

**Metal Mediated Novel Nitro-Alkyne Cycloisomerizations:
Studies Toward the Total Synthesis of Isatisine A**

A THESIS
SUBMITTED FOR THE DEGREE OF
DOCTOR OF PHILOSOPHY
(IN CHEMISTRY)

TO
UNIVERSITY OF PUNE

BY
Pitambar Patel

Dr. C. V. Ramana
(Research Guide)

ORGANIC CHEMISTRY DIVISION
NATIONAL CHEMICAL LABORATORY
PUNE-411008
APRIL-2012

*DEDICATED
TO
MY Mother*

DECLARATION

The research work embodied in this thesis has been carried out at National Chemical Laboratory, Pune under the supervision of **Dr. C. V. Ramana**, Organic Chemistry Division, National Chemical Laboratory, Pune – 411008. This work is original and has not been submitted in part or full, for any degree or diploma of this or any other university.

Organic Chemistry Division
National Chemical Laboratory
Pune – 411008
October–2010

(Pitambar Patel)

Dr. C. V. Ramana

Phone: +91-20-25902577

+91-20-25902455

E-mail: vr.chepuri@ncl.res.in

CERTIFICATE

The research work presented in thesis entitled “**Metal Mediated Novel Nitro-Alkyne Cycloisomerizations: Studies Toward the Total Synthesis of Isatisine A**” has been carried out under my supervision and is a bonafide work of **Mr. Pitambar Patel**. This work is original and has not been submitted for any other degree or diploma of this or any other University.

Pune – 411008

April – 2012

Dr. C. V. Ramana

(Research Guide)

Acknowledgements

Completing my PhD degree is probably the most challenging activity of my life so far. The best and worst moments of my doctoral journey have been shared with many people. It has been a great privilege to spend several years in the Division of Organic Chemistry at National Chemical Laboratory and its members will always remain dear to me.

My first debt of gratitude must go to my advisor, **Dr. C. V. Ramana** for his brilliant guidance, unmatched humanity. He patiently provided the vision, encouragement and advice necessary for me, throughout the doctorate programme. I consider myself very fortunate to have been a part of his research group. I sincerely thank him for instilling excellent work ethic in me. I wish to emulate the decency and dignity with which he lives life.

I express my profound gratitude to Dr. Kumar Vanka for introducing me to the field of theoretical chemistry (DFT study) and also for his genuine and valuable suggestion for my work. I also express my profound gratitude to Dr. B. L. V. Prasad for introducing me to the world of Nano Science, friendly attitude and valuable suggestion for my work.

I also thanked HOD, Division Organic Chemistry and Director, NCL for providing infrastructural facilities. I gratefully acknowledge Dr. Srinivas Hotha, Dr. S.P. Chavan, Prof. D. D. Dhavale, Dr. Thulsiram, Dr. Borate, Dr. R. A. Joshi, Dr. (Mrs.) R. R. Joshi, Dr. D. K. Mohapatra and Dr. P. K. Tripathy for their valuable suggestions. I sincerely thank Mrs. Raphael, Mrs. Kulkarni and all OCD office staff for their cooperation. Help from the spectroscopy, analytical and mass group is gratefully acknowledged. I sincerely thank Dr. Rajmohan, Dr. Gonnade, Mrs. Santhakumari and Mr Ajit (for HRMS) for their unhesitant support and assistance. My special thanks to the entire NMR faculty.

I gratefully acknowledge the training and support extended by my senior colleagues Dr. Bagawat, Dr. N. Raghupathi, Dr. Soumitra, Dr. Nageswar, Dr. Sumantha, Dr. Srinivas, Dr. Indu, Dr. Chandrakiran, Dr. Anuj, Dr. Mondal, Dr. Kullu, Dr. Sharad, Dr. Giri, Dr. Vikhe, Dr. Pandey and Senthil during the tenure of my Ph.D life. I would like to thank all my colleagues Rahul, Suneel, Narendra, Ashish, Yadagiri, Mangesh, Atul, Paresh, Yogesh, Shyam, Chandrababu, Sachin, Ajay, Vilas, Sridhar, Ketan, Tejas, Dinesh, Srinivas & all my other colleagues at NCL for their cheerful support.

On the same note, I sincerely thank to my G. J. hostel and NCL friends for making life easy and pleasant whenever it seemed to be getting tough.

I gratefully acknowledge "Oriya Mandali" members— Seetaram bhai, Sabita apa, Sashi bhai, Debashish Bhai, Sahoo Bhai, Rosy Apa, Manaswini Apa, Suman Apa,

Bhuban, Ramakanta, Subash & Karubaki, Tini, Jitu, Manda, Chaka, Raju, Subash, Rinki, Khirodra and Bisnu for creating a sweet home away from home ambiance.

It is impossible to express my sense of gratitude for my parents in mere words, specially my mother. The existence of my life, wheather it is present or future is because of her enormous blessings, commitments to my ambitions and selfless sacrifices. I am thankful to my sisters; Saraswati, Tapaswin, Jogeswari and brother-in Laws; Bhogilal, Gunanidhi, Pitambar. Words fall short to thank my niece Sunita, Sanjukta, Ankita, Alibha, Dimpal and nephew Manas for their love during my home visit.

I would also like to show my deep gratitude to my M. Sc. Teachers and seniors in Jyotivihar University–Prof. B. K. Mishra, Prof. R. K. Behera, Prof. A. K. Panda, Dr. A. Panda and Dr P. K. Behara for their unique way of teaching & inspiration in life and Anita Nani, Sushanta Da for their constant encouragement.

I am also thankful to UGC, New Delhi for the financial assistance in the form of a fellowship. Finally, my acknowledgement would not be complete without thanking the Almighty, for the strength and determination to put my chin up when faced with hardships in life.

Pitambar Patel

“God, grant me the serenity to accept the things I cannot change, the courage to change the things I can, and the wisdom to know the difference”

R. Niebuhr.

DEFINATIONS AND ABBREVIATIONS

Ac	–	Acetyl
aq.	–	Aqueous
Bn	–	Benzyl
Bu	–	Butyl
Cat.	–	Catalytic/catalyst
DCE	–	1,2-Dichloro ethane
Conc.	–	Concentrated
COSY	–	Correlation spectroscopy
DMF	–	<i>N,N</i> -Dimethylformamide
DMAP	–	<i>N,N'</i> -Dimethylaminopyridine
DMSO	–	Dimethyl sulfoxide
Et	–	Ethyl
HRMS	–	High Resolution Mass Spectrometry
LDA	–	Lithium diisopropylamide
<i>m</i> -CPBA	–	meta-Chloroperbenzoic acid
NMR	–	Nuclear Magnetic Resonance
NOESY	–	Nuclear overhauser effect spectroscopy
ORTEP	–	Oak Ridge Thermal Ellipsoid Plot
Py	–	Pyridene
Ph	–	Phenyl
rt	–	Room temperature
Sat.	–	Saturated
TBSCl	–	<i>tert</i> -Butyldimethylsilyl chloride
TBAF	–	<i>tetra-n</i> -butylammonium fluoride
THF	–	Tetrahydrofuran
TPP	–	Triphenylphosphine

Abbreviations used for NMR spectral informations:

br	Broad	q	Quartet
d	Doublet	s	Singlet
m	Multiplet	t	Triplet

GENERAL REMARKS

- ^1H NMR spectra were recorded on AV-200 MHz, AV-400 MHz, and DRX-500 MHz spectrometer using tetramethylsilane (TMS) as an internal standard. Chemical shifts have been expressed in ppm units downfield from TMS.
- ^{13}C NMR spectra were recorded on AV-50 MHz, AV-100 MHz, and DRX-125 MHz spectrometer.
- EI Mass spectra were recorded on Finnigan MAT-1020 spectrometer at 70 eV using a direct inlet system.
- The X-Ray Crystal data were collected on *Bruker SMART APEX* CCD diffractometer using Mo K_α radiation with fine focus tube with 50 kV and 30 mA.
- Infrared spectra were scanned on Shimadzu IR 470 and Perkin-Elmer 683 or 1310 spectrometers with sodium chloride optics and are measured in cm^{-1} .
- Optical rotations were measured with a JASCO DIP 370 digital polarimeter.
- All reactions are monitored by Thin Layer Chromatography (TLC) carried out on 0.25 mm E-Merck silica gel plates (60F-254) with UV light, I_2 , and anisaldehyde in ethanol as developing agents.
- All reactions were carried out under nitrogen or argon atmosphere with dry, freshly distilled solvents under anhydrous conditions unless otherwise specified. Yields refer to chromatographically and spectroscopically homogeneous materials unless otherwise stated.
- All evaporations were carried out under reduced pressure on Buchi rotary evaporator below 45 °C unless otherwise specified.
- Silica gel (60-120), (100-200), and (230-400) mesh were used for column chromatography.
- Different numbers were assigned for compounds in Abstract and in present work.
- Spectra of some selected compound are only given, as all the spectra are given in supplementary information of the published paper.

CONTENTS

Sr. No.	Subject	Page No
1	Abstract	i–viii
2	Introduction	1–34
3	Result and discussion	35–105
4	Experimental	106–154
5	References	155–163
6	Spectra	164–202
7	No. of publication	203
8	Erratum	204

ABSTRACT

ABSTRACT

The thesis entitled “**Metal Mediated Novel Nitro-Alkyne Cycloisomerizations: Studies Toward the Total Synthesis of Isatisine A**” consists of five parts - namely i. Introduction, ii. Results and Discussion, iii. Experimental Details, iv. References and v. Spectra. The thesis describes the details of the total synthesis of Isatisine A and the new methods developed in this context. The introductory part provides the origin and precedences of the reactions that we have attempted to develop and the details of the total syntheses of four isatisine A's that have been reported by other groups. The second part comprises the complete details of the new methods that we have developed focussing on the nitroalkyne cycloisomerization and some mechanistic insights into this reaction with the help of DFT calculations. The second part also discusses the conceptualization and the execution of the nitroalkynol cycloisomerization reaction. The products of these cyclizations (isatogens, indolin-3-ones) have been further used to develop two subsequent [metal]-mediated reactions by which the synthesis of tricyclic core of isatisine A has been realized. Finally, the total synthesis of Isatisine A has been completed by employing all the indigenous reactions that we have developed.

Isatisine A

Isatisine A (**1**) (Figure 1) is a complex alkaloid having bisindole, isolated from the leaves of *Isatis indigotica* Fort, an herbaceous plant species used in Chinese folk medicine. The acetonide derivative **2**, which is an artifact during the isolation, was found to exhibit cytotoxicity against C8166 with $CC_{50} = 302 \mu\text{M}$ and anti-HIV activity of $EC_{50} = 37.8 \mu\text{M}$. The challenging structural features of isatisine A (**1**) was characterized by the presence of a fused tetracyclic system comprising mainly of furanose and an indolin-3-one units. These two units are connected through a C-anomeric linkage at C(2)- of the indolinione and an amide bridge between the C(2) of

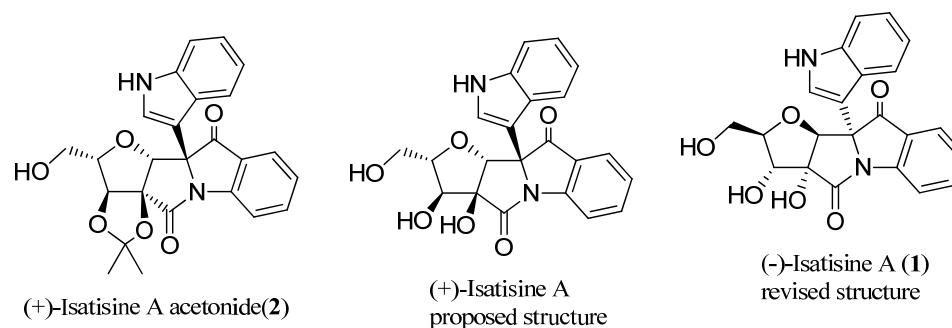
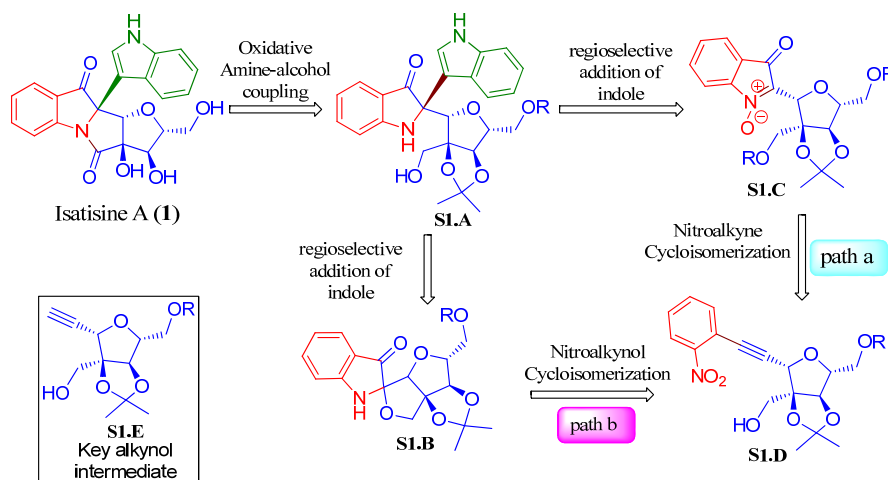


Figure 1: Proposed structure of *Isatisine A*

furanose and nitrogen of the indolinone. There is an indole unit as a substituent at C(2)- of indolinone connected with its C(3). Keeping the promising biological activity in mind, taken together with its unique structure, a program aiming its total synthesis has been initiated immediately after its isolation.

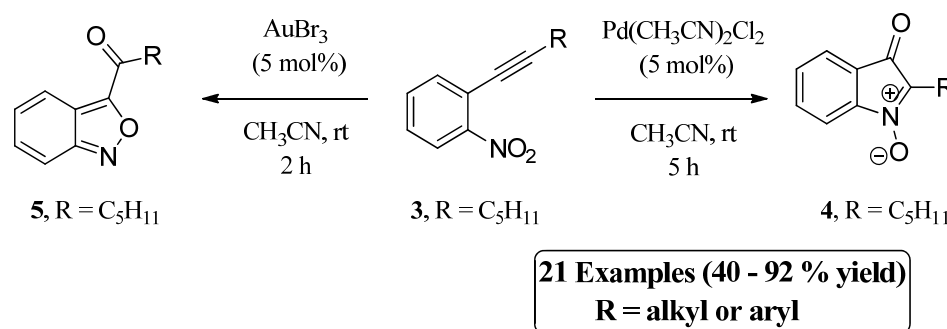


Scheme 1: Key retro synthetic disconnection for *Isatisine A*

Scheme 1 shows the details of our retrosynthetic disconnections. The construction of the central lactam ring has been planned as the final event in our total synthesis via a metal-mediated oxidative cyclization of a γ -aminoalcohol. The synthesis of γ -aminoalcohol has been planned *via* two different routes both featuring a metal/Lewis-acid mediated addition of indole to either a spiro-3-indolinone derivative or to an isotogen. For the synthesis of these intermediates, we designed two novel nitroalkyne cycloisomerizations.

1. Pd(II) catalyzed nitroalkyne cycloisomerization for Isatogens synthesis

Our journey in this regard began with developing methods for the above-mentioned key intermediates, namely for isatogens and for 2,2-disubstituted-spiroindolin-3-ones. Isatogens are the unnatural scaffolds known since the last 130 years. However, the available methods have been mainly limited to the synthesis of 2-aryl isatogens synthesis. The 2-alkyl isatogens are rarely made and generally involve harsh conditions and multi-step protocols. In the quest for a general, mild, and substituent independent method for isatogens synthesis, after an initial consultation with the mechanisms available for cycloisomerization of nitrotolans leading either to isatogens (photochemical) or to the anthranils ([Ir]-/[Au]-catalyzed), we hypothesized [Pd]-catalyzed nitroalkyne cycloisomerization for synthesis of isatogens and executed it successfully employing diverse substrates with different protecting groups (Scheme 1).



Scheme 2: [Pd]-Catalyzed nitroalkyne cycloisomerization for isatogens synthesis

For example, protecting groups such as TBS, isopropylidene, and benzyl ethers were intact under the conditions employed, and also these conditions accommodated diverse substituent functionalities that included free alcohols, β -lactams, heterocycles, and olefins. Next, a preliminary screening of the available isatogens revealed the 2-alkyl isatogens to be novel ROS scavengers capable of inhibiting cellular necroptosis.

2. Mechanistic Investigation of Nitroalkyne Cycloisomerization using Density Functional Theory (DFT)

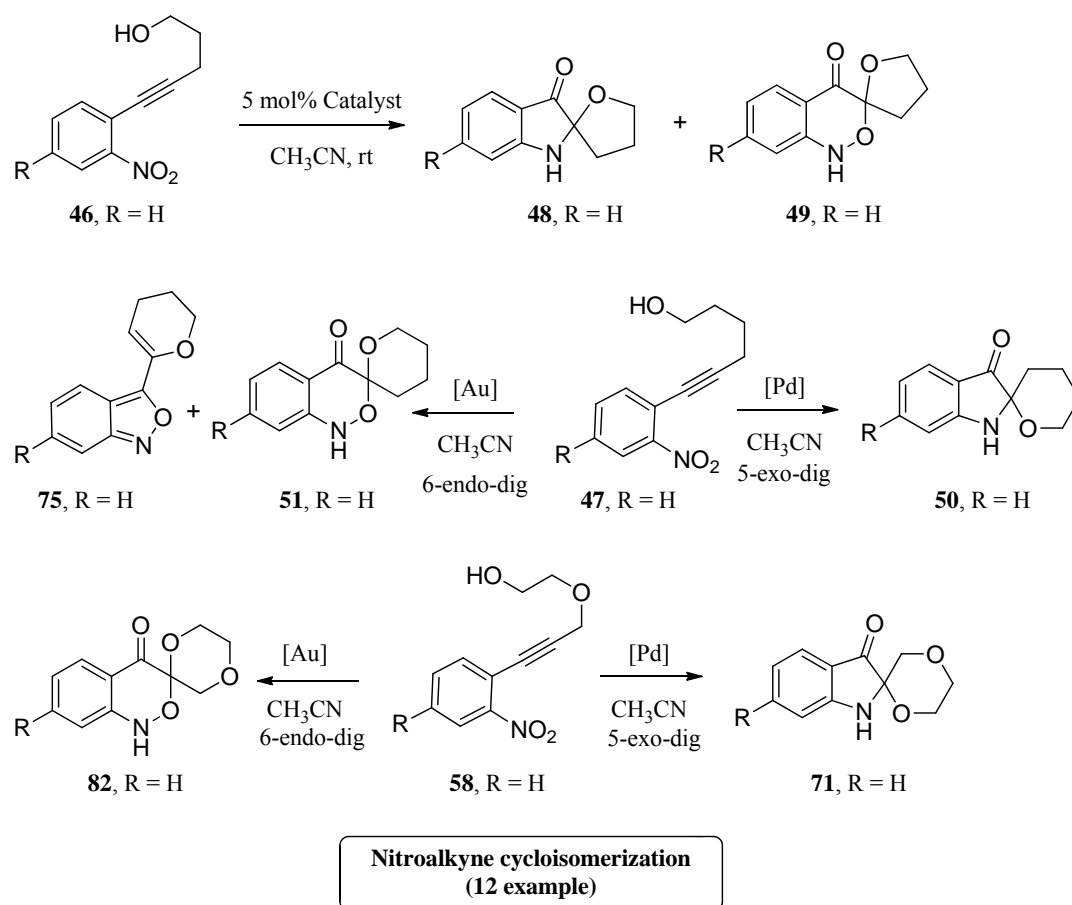
After having an established method for isatogens synthesis, the detailed mechanism of the above reaction was studied with the aid of density functional theory (DFT). For this, three possible pathways for the palladium-mediated nitroalkyne cycloisomerization and for the internal redox have been considered; namely i) the chloro palladation approach based upon Huisgen's mechanism for pyridine mediated isatogens synthesis; ii) palladium assisted 5-*exo*-dig mode route for transfer of oxygen from nitro to alkyne; and iii) the corresponding competitive 6-*endo*-dig route.

The detailed analysis of these three paths through the identification of the various transition states involved and their energy requirements, led to the conclusion that the 5-*exo*-dig route to isatogen formation had significant advantages over the other two routes involving halo-palladation or the 6-*endo*-dig mode cyclization. For example, the route we identified for the 5-*exo*-dig path way is significantly simpler, having three transition states as opposed to five for the halo-palladation, and also requiring only the presence of one PdCl₂ molecule as the catalyst instead of two PdCl₂ and a CH₃CN solvent molecule as required for the halo-palladation process. Moreover, the rate determining step had a barrier of 24.8 kcal/mol, which was 5.7 kcal/mol lower than the rate determining barrier in the halo-palladation case (for the oxygen transfer). Next, we have also considered the possibility of isatogen formation *via* a 6-*endo*-dig fashion and found the pathway to be significantly disfavoured over the 5-*exo*-dig route, as the energy barrier for both transition states is quite high (barrier: 24.8 kcal/mol).

3. Metal Catalyzed Nitroalkynol Cycloisomerization

After our initial success with the nitroalkyne cycloisomerization, we next hypothesized a new nitroalkynol cycloisomerization route leading to the synthesis of N-hydroxy spiroindolin-3-one and/or spirobenzoxazinone, the former compounds bearing the advanced structural unit that was identified in the total synthesis of Isatisine A and the latter being an unprecedented structural unit. The 5-(2-nitrophenyl)pent-4-yn-1-ol (**46**) and 6-(2-nitrophenyl)hex-5-yn-1-ol (**47**) complexes

have been employed as model substrates and various [Pd] and [Au] complexes have been screened to realize the nitroalkynol cyclization. With the pentynol derivative **46** Pd(CH₃CN)₂Cl₂ (5 mol%) in acetonitrile solvent, the nitroalkynol cyclization furnished the spiroindolin-3-one **48** derivatives (resulting from the N–O reduction) instead of the corresponding N-hydroxy derivative along with the anticipated benzoxazinone **49**. Similarly, with the other pentynol derivatives, the [Pd]-catalyzed cyclizations gave both the products in a ~1:1 ratio. The cyclization of the hexynol and propargyl glycol derived nitroalkynols gave spiroindolin-3-one as the sole product. The gold catalyzed nitroalkynol cyclization of the hexynol derivative led to the formation of spirobenzoxazinone **51** along with a minor amount of anthranil derivative **75** (Scheme 3). On the other hand, the propargylglycol derivatives gave exclusively the benzoxazinones.



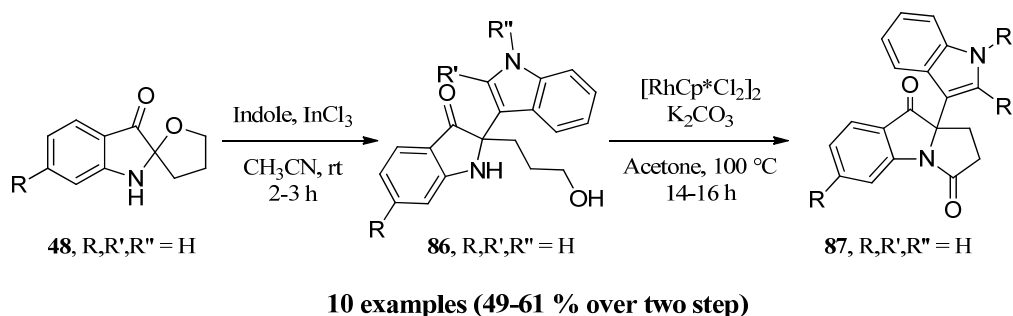
Scheme 3: [Pd] and [Au] mediated nitroalkynol cyclization

4. Friedel-Craft alkylation of spiroindolin-3-ones: A sequential metal catalyzed approach for the central tricycle core structure of Isatisine A

The next requirement in the planned synthesis of Isatisine A was to develop methods for the addition of indoles to isatogen or to spiroindolin-3-one derivatives followed by oxidative lactamization. In this context, prior to the starting the synthesis of Isatisine A, we were interested in executing a model study for the core structure of the molecule. During this period, our group has developed [In]-mediated of addition of indoles to isatogens to procure either the 2,2-disubstitutedindolin-3-ones or the corresponding N-hydroxy derivatives by employing InCl_3 as a reagent or the catalyst. The same InCl_3 has been explored for the addition of indole to spiroindolin-3-ones. The optimized conditions involve the use of InCl_3 (1 eq.) in acetonitrile solvent and the reactions in general were found to be completed within 1h with isolation of the products in excellent yields.

Next, we screened a couple of complexes that have been used for the oxidative cyclization of γ -amino alcohols which led to the identification of the $[\text{RhCp}^*\text{Cl}_2]_2$ species as the catalyst of choice. The conditions employed involve the heating of the γ -amino alcohol with 5 mol% of $[\text{RhCp}^*\text{Cl}_2]_2$ and K_2CO_3 (0.05 eq.) in acetonitrile solvent at 100 °C. The corresponding tricyclic lactam was obtained in moderate yields. The approach was generalized by synthesizing a library of compounds.

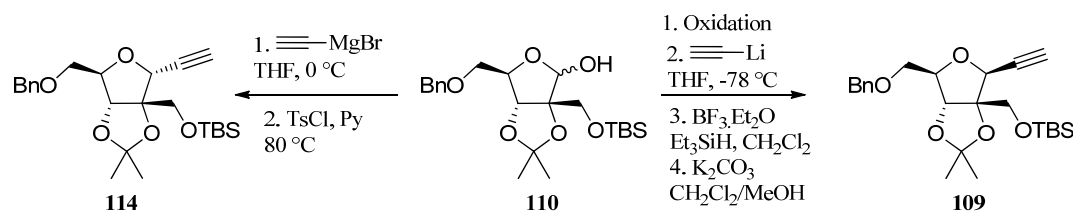
To this end, we have now developed a convergent strategy that comprises of four consecutive [metal]-catalyzed/mediated reactions to convert a simple alkynol into a tricyclic core of the isatisine A (Scheme 4).



Scheme 4: A sequential approach for core of Isatisine A

5. Total synthesis of Isatisine A

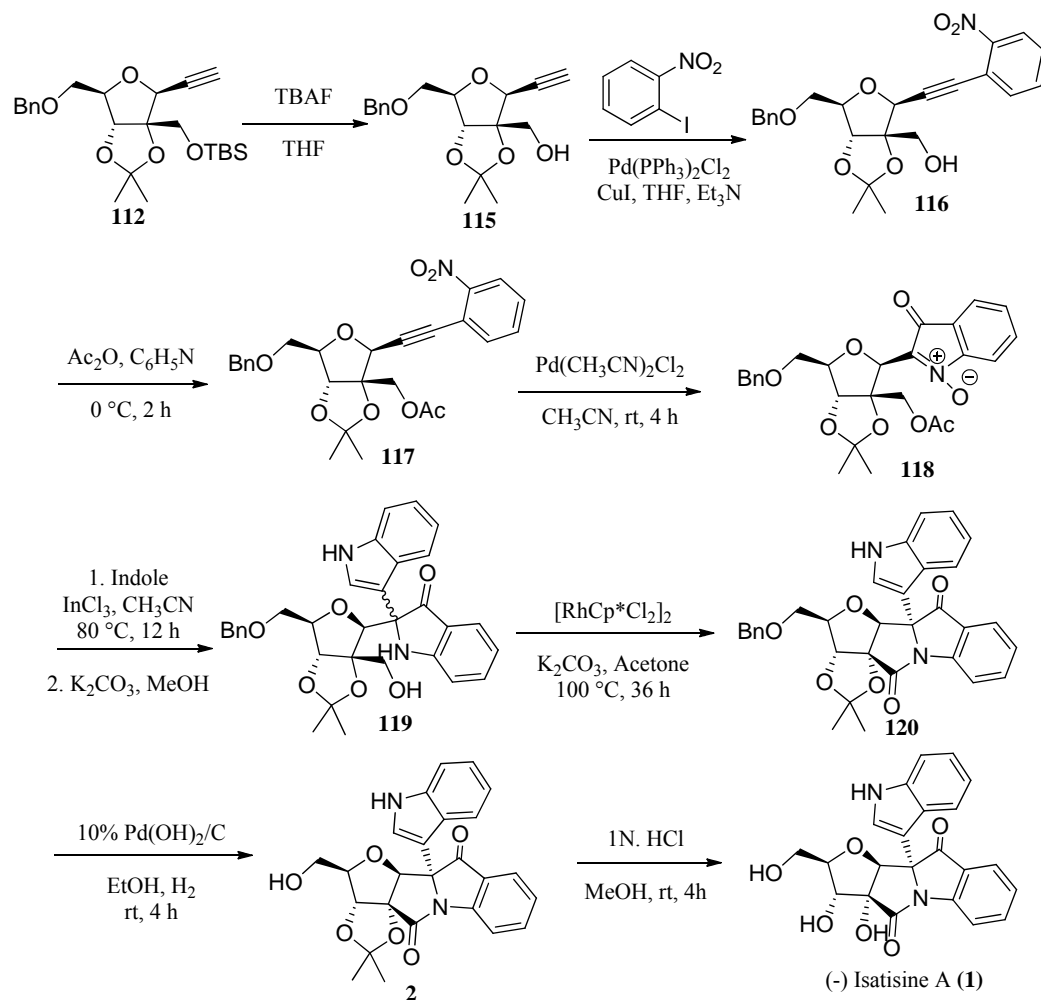
After successful development of the novel nitroalkyne/nitroalkynol cycloisomerization, as well as subsequent methods for the indole addition and oxidative cyclizations, we next focused our attention on the total synthesis of Isatisine A. A careful analysis of the revised structure of isatisine A led to the identification of the D-ribose as the suitable starting material and the alkynol **109** as an advanced intermediate to apply to our four-step sequence leading to the total synthesis of Isatisine A.



Scheme 5: Synthesis of the key alkynol

The synthesis started with the conversion of D-ribose to the corresponding lactol by using the available procedures. The cross aldol reaction of **111** with formaldehyde followed by selective 1-OH protection as its TBS ether gave **112**. The addition of ethynylmagnesium bromide followed selective tosylation of propargylic OH and subsequent cyclization gave the C-ethynyl furanose **114**, which turned out to be the undesired α -anomer. Alternatively the oxidation of lactol to the corresponding lactone and subsequent addition of lithiated TMSacetylene and the reduction of intermediate hemiacetal provided the α - and β - anomers in a 1:3 ratio. The requisite β -anomer **117** was then subjected for the Sonogashira coupling to obtain the key nitroalkyne **118**. However, the attempted cycloisomerization of **118** resulted in an intractable complex mixture. Whereas, the cycloisomerization of the corresponding acetate protected nitroalkyne **119** was smooth and the resulting isatogen derivative **120** was subjected for the indole addition followed by deacetylation to arrive at the γ -amonalcohol **106**. The γ -amino alcohol **106** was converted into the benzyl protected Isatisine acetonide by oxidative amidation employing the complex as the catalyst. The stepwise deprotection of benzyl and acetonide groups of the resulting lactam led to

the completion of the total synthesis of Isatisine A. The spectral and analytical data of Isatisine A were in full agreement with the data reported for the natural product.



Scheme 6: Total synthesis of Isatisine A

At the outset, a highly modular total synthesis of Isatisine A has been developed that has the potential for the synthesis of related isatisine like small molecule libraries. Starting from the known intermediate derived from D-ribose, isatisine A has been synthesized in 9 steps. Our approach is unique in its own as it involved four consecutive metal catalyzed/mediated transformations addressing two each of C–C and C–hetero atom bond formations and finally global deprotection using TiCl_4 to furnish Isatisine A.

INTRODUCTION

INTRODUCTION

Since their co-existence and their optimization along with the evolution of life, natural products were regarded as pre-validated lead structures for chemical biology and medicinal chemistry research.¹ Secondly, because they have been accommodated in some living organism, either during their own bio-synthesis or through their involvement in the modulation of respective biological processes, natural products, and to a major extent natural product like small molecules, can move fast across the critical pharmacokinetic and bioavailability barriers when compared with a randomly synthesized small molecule. Though natural products have served as platforms since the beginning of the drug discovery programs, in the early 90's of the last century however, they have been ignored across all the major pharmaceutical companies. This was partly due to the needs of rapid development in biology and the availability of high throughput screenings and partly because of the uncertain IP protocols. During this period, combinatorial chemistry has emerged as a promising approach aided with the development of robotic hands for small molecule libraries synthesis. However, the combinatorial libraries have failed miserably at delivering a magic bullet and again, the attention have focused back on the complexity and diversity of nature's small-molecules in the new drug discovery programs.² The focus has shifted towards using total synthesis as a platform for focused small molecule libraries synthesis by applying the combinatorial technologies and the discovery of new biologically active small molecules.³

The total synthesis of complex natural products remains the challenging, educative, and continuously contemporary area in organic chemistry.⁴ As a part of our total synthesis program, we aim to develop new strategies and methods that make the process of synthesizing natural products as efficient and flexible as possible.⁵ Needless to say, the design of an overall synthetic plan of the total synthesis is an important aspect as well as the development of new methods, especially the catalytic ones, which address the skeletal complexity of the targeted molecules. Our group has been actively engaged in developing a new philosophy of synthesizing molecules which is rightly called as the target cum flexible synthesis platform; wherein, we emphasize that the right selection of building blocks and reactions must enable *not* one single target molecule but should result in a collection of small molecules having

the similar core.^{5,6} In this context, we have selected the total synthesis of Isatisine A (**1**). The acetonide of isatisine A (**2**), an artifact during the isolation, has shown promising anti-HIV⁷ activity and our intention was to develop a highly modular strategy that involves mainly the catalytic transformations in the final stages so as to also address the synthesis of focused isatitisine A like small molecule libraries.

Acquired immunodeficiency syndrome (AIDS) is a clinical syndrome that is the result of infection with human immunodeficiency virus (HIV), which causes profound immunosuppression.⁸ It has been a serious, life-threatening health problem and is the most quickly spreading disease of the century. Since the epidemic began, more than 60 million people have been infected with the virus. HIV/AIDS is now the leading cause of death in Sub-Saharan Africa. Worldwide, it is the fourth biggest killer. Most of the clinically useful anti HIV agents are nucleosides but their use is limited due to their severe toxicity and emerging drug resistance.⁹ Natural products, of which structural diversity is very broad, are good sources for the effective discovery of anti HIV agents with decreased toxicity.¹⁰

Biodiversity of the plant kingdom has always provided a source of new drug candidates for almost all disease areas. Over the past decade, substantial progress has been made in research on the natural products possessing anti-HIV activity.¹⁰ A variety of secondary metabolites obtained from natural origin showed moderate to good anti-HIV activity. A variety of alkaloids have been found to possess HIV-inhibitory activity. As mention earlier, from the vast library of alkaloids, our attention was drawn towards indole alkaloids, named Isatisine A, isolated in 2007, from a Chinese plant.

1.1 Isatisine A

1.1.1 Isolation, Structural Features and Biological Activity

Isatis indigotica Fort. (family *Cruciferae*) is a biennial herbaceous plant distributed widely in Changjiang River valley. Its roots and leaves commonly used as traditional Chinese medicine are named "Ban-Lan-Gen" and "Da-Qing-Ye" in China. The term "Ban-Lan-Gen" is an official crude drug that has been recorded in Chinese

Pharmacopeia for a long time. The purified extracts of "Ban-Lan-Gen" have been subjected to make various preparations which are popularly used in clinical practice



Figure 1: (A) Leaf of *isatis indigotica*, (B) Tea made from leaves of *isatis indigotica* fort.

for treatment of influenza, epidemic hepatitis, epidemic encephalitis B, carbuncle, erysipelas etc. The chemical investigation of this plant has led to the isolation of indigotin, indirubin, epigotrin, 2-hydroxy-3-butenyl thiocyanate etc., among which indirubin has been proven to be an anticancer agent used in the clinic for chronic granulocytic leukemia.¹¹ Recently, several "Ban- Lan-Gen" injections manufactured by different factories showed antiendotoxic effects in experimental studies. In search of an active anti-HIV compound, the leaves of *I. indigotica* ("Da-Qing-Ye") were investigated and many known compounds were reported.¹² From the methanol extract of the leaves, compound **2** (64 mg) was isolated.

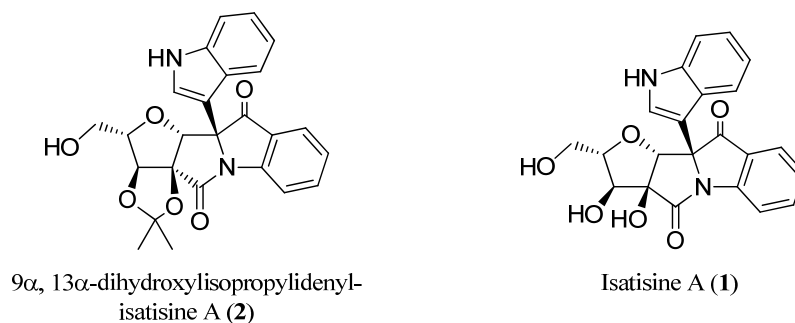


Figure 2: proposed structure of *Isatisine A*

Initially, isatisine A was isolated as its acetonide derivative **2** and the structure elucidation was done by 1D and 2D NMR experiments. Then subsequent X-ray crystallographic analysis secured the structural assignment as well as the relative stereochemistry. Biological evaluation of the acetonide derivative **2** reveals that this material exhibits cytotoxicity against C8166 with $CC_{50} = 302 \mu\text{M}$ and anti-HIV activity of $EC_{50} = 37.8 \mu\text{M}$. However, its unusual dioxolane group, which is rarely found in natural products, led to further investigations to determine whether the acetonide derivative **2** was the natural product or an artifact compound formed during the isolation (acetone was used as an eluent). Suspecting this, isatisine A (**1**) was prepared by hydrolysis of **2** and matched with an HPLC trace of a crude extract, leading to the supposition that **1** and not **2** was in fact the biogenetic product (Figure 2). Although the relative stereochemistry of **2** (and consequently **1**) was confirmed by single crystal X-ray diffraction studies of acetonide **2**, the absolute stereochemistry remained unknown (Figure 3). However, the biological properties of natural product **1** were not reported due to insufficient amount of the compound. The challenging structural features of isatisine A (**1**) which contains an unprecedented fused tetra cyclic framework with five contiguous stereogenic centers, two of which are fully substituted, as well as a densely functionalized tetrahydrofuran moiety and an indole ring attached to one of its quaternary center. Keeping the promising biological activity in mind as well as the unique structure of the compound, a program aiming at the total synthesis has been initiated in our group immediately after its isolation.

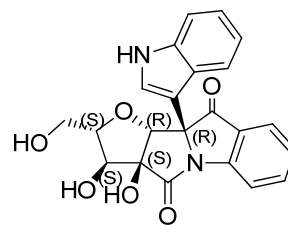
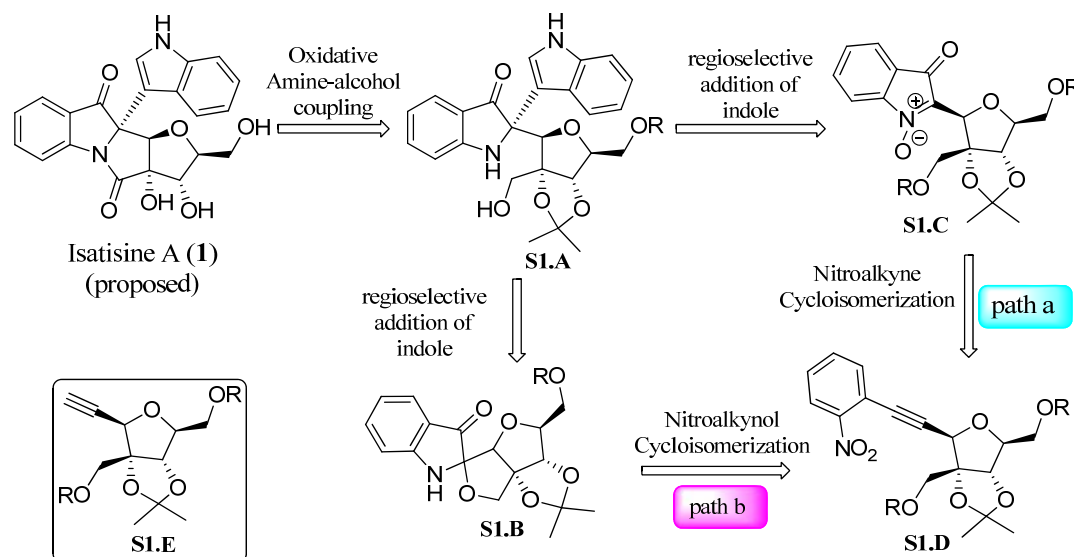


Figure 3: Stereochemistry of isatisine A

1.1.2. Retro Synthetic Analysis of Isatisine A

The structure of isatisine A was characterized by the presence of a fused tetracyclic system comprising mainly a furanose unit and an indolin-3-one unit. These two units are connected through a C-anomeric linkage at C(2) of the indolin-3-one and an amide bridge between the C(2) of furanose and nitrogen of the indolinone. There is an indole ring as a substituent at C(2) of indolinone connected with its C(3). Scheme 1 describes the key retrosynthetic disconnections for the isatisine A. The

construction of the central lactam ring had been planned as the final event in our total synthesis *via* a metal-mediated oxidative cyclization of a γ -amino alcohol, thus identifying **S1.A** as the corresponding retron. The synthesis of **S1.A** was planned *via* two different routes, both featuring a metal/Lewis acid-mediated addition of indole to either to an isatogen **S1.C** or to a spiro-3-indolinone derivative **S1.B**. The synthesis of both key intermediates **S1.C** and **S1.B** feature a novel nitroalkyne cycloisomerization. In one case it was nitroalkyne cycloisomerization leading to isatogens and in another case it was a nitroalkynol cyclization leading to a spiro-*N*-hydroxyindolinone. The alkynol **S1.D** was identified as the common starting point for both these approaches. **S1.D** Can be made from the alkynenol **S1.E**. After having an initial blueprint of the retrosynthetic strategy for the isatisine A total synthesis, our next concern was the development of methods for the above-mentioned key transformations, namely– i. a nitro-alkyne cycloisomerization leading to isatogens or, in other words, methods for the synthesis of isatogens; ii. a nitroalkynol cyclization leading to spiro-*N*-hydroxy-indolinones which is unprecedented; iii. methods for the addition of indole either to isatogen or to a 2,2'-spiroindolin-3-one; and iv. the scouting for a suitable metal complex for the catalytic oxidative cyclization. In the following sections, a brief review of the literature related to the above-mentioned aspects will be dealt in detail.

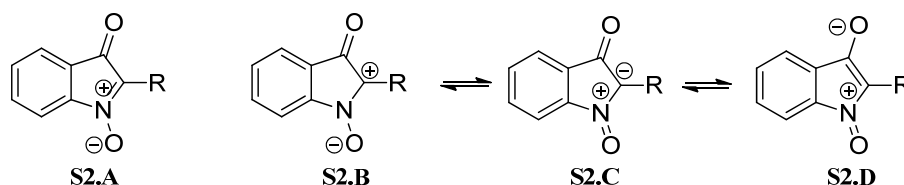


Scheme 1: Retrosynthetic disconnection for Isatisine A

1.2. Isatogen

1.2.1. Structural features

The isatogens are non-natural compounds and comprehensively named as 3-oxo-3*H*-indole-1-oxides.¹³ The first members of this group of compounds were prepared by Bayer¹⁴ in 1881, during the course of his classic research on indigo. Ethyl isatogenate was obtained by the rearrangement of ethyl *o*-nitrophenylpropiolate under the influence of cold concentrated sulphuric acid. Isatogens, are usually represented as **S2.A**, but they are more fully described by the additional canonical structures **S2.B–D**



Scheme 2: Structure of isatogen and its canonical structure

(Scheme 2). The addition of nucleophiles and some dipolarophiles is indicated by **S2.B**, whereas the back polarization represented in **S2.C** is well known in cyclic nitrones and aromatic N-oxides.¹⁵ The parent isatogen (R = H) has not been unequivocally identified and only few 2-

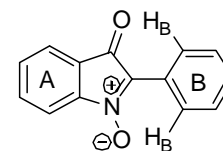
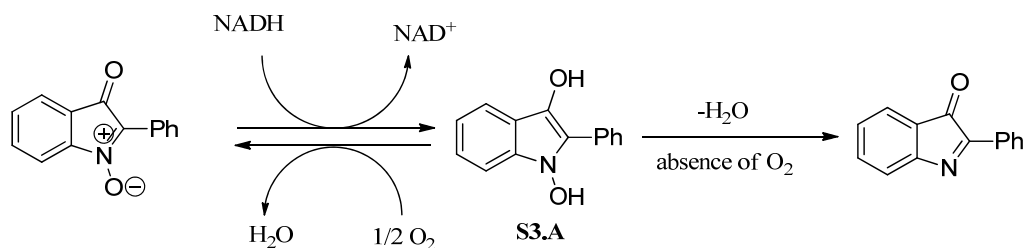


Figure 4

alkylisatogens (R = alkyl) have been prepared. The infrared spectra of isatogens show strong carbonyl absorption at 1700–1720 cm^{-1} which is characteristic of conjugated carbonyl groups in five membered ring compounds. A band at 1175 cm^{-1} has been assigned to the N–O stretching vibrations. The NMR spectra of isatogens are characterized by the almost equivalent values for all four protons in ring A (figure 4), the carbonyl and nitronium groups having similar effects. In 2-arylisatogens, the four protons of ring A, form multiplet whereas the ortho protons H_B of aryl ring B are more deshielded by the carbonyl and nitronium groups.

1.2.2. Biological properties of Isatogens

2-Aryl isatogens show significant antimicrobial activity against bacteria,¹¹ mycoplasma organisms and the mold *Candida albicans*.¹⁶ A detailed study of the biochemical effects of 2-phenylisatogen xx, shows that it executes a range of actions on mitochondrial respiration. It inhibits the uptake of phosphate, glutamate and calcium ions into mitochondria. The effect on phosphate transport closely resembles that of organic mercury compounds which are known to interact with thiol groups. The inhibition of oxidative phosphorylation by the compound, originally thought to be analogous to the action of aurovertin and oligomycin is now recognized to arise from the blockade of phosphate transport.¹⁷ In contrast, 2-phenylcarbamoylisatogen (R = CONHPh) acts as a classical uncoupling agent and releases the inhibition of ATP synthesis caused by 2-phenyl isatogen and oligomycin.¹⁸ 2-Phenylisatogen, which oxidizes thiol compounds, has a similar effect on the transhydrogenase system only when the mitochondrial particles are prepared in the presence of the isatogen. This observation has been used in locating the site of this enzyme system on the outside of the inner mitochondrial membrane.¹⁹

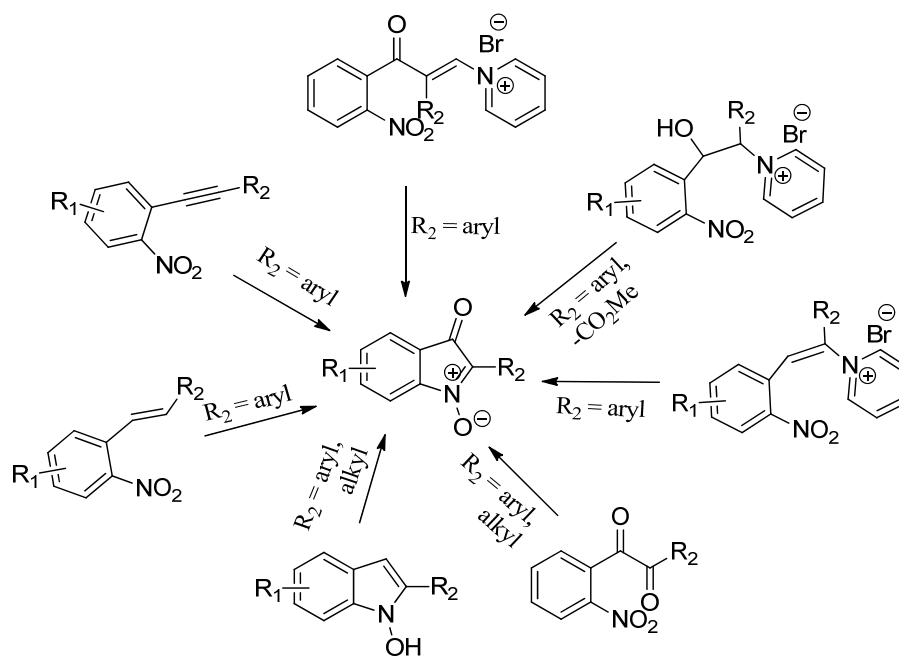


Scheme 3: *Isatogen as a hydrogen carrier in mitochondria*

In the latter case, however, the picture is complicated by the ability of 2-phenylisatogen to function as a hydrogen acceptor in the mitochondrial oxidation of NADH (scheme 3). This effect is not due to the direct oxidation of NADH by the isatogen and in the presence of oxygen 2-phenylindolone is not formed. It is proposed that under these conditions 2-phenyl isatogen acts as a reversible hydrogen carrier by formation of the unstable dihydroxyindole **S3.A**. In the absence of oxygen, 2-phenylindolone is formed *via* an irreversible step.

1.2.3. Synthesis of isatogens

Generally, isatogens have been synthesized *via* two main methods involving either the oxidation of a 1-hydroxy-2-substituted indole or the intramolecular cyclization of an *ortho*-substituted nitrobenzene precursor¹³ (Scheme 4). However, the first strategy, applicable to both alkyl and aryl substituted isatogens, requires a multi-step preparation of the indole intermediate and the second synthetic approach is limited to 2-aryl 3*H*-indol-3-one *N*-oxides. Recently, the synthesis of isatogens was reported by metal mediated cycloisomerization of *o*-nitroalkynebenzene derivatives. A brief account about the reported methods for the nitroalkyne cycloisomerizations have been described below.



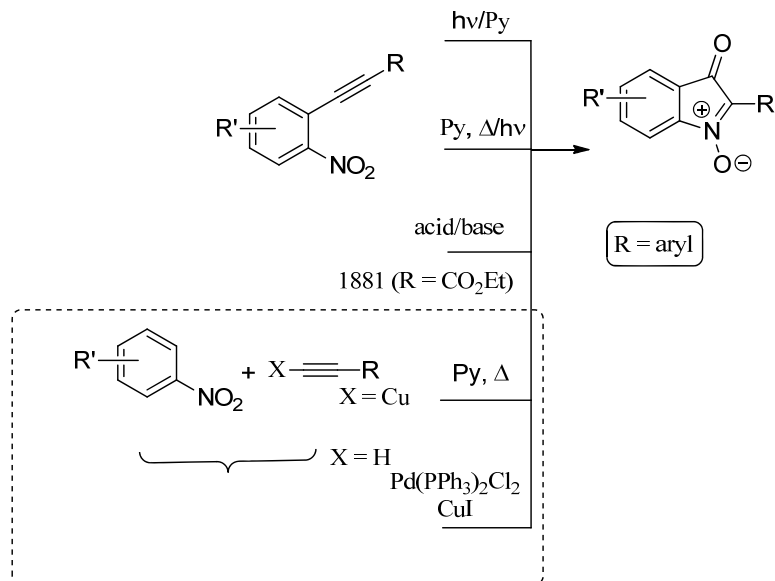
Scheme 4: Available Approaches for the Synthesis of Isatogens

1.2.3.1. Intramolecular cyclizations

1.2.3.1.1. Nitroalkyne cycloisomerization

The cyclization of 2-nitrophenylacetylene derivatives (trivially known as *o*-nitrotolans) provides a simple route to isatogens bearing mainly aryl, arylcarbamyl or

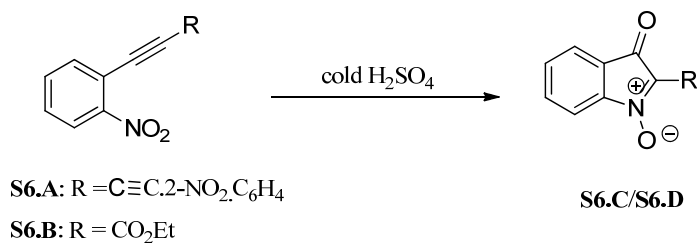
alkoxycarbonyl substituents in the 2-position under different conditions¹⁶ (Scheme 5). The different conditions used for cyclization of 2-nitrophenylacetylene for isatogen synthesis are discussed below.



Scheme 5: Reagents/Conditions Employed for the cyclization of 2-o-nitrotolans

i) Sulphuric Acid

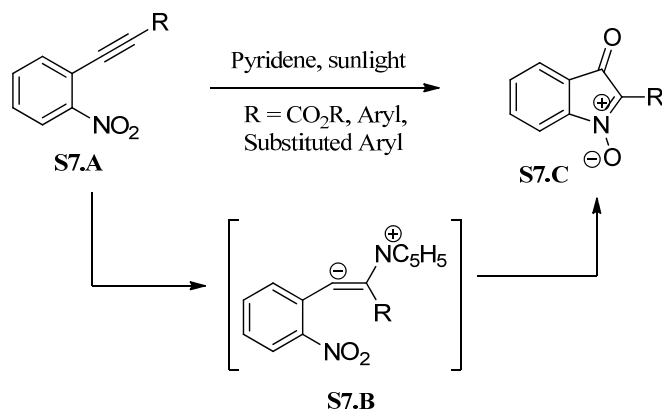
The inaugural synthesis of isatogens was reported by Baeyer¹⁴ using sulphuric acid mediated nitroalkyne cyclization. Compound **S6.A** and **S6.B** on treatment with cold concentrated sulphuric acid, cyclizes to the corresponding isatogens (Scheme 6).



Scheme 6

ii) Pyridine and Sunlight

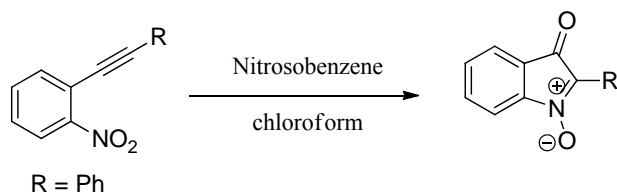
When pyridine solution of 2-nitrophenylacetylenes was exposed to sunlight, the corresponding isatogens²⁰ were obtained in good to moderate yields (Scheme 7). Huisgen suggested the reaction mechanism through the formation of the betaine **S7.B** as a key intermediate. Although the mechanism seems to be reasonable it lacks experimental support, as none of the proposed intermediates have been isolated or trapped.



Scheme 7: Pyridine and light mediated isatogen synthesis

iii) Nitrosobenzene and Chloroform

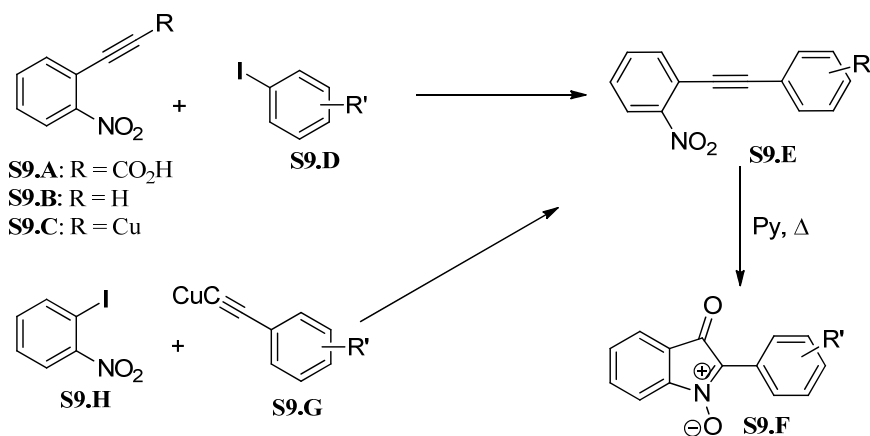
Alessandri and Ruggli²¹ found that chloroform solution of 2-nitrophenylacetylenes in the presence of nitrosobenzene formed isatogens in the absence of light. The reaction is very slow (take several days for completion) which can be reduced to 2 hours by simply heating the reaction mixture (Scheme 8).



Scheme 8

iv) Pyridine and Heat

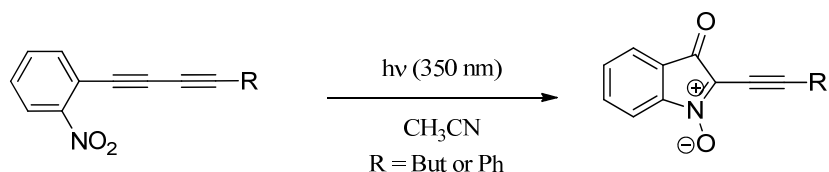
The Castro and Stephens²² method for the preparation of unsymmetrical disubstituted acetylenes involves the reaction of copper (I) acetylides with aromatic iodo compounds. Bond and Hooper extended this route to the synthesis of 2-arylisatogens. The reaction involves the formation of acetylene **S9.B** by the decarboxylation of 2-Nitrophenylpropionic acid (**S9.A**) (Scheme 9).²³ Compound **S9.B**, on treatment with CuCl gives **S9.C** which, on reaction with aromatic iodo compounds under pyridine and heating conditions gives the corresponding isatogens (**S9.F**) the formation of acetylene intermediates **S9.E**. The alternative route (**S9.H** + **S9.G** → **S9.E**) has been used very little.



Scheme 9: Isatogen synthesis using pyridine in heating condition

v) Irradiation of Nitroalkyne

Photocyclization of *o*-nitrophenyl-1,3-butadiynes provided a simple, clean and efficient synthetic method for the synthesis of isatogen derivatives in a very short reaction time.²⁴ The reaction can be carried out in various solvents and the starting

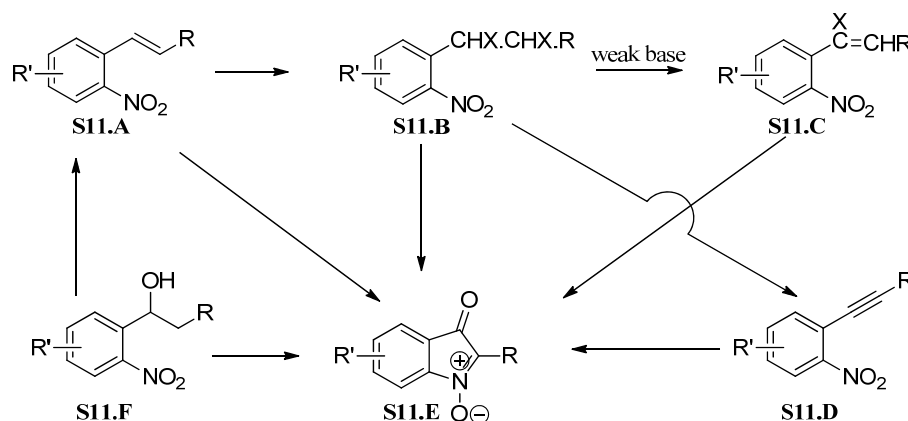


Scheme 10

material can be quantitatively converted into isatogen derivatives (Scheme 10).

1.2.3.1.2. From stilbenes and their derivatives

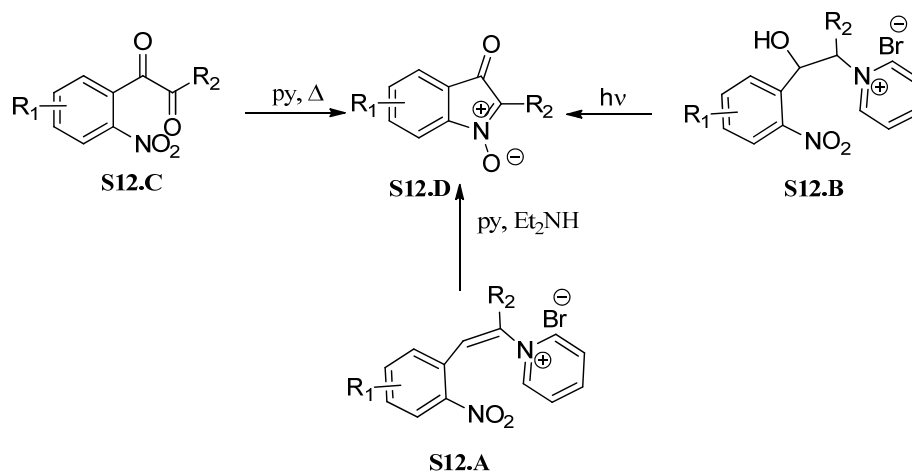
The addition of halogens to stilbenes (**19**) gives stilbene dihalides (**20**), which on treatment with strong base furnished the 2-nitrophenylacetylene which subsequently isomerized to form isatogens.²⁵ Only the *trans*-stilbenes undergo this reaction (Scheme 11). Compounds **11.B**, **11.C** on exposure to sunlight in the presence of pyridine slowly converted into isatogens. Stilbenes with strongly electron-withdrawing groups (4-NO₂, 4,6-di-NO₂ etc) cyclized to isatogens even in the absence of a base.



Scheme 11: Synthesis of isatogens from stilbenes

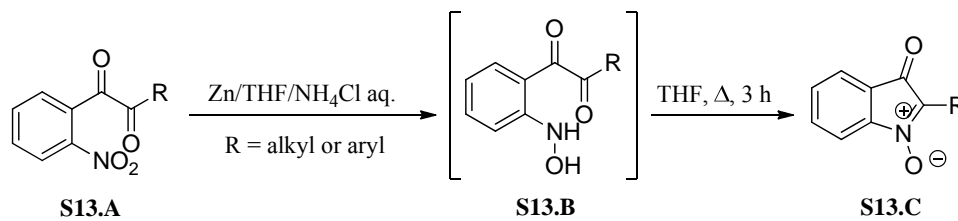
1.2.3.1.3. Miscellaneous intramolecular cyclization reaction

Isatogen syntheses which may be mechanistically related to the o-nitrophenylacetylene cyclizations involve the base-catalyzed conversions of o-nitrostyrylpyridinium salts (**S12.A**) into the 2-arylisatogens (**S12.D**) (Scheme 12). Either sodium carbonate or pyridine in combination with diethylamine can be used as the base, the former giving the best yields though the use of the latter is more convenient in practice. Similarly, the hydroxy compound **S12.B** in the presence of light affords 2-phenylisatogen.²⁶



Scheme 12

Reductive cyclization of 2-nitrobenzyl (**S13.A**) was reported to give the isatogen **S13.C** via the intermediate hydroxylamino compound **S13.B**.²⁷ This method can be used for the synthesis of both aryl as well alkyl substituted isatogens.

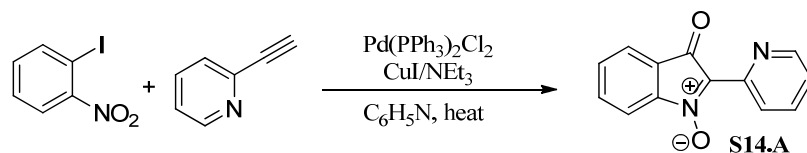


Scheme 13

1.2.3.3. Transition metal catalyzed Nitroalkyne cycloisomerization

1.2.3.3.1 Rosen's synthesis of Isatogen

Recently, transition metal catalyzed cycloisomerization of 2-nitrophenylacetylene has been reported for the synthesis of isatogens. Rosen²⁸ *et al.* reported a one step synthesis of isatogen **S14.A** from 2-iodonitrobenzene and 2-ethynyl-pyridene under Sonogashira conditions and then heating in pyridine (Scheme 15). The yields reported are moderate and the role of [Pd] over the cyclization is not very clear.



Scheme 14: Rosen's isatogens synthesis

1.2.3.3.2 Yamamoto's isatogen synthesis

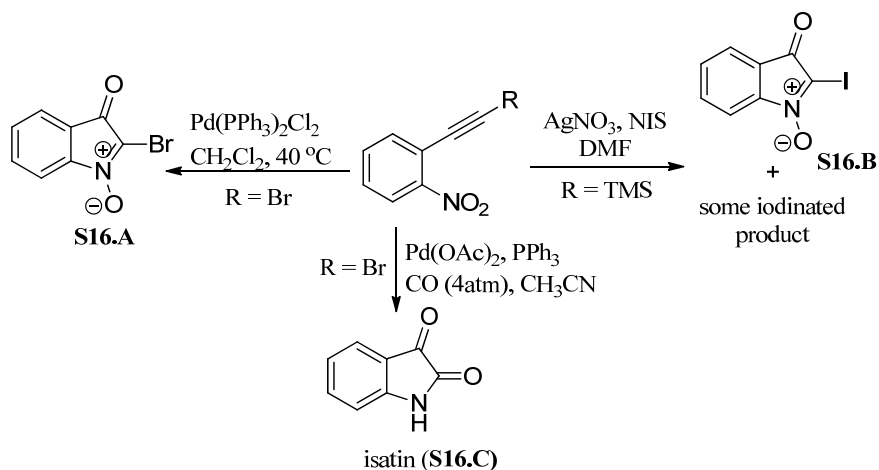
Yamamoto²⁹ et al. reported a substrate dependent gold(III) catalyzed synthesis of isatogens from 2-nitrophenyl acetylene. Interestingly, an aromatic group on the alkyne provides good yield of isatogens **S15.B** along with the anthranils **S15.C**, whereas alkyl substituent on alkyne gives predominantly the anthranil derivatives **S15.C** (Scheme 8).



Scheme 15: Yamamoto's isatogens synthesis

1.2.3.3.3 Söderberg's isatogen Synthesis

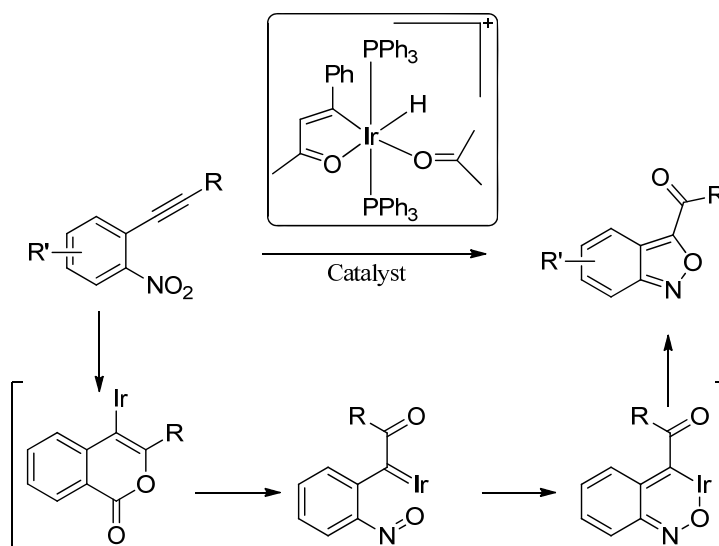
Later in 2009, silver and palladium catalyzed isatogen synthesis was reported by Söderberg³⁰ *et al.* (Scheme 16). 1-(Bromoethynyl)-2-nitrobenzene on treatment with Pd(II) in dichloromethane solvent at 40 °C gives the 2-bromoisatogen product **S16.A**. In contrast, the reaction of the same compound with carbon monoxide in the presence of a catalytic amount of palladium diacetate and triphenyl phosphine exclusively gave the isatin (Scheme 16). Trimethyl((2-nitrophenyl)ethynyl)silane on reaction with NIS in the presence of AgNO₃ in DMF solvent gives the corresponding 2-iodoisatogen. This method was selective for the alkynylhalides and was not generalized for the synthesis of alkyl or aryl isatogens.



Scheme 16: Söderberg's isatogen synthesis

1.2.3.3.4. Crabtree's nitroalkyne cycloisomerization

Crabtree³¹ and co-workers reported the formation of the anthranil derivative from iridium(III) hydride mediated nitroalkyne cycloisomerization (Scheme 17). This reaction was proposed to involve an analogous addition–elimination process to give an oxo-carbenoid, followed by 6e⁻ electrocyclicization to afford an N-bound anthranil complex. In this case, the role of the iridium(III) center has been regarded as that of a Lewis acid.



Scheme 17: Crabtree's anthranil synthesis

1.3. Spiroindolin-3-one

1.3.1. Structural features

The Spiroindolin-3-one (**F5.A**) unit, trivially known as the indoxyl unit, is an important structural feature or an advanced intermediate for many important biologically active natural products. The main importance of this structural unit is the easy formation of the 2,2-disubstituted indoxyl (**F5.B**) group by the simple Lewis acid catalyzed addition of nucleophile. The 2,2-disubstituted indoxyl is again an advanced intermediate for many natural products. For example: isatisine A, brevinamide, secoleuconoxin, mersicarpine, austamide, notoamide O.³² However, the chemistry of spiroindolin-3-one have not been well explored and only few methods have been reported in the literature for its synthesis. All the approaches reported in general involve either the oxidation of corresponding substituted indole or the intramolecular alkyl migration from the C3 to the C2 carbon of indole for constructing the indolinone unit. Below are the few synthetic efforts for the spiroindolin-3-one derivatives.

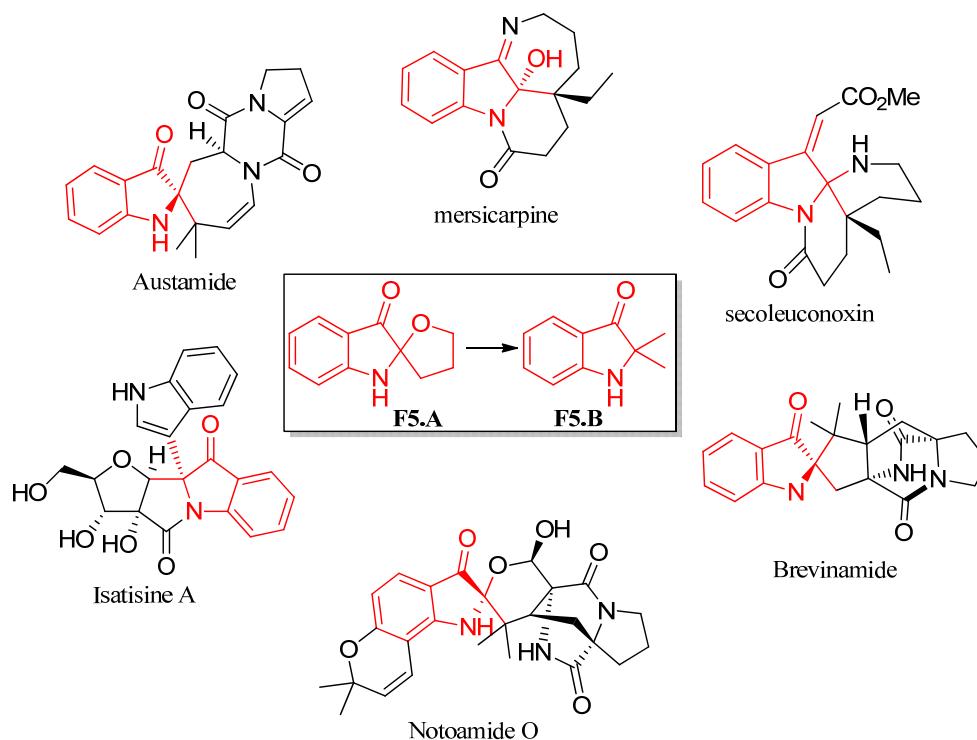
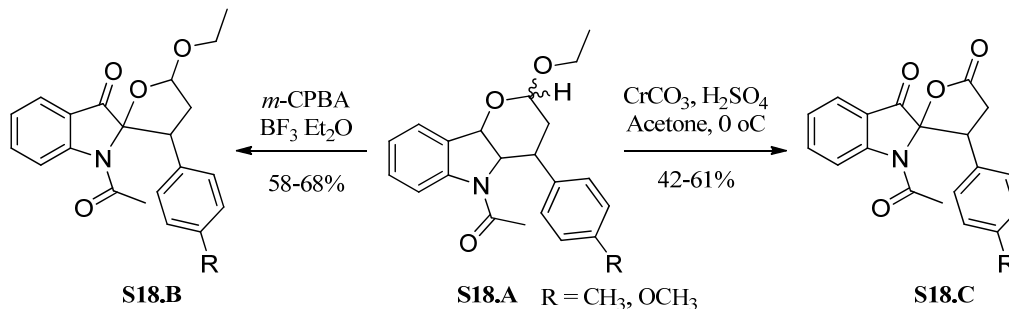


Figure 5: Natural products having pseudoindoxyl unit.

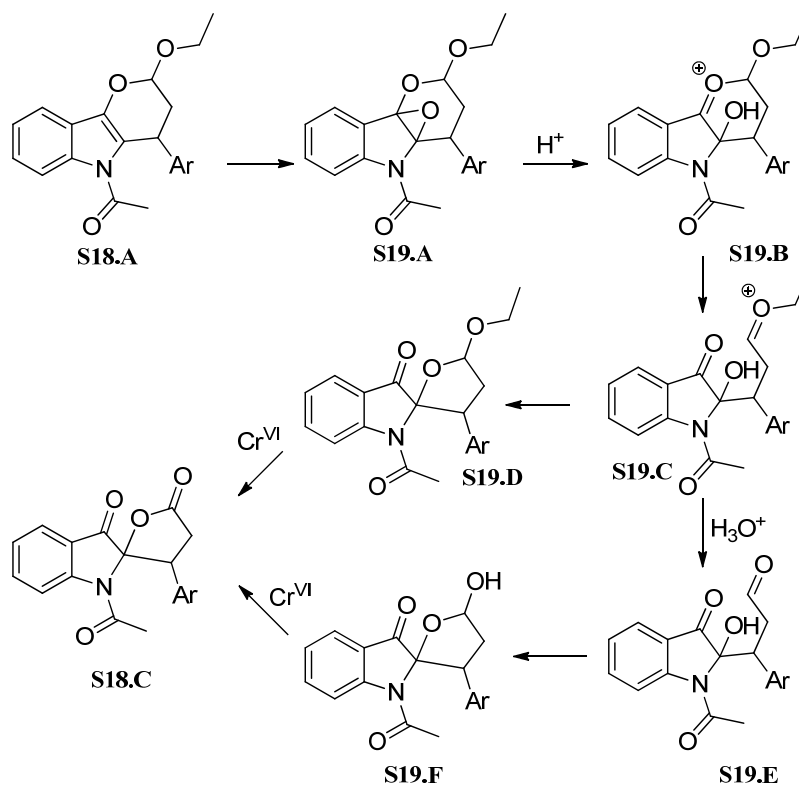
1.3.2 Synthesis of Spiroindolin-3-one

1.3.2.1 Mérou's approach



Scheme 18: Synthesis of spiroindolinone by Mérou group

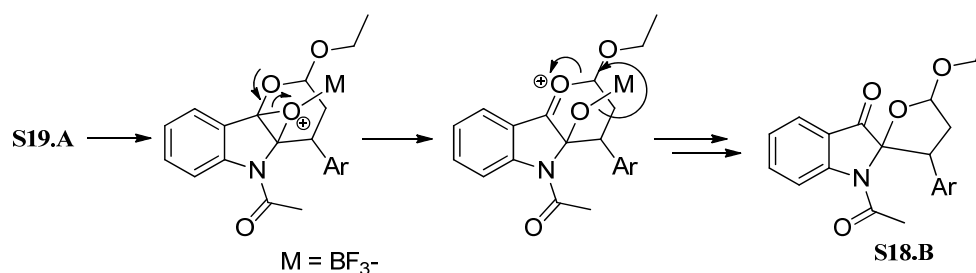
Mérou *et al.*³³ reported the oxidation of compound **S18.A** using Jones reagent to form spiro lactones **S18.C** or the oxo-acetals **S18.B** with *m*-CPBA/ $BF_3 \cdot Et_2O$. The results with Jones reagents were consistent with a mechanism (Scheme 19) involving initial epoxidation. The opening of the oxirane ring with a concomitant opening of the



Scheme 19: Possible mechanism for spiro lactone formation

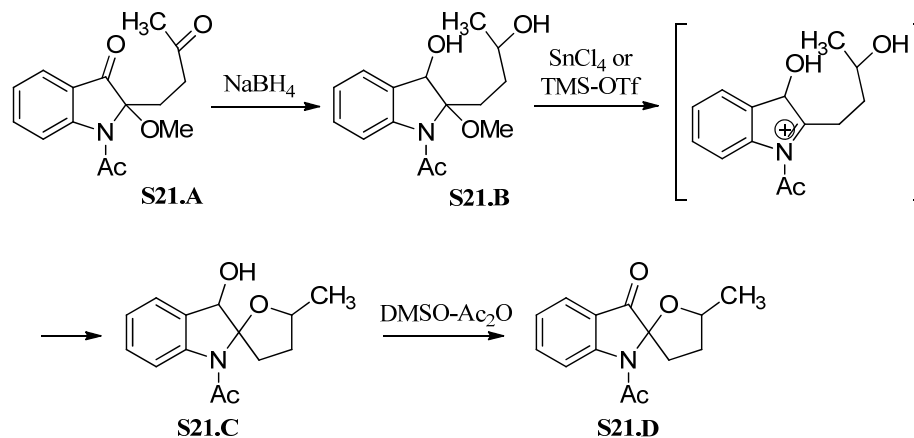
pyrano ring generates the intermediate oxonium ion (**S19.C**). The oxonium ion may give either the spiro compound **S19.D** which was further oxidized to the lactone **S18.C**; or a hydroxyaldehyde which afforded **S18.C** after an oxidation *via* its hemiacetal.

Similarly, the possible mechanism for the transformation of **S18.A** into **S18.B** will be - the epoxidation of the ethylenic bond followed by an intramolecular nucleophilic opening of the oxirane by the anomeric carbon to afford **S18.B** (Scheme 20).



Scheme 20: Possible mechanism for spiroindolinone formation

1.3.2.2 M. Sakamoto *et al.*

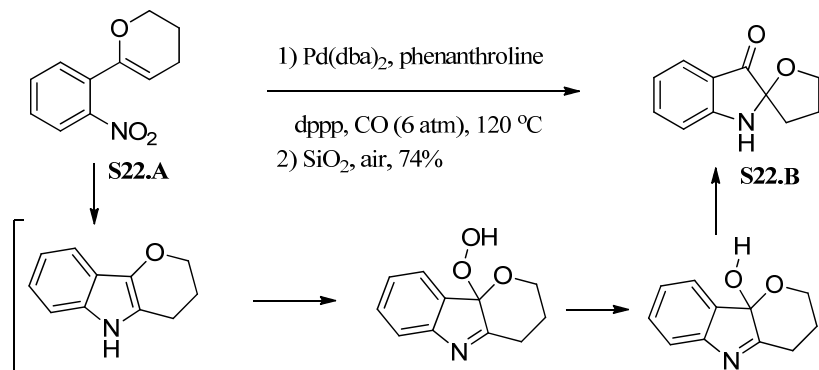


Scheme 21: Sakamoto approach for the synthesis of spiroindolinone derivatives

Sakamoto³⁴ *et al.* reported the synthesis of the spiroindolinone derivative from compound **S21.A**. Compound **S21.A** on reduction with sodiumborohydride gave the dihydroxy compound **S21.B** which, on treatment with SnCl_4 or TMS-OTf gave compound **S21.C**. Compound **S21.C**, upon oxidation gave the spiroindolinone **S21.D**.

1.3.2.3 B. C. G. Söderberg *et al.*

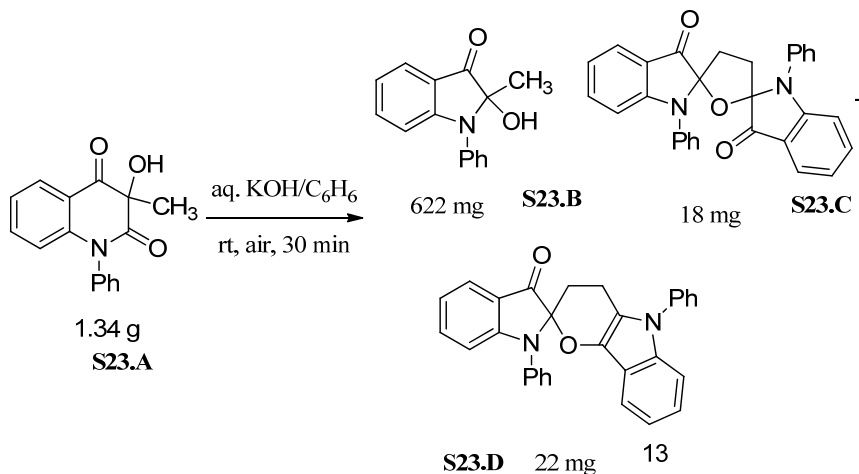
Söderberg³⁵ *et al.* report the formation of spiroindolinone **S22.B** from compound **S22.A**, *via* palladium-catalyzed reductive N-heteroannulation using carbon monoxide as the reducing agent.



Scheme 22: Söderberg approach for the synthesis of spiroindolinone derivatives

1.3.2.4 Janez Košmrlj *et al.*

In 2007, Košmrlj³⁶ *et al.* reported the formation and structure elucidation of

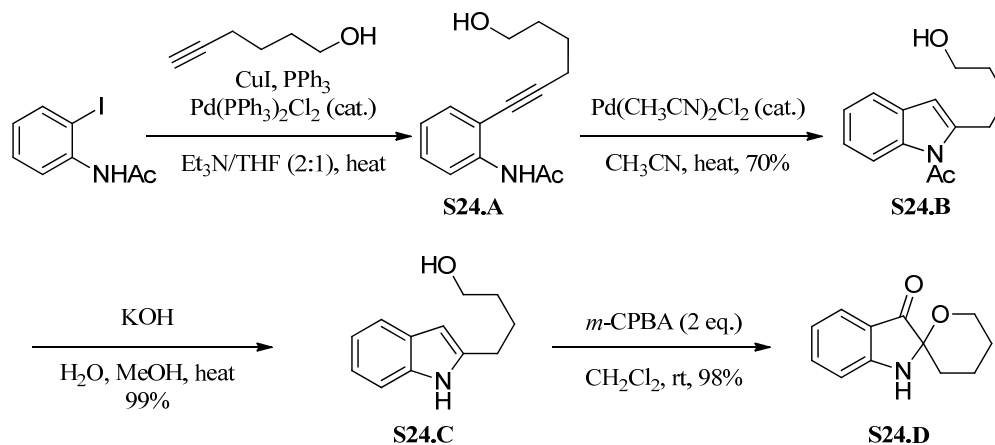


Scheme 23: Košmrlj approach for the synthesis of spiroindolinone derivatives

compound **S23.B** and **S23.D**, from compound **S23.A** on treatment with an aqueous KOH/benzene mixture under reflux conditions in the presence of air.

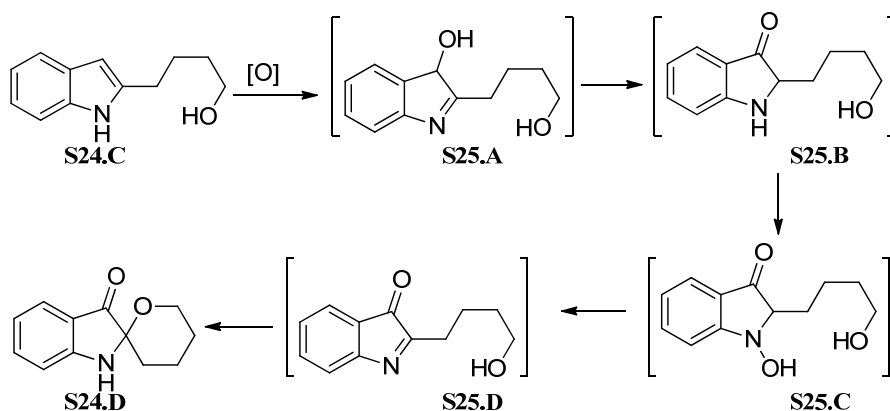
1.3.2.5 Yoshihisa Kobayashi *et al.*

In the course of synthetic studies towards lundurine A, Kobayashi³⁷ *et al.* discovered that oxidation of 2-(4-hydroxybutyl)indole **S24.C** with two equivalents of *m*CPBA in CH₂Cl₂ furnished indolinone spiro-*N,O*-ketal **S24.D** in excellent yield



Scheme 24: Kobayashi approach for the synthesis of spiroindolinone derivatives

(Scheme 24). The starting compound **S24.A** was prepared as shown in Scheme 24. A possible reaction mechanism of the one-pot oxidation could be as shown in Scheme 25. After initial oxidation of indole **S24.C** with *m*CPBA, facile Amadori rearrangement of 3-hydroxyindolenine **S25.A** gave the mono-substituted indolinone **S25.B**. The lack of substituents at the 3-position could avoid the undesired oxidative cleavage due to this rearrangement. The resulting indolinone **S25.B** was oxidized to **S25.C** by excess *m*CPBA and then dehydrated to give 2-substituted indolone **S25.D**. Finally, the butanol side chain at the 2-position of indolone **S25.D** trapped the imine to form the indolinone *N,O*-ketal **S24.D** without isomerization to an exocyclic unsaturated isomer. It was protected from further oxidation of nitrogen due to steric bulk of the adjacent quaternary center and electronic effects (*N,O*-ketal). The same reaction of 2-(4-acetoxybutyl)indole furnished a nitronone derived from indolone **S25.D** without spiro-ketal formation. This supports the suggested intermediates in the proposed reaction mechanism.



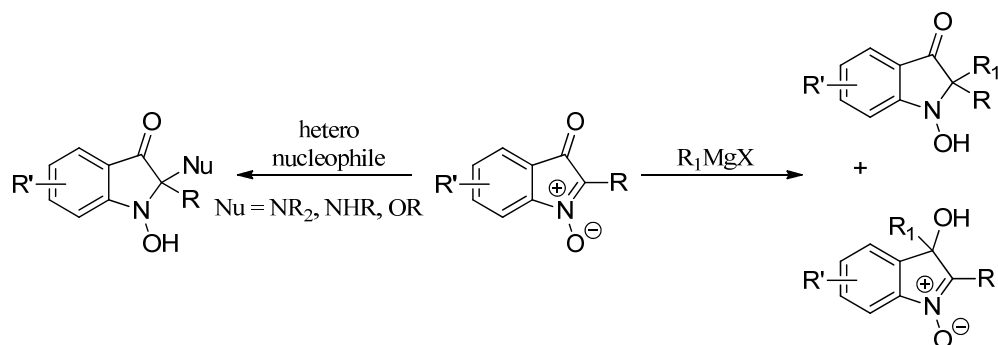
Scheme 25: Possible mechanism for spiroindolin-3-one formation by oxidation of indole

1.4. C(2) alkylation of isotogens/spiroindolin-3-one: synthesis of 2,2-disubstituted indolinone derivative

As per the retrosynthetic approach for Isatisine A, generation of 2,2-disubstituted indolinone intermediate should be through the C(2)-alkylation of either isotogens or spiroindolin-3-ones with indole. However, the addition of indoles to isotogens were not reported and while our work was in progress, the addition to spiroindolin-3-ones was reported by Kobayashi's group. Some of the reactions of isotogens and spiroindolin-3-ones are discussed in brief below.

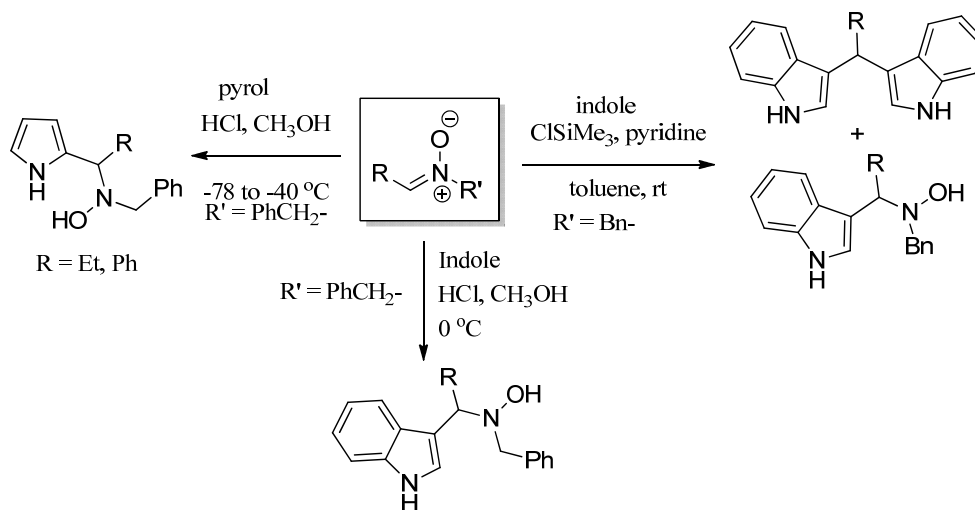
1.4.1. C(2)-alkylation of isotogens

Isatogens exhibit reactions characteristic of both nitrene and carbonyl groups. The carbon atom of the nitrene group is a much more reactive site, generally behaving as an electron-deficient centre. The reactivity of isotogens towards the nucleophiles has been documented: hetero atom centered nucleophiles are known to add at the C(2) of the nitrene unit³⁸ and the addition of carbon centered nucleophiles such as alkyl/aryl Grignard reagents are in general non-regioselective [C(2)/C(3)]³⁹ with the addition to the carbonyl carbon being the dominating reaction (Scheme 26).



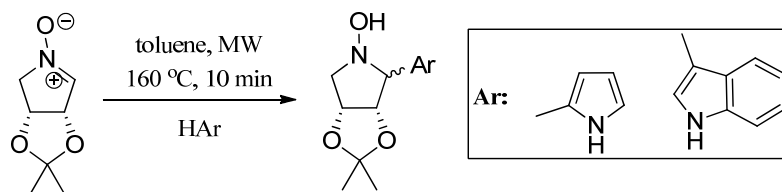
Scheme 26

Though the addition of indoles to isotogens has not yet been explored, the Friedel-Craft type alkylation of indoles with simple nitrones employing either Lewis acids or Brownsted acids have already been documented.⁴⁰ The reaction of nitrones with indoles in the presence of HCl gives indolyl N-hydroxylamines. In the presence of Me₃SiCl, symmetrical diindolylalkanes are obtained (Scheme 27). The addition goes mainly to the C(3) position of indole when it is free.



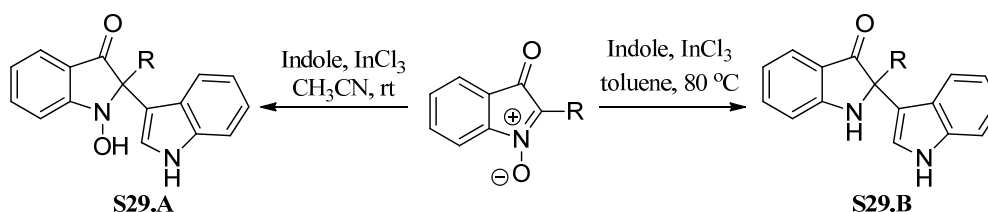
Scheme 27

Similarly, when pyraxone or even furans were used as a nucleophile in presence of HCl in methanol, the corresponding C(2) alkylated products were obtained. In general, the alkylation occurs at the C(3) position of indole, but if the C(3) position of indole is substituted, alkylation goes to the C(2) position (scheme 28).



Scheme 28: Alkylation of cyclic nitrones with indole or pyrrol

Recently in our group,⁴¹ an indium(III) chloride catalyzed Friedel-Crafts type alkylation of isotogens with indole has been studied in detail (Scheme 29). Treatment of isotogen with indole in acetonitrile solvent at room temperature gave the indole addition product **S29.A** with an N–OH group. On the other hand, the same reaction when carried out with 1.5 eq. of indium chloride in toluene at 80 °C gave the 2,2'-spiroindolin-3-one **S29.B** due to the addition and reduction of the N–O bond.



Scheme 29: Friedel-Crafts alkylation of isotogens with indoles

1.4.2. C(2)-Alkylation of spiroindolin-3-ones

Despite having important synthetic utility, the chemistry of spiroindolin-3-one has not been well explored so far. Kobayashi *et al.* reported the first Lewis acid mediated C(2) alkylation of spiroindolin-3-one, which allowed the construction of the nitrogen-containing quaternary center of a 2,2-disubstituted indolin-3-one through a

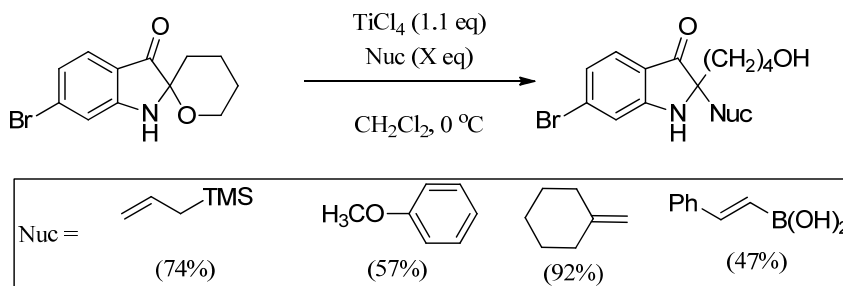
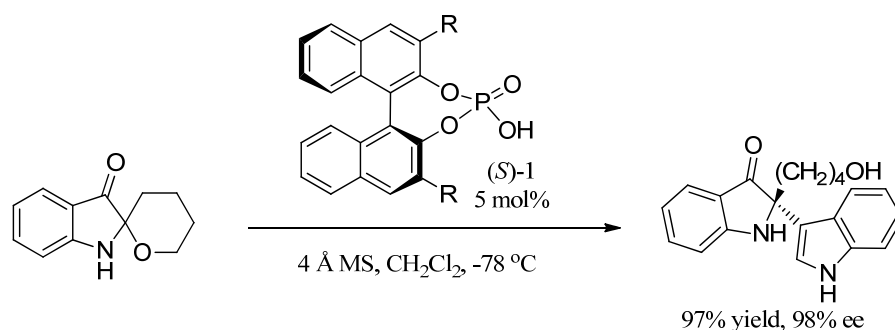


Table 1: Other nucleophiles for the synthesis of indolin-3-ones

Mannich-type reaction. After screening different Lewis acids, TiCl_4 has been selected as a suitable reagent for the alkylation with different nucleophiles (Table 1).

Very recently, when we had already established a method for the alkylation of indole to spiroindolin-3-one, Shu-Li You *et al.* reported a chiral phosphoric acid catalyzed alkylation of spiroindolin-3-one with indole to get the enantioselective alkylated product (Scheme 30). The reaction with 5 mol% (S)-TRIP and 4 Å MS in dichloromethane at $-70\text{ }^\circ\text{C}$ led to the best combination of isolated yield and enantioselectivity.



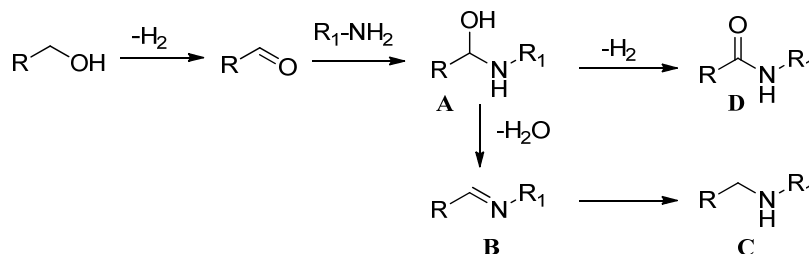
Scheme 30: *Asymmetric Friedel–Craft reaction of spiroindolin-3-one with indole*

From the above discussion, it is clear that the nucleophilic addition reaction with isotogen seems to occur mainly at the C(2) carbon rather than the carbonyl carbon. Similarly, the Lewis acid mediated alkylation of spiroindolin-3-one goes to the C(2) position. However the chemistry of spiroindolin-3-one is not well explored.

1.5. Oxidative amide synthesis directly from alcohols with amines

The amide bond is one of the most important linkages in organic and biological chemistry. Amides are usually prepared by the coupling of carboxylic acids and amines by the use of either a coupling reagent or by prior conversion of the carboxylic acid into an active derivative. Alternative procedures include the Staudinger ligation, aminocarbonylation of aryl halides and oxidative amidation of aldehydes.⁴² However, all these methods require stoichiometric amounts of reagents employed and result in equimolar amounts of byproducts. In special cases, amides can be formed by catalytic procedures such as the Schmidt reaction between ketones and

azides, the Beckmann rearrangement, and the amidation of thioacids with azides. The transition metal catalyzed oxidative coupling of alcohols and amines leading to amides (Scheme 31) is one of the contemporary reactions and has been identified as an atom economical and environmentally benign method for the amidation. The reaction path involves the initial oxidation of alcohol to the corresponding aldehyde that reacts with an amine to produce a hemiaminal intermediate (**A**). There are two possible further pathways for the hemiaminal—either it would form an imine (**B**), which could subsequently be hydrogenated to an amine (**C**) or would be further oxidized to the corresponding amide (**D**). The pathway of the dehydration and the hydrogenation of **A** and the overall alkylation of the amine has been extensively reported.⁴³ Recent examples have shown that further dehydrogenation of **A** producing amides can be achieved instead, depending on the nature of catalysts, ligands, and substrates.



Scheme 31: Direct amide synthesis from alcohols and amines

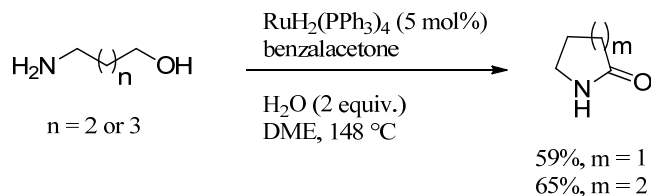
1.5.1. Literature report for oxidative amide bond formation

Oxidative amide synthesis from alcohols and amines is mainly promoted through homogeneous catalysts using Ru- and Rh- based complexes. A heterogeneous Ag-based catalyst was recently reported.

1.5.1.1. Ru-based catalytic systems

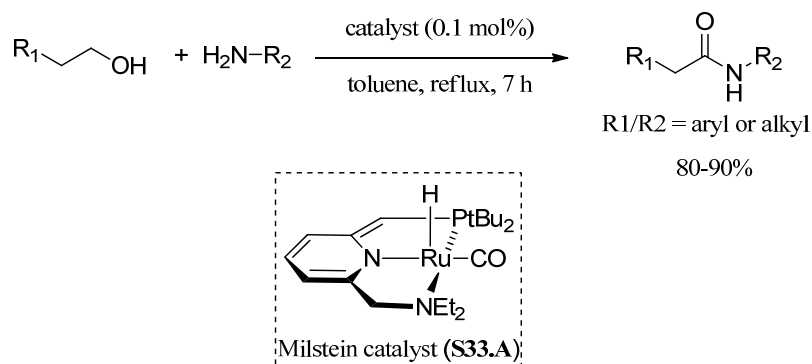
In 1991, Murahashi and Naota reported the first example of the reaction by synthesizing lactams with 1,4- and 1,5-amino alcohols in an intramolecular amidation process (Scheme 32).⁴⁴ Using $\text{RuH}_2(\text{PPh}_3)_4$ as a catalyst and a hydrogen acceptor such as benzalacetone, lactams were formed in good yields. When the reaction was run without the hydrogen acceptor, only cyclic amines were obtained. Two equivalents of

water had to be added so as to avoid the formation of cyclic amines if there was a primary amine group in the amino alcohol, while addition of water was not required in the case of amino alcohols bearing a secondary amine group.



Scheme 32

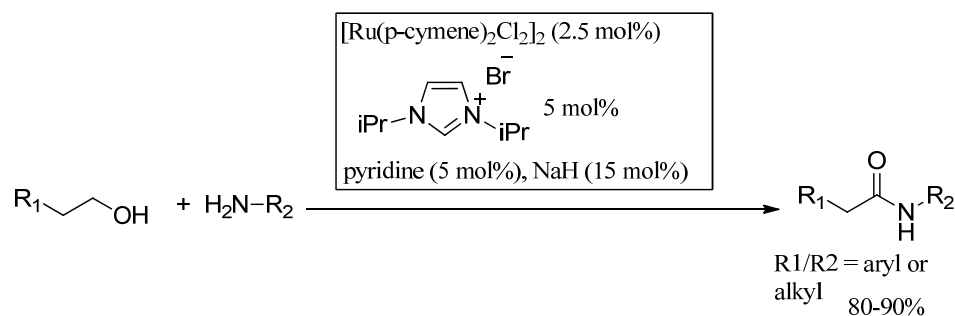
Recently, the Milstein group employed a Ru PNN pincer complex **S33.A** for the direct amide synthesis from alcohols and primary amines without any base, acid promoter or hydrogen acceptor (Scheme 33).⁴⁵ It was the first example of allowing the direct amidation of alcohols with amines in an intermolecular fashion. To facilitate the removal of hydrogen gas, the reactions were carried out under a flow of argon. Excellent yields for sterically non-hindered substrates and slightly reduced yields for moderately hindered substrates were obtained.



Scheme 33

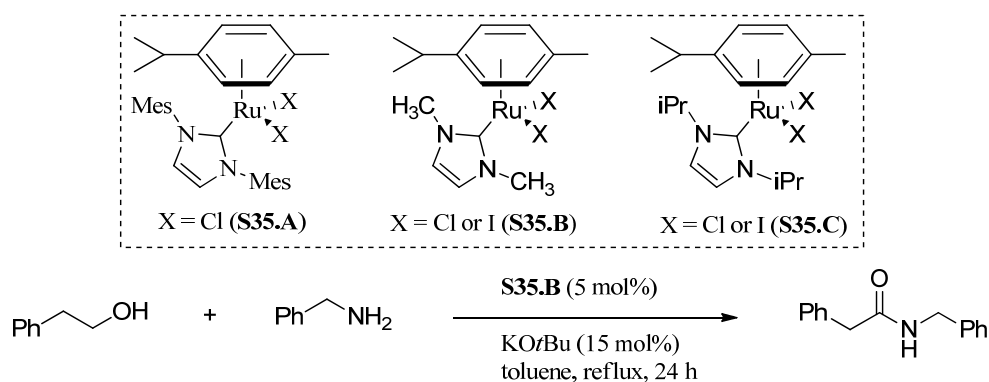
Phosphine-free ruthenium catalytic systems for effective amide synthesis from alcohols and amines were also reported by Hong and coworkers.⁴⁶ The catalytic systems consist of $[\text{Ru}(p\text{-cymene})\text{Cl}_2]_2$ or $[\text{Ru}(\text{benzene})\text{Cl}_2]_2$, an NHC precursor, pyridine or acetonitrile, and NaH as a base (Scheme 34). Sterically non hindered substrates worked smoothly and moderately hindered ones reacted reasonably well.

Limited yields were found for the sterically bulky substrates such as neopentyl alcohol.

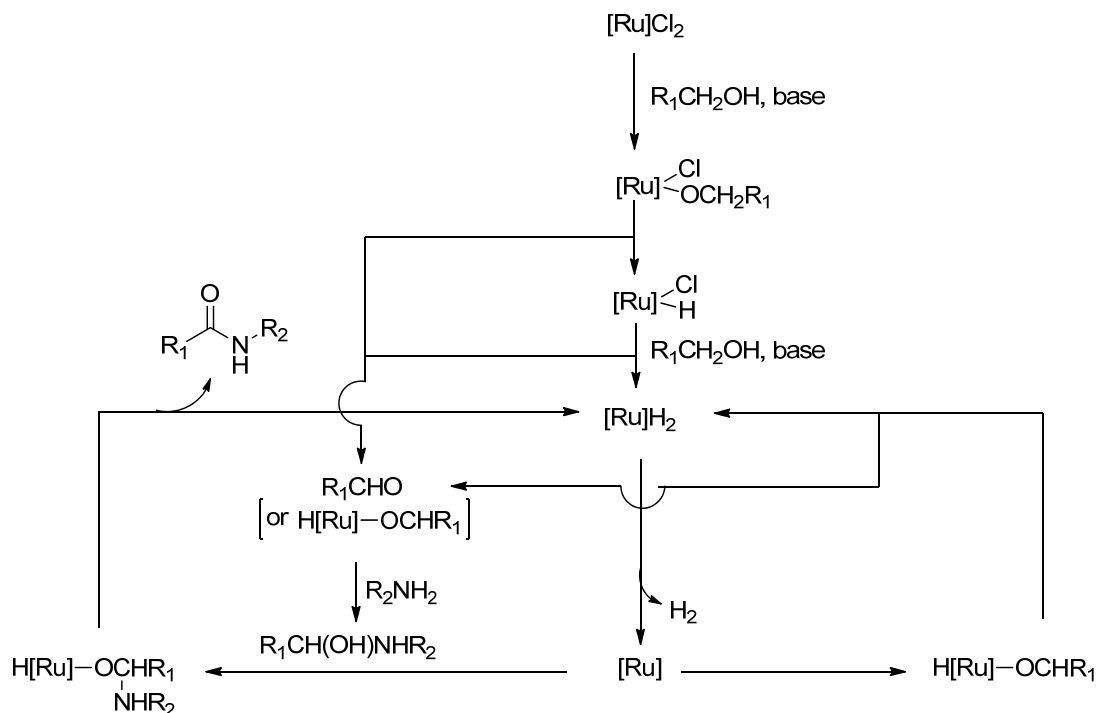


Scheme 34

Based on the reported phosphine-free *in situ* NHC-based Ru catalysts, the Hong group investigated complexes **S35.A–S35.C** (Scheme 35) as pre-catalysts for the direct amide synthesis.⁴⁷ When the activity was screened only with the NHC-Ru complexes, there was no formation of the amide from 2-phenylethanol and benzylamine. It was found that at least 2 eq. of a strong base *versus* the pre-catalyst is necessary for the catalytic cycle to proceed. A higher amount of the base was detrimental to the catalytic activity, suggesting that the role of the base is related to the activation of the pre-catalyst.



Scheme 35: Hong's method for amide synthesis



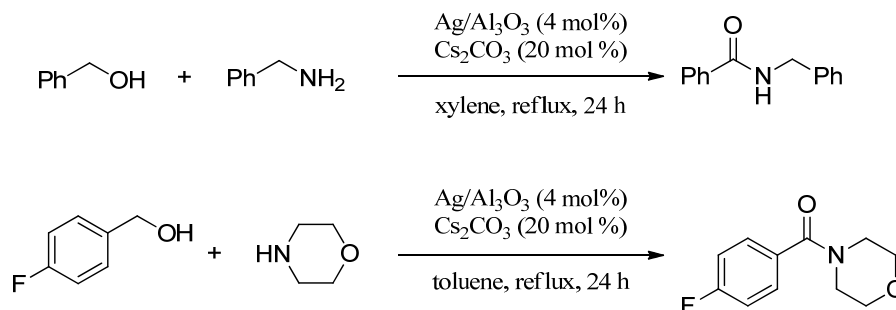
Scheme 36: possible mechanism for $[\text{Ru}]$ mediated amide formation

A mechanism involving a $\text{Ru}(0)/\text{Ru}(\text{II})$ cycle was proposed on the basis of the investigation (Scheme 36), especially elucidating the reason why free aldehyde was not so active under the reported catalytic systems—less efficient formation of active $[\text{Ru}]\text{H}_2$ from $[\text{Ru}]\text{Cl}_2$ and an aldehyde without the help of a primary alcohol.

1.5.1.2. Ag-based heterogeneous catalyst

A heterogeneous Ag-based catalyst for the direct amidation of alcohols with amines was reported by Shimizu and coworkers (Scheme 37).⁴⁸ The alumina-supported silver cluster with Cs_2CO_3 was active for the amide synthesis with primary amines, cyclic secondary amines, and less sterically hindered non-cyclic secondary amines such as N-benzylmethylamine. Mechanistic investigations suggested that the reaction goes through an aldehyde-like species that was adsorbed on the catalyst, as there was no amide formation from an ester, a free aldehyde, or imine. Subsequent attack on the aldehyde-like species by an amine afforded the hemiaminal, and then the amide was formed after hydride elimination by the silver cluster. Based on these

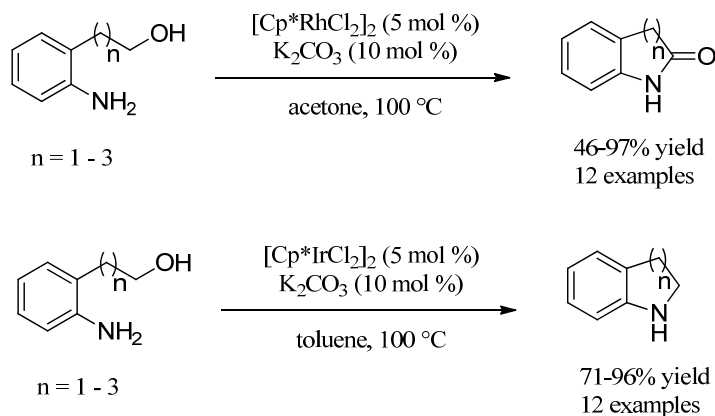
kinetic studies, C–H cleavage of the alkoxide or hemiaminal by the silver cluster was proposed as the rate-determining step.



Scheme 37

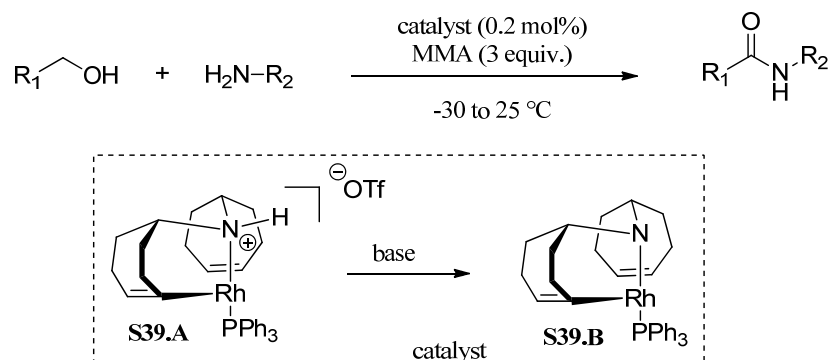
1.5.1.3. Rh-based catalytic systems

Fujita, Yamaguchi and coworkers reported the first Rh-based catalyst system, using $[\text{Cp}^*\text{RhCl}_2]_2$ and K_2CO_3 in acetone, for the lactamization of amino alcohols.^{49a} This catalytic system is active for the synthesis of five-, six- and seven-membered benzofused lactams. Acetone was used as a hydrogen acceptor as well as the solvent. A rhodium hydride species generated by the β -hydrogen elimination of alkoxide was also proposed as an active catalytic intermediate similarly to the Ru catalysts. It was also noted that selective synthesis of *N*-alkylated or lactamized products from the same amino alcohols can be achieved by altering catalytic systems— $[\text{Cp}^*\text{IrCl}_2]_2$ in toluene for *N*-alkylation^{49b} or $[\text{Cp}^*\text{RhCl}_2]_2$ in acetone for lactamization (Scheme 38).



Scheme 38

A Rh-based catalyst **S39.B** for intermolecular amide synthesis was developed by Grützmacher and co-workers (Scheme 39).⁵⁰ A hydrogen acceptor such as methylmethacrylate (MMA) was required to generate primary and secondary amides in excellent yields. The reaction occurs under much milder conditions than with the Ru-based catalyst systems, even at room temperature. This method has good functional group tolerance and chemoselectivity with low catalyst loading. The amido function in **S39.B** is the Lewis basic site which may be crucial for the catalytic cycle. A computational study illustrated that the rhodium monohydride species is an important intermediate in the whole cycle. Notably, this was the first example of the synthesis of primary amides directly from primary alcohols and ammonia.



Scheme 39

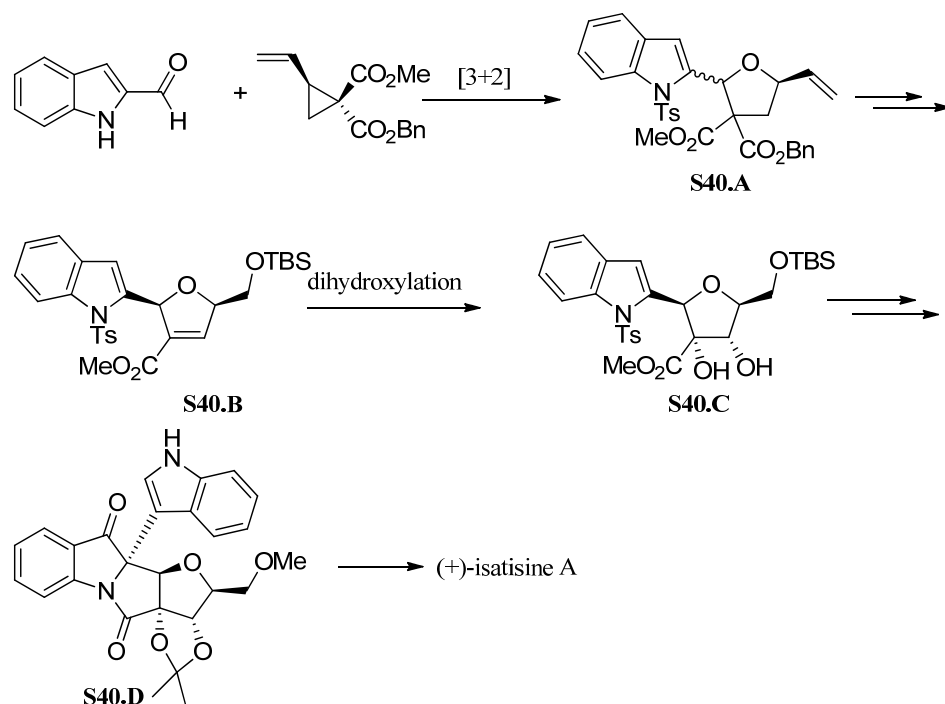
1.6. Literature reports on Total synthesis of Isatisine A

During our study on the total synthesis of Isatisine A, four reports for the total synthesis of Isatisine A,⁵¹ were published from different groups, which are briefly discussed below.

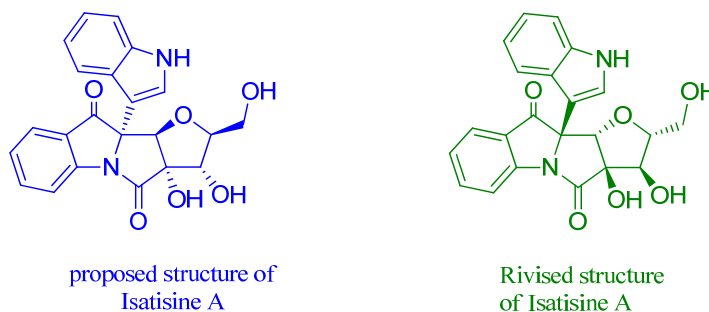
1.6.1. First total synthesis of (+)-Isatisine A and structural reassignment

Kerr *et al.* reported the first total synthesis of Isatisine A,⁵¹ which commenced with the key Johnson tetrahydrofuran synthesis⁵² using the indole-2-carboxaldehyde and the homo-chiral (*S*)-vinylcyclopropane diester under the catalytic influence of Sn(OTf)₂ (Scheme 40) to obtain the tetrahydrofuran derivative **S40.A** in 89% yield as an 11:1 mixture of the 2,5-cis:2,5-trans (furan numbering) isomers. Compound **S40.A** on functional group manipulation converted into the required diol compound **S40.C**.

On treating compound **S40.C** with *m*CPBA the 2:1 epimeric mixture of ainals was obtained, which on



treatment with indole and camphorsulfonic acid resulted in a 3:1 ratio for the indole addition product. Keeping the reaction for a long time resulted in the formation of the Isatisine A acetonide derivative **S40.D** in one pot up to 50% yield. The deprotection

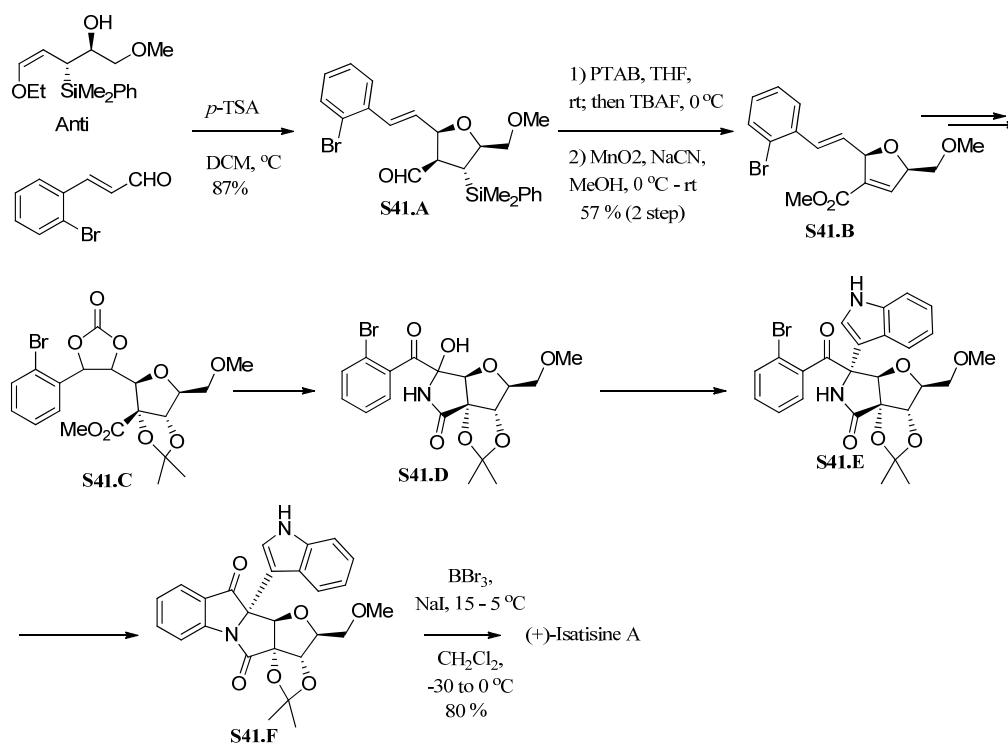


of the acetonide moiety gave Isatisine A. The specific rotation of the synthetic acetonide and isatisine A (**1**) were $[\alpha]_D^{25} = +271$ and $[\alpha]_D^{25} = +274$, respectively, which is essentially equal and opposite to that reported in the isolation paper ($[\alpha]_D^{25} =$

-283 ($c = 0.46$, MeOH)). Since the synthesized product is C2(*R*), C9(*S*), C10(*R*), C12(*S*), C13(*S*), the natural product must be C2(*S*), C9(*R*), C10(*S*), C12(*R*), C13(*R*) which is antipodal to the structural depictions in the isolation paper.

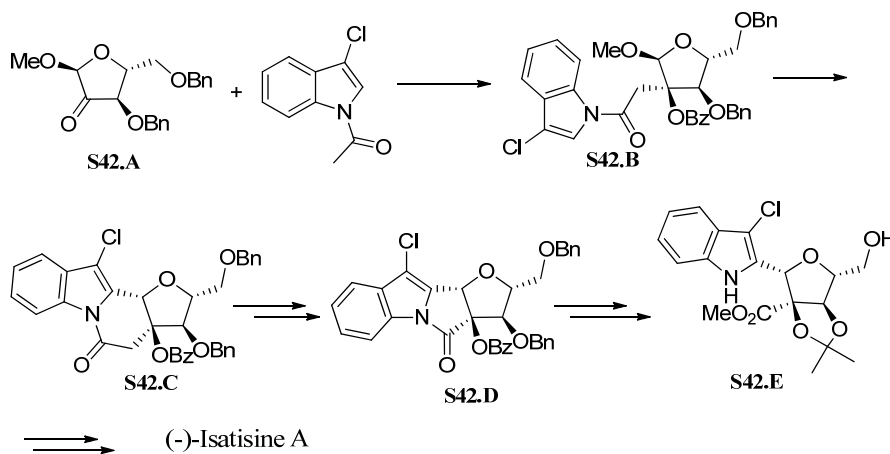
1.6.2. Total Synthesis of (+)-Isatisine A by Panek *et. al.*

Pank's approach^{51c} for the total synthesis of Isatisine A was based on the application of the silyl-directed Mukaiyama-type [3 + 2]-annulation for the preparation of the fully substituted furan core **S41.A**. The indole branch forming the quaternary carbon center at C2 was constructed by addition to an intermediate N-acyliminium ion derived from aminal. Finally, the fused tetracyclic framework including furan core **S41.F** was built up using modified Buchwald amidation conditions. One pot demethylation and acetonide deprotection under BBr₃ and NaI condition afford Isatisine A.



Scheme 41: Panek's approach for total synthesis of Isatisine A

1.6.3. Total Synthesis of (-)-Isatisine A by Liang *et. al.*



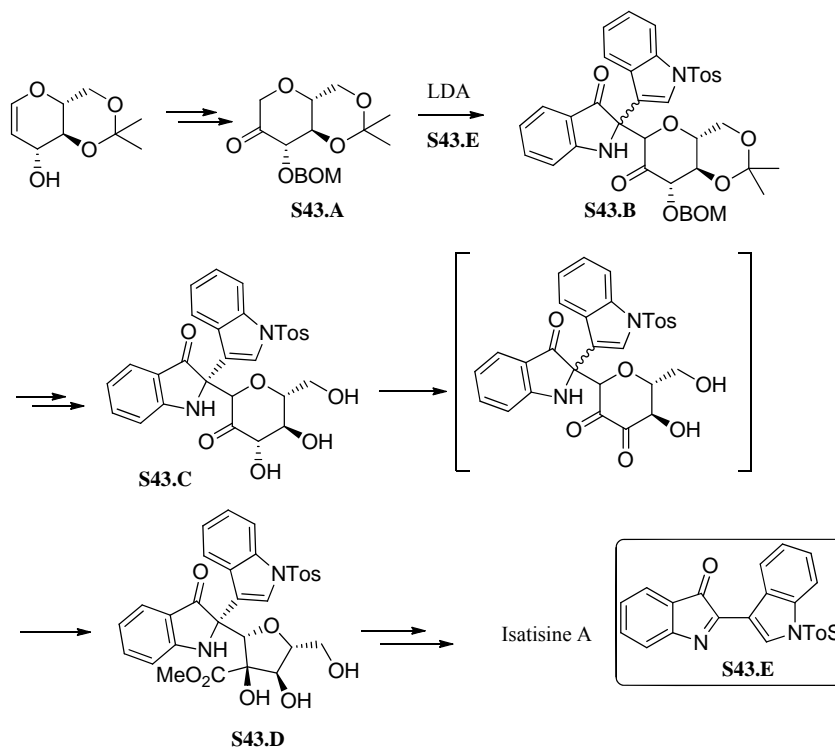
Scheme 42: Liang's synthesis of Isatisine A

Liang *et. al.* reports the chiral pool approach^{51d} for the synthesis of Isatisine A from compound **S42.A**. The synthesis commenced with the aldol reaction of **S42.A** with acetylindole to give compound **S42.B**. Intramolecular C-glycosylation of compound during benzoyl protection of tertiary hydroxyl group followed by functional group manipulation leads to chloroindole derivative **S42.E**. Oxidation of the chloroindole moiety in **S42.E** with *m*CPBA following the reaction sequence of Kerr's group furnishes Isatisine A. The specific rotations of the synthetic Isatisine A obtained was $[\alpha]_D^{25} = -240 \text{ deg cm}^3 \text{ g}^{-1} \text{ dm}^{-1}$ ($c = 0.43 \text{ g cm}^{-3}$, MeOH) which is nearly equal to the isolated value ($[\alpha]_D^{25} = -283$ ($c = 0.46$, MeOH)).

1.6.4. Xie's approach for total synthesis of Isatisine A

In 2012, Z. Xie *et. al.* reported the biogenetic synthetic pathway toward (-)-isatisine A.^{51e} Based on the biogenetic pathway, the biomimetic total synthesis of (-)-isatisine A has been accomplished from 4,6-O-isopropylidene-protected glucal. The synthetic routes involve a nucleophilic addition and an unprecedented biomimetic benzilic ester rearrangement as key steps (Scheme 45). The first key reaction involves the coupling of **S43.A** and **S43.E** using LDA at $-78 \text{ }^\circ\text{C}$ to furnish compound **S43.B** which was then converted to **S43.C**. Compound **S43.C** on treatment with CuCl underwent tandem biomimetic oxidation and benzilic ester rearrangement to

compound **S43.D**. Finally, compound **S43.D** was converted to Isatisine A following the known procedure.



Scheme 43: Xie's synthesis of Isatisine A

From the above discussion it is clear that though isatogens are known from Bayer's time, a general method for their synthesis is still awaiting. Also, this is the same case with 2,2'-spiroindolin-3-ones, which have not yet got the popularity as the targets for the methodology development. According to the retrosynthetic strategy for we devised for the isatisine A total synthesis, our immediate concern was the development of methods for the substrate independent isatogens synthesis and a nitroalkynol cycloisomerization leading to spiro-*N*-hydroxy-indolinones. Once we have methods for these two skeletons, the next will be scouting for the suitable catalyst/reagents for the addition of indole to 2,2'-spiroindolin-3-one and for a suitable metal complex for the catalytic oxidative cyclization. In the following sections, a detail study regarding above issues have been discussed in details along with the realization of our ultimate target isatisine A.

RESULT & DISCUSSION

2.1. Palladium Catalyzed Nitroalkyne Cycloisomerization for Synthesis of Isatogens

Construction of architecturally complex molecules from simple building blocks has emerged as a powerful tool in synthetic organic chemistry because of the increasing demand for molecules with unprecedented diversity. Designing effective routes to construct complex cyclic structures through organotransition-metal catalyzed reactions provides many attractive possibilities, which, by conventional procedures, would need a large number of synthetic transformations. The formation of carbon-carbon and carbon heteroatom bonds are extremely important for the synthesis of biologically active natural products.⁵³ The use of transition metals, especially Pd, for the formation of C-C and carbon-hetero atom bonds have been extensively documented as demonstrated by numerous reviews and books.⁵⁴ The great interest in palladium catalysis stems from the fact that they often provide greater chemo, regio and enantioselectivity, tolerate a wide range of functional groups and relatively inexpensive in comparison to the traditional organic synthetic routes. For many years, Pd-catalyzed reactions have served as one of the most reliable and versatile methods for the synthesis of organic compounds.⁵⁵ In particular, great attention has been given to Pd-catalyzed ring-forming processes.⁵⁶ Our group has been interested in the development of new Pd-catalyzed cyclization methods for the synthesis of functionalized heterocyclic compounds from relatively simple and readily accessible starting materials.⁵⁷ The discussion below describes substrate independent Pd-catalyzed nitroalkyne cycloisomerization process which result in the formation of isatogens.

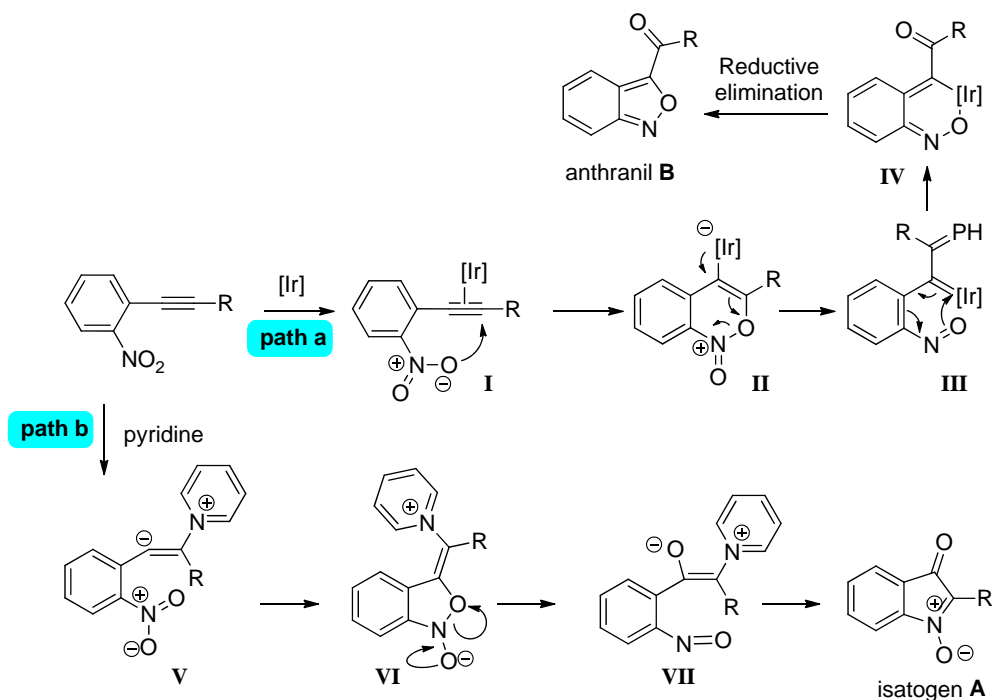
2.1.1 Concept of Nitroalkyne Cycloisomerization

The inaugural report of Bayer in 1881 on the cycloisomerization of *o*-nitrophenylpropiolates documented the first synthesis of isatogens.¹⁴ To address the harsh reaction conditions employed initially, several approaches have been put forward to facilitate the nitro-alkyne cycloisomerization.¹⁶ Amongst these, the base mediated cycloisomerization of (*o*-alkynyl)-nitrobenzene derivatives (trivially known as *o*-nitrotolans) under photochemical or thermal conditions has conventionally been

employed for the synthesis of isatogens²⁰⁻²³ (Scheme 5). However, all the above mentioned methods and the other methods generally employed for isatogen syntheses involve either harsh reaction conditions, prolonged reaction times or are substrate dependent. Also, the functional units at the C(2)-position of reported isatogens are limited mainly to aryl groups and reports dealing just with C(2)-alkyl groups are scarce.^{23b, 26c} It has been recently reported that the nitro-alkyne cycloisomerization can also be effected under mild conditions by gold (III) bromide or an iridium hydride complex. However, the outcome of the cyclization is dictated by the nature of the alkyne substituent.²⁹ For instance, *o*-(arylalkynyl)-nitrobenzenes were seen to give a mixture of isatogens **A** and anthranils **B** in the presence of catalytic amounts of gold bromide, whereas anthranils were formed exclusively from *o*-(alkylalkynyl)-nitrobenzenes with gold bromide²⁹ or with an iridium hydride³¹ complex. Thus, the available catalytic transition metal protocols which are compatible only for the 2-aryl isatogens synthesis have serious limitations for the synthesis of isatogens with 2-alkyl substituents. Developing a widely applicable catalyst that promotes the nitro-alkyne cycloisomerization leading selectively to isatogens will be the major bottle-neck in our program, since the advanced intermediate that we employ for this cycloisomerization is going to have a furanosyl unit, with its hydroxyl groups being protected differently.

In order start in this direction, we have initially examined the mechanisms that have been proposed for complementary nitro-alkyne cycloisomerizations i. by Huisgen²⁰ for the pyridine mediated formation of isatogen under photochemical conditions and ii. that by Crabtree³¹ given for the anthranil formation with the [Ir]-hydride complex. The given mechanism for anthranil formation involves the initial nucleophilic attack of one of the oxygens of the -NO₂ group on the β -carbon of the metal co-ordinated triple bond in an 6-*endo* fashion which subsequently leads to a metal carbene intermediate **III** after the initial oxygen transfer through an internal redox process. This iridium carbene can then undergo a Cope-like rearrangement to yield an iridium vinyl; followed by C-O reductive elimination to afford the iridium-anthranil complex **IV**. In the pyridine mediated isatogen synthesis, pyridine acts as a nucleophile, and assists in the formation of intermediate **VII** via the 5-*exo* transfer of oxygen (Scheme 44) through the initial formation of a betaine **V** and its addition

across the nitro unit leading to the nitronate **VI**. The intermediate **VII** then undergoes an intramolecular cyclization and subsequent elimination of the pyridine to form the

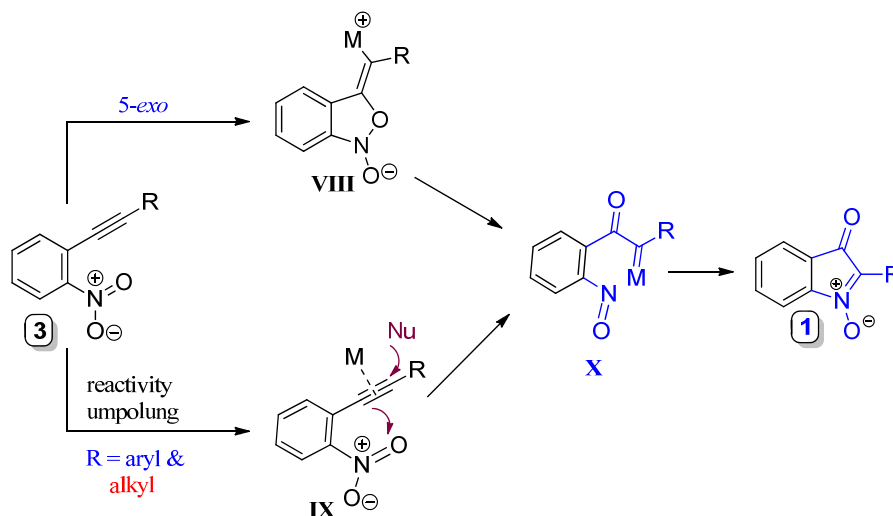


Scheme 45: Carbtree mechanism for anthranil formation (path a) and Huisgen mechanism for isatogen synthesis from nitroalkyne cyclization (path b)

isatogen unit. It was clear from the above-mentioned mechanisms that they differ fundamentally on how the $-\text{NO}_2$ group participates in the cyclization – does it act like a nucleophile or an electrophile? The outcome of the nitroalkyne cycloisomerization and product formation i.e either isatogen or anthranil, depends on the mode of oxygen transfer from the nitro group to alkyne, i. e. the 5-*exo* mode of oxygen transfer leads to the formation of isatogen whereas the 6-*endo* mode of oxygen transfer leads exclusively to the formation of anthranils.

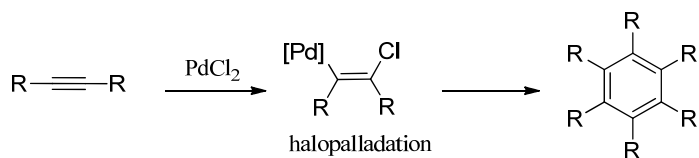
Considering these two aspects, we envisaged that a reactivity umpolung at the nitro group leading to the isomeric metal carbene **IX**, similar to what is done by pyridine, could provide substituent independent isatogen synthesis (Scheme 45). We hypothesized the halopalladation of the alkyne unit for such a reactivity umpolung, with the chloride being the transient nucleophile-cum-leaving group,⁵⁸ albeit not

ruling out such a possibility through the addition of nitro-oxygen in a 5-*exo*-dig fashion. However, earlier investigations from our group and from other groups have



Scheme 45: The proposal for general isatogen synthesis either through halopalladation or through 5-*exo* addition

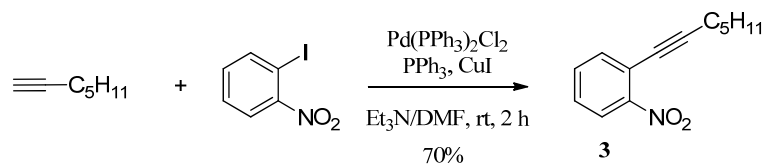
revealed that when another internal nucleophile is present, the NO₂ group remains as a spectator group and facilitates the addition of the nucleophile on the β-carbon of the alkyne.⁵⁹



Scheme 46: The halopalladation and synthesis of benzene from acetylene

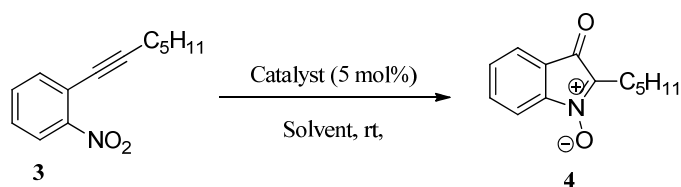
2.1.2 Results and discussion

To start with, 1-nitro-2-(hept-1-ynyl)benzene (**3**) was prepared (Scheme 47) as a model substrate and the feasibility of the nitro-alkyne cycloisomerization was examined with various Pd(II) complexes as catalysts. The cyclization was facile with PdCl₂, PdBr₂ and with their acetonitrile and benzonitrile complexes. Amongst these complexes, Pd[CH₃CN]₂Cl₂ gave better yields of 2-pentyl isatogen **4**. The reaction



Scheme 47: Synthesis of compound 3

with PdI₂ did not proceed at all, which may be due to the poor solubility of PdI₂ in almost all the solvents used (Table 2). The reactions were found to be clean in acetonitrile whereas protic solvents resulted in several other byproducts. Pd(OAc)₂ or Pd[PPh₃]₂Cl₂ were found to be inefficient for this nitro-alkyne cycloisomerization. The product was confirmed by NMR, IR and mass spectra and also by comparison with the reported data for isotogens. The four aromatic protons of the benzene ring give a multiplet in the range δ 7.50–7.66 and the two protons of the first CH₂ group resonate at δ 2.67 compared to δ 2.42 in the case of starting compound, which is in accordance with the literature¹³ (deshielded by δ 0.25). Similarly, in the ¹³C NMR spectrum of compound 4, the peak at δ 186.8 (s) corresponds to a carbonyl group while the peak at δ 125.5 (s) corresponds to the newly generated quaternary carbon atom. In the IR spectra of compound 4, the peaks at 1711 and 1695 cm⁻¹ are due to the carbonyl and N–O group respectively.

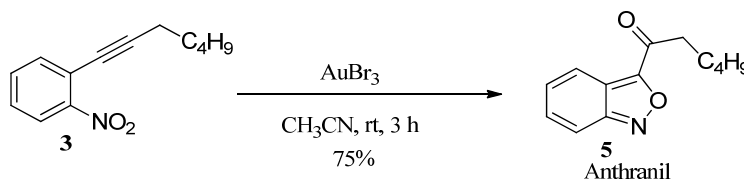


S.No.	Catalyst	Solvent	Product (% Yield)
1	Pd(PPh ₃) ₂ Cl ₂	CH ₃ CN	No reaction
		DMF	No reaction
2	Pd(CH ₃ CN) ₂ Cl ₂	CH ₃ CN	69
		MeOH	42
		CH ₂ Cl ₂	48
		Toluene	32

3	Pd(PhCN) ₂ Cl ₂	CH ₃ CN	17
		DMF	Traces of product
4	PdCl ₂	CH ₃ CN	59
		Toluene	22
		MeOH	10
		CH ₂ Cl ₂	34
5	PdBr ₂	CH ₃ CN	48
6	PdI ₂	CH ₃ CN	No reaction
		MeOH	No reaction
		DMSO	No reaction
		DMF	No reaction
7	Pd(OAc) ₂	CH ₃ CN	No reaction
		DMF	No reaction

Table 2: Screening of different Pd complexes for the cycloisomerization reaction

As a control experiment, when **3** was exposed to AuBr₃ in acetonitrile solvent at room temperature, anthranil **5** (Scheme 48) was obtained as the main product which was in accordance with the earlier report by Yamamoto *et al* where dichloromethane was used as the solvent instead of acetonitrile in the present case. The structure of the anthranil derivative was confirmed by spectral and analytical data. For example, in the ¹H NMR of compound, unlike the corresponding isatogen **4**, all the aromatic ring –H are well separated. In the ¹³C NMR spectrum, the peak at δ 190.5 is due to the newly generated carbonyl carbon and at δ 119.1 corresponds to the new quaternary center. Table 3 provides a brief comparison of NMR data of **3**, **4** and **5**.



Scheme 48: Gold catalyzed nitroalkyne cycloisomerization

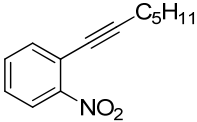
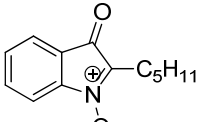
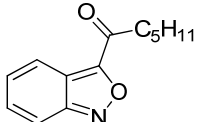
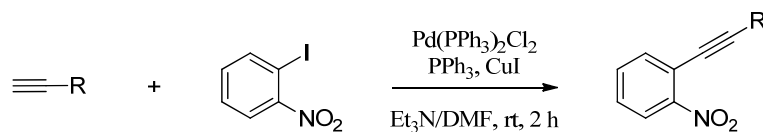
Proton/ Carbon	 3	 4	 5
Aromatic protons	7.33 (br. ddd, 1 H) 7.46 (dt, 1 H) 7.51 (dd, 1 H) 7.90 (dd, 1 H)	7.50–7.56 (m, 2 H) 7.60–7.66 (m, 2 H)	7.27 (ddd, 1 H) 7.40 (ddd, 1 H) 7.73 (dt, 1 H) 8.05 (dt, 1 H)
≡C-CH ₂ -	2.42 (t, <i>J</i> = 7.2 Hz)	2.67 (t, <i>J</i> = 7.4 Hz)	3.17 (t, <i>J</i> = 7.4 Hz),
-C≡C- carbons	75.9 (s) 99.2 (s)	186.8 (s) 123.1 (s)	190.5 (s) 119.1 (s)
-C=O carbon	---	186.8 (s)	190.5 (s)

Table 3: Comparison of spectral data of **4** and **5** with starting nitroalkyne **3**

From the above preliminary experiments, it was observed that palladium catalyzed nitroalkyne cycloisomerization gives exclusively isatogens whereas the gold catalyzed case mainly provides anthranil products. To examine the scope of this palladium catalyzed reaction, different nitroalkyne substrates (**6** – **15**) were prepared using a variety of aliphatic alkynes,⁶⁰ functionalized substrates with free hydroxyl groups, different protecting groups, a lactam ring and a sugar derivative (Table 4) using Sonogashira coupling.⁶¹



Scheme 49: Synthesis of nitroalkyne substrate

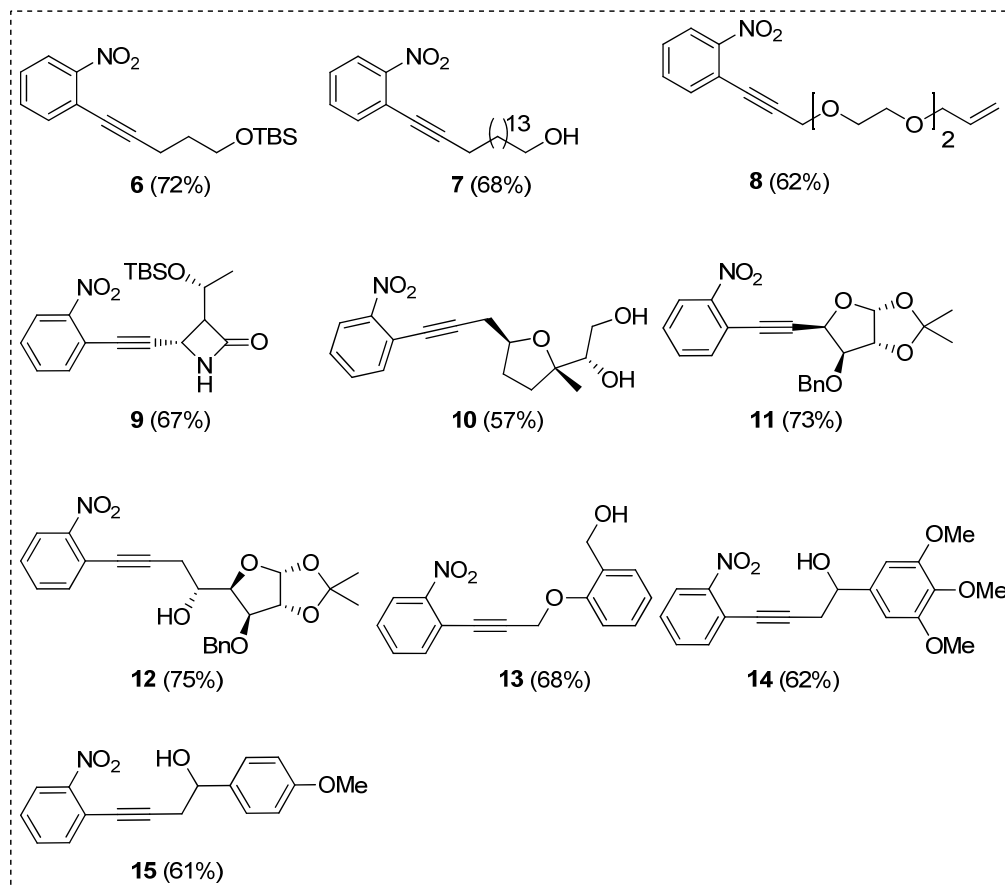
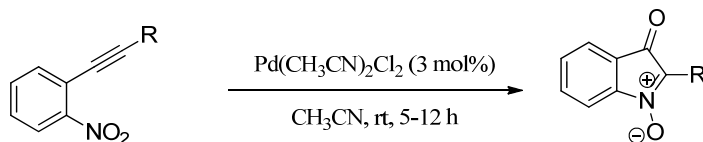


Table 4: Starting compounds for the synthesis of alkyl isotogens

The cyclization of all these substrates **6** – **15** was examined under the above conditions. Gratifyingly, in all the cases, the cyclization showed excellent selectivity that was independent of alkyne substituents (Table 5) and provided the isotogens **16** – **25** respectively from **6** – **15** in moderate to excellent yields. From the substrates employed, it was evident that the conditions we developed were tolerable for commonly employed protecting groups such as TBS, isopropylidene and benzyl ethers and accommodated the substituent functionality including free alcohols, β -lactams, heterocycles and olefins.



Scheme 50: Generalization of method for alkyl isatogens synthesis

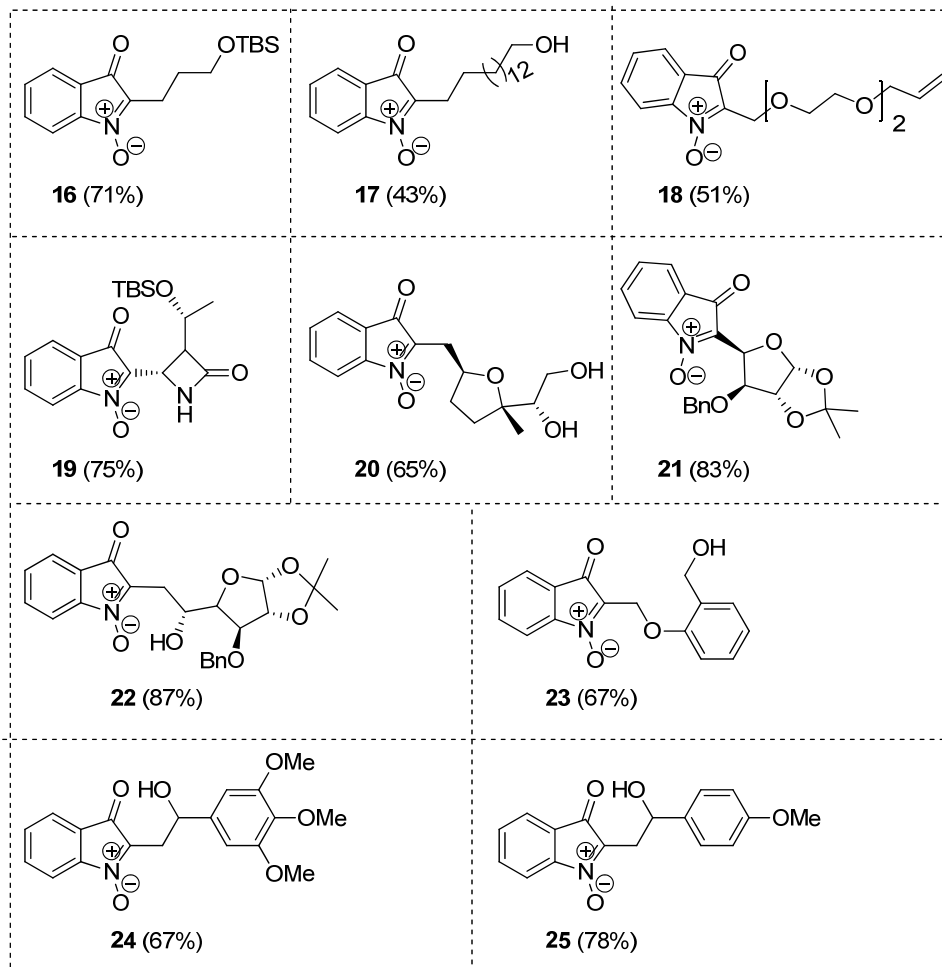
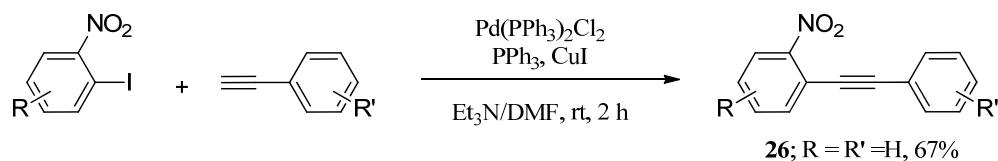


Table 5: Synthesis of various 2-alkyl isatogens

After successful synthesis of various 2-alkyl isatogens, we next examined the scope of our current catalyst-conditions for synthesis of 2-aryl isatogens. The compound **26** was prepared from the Sonogashira coupling of 2-iodonitrobenzene with phenyl acetylene (Table 6). The Pd-mediated nitroalkyne cycloisomerization of **26** proceeded smoothly and provided exclusively the known 2-phenyl isatogen **36** in



Scheme 51: Synthesis of aryl starting compound

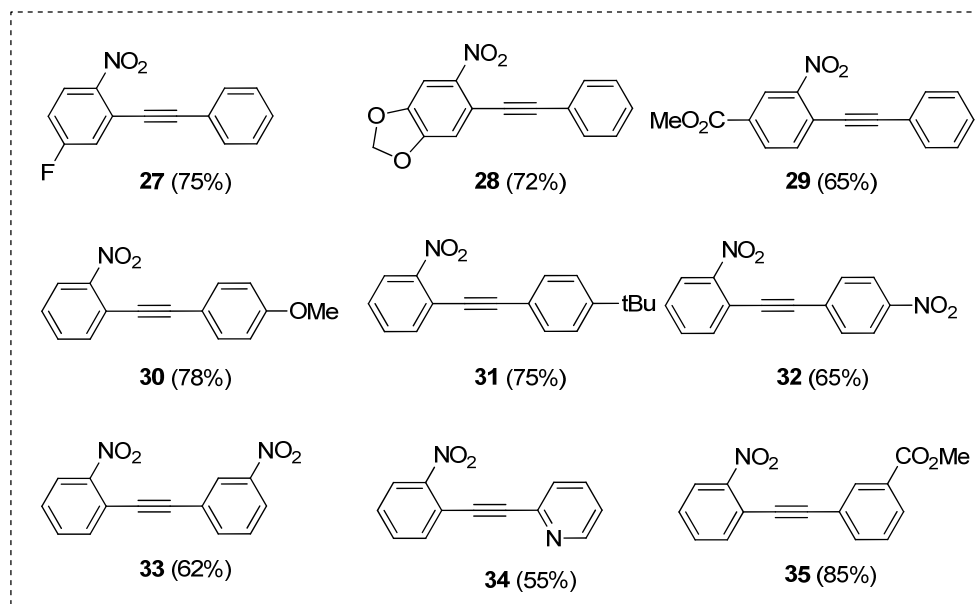
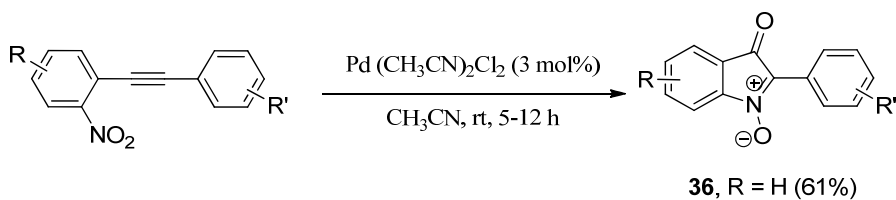


Table 6: Starting compounds for nitroalkyne cycloisomerization

61% yield. The spectral data matches with the reported values.¹³ In the ¹H NMR spectra of **36**, deshielding of both the *ortho* protons of phenyl ring which resonate at δ 8.64 was observed. In the ¹³C NMR spectra of **36**, the carbonyl and the newly generated quaternary centers are seen at δ 125.9 and 186.7 respectively. An important point worth mentioning here is that the formation of isotogens during the preparation/purification of the nitroalkyne **26**. It was observed that the column fraction containing the compound **26**, slowly converted into isotogen without the addition of any reagent. This may be due to the cyclization of nitroalkyne in the presence of light, as reported previously in the literature.²² However, such type of cyclization was not observed in the case of alkyl isotogens - in fact, the starting materials for the alkyl isotogens are stable at rt, and can be stored for months at low temperature.



Scheme 52: Generalization of method for aryl isatogen synthesis

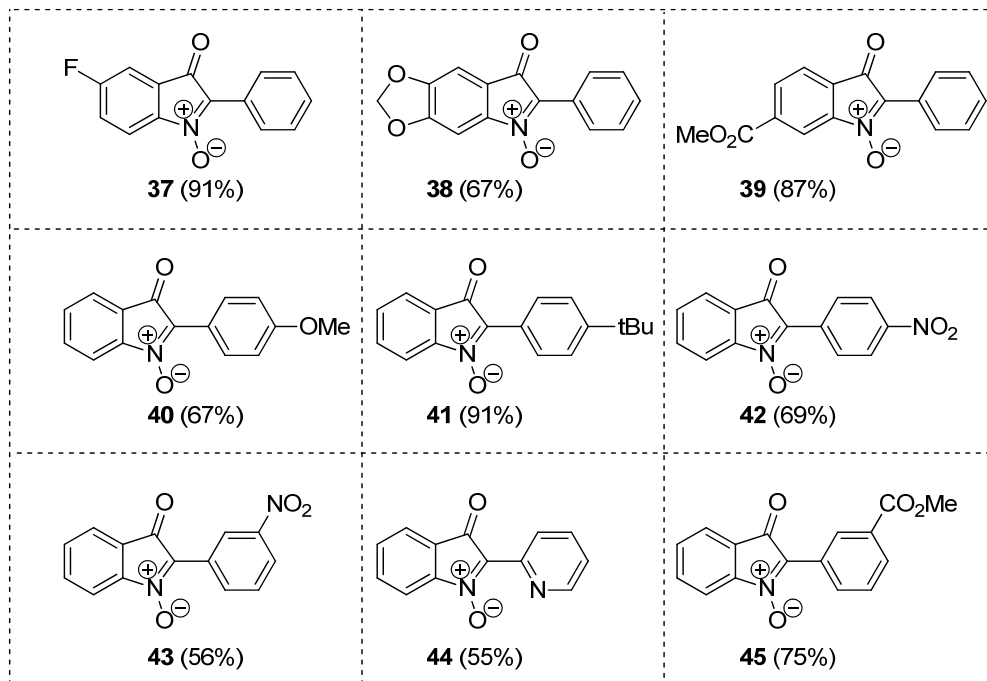


Table 7: Synthesis of aryl isatogens

Next, we examined the generality of the 2-arylisatogens synthesis. Various nitroalkyne derivatives **27–35** having different substituents on both the aryl rings have been prepared from the corresponding iodo and alkyne compounds by using the Sonogashira reaction. Afterwards, all the compounds **27–35** were subjected for palladium catalyzed cycloisomerization to give the corresponding isatogens **37–45** in good to excellent yields (Table 7).

2.1.3. Evaluation of isatogens as modulators of ROS-mediated cell death

Isatogens show a variety of biological properties such as significant activity against a range of bacteria,⁶² mycobacteria⁶³ and fungi⁶⁴ and are also able to antagonize the relaxant response to adenosine-5-triphosphate in mammals.⁶⁵ In

addition, they are also able to trap oxygen and carbon-centered radicals as reported by different groups.⁶⁶ Isatogens form spin trap adducts capable of trapping hydroxyl and superoxide radicals.⁶⁷

After having synthesized a diverse collection of isatogens, we next proceeded to evaluate their efficiency in inhibiting ROS-mediated necroptotic cell death. This is because the generation of ROS is a key downstream execution event in necroptotic cell death.⁶⁸ The isatogen nucleus was identified on consideration of its ability to trap hydroxy and superoxide radicals. These experiments employed mouse fibrosarcoma L929 cells treated with TNF α . As shown in Figure 7A, isatogens indeed displayed significant protection from necroptosis. The EC₅₀ values of some of the active

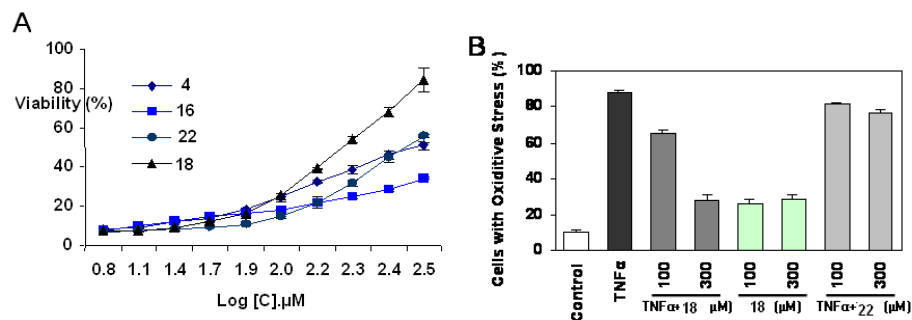


Figure 7. Inhibition of necroptosis (A) and oxidative stress (B) in L929 cells by isatogens. L929 cells were treated with 10 ng/ml mouse TNF α (Cell Sciences, Canton, MA) in the presence of the indicated concentrations of the compounds for 24 hr. Cell viability was measured using Cell Titer-Glo assay (Promega, Madison, WI). ROS levels were determined by measuring fluorescence of the cells stained with 10 μ M Mito Sox reagent (BD Biosciences, Eugene, OR) by FACS analysis

Compounds	4	22	16	18
EC ₅₀ (μM)	327.34	879.02	299.92	188.36

Table 8. The EC₅₀ value of selected compounds

compounds are shown in Table 2. Compound **18** displayed the highest activity ($EC_{50} = 188 \mu\text{M}$), while other molecules were found to lack activity. To confirm that the inhibition of cell death was related to the suppression of ROS, the production of mitochondrial superoxide in necroptotic L929 cells was directly measured. As shown in Figure 7B, **18** indeed efficiently suppressed TNF α -induced ROS, in contrast to the related inactive analogue. The inhibition of necroptosis selectively by 2-alkylisatogens and not by 2-arylisatogens can be explained by considering the superior spin trapping abilities as well as the longer half-life times of the corresponding spin adducts of the former. Overall, these data confirm that isatogens represent a new family of ROS scavengers capable of inhibiting cellular necroptosis. Because of their proximity to the reactive center, the electronic and steric influence of the substituents at the C(2)-position are critical for the modulation of the reactivity of the *N*-oxides.

Thus, after their inaugural synthesis about 130 years back, a general and mild method for the synthesis of isatogens has been developed. The electrophilic palladium(II) complex has been shown to bring the requisite nitroalkyne cycloisomerization of (*o*-alkynyl)nitroaryls with complete region-selectivity and deliver the isatogens without any interference from the alkyne substituents. 2-alkyl isatogens were identified as new candidates for inhibiting the necroptosis mediated cell death through the efficient trapping of the reactive oxygen species. The present reaction conditions employed are catalytic in nature, mild, accommodate both aryl and alkyl substituents and tolerate commonly employed protecting groups/functional units.

2.2. Mechanistic Investigation of Nitroalkyne Cycloisomerization using Density Functional Theory (DFT) Study

After having developed a general and efficient method for the synthesis of isotogen by palladium catalyzed nitroalkyne cycloisomerization, the detailed mechanism of the above reaction was studied with density functional theory (DFT) in order to check our hypothesis of chloropalladation. These calculations now provides the necessary structural and energetic information about the products formed in the reaction as well as the important intermediates and transition states involved. By eliminating reaction pathways with high energy barriers, we have been able to derive a reaction mechanism that explains the salient aspects of the experimental observations. Before going to the reaction mechanism of nitroalkynol cycloisomerization, the basic aspects of theoretical calculations has been discussed in brief.

2.2.1. Theoretical methods

Because of the rapid progress of computers and processing speed, the area of computational chemistry has developed extremely quickly in the past few decades. Beginning from small systems, consisting of only a few atoms that could be managed at the end of the 1980s, the computational chemists of today can handle enzymatic systems with several thousand atoms.

2.2.1.1. Wave function methods

One of the important developments for calculations in organic chemistry was the *Hartree-Fock* (HF) method, in which the Schrödinger equation (Equation 1) can be solved iteratively.⁶⁹

$$H\Psi = E\Psi \dots\dots\dots(\text{eq. 1})$$

However, HF calculations use the approximation that each electron interacts with the average of all the other electrons, and ignores the important *electron correlation*, which postulates that when one electron moves to a certain point in

space, all the other electrons must move away from that point. In spite of this simplification, the HF method is able to give fairly accurate total energies for molecules, as well as molecular geometries and reaction barriers. In cases with higher electron densities, such as transition metals, the electron correlation is large enough to give significant errors for HF results. Therefore, other more accurate methods are needed in these situations.

Small perturbations can be introduced to the HF wavefunction, in order to obtain a more accurate solution. An easy way to do this is to mix the ground state with other low-energy states. In the *many-body perturbation theory* (MBPT), or *Møller-Plesset theory* (MP), the HF excited states are used in this way.⁶⁹ MP2 uses the single and double excitations. Three or more electrons can be excited simultaneously in MP3, MP4 and MP5 methods, of course at a much greater computational cost. A development of this technique is the *coupled-cluster theory*, the variant termed CCSD(T) is used today as a “gold standard” for computational benchmarking, but this method is very costly, and is practical only for up to around a dozen atoms.

2.2.1.2. Density functional theory

An alternative to the wavefunction methods is density functional theory (DFT) which, unlike the above-mentioned methods, does not solve the Schrodinger equation; instead it solves a corresponding equation for the electron density. Initially, DFT was used to calculate the total energy of a system by considering the electron density at each point in space, the *local density approximation* (LDA). The further development of this technique resulted in the *non-local density approximation* (NLDA or GGA) where the variation in density, the gradient, was taken into account. This approach was at least as accurate as HF methods and had a lower computational cost.⁷⁰ In more recent years, new improvements have resulted in a method that is as fast as HF calculations and has the accuracy of the MP methods. Particularly the work from Becke providing the hybrid theory, a merge between HF and DFT has been instrumental in the development of DFT as the standard method of today.⁷¹ The hybrid theory uses a combination of a partially exact treatment of the exchange term and an approximation of the electron correlation term to generate a more accurate and generalized DFT method. Most of the published computational studies today employ

Becke's hybridization methods,⁷² especially the B3LYP variant.⁷³ Even more recent improvements of these methods involve accounting for van der Waals dispersion forces, for example by a parameterized functional, such as M06-2X,⁷⁴ or by calculation of a correction term.⁷⁵

2.2.1.3. Basis sets

All of the aforementioned methods require a mathematical description of the distribution of electrons in space. In an atom, the electrons are distributed in *orbitals*, with each orbital able to confine two electrons. The atomic orbitals are the well-known 1s, 2p and so on, orbitals. Usually the molecular orbitals are constructed from the atomic orbitals: this is called *linear combination of atomic orbitals* (LCAO). In trivial cases, the simple atomic orbitals are employed, but in more complex examples, the requirement of accurate results demands the need of the orbitals to be able to change size and shape. Giving each orbital two different sizes is denoted as double- ζ (DZ), whereas using three different sizes is termed triple- ζ (TZ). Sometimes, very large orbitals are used, especially when anions need to be accounted for. These are called diffuse orbitals and are indicated by a "+" or "aug-" in the name of the basis set.

The shape of the orbitals can be adjusted by adding orbitals of a higher quantum number. The mixing of these different orbitals result in new orbitals that better describe chemical bonds, such as π -bonds. The use of the extra orbitals is called polarization and is denoted with a "*" or "***" describing the use of an extra set of d-orbitals on heavy atoms and p-orbitals on hydrogens, respectively. Another way to indicate this is by adding (d) or (d,p) to the name of the basis set. The large number of electrons in the heavier elements is a problem in calculations since they increase the required time for each calculation, without significantly changing the result. Because it is the valence electrons that constitute the part of the atom that contributes to bonds and other interactions, it is these that will give changes to the total energy. Therefore, the core electrons of heavy atoms are sometimes treated with an *effective core potential*⁷⁶ (ECP). This greatly reduces the basis set size.

2.2.1.4. Solvent

Since most organic reactions are carried out in a solvent, and not in the ideal “gas phase” that makes up the best arena for calculations, some consideration must be spent to account for the implementation of the influence of the solvent. Most structures will be reasonably accurate when optimized in the gas phase, as long as they do not carry opposite charges. This problem occurs when dealing with, for example, two ionic species of opposite charge. The reaction between these will generally be barrier-less in gas phase, something that can be far from the reality in solution. The most popular way to answer this problem is to use a continuum solvent model. Several are available and one of the most common is the *polarizable continuum model*⁷⁷ (PCM). It encloses the molecule with a cavity dotted by parameterized point charges, which has been modeled to simulate the average influence of the solvent. The method employed in this thesis is a variant of the PCM method, the *Poisson-Boltzmann finite continuum model* (PBF).⁷⁸ This method uses two parameters to describe different solvents, the *probe radius*, derived from the size of the solvent molecule and used to construct the solvent accessible surface area, and the *dielectric constant* of the solvent.

2.2.1.5. Calculating energies and analyzing results

A simple DFT optimization of an organic molecule in the gas phase results in a large amount of information. The most important property is the energy of the molecule. It is provided in the unit Hartree and can only be used as a relative value. The energy can only be compared to other calculated energies with the same setup as the first one. This is the *potential energy* of the molecule. A more accurate energy for the molecule is the *Gibbs free energy*, denoted G , which can be calculated by adding the thermodynamic and solvation effects. The method employed in this thesis approximates this by adding the vibrational contributions to the single-point energy with the solvation of an optimized gas-phase structure.

The easiest way to analyze a chemical reaction computationally is to construct a reaction profile; a *free energy surface* (FES), where the starting point is the sum of all starting reactants, and consequently, the end point is the sum of all the products.

All intermediate points are the sum of the relevant intermediates, not yet consumed reactants and already formed products. In catalytic systems, it is important to note that the starting point is arbitrary. The relationship between all steps are easiest seen when drawing two full catalytic cycles after each other, as depicted in Figure 8.⁷⁹

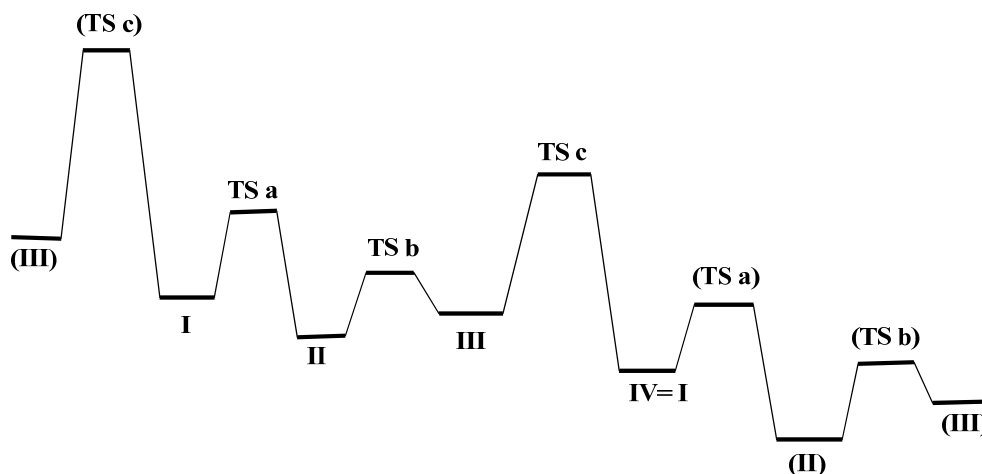


Figure 8: Free energy surface (FES) for a catalytic reaction

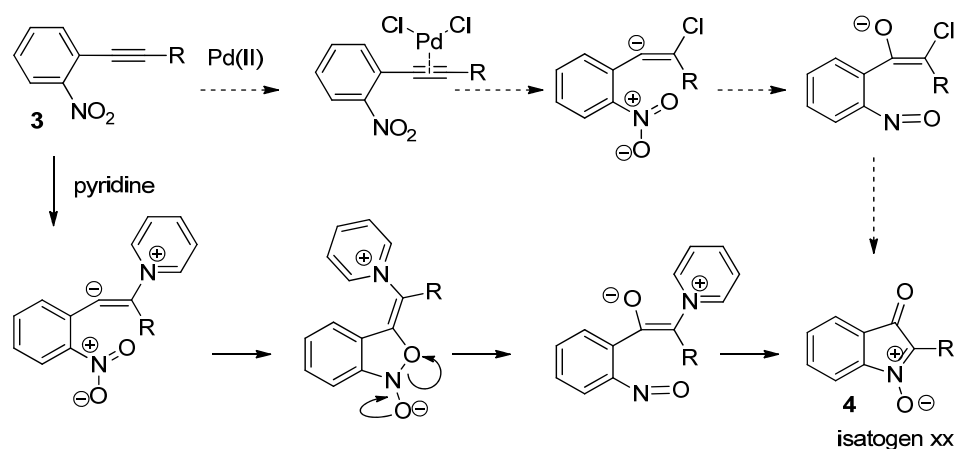
The overall exergonicity of the reaction can be seen as the difference between the same point in two subsequent catalytic cycles (e.g. between I and IV in Figure 8). The interpretation of the surface reveals several interesting points. First of all, all transition states those are higher than all the subsequent points can be identified as *effectively irreversible*. In Figure 1 this is true for **TS c**, may be also for **TS a**, even if the difference between these points is hard to determine, and can be within the accuracy limit of the method employed. However, these transition states are selectivity determining for the bonds formed in the corresponding step. **TS b**, on the other hand, is a completely reversible step, and will not have any influence on the reaction. This is a classic Curtin-Hammett situation where **II** and **III** are in rapid equilibrium.⁸⁰ With the important **TS a** and **TS c** established, the activation free energy can be calculated as the difference between the TS and the lowest preceding point. In Figure 1 the barriers correspond to $G(\text{TS a}) - G(\text{I})$ and $G(\text{TS c}) - G(\text{II})$. The rate determining step is the one with the highest barrier (**TS c** in Figure 1) and the resting state is the lowest preceding point (**II** in Figure 1). Other ways to analyze free energy surfaces are present in the literature; one example is the *energetic span model* by Shaik and co-workers.⁷⁹

The *ab initio* calculations were done with the software Turbomole 5.10⁸¹ using the TZVP⁸² basis set and the BP-86⁸³ functional. The values provided here are the ΔE values, calculated after the incorporation of solvent effects, taking acetonitrile ($\epsilon=37.5$) as the solvent. The barriers calculated must be compared to the reaction conditions, especially the temperature, which of course is the factor that most greatly influences the possibility for the reaction to progress. At room temperature, a good estimate is that a barrier should not be above 25 kcal/mol in order to proceed at an acceptable rate.

2.2.2. Chloropalladation approach for nitroalkyne cycloisomerization

For the mechanism of the nitroalkyne cycloisomerization reaction, first we consider according to our hypothesis, the cycloisomerization i.e. the chloropalladation approach. According to our hypothesis, chlorine is acting as a nucleophile which initiates the transfer of oxygen to the α carbon of the alkyne, and then can act as a living group to give the isatogen (Scheme 53). The compound **3** was taken as a model substrate.

To begin with, substrate **3** reacts with one molecule each of $\text{Pd}(\text{CH}_3\text{CN})_2\text{Cl}_2$ and PdCl_2 to produce the alkene coordinated complex **A**, and release one molecule of CH_3CN . This reaction is exothermic by 36.7 kcal/mol (see Figure 9). Subsequent to



Scheme 53: Huisgen's pyridine mediated mechanism for isatogen formation and proposed chloropalladation path way for the formation of isatogens

this step, the system goes through a transition state **TS1**, where a leaving palladium species donates a chlorine atom to the β carbon of the alkyl chain and extracts a

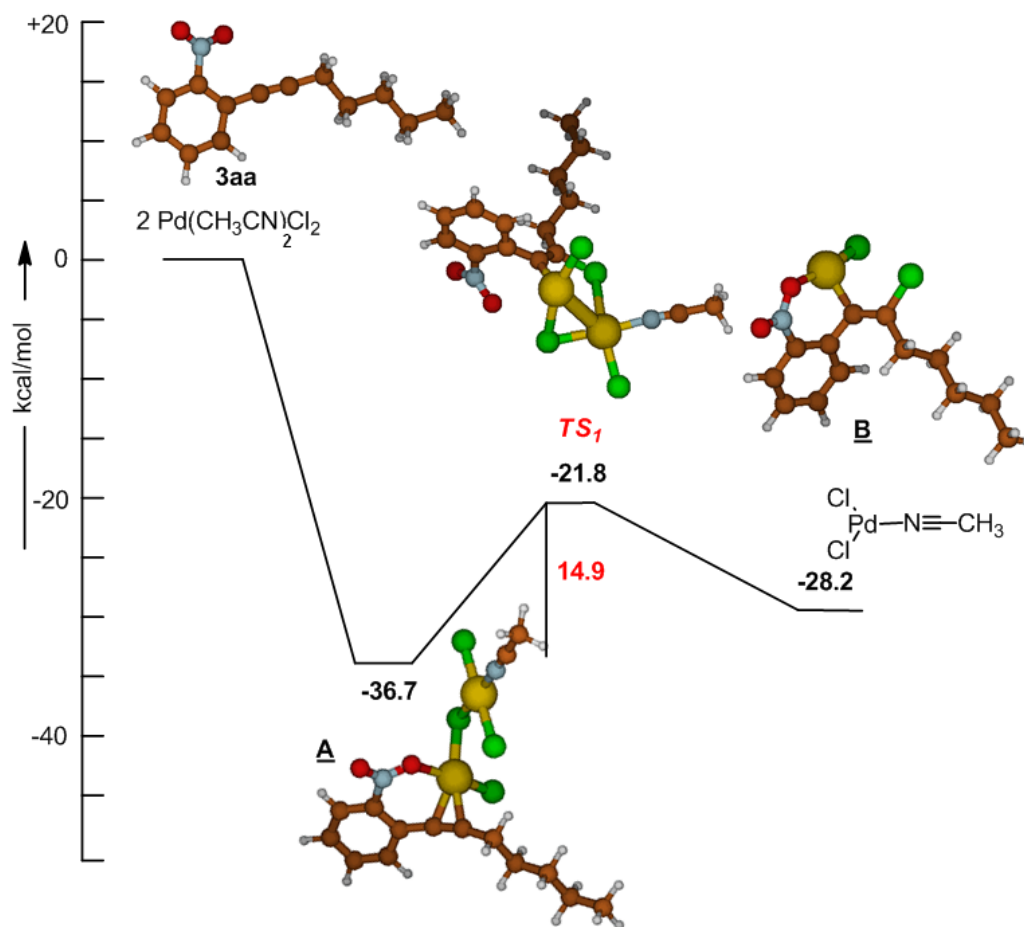


Figure 9. The energy profile for the first steps of the catalysis: the conversion of the substrate **3** to **B**, with the aid of two palladium chloride molecules; all the reported energies have been calculated using DFT, all values are in kcal/mol.

chlorine from the palladium atom that remains coordinated to the original substrate complex. The barrier for the reaction is 14.9 kcal/mol. The subsequent dissociation reaction to yield PdCl₂(CH₃CN) and the *cis*-chloropalladated species **B** (see Figure 9)⁸⁴ is downhill in energy with respect to the transition state **TS1** by 6.4 kcal/mol, and the overall reaction converting **A** to **B** and the PdCl₂(CH₃CN) complex is slightly endothermic, by 8.4 kcal/mol.

Figure 10 continues the reaction cycle, with **B** being converted to the oxirane **C** via the transition state **TS2**. The earlier reports by Andrews and Chen on the epoxidation of cycloalkenes employing stoichiometric or catalytic amounts of Pd[CH₃CN]₂NO₂Cl complexes at ambient temperatures supports the intermediacy of

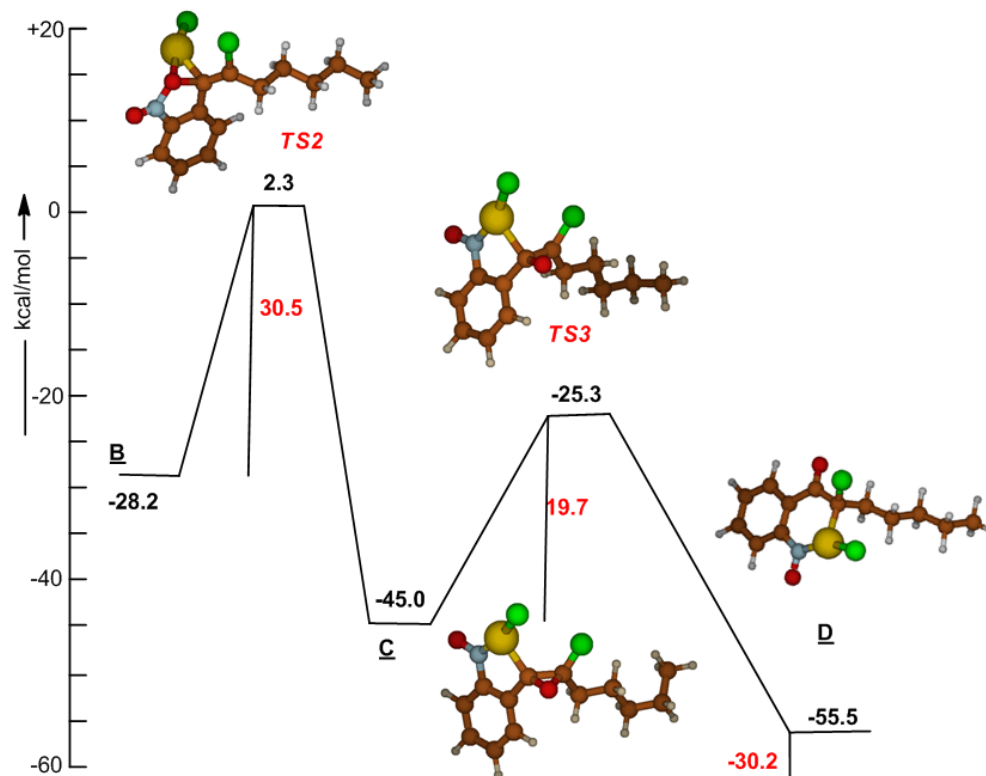


Figure 10. The energy profile for the continuing steps in the catalysis: the conversion of the species **B** to **D** through two transition states that shift an oxygen atom from the nitrogen (in **B**) to the carbon (in **D**), with the help of an interacting palladium species; all the reported energies have been calculated using DFT; all values are in kcal/mol.

C in our mechanistic route.⁸⁵ The conversion taking place here is the transfer of an oxygen atom from the nitro group to the α carbon of the alkyl chain connected at the *ortho* position of the phenyl ring. The transition state for this has the oxygen atom coordinating to the palladium, and also beginning to form a bond with the α carbon (The breaking N-O bond distances in **B** and **TS2** are 1.28 and 1.41 Å whereas the newly forming C-O bond distances are 2.75 and 1.67 Å respectively). The barrier for this reaction is 30.5 kcal/mol, which is the highest barrier in the entire catalytic cycle

described over the four figures 9–12. This step is therefore the slowest step – the rate determining step – in the reaction cycle.

The next step in the reaction cycle is the conversion of the oxirane **C** to **D**, shown in Figure 10, where the palladium has shifted its bond from the α to the β carbon of the alkyl chain. The barrier for this step is 16.4 kcal/mol. This conversion is exothermic by 7.8 kcal/mol. In Figure 11 is shown the continuation of the reaction cycle, moving from the species **D** to **E**. For this conversion, there is need of an extra molecular species: $\text{Pd}(\text{CH}_3\text{CN})_2\text{Cl}_2$, that can act as a catalyst to essentially transfer a chlorine atom from the β carbon of the alkyl chain to the palladium atom. The way it does so is by acting as a “chlorine shuttle” – forming a five-membered transition state complex **TS4** by coordinating to species **E** (see Figure 11) - and then proceeding to extract a chlorine from the β carbon of the alkyl chain while simultaneously giving its own chlorine atom to the palladium, to eventually yield intermediate **E**. As shown in Figure 11, this reaction is quite facile: the formation of **E** from **D** and $\text{Pd}(\text{CH}_3\text{CN})_2\text{Cl}_2$ is only marginally uphill by 4.8 kcal/mol, and the barrier of the conversion of **TS4** to **E** is only 12.6 kcal/mol (see Figure 11). It is interesting to note that an acetonitrile solvent molecule, originally coordinated to the chlorine shuttling $\text{Pd}(\text{CH}_3\text{CN})_2\text{Cl}_2$ species is dissociated from the palladium centre in the intermediate species **E** (the distance of the nitrogen atom of the dissociating acetonitrile solvent molecule from the palladium centre is 2.02 Å in $\text{Pd}(\text{CH}_3\text{CN})_2\text{Cl}_2$ and 3.57 Å in the intermediate **E**). This is the bond that the palladium sacrifices in order to coordinate to the species **D**. However, at the transition state **TS4**, this acetonitrile molecule re-coordinates to the palladium centre (Pd-N distance at the transition state is 2.27 Å). This is because, at the transition state, the two palladium-chlorine bonds in $\text{Pd}(\text{CH}_3\text{CN})_2\text{Cl}_2$ have been weakened due to the exchange of chlorines - one being given to the palladium and one taken from the β carbon of the alkyl chain in the original species **D**. This re-coordination of the solvent molecule is significant, because it serves to reduce the barrier to only 12.6 kcal/mol, by providing stability to the palladium centre whose bonding to the transferred chlorine atom is reduced at the transition state.

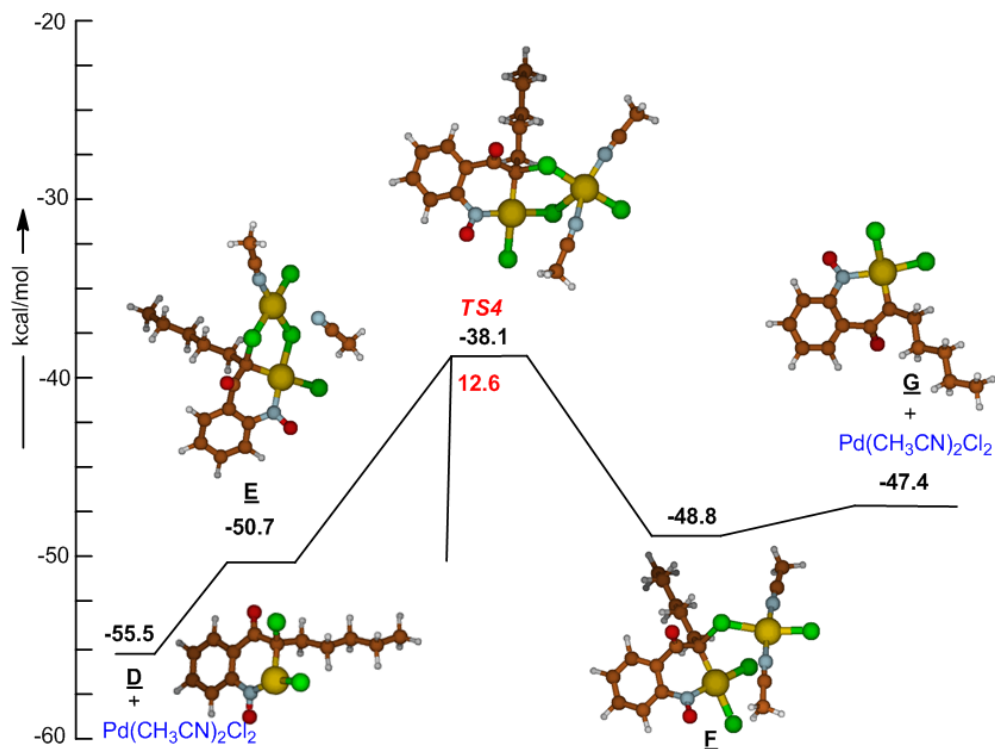


Figure 11. The energy profile for the continuing steps during the catalysis: the conversion of the species **D** to **G** with the help of a “chlorine shuttling” $\text{Pd}(\text{CH}_3\text{CN})_2\text{Cl}_2$ species; all the reported energies have been calculated using DFT; all values are in kcal/mol.

Again here, the dissociation and re-coordination of the labile acetonitrile species serves the crucial purpose of reducing the reaction barrier, and thus once again has a significant influence on the reaction cycle in our proposed mechanism. Recent work by Popp *et al.*⁸⁶ shows that labile monodentate ligands can associate and dissociate readily from the palladium centre and have a significant influence on the mechanism of the palladium mediated catalysis reactions. The labile ligand in the palladium catalyst system reported by Popp *et al.* was pyridine; in our system, the labile ligand is the acetonitrile solvent molecule. The intermediate species **F** then undergoes a marginally downhill (by 0.6 kcal/mol) conversion to the species **G** where the palladium complexes preferentially with the nitrogen of NO.⁸⁷ The involvement of such stable Pd(II)-carbene species and subsequent electrocyclizations is well documented.⁸⁸

The final figure 12, for the mechanistic cycle shows the last few steps in the catalysis. Here, we show the calculations illustrating the conversion of the species **G** to **H**, going through the transition state **TS5**. This conversion involves the bonding of the nitrogen, attached in structure **G** to the palladium atom, to the β carbon of the alkyl

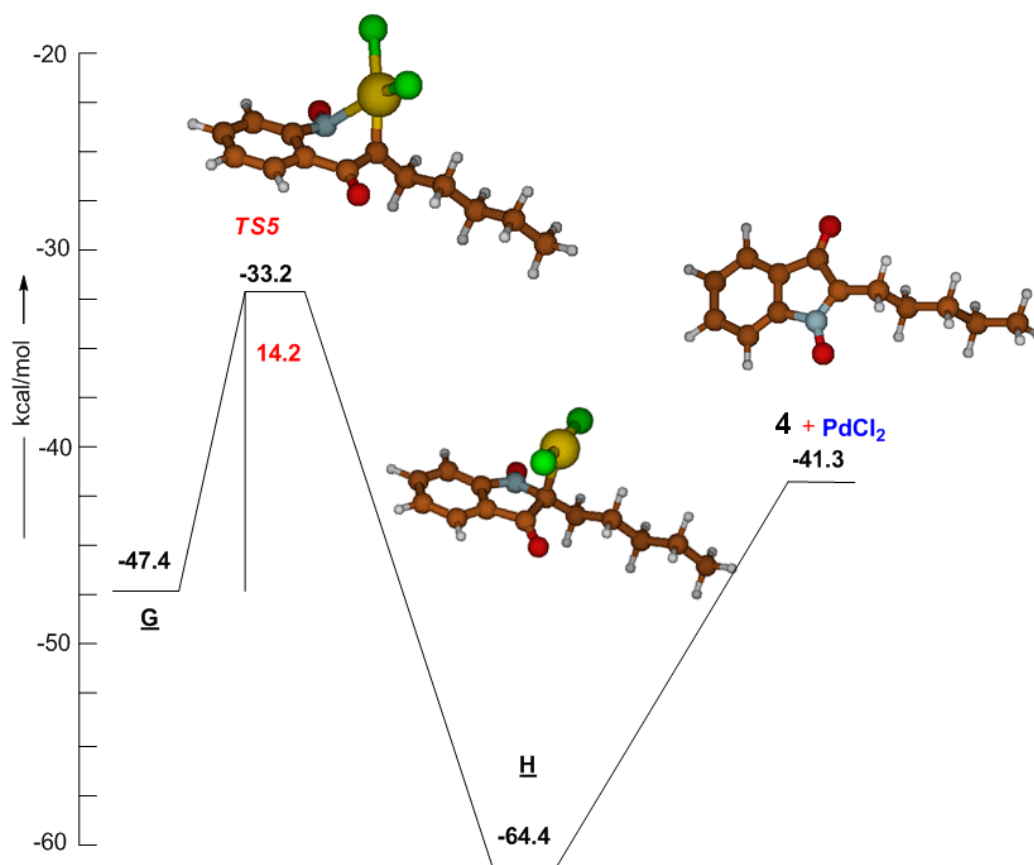


Figure 12. The energy profile for the final steps of the final steps in the catalytic cycle: the conversion of **G** to the final product **Iaa**, occurring through the elimination of the PdCl_2 species; all the reported energies have been calculated using DFT; all values are in kcal/mol.

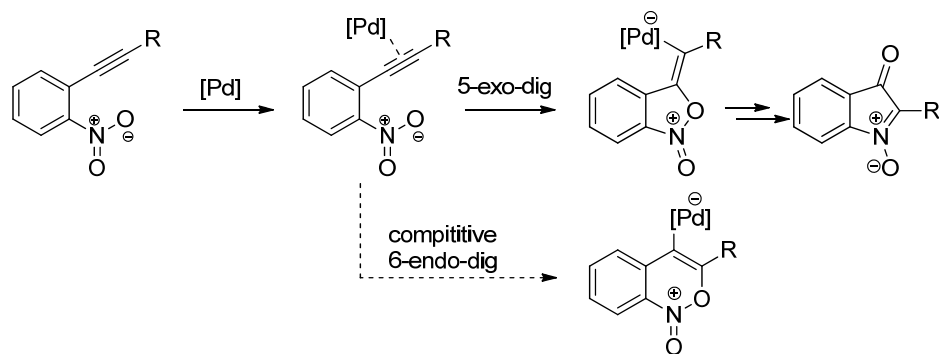
chain – leading to structure **H** that has the palladium atom coordinated to the β carbon, and two chlorine atoms, having relinquished its bonding to the nitrogen. This reaction is exothermic by 17.0 kcal/mol, and has a barrier of only 14.2 kcal/mol, suggesting that it is quite feasible. Once **H** has been formed, it can dissociate to give the desired product **4** and the PdCl_2 catalyst. On the potential energy surface, this

reaction is endothermic by 21.3 kcal/mol, but since the reaction is favourable entropically, yielding two species (**4** and PdCl₂) from one (**H**), such a dissociation is likely to occur at room temperature.

The mechanism discussed above shows the PdCl₂ catalyzed halo-palladation route to isatogen formation. While it was halo-palladation that had been envisaged by us in deciding the use of palladium as the catalyst for isatogen synthesis, a perusal of the mechanism makes it clear that it suffers from several problems: (i) it is very circuitous and complicated, (ii) it is likely to be entropically disfavoured since two PdCl₂ as well as a CH₃CN solvent molecule have to be invoked to catalyze the reaction, (iii) the barrier for the rate determining step: 30.5 kcal/mol, is on the higher side for a reaction taking place at room temperature. These considerations compelled us to consider the possibility that the transformation might be taking place through an alternative pathway - the 5-*exo*-dig route, as discussed earlier and elucidated in Scheme 54.

2.2.3. 5-*Exo*-dig mode of nitroalkyne cyclization

Having found unsatisfactory results in the chloropalladation approach for the nitroalkyne cycloisomerization, we focused on the alternative 5-*exo*-dig mode of



Scheme 54: The alternative 5-*exo*-dig mode of cyclization and possible competitive 6-*endo*-dig mode of cyclization

cyclization. The basic approach for this is outlined in schemes 54. The first step is the complexation of Pd with alkyne, followed by the 5-*exo*-dig mode attack of oxygen

atom of nitrogroup which finally leads to the formation of the isatogen. Calculations were carried out to determine the feasibility of this route, and the potential energy

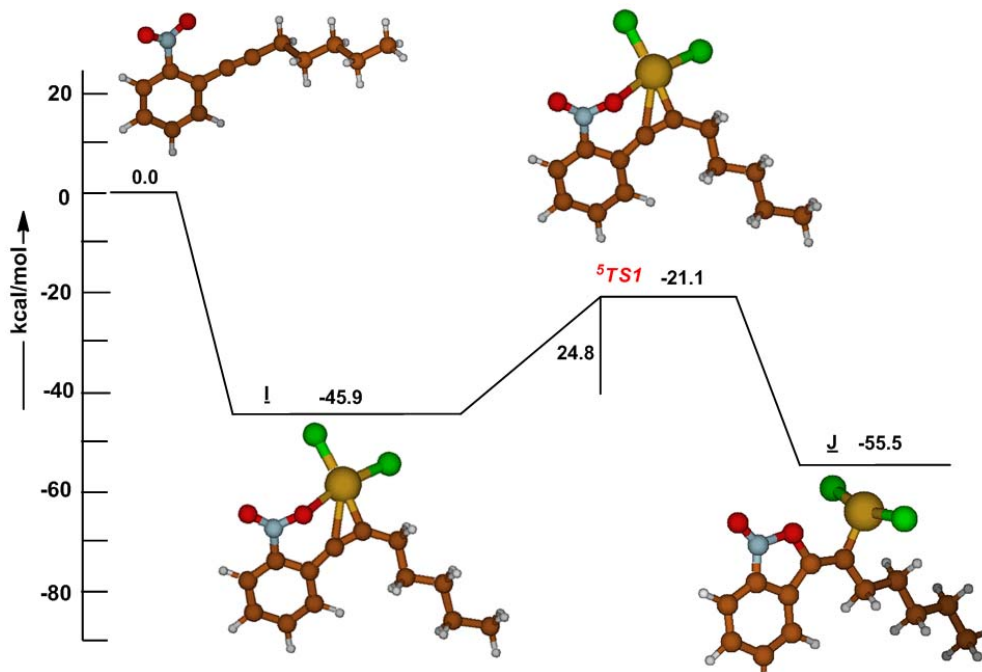


Figure 13. Energy profile for the Pd-mediated 5-exo-dig addition of the nitro-group oxygen atom; all values are in kcal/mol

surface for the mechanistic route is shown in Figure 13 and Figure 14, below. The addition of a PdCl₂ molecule to the substrate **3** leads to the formation of the complex **I** that lies 45.9 kcal/mol below the reactant on the potential energy surface. This complex has the PdCl₂ bound to the two alkyne carbons as well as to one of the oxygens of the NO₂ group (see Figure 13). The high exothermicity of this reaction makes it quite feasible. From here on, the next step involves the transformation to the intermediate species **J**, which has the oxygen of the nitro group coordinated to the α carbon of the alkyne, while the palladium has lost its coordination to the α carbon as well as the oxygen and is now bound to the β alkyne carbon. This species lies 5.6 kcal/mol below the species **I**, and is therefore 55.5 kcal/mol below the original reactant species (see Figure 13). The transition state that connects the two species **I** and **J**, ⁵TS1, lies 24.8 kcal/mol above **I**, and features a lengthening of the N–O bond as well as of the Pd– α carbon bond (The N–O and Pd– α bond length in **I** is 2.16 and

1.27 Å whereas that of ${}^5\text{TS1}$ is 2.57 and 1.33 Å) while the palladium is seen to come closer to the β carbon of the alkyne.

Subsequent to the formation of the species **J**, the system undergoes further transformation to the species **K**, where the palladium is bound to the nitrogen as well as to the β carbon of the alkyne. This occurs via transition state ${}^5\text{TS2}$, where the oxygen has lost its coordination to the nitrogen and is now bound in an epoxy fashion

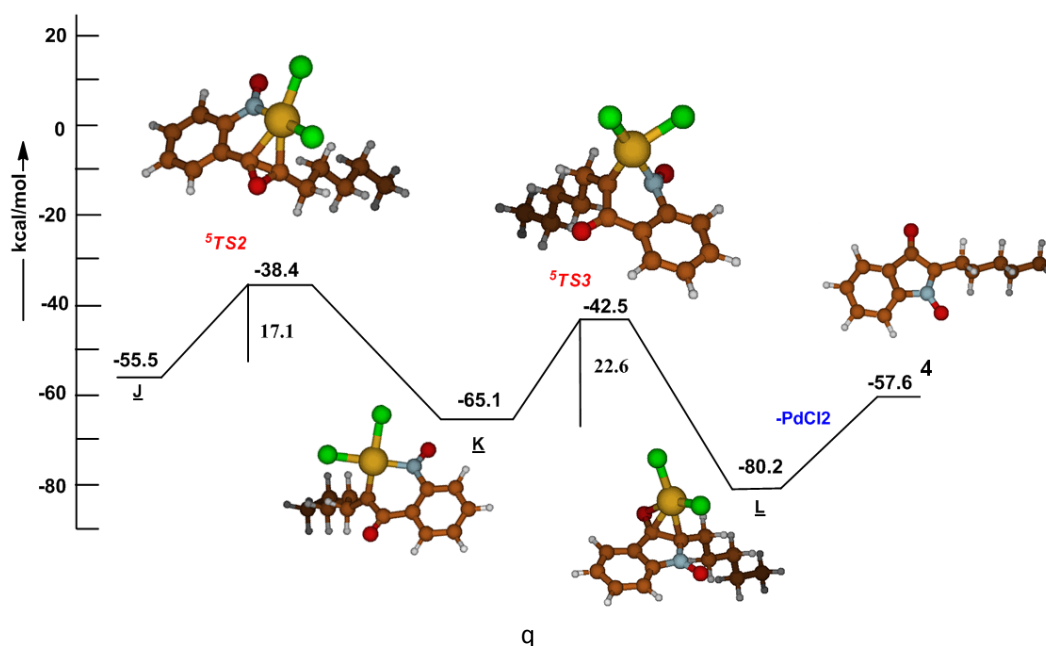


Figure 14. The energy profile for the final steps in the catalytic cycle: the conversion of **J** to the final product **1aa**, occurring through the elimination of the PdCl_2 species; all the reported energies have been calculated using DFT; all values are in kcal/mol.

to the two alkyne carbons, while the palladium, approaching the nitrogen, is bound to both the alkyne carbons (see Figure 14). This transition state lies 17.1 kcal/mol above species **J**, while the formed intermediate **K** is more stable than **J**, and lies 65.1 kcal/mol below the reactants on the potential energy surface. From this point, intermediate **K** is converted to the species **L** which has the nitrogen bound to the β alkyne carbon, while the palladium has bonds to both the atoms. This structure is stitched via the transition state ${}^5\text{TS3}$, which features a shortening of the nitrogen and β alkyne carbon atoms and has a barrier of 22.6 kcal/mol. Species **L** is in essence the

isatogen with a coordinating PdCl₂ species, the loss of which gives the final desired product **4**, at an energy cost of 22.6 kcal/mol.

This 5-*exo-dig* route to isatogen formation has significant advantages over the halo-palladation. To begin with, it is significantly simpler, having three transition states as opposed to five for the halo-palladation, and also requiring only the presence of one PdCl₂ molecule as the catalyst instead of two PdCl₂ and a CH₃CN solvent molecule as required for the halo-palladation process. Moreover, the rate determining step has a barrier of 24.8 kcal/mol, which is 5.7 kcal/mol lower than the rate determining barrier in the halo-palladation case (for the oxygen transfer). Indeed, since the reaction takes place at room temperature, the necessity of the barrier for the reaction to be less than 25.0 kcal/mol strongly suggests the favourability of the 5-*exo-dig* route. Finally, it is interesting to note that every succeeding step in the reaction pathway for the 5-*exo-dig* route to isatogen formation features an intermediate that is lower in energy than the previous intermediate species (see Figure 14). This suggests that every successive step would be thermodynamically favoured in this route, which makes this mechanism highly feasible.

2.2.4. 5-*Exo-dig* Vs 6-*Endo-dig* mode of nitroalkyne cyclization

It is also noted here that we have also considered the possibility that species **I** could proceed via a 6-*endo-dig* fashion to produce the regiomer carbene **K**, which has been postulated by Crabtree and co-workers as a possible intermediate when iridium was used as the catalyst. As shown in Figure 15, this pathway is significantly disfavoured, ⁶TS1 lying 43.6 kcal/mol higher in energy than **I** on the potential energy surface. As also shown in Figure 15, species **I** has the much more energetically favourable choice of passing through transition state ⁵TS1 (barrier 24.8 kcal/mol) to give the 5-*exo-dig* intermediate **J**, which renders the 6-*endo-dig* pathway unlikely and helps explain why the isatogen is formed exclusively while the carbene **M**, resulting from the 6-*endo-dig* pathway leading to anthranil **5**, is not formed. The reason for the high barrier for this route is the steric strain that is involved – the transition state ⁶TS1 has a strained nitro group where both oxygens have bonds to two atoms, thereby giving rise to two different rings. Therefore, when PdCl₂ is used as the catalyst, the results from the DFT calculations indicate that the route to isatogen formation

exclusively involves the formation of the 5-*exo*-dig species. Calculations are currently being done to determine the barrier heights for the analogous reactions when using iridium and gold catalysts in place of palladium (work in progress).

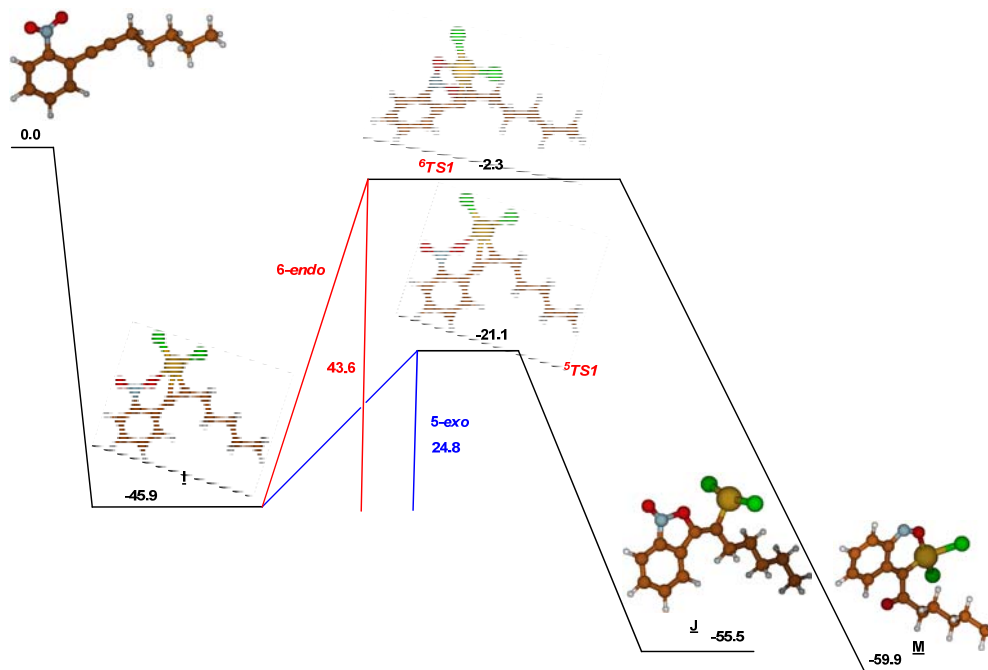


Figure 15. Difference in the activation energies for the addition of the nitro-group oxygen atom in 5-*exo* or 6-*endo*-dig modes; all values are in kcal/mol.

In conclusion, the mechanistic investigation of palladium catalyzed isotogen synthesis from nitroalkyne cycloisomerization has been carried out using density functional theory (DFT). All the three possible modes of oxygen transfer from nitrogroup to the alkyne carbon; i) the halopalladation approach, ii) the 5-*exo*-dig mode and iii) the 6-*endo*-dig mode, has been studied in detail. The energy for different transition states has also been calculated. It was found that the 5-*exo*-dig mode of nitroalkyne cycloisomerization was the low energy and feasible mode of cyclization.

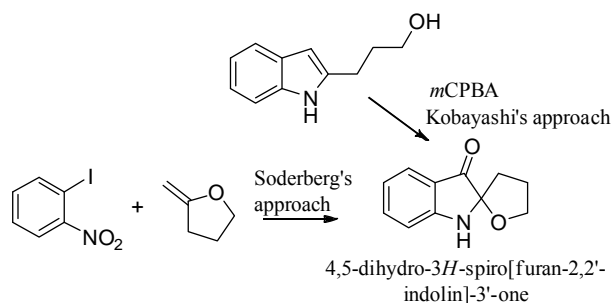
2.3. Metal Catalyzed Nitroalkynol Cycloisomerization

Over the past few years, the use of transition metal complexes has provided important new methodologies for the stereospecific elaboration of a variety of carbocyclic and heterocyclic, sometimes *via* cascade reactions. Palladium-catalyzed cyclization processes provide a powerful methodology for the elaboration of carbocyclic as well as heterocyclic derivatives, allowing for example the stereoselective formation of bridged rings or spirocycles. Transition metal mediated addition of C- and heteroatom nucleophiles across the carbon-carbon double and triple bonds, is one of the most interesting and important reactions in organic chemistry.⁵³ The intramolecular version of this reaction falls under the broad category of cycloisomerization reactions. Recent programmes in our laboratory have been concerned with understanding the regioselectivity of [Pd]-mediated alkynolcycloisomerization reactions and their application in the total synthesis of various natural products having bridged bicyclic ketal, spirobicyclic ketal or C-glycosidic units.⁵⁶

Some of our model substrates employed in the alkynol cycloisomerization reactions possess the *o*-nitrophenyl acetylene sub-units which essentially could undergo a nitroalkyne cycloisomerization leading to isatogens. However, the alkynol cyclization was a predominant pathway and the nitro group was only a spectator.⁵⁹ Quite interestingly, these model alkynols contain an –OH group positioned for a 5-*exo*-dig mode of addition across the alkyne. This is a favoured event as both energetic and electronic factors operate in a synergetic fashion. In addition, the propargylic carbon is a tertiary carbon with an OH group which might be hindering the nitroalkyne cycloisomerization. To this end, we asked a simple question: what happens with the simple nitroalkynols such as 5-(2-nitrophenyl)pent-4-yn-1-ol where both the alkynol and nitroalkyne cycloisomerizations are sterically unbiased? Herein we report the development of a new reaction comprising the nitroalkynol cycloisomerization for the synthesis of spiroindolin-3-one and spirobenzoxazinone derivatives, the latter being the unprecedented skeletons in organic chemistry.

2.3.1. Concept of nitroalkynol cycloisomerization

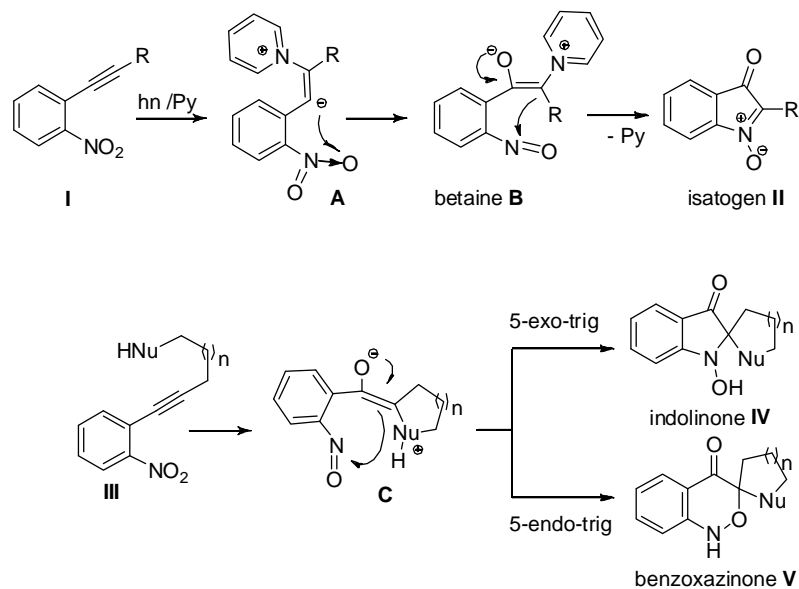
Oxidation of 2,3-disubstituted indole followed by alkyl group migration is a well-known method to obtain indolin-3-one derivatives, which, trivially, are known as indoxyls.³⁴⁻³⁷ This reaction is usually successful in the case of ring contraction reaction to form spiro-indolin-3-one (spiro-indoxyl). Recently, Kobayashi³⁷ *et al.* reported a one-pot oxidation method of indoles to give 4,5-dihydro-3*H*-spiro[furan-2,2'-indolin]-3'-ones, and discussed their utility as versatile precursors to obtain a variety of 2,2-disubstituted indolinones with two different substituents. Although the above method is convenient to synthesize spiroindolin-3-one, it takes many steps and excess use of *m*CPBA. A multi-step approach for the synthesis of these spiroindolinones has been reported by Söderberg's³⁵ group (Scheme 55). While our work was in progress, a similar intermediate was reported by Karadeolian and Kerr in the total synthesis of isatisine A.



Scheme 55: pyridine mediated photochemical isatogen synthesis

As mentioned above, our interest in this regard was to develop a nitroalkynol cycloisomerization for the synthesis of *N*-hydroxy spiroindolin-3-ones. Scheme 56 describes the general concept and the originating pyridine mediated photochemical isatogen synthesis.²⁰ In the reaction mechanism proposed for the pyridine mediated nitroalkyne cyclization, pyridine acts as a nucleophile, which attacks the electron deficient external alkyne carbon, followed by oxygen transfer from nitro group to internal alkyne carbon *via* the pyridinium betaine intermediate **B** formation, followed by its spontaneous conversion to isatogen **II**. We speculated that when the substrate has an internal nucleophile, such a transient betaine **C** can be generated by an intramolecular nucleophilic addition across the alkyne,⁸⁹ and then it should undergo

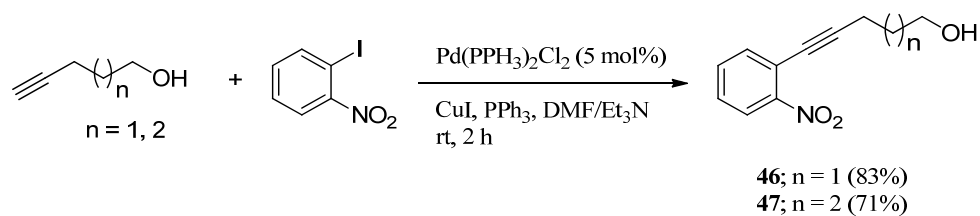
similar post photochemical transformations of isatogen synthesis, leading finally either to a *N*-hydroxy-spiroindolinone derivative **IV** or a spirobenzoxazinone derivative **V** depending upon the preference of approach of the nucleophile either for the N or the O of nitroso group (Scheme 56) in a stepwise or synchronous manner⁹⁰ (1,5- or 1,6- electrocyclizations).



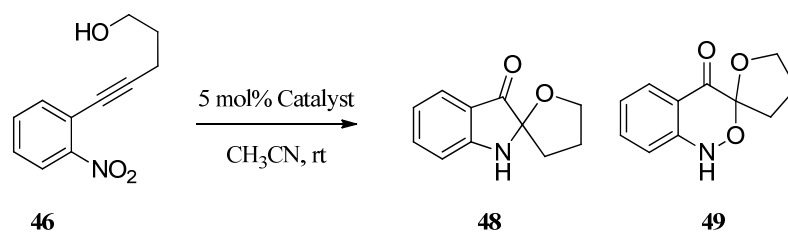
Scheme 56: *Pyridine mediated photochemical isatogen synthesis & hypothetical mechanism for the synthesis of indolinones/benzoxazinones via nitroalkynol cycloisomerization*

2.3.2 Results and discussion

With this concept in mind, the nitroalkynols **46**⁹¹ and **47** were prepared under standard Sonogashira⁶¹ conditions. The feasibility of the proposed cycloisomerization has been examined by screening **46** with various Pd(II) complexes⁵⁵ in different



Scheme 57: *Synthesis of model substrates for cycloisomerization*



Entry	Catalyst	Solvents	Product(s) (48:49)
1	PdCl ₂	CH ₃ CN	1 : 1
2	PdBr ₂	CH ₃ CN	1 : 1
3	PdI ₂	CH ₃ CN	No reaction
		CH ₂ Cl ₂	No reaction
		DMSO	Complex mixture
4	Pd(OAc) ₂	CH ₂ Cl ₂	No reaction
		CH ₃ CN	No reaction
5	Pd(CH ₃ CN) ₂ Cl ₂	CH ₃ CN	1.1 : 1
6	Pd(PhCN) ₂ Cl ₂	PhCN	No reaction

Table 9: Catalysts screened for the nitroalkynol cyclization of **46**

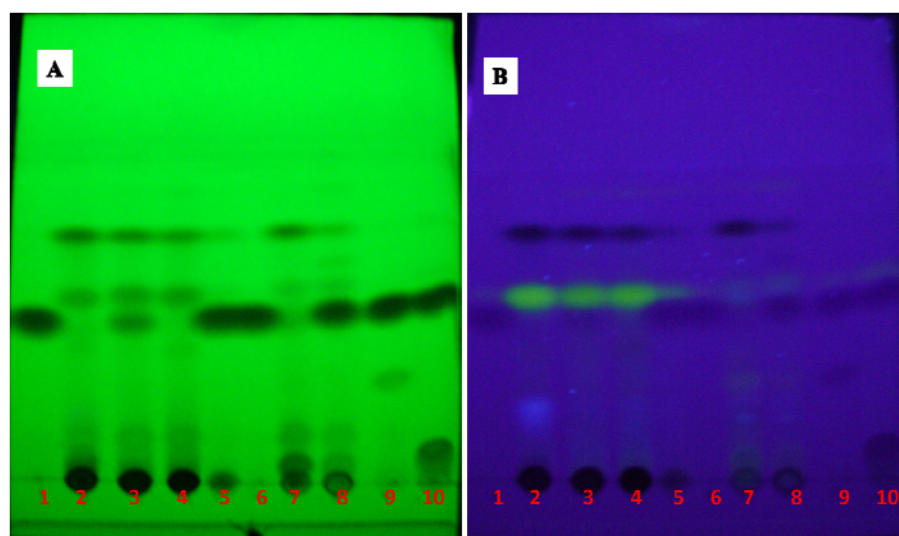


Figure 16: 1- starting, 2- PdCl₂, 3- PdBr₂, 4- Pd(CH₃CN)₂Cl₂, 5,6- PdI₂, 7- PdI₂ in DMSO, 8- Pd(PhCN)₂Cl₂, 9,10 - Pd(OAc)₂Cl₂

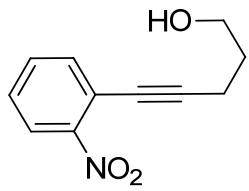
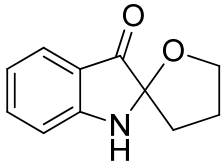
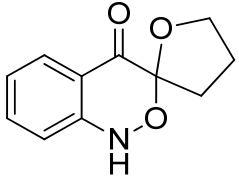
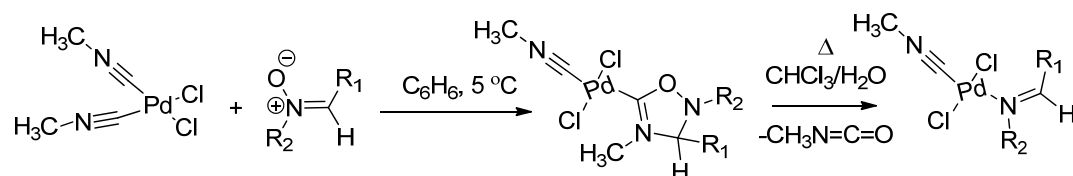
Proton/C arbon			
Aromatic protons	7.38 (ddd, $J = 2.1, 6.6, 8.1$ Hz, 1H), 7.51 (dt, $J = 1.4, 7.8$ Hz, 1H), 7.56 (dd, $J = 2.2, 7.6$ Hz, 1H), 7.95 (dd, $J = 1.3, 7.8$ Hz, 1H)	6.74 (d, $J = 8.1$ Hz, 1H), 6.81 (t, $J = 7.4$ Hz, 1H), 7.41 (ddd, $J = 1.3, 7.3, 8.4$ Hz, 1H), 7.56 (d, $J = 7.7$ Hz, 1H)	6.85 (d, $J = 8.2$ Hz, 1H), 7.05 (t, $J = 7.5$ Hz, 1H), 7.43 (ddd, $J = 1.4, 7.3, 8.3$ Hz, 1H), 7.94 (dd, $J = 1.4, 7.9$ Hz, 1H)
-CH ₂ -OH	3.83 (t, $J = 6.1$ Hz, 2H)	4.02–4.18 (m, 2H)	4.05–4.24 (m, 2H)
≡C-CH ₂ -	2.60 (t, $J = 6.8$ Hz, 2H)	2.21–2.32 (m, 2H)	1.93–2.19 (m, 1H), 2.70–2.85 (m, 1H)
Aromatic Carbon	118.9 (s), 124.3 (d), 127.9 (d), 132.6 (d), 134.6 (d), 149.8 (s)	112.1 (d), 119.0 (s), 119.6 (d), 125.0 (d), 137.8 (d), 159.6 (s)	114.7 (d), 117.7 (s), 122.4 (d), 127.7 (d), 134.8 (d), 150.4 (s)
-C≡C-carbon	76.3 (s) 98.3 (s)	95.0 (s) 200.9 (s)	107.5 (s) 185.1 (s)

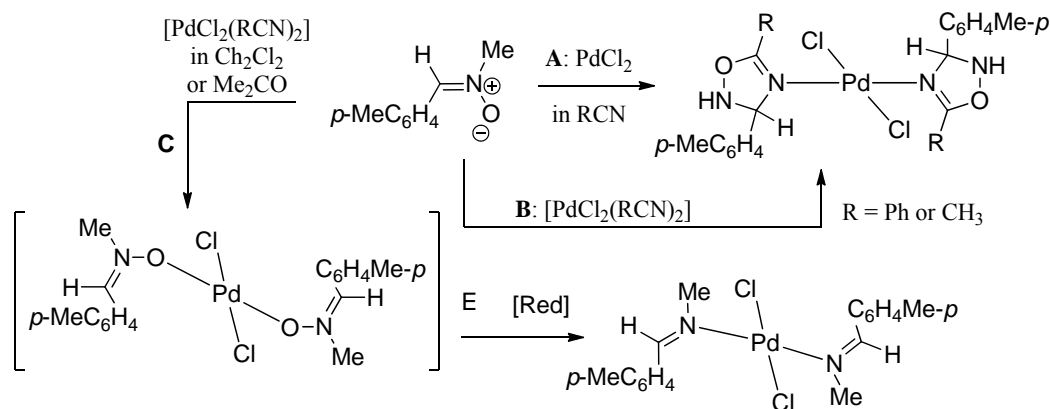
Table 10: Brief comparison of NMR of products with starting compound.

solvents. The cycloisomerization of **46** with a majority of the palladium (II) complexes resulted in the formation of two distinct products (Table 9). The TLC diagram provided in Figure 16 provides a visual indication of the progress/efficiency of the reaction with various complexes. It was observed that PdI₂ is sparingly soluble in a majority of the solvents used and that it has good solubility in DMSO. However, the attempted cycloisomerization with PdI₂ in this solvent gave an intractable complex mixture. Among these complexes, the reaction with Pd(CH₃CN)₂Cl₂ was found to be clean, with a complete conversion of **46** within 6 h at room temperature giving two compounds in a ~1:1 ratio. One of these compounds was shown to fluoresce. The characterization of these compounds was carried out after their separation by column chromatography. Table 10 shows the brief comparison of the ¹H and ¹³C data of the two products with the starting compound. One of the compounds

was found to be the anticipated spirobenzoxazinone derivative **49** whereas the other one which is fluorescent was found to be the spiroindolin-3-one



a) Reactions between *cis*-[PdCl₂(CN-R)₂] and acyclic nitrones

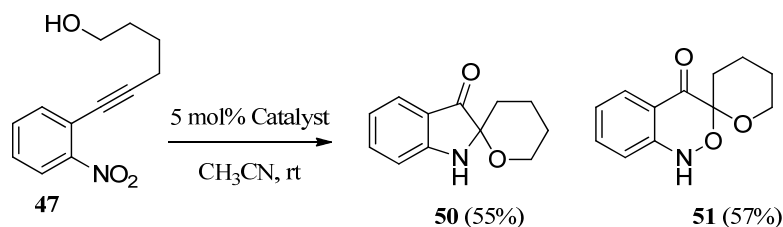


Scheme 58: b) Interplay between Nitrones and (Nitrile)Pd(II) Complexes

derivative **48**. The formation of **48** indicates the reduction of the anticipated *N*-hydroxy indolin-3-one derivative **IV** (Scheme 56) during the course of the reaction. The breakdown of the N–O bond with electrophilic Pd(II)-complexes is a rare example, but it is not unprecedented⁹² (Scheme 58).

To check whether both the products are formed from the same intermediate, we performed controlled experiments such as varying the temperature of the reaction and stirring isolated benzoxazinone **49** in the presence of the Pd(II)-complex. However, it was found that increasing the temperature had no effect on the products ratio and also that **49** was stable in the presence of the Pd(II)-complex employed. The later observation reveals that the indolinone **48** and benzoxazinone **49** are formed *via* independent pathways.

A similar set of catalysts were employed for the cycloisomerization of the hexynol derivative **47** (Table 11). The cycloisomerization of **47** with PdCl₂, PdBr₂ and Pd(CH₃CN)₂ gave exclusively the spiroindolinone **50**,⁹³ whereas the nitro and acetate



Entry	Catalyst	Solvent	Product(s)* (50:51)
1	PdCl ₂	CH ₃ CN	5 : 1
2	PdBr ₂	CH ₃ CN	5 : 1
3	PdI ₂	CH ₃ CN	No reaction
		CH ₂ Cl ₂	
		DMSO	
4	Pd(NO ₂) ₂	CH ₃ CN	No reaction
		CH ₂ Cl ₂	
5	Pd(OAc) ₂	CH ₃ CN	No reaction
		CH ₂ Cl ₂	
6	Pd(CH ₃ CN) ₂ NO ₂ Cl	CH ₃ CN	slow reaction
		CH ₂ Cl ₂	
7	Pd(CH ₃ CN) ₂ Cl ₂	CH ₃ CN	1 : 0
8	Pd(PhCN) ₂ Cl ₂	PhCN	No reaction

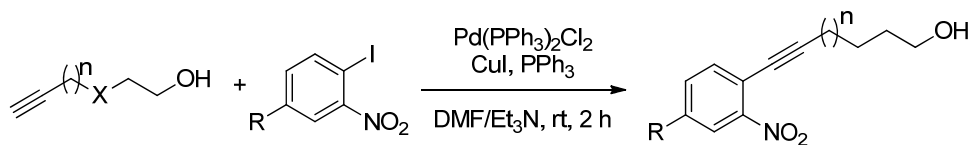
*All the ratios are given on the basis of NMR of crude product.

Table 11: Catalysts screened for the nitroalkynol cycloisomerization of **47**

salts of palladium were found to be inactive for the cycloisomerization reaction. Similar to the previous case, the reaction with Pd(CH₃CN)₂Cl₂ in acetonitrile solvent was clean and gave high yields as compared to other catalysts. The reaction with PdI₂ gave results similar to that obtained with the pentynol derivative.

After a preliminary screening of various metal complexes, the next step was to extend the scope and generality of the palladium mediated nitro-alkynol

cycloisomerization. For this, a variety of nitroalkynol derivatives were prepared by using three different alkynols and various substituted o-iodonitrobenzene derivatives



Scheme 59: preparation of nitroalkynol substrates

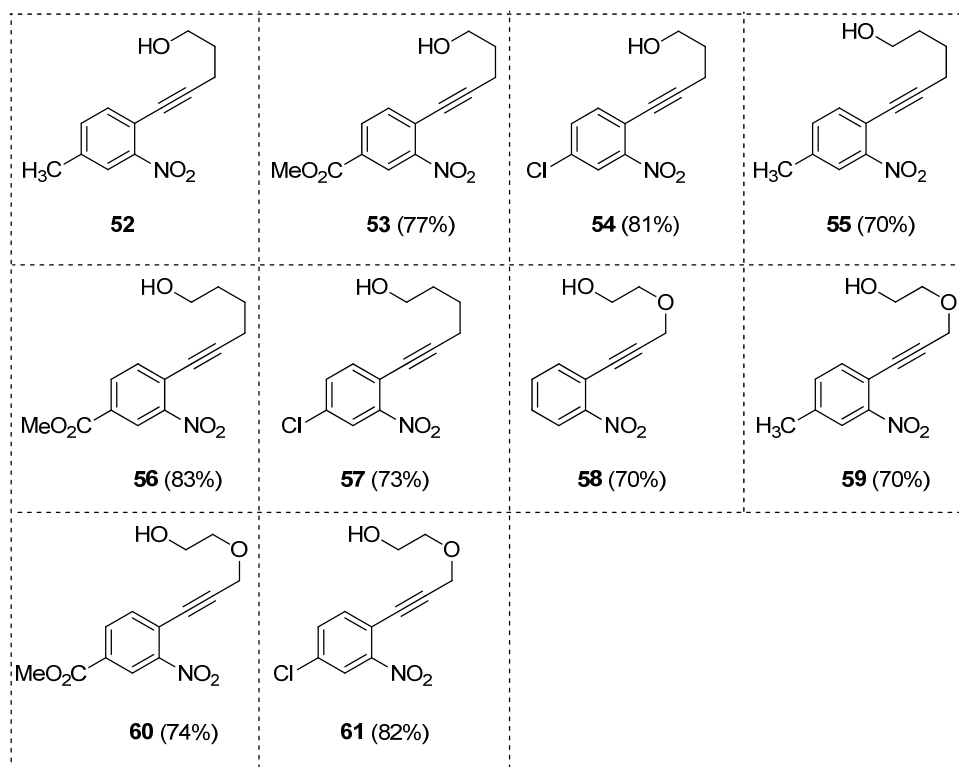
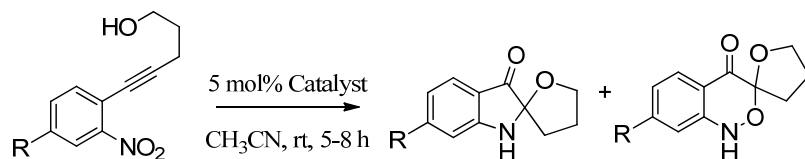


Table 12: Preparation of substrate for nitroalkynol cycloisomerization by Sonogashira coupling.

(Table 12). Quite interestingly, the isolation and characterization of compound **52** was found to be difficult due to the cyclization of purified **52** (in CDCl_3 solution). This might be resulting from the presence of trace amounts of palladium complex from the Sonogashira coupling reaction.

The [Pd]-catalyzed cycloisomerization of all the synthesized nitroalkynols **52**–**61** was carried out under established conditions (Table 13). The cycloisomerization of

all the pentynol derived nitroalkynols gave a mixture of both spirobenzoxazinone and spiroindolin-3-one derivatives in equal amounts. For a solid structural confirmation,



Entry	Nitro-Alkynol	Products/Yield (%)	
1	 52	 62 (36%)	 63 (34%)
2	 53	 64 (38%)	 65 (34%)
3	 54	 66 (32%)	 67 (31%)

Table 13: Screening of various nitropentynol derivatives for cyclization

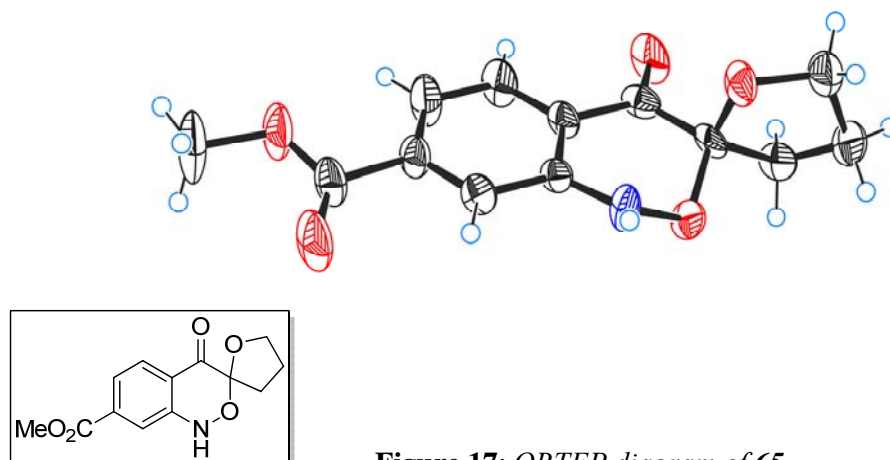
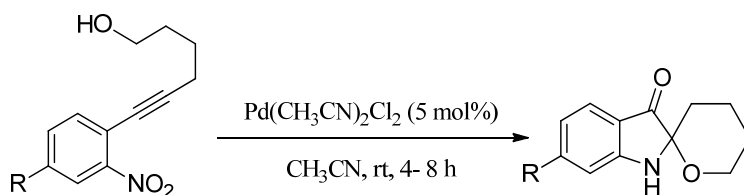


Figure 17: ORTEP diagram of **65**

the single crystal X-Ray structure of spirobenzoxazinone compound **65** has been carried out which confirmed its proposed structure (Figure 17). The structural integrity of other compounds has been established by spectral and analytical data and by comparing the ^1H NMR spectral data with that of the parent benzoxazinone or the indolinones.

Similarly, the hexynol derived nitroalkynol substrates were subjected for cycloisomerization with $\text{Pd}(\text{CH}_3\text{CN})_2\text{Cl}_2$. Exclusive formation of spiroindolin-3-ones

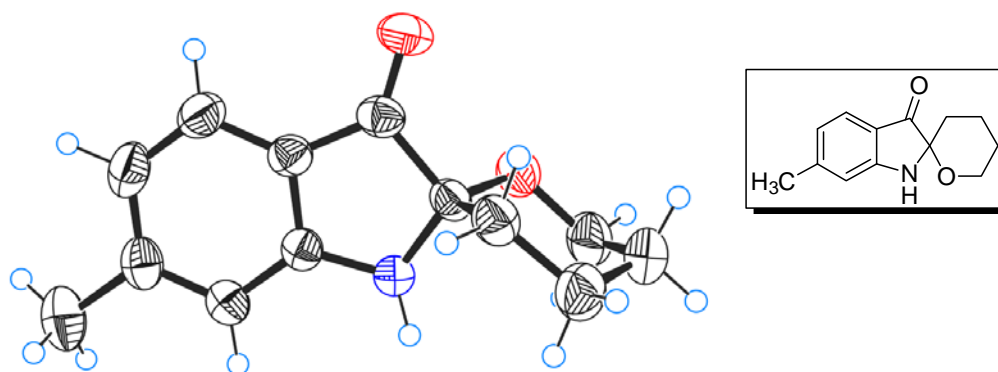


Scheme 60: Pd mediated nitroalkynol cycloisomerization

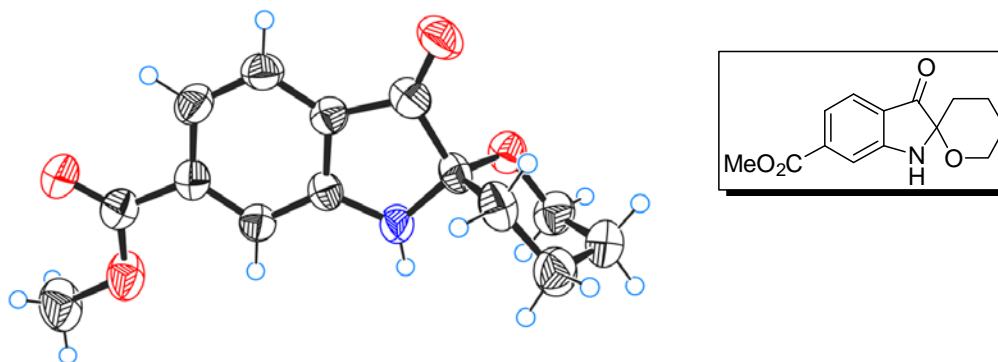
Entry	Nitro-Alkynol	Products/Yield (%)
4	 55	 68 (79%)
5	 56	 69 (84%)
6	 57	 70 (82%)

Table 14: Screening of various nitro-alkynol derivatives for Pd- cycloisomerization

was observed with all the hexynol derivatives (Table 14). The structures of the compounds were confirmed by spectral and analytical data. Furthermore, the structures of the spiroindolin-3-ones **68** and **69** were confirmed by single crystal X-ray (Figure 18) analysis.



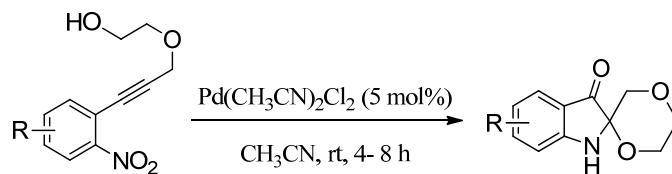
(a) ORTEP diagram of **68**



(b) ORTEP diagram of **69**

Figure 18: ORTEP diagram for the titled compounds.

The cycloisomerization method was also applied to propargyl glycol derivatives **58–61**, and the spiroindolin-3-one derivatives were isolated exclusively in good to excellent yields (Table 15). The structures of the compounds were confirmed from NMR and HRMS data. For example, in the ^{13}C NMR of compound **71**, peaks at δ 86.6 (s) and 195.9 (s) correspond to the newly generated quaternary center and carbonyl carbon respectively. HRMS for the same compound was found to be 228.0598 ($[\text{M}+\text{Na}]^+$) against the calculated value of 228.0637 ($[\text{M}+\text{Na}]^+$).

**Scheme 61:** Pd mediated nitroalkynol cyclisomerization

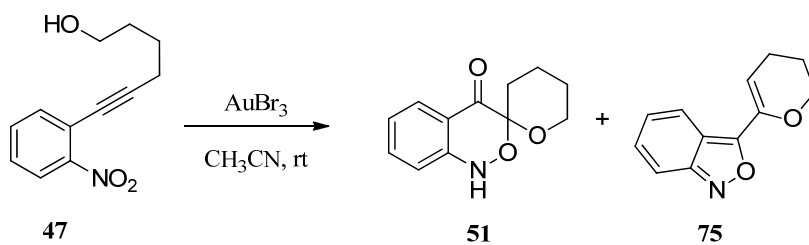
Entry	Nitro-Alkynol	Products/Yield (%)
1	 58	 71 (64%)
2	 59	 72 (80%)
3	 60	 73 (82%)
4	 61	 74 (78%)

Table 15: Screening of various nitro-alkynol derivatives for Pd- cyclisomerization

From the above observations, we can conclude that the cyclisomerization of pentynol derived nitroalkynols results in the formation of both spiroindolin-3-one and spirobenzoxizin-4-one in nearly equal amounts. On the other hand, the hexynol derived nitroalkynol substrates gave only the spiroindolin-3-one products. The

exclusive formation of indolinones with hexynols is quite remarkable and indicates that the nitroalkyne cycloisomerization leading to the isatogens is in operation than the alkynol cyclization and subsequent events as proposed in the Scheme 56. Considering our previous experience with the cycloisomerization of simple *o*-(alkylalkynyl)-nitrobenzenes and divergent products resulting from the [Pd]- and [Au]-catalyzed reactions (Schemes 49 and 50) we were interested to explore the [Au]-mediated nitroalkynol cycloisomerizations and learn about the difference in the mode of the reactivity of these complexes when compared to that of the [Pd]-complexes.

Initially, we used the pentynol **46** as a substrate and its cycloisomerization was attempted with AuCl₃ and AuBr₃. However, with both the salts, the reactions led to the formation of a polar mixture the identity of which could not be determined.



Entry	Substrate	Catalyst	solvent	Product (72:73 , % yield)
1	46	AuBr ₃	CH ₃ CN	Complex Mixture
2		AuCl ₃	CH ₂ Cl ₂	Complex Mixture
3	53	AuBr ₃	CH ₃ CN	Complex Mixture
4	47	AuBr ₃	CH ₃ CN	3.6 : 1
5		AuBr ₃	CH ₂ Cl ₂	4 : 3
6		AuCl ₃	CH ₃ CN	Complex Mixture
7		AuCl ₃	CH ₂ Cl ₂	4 : 3
8		HAuCl ₄	CH ₃ CN	Complex Mixture
9		HAuCl ₄	CH ₂ Cl ₂	5 : 6
10		(PPh ₃) ₃ (O)Au ₃ BF ₄	CH ₃ CN	Complex Mixture

11		$(\text{PPh}_3)_3(\text{O})\text{Au}_3\text{BF}_4$	CH_2Cl_2	1.5 : 1
12		<i>cis</i> -Pt(CH ₃ CN) ₂ Cl ₂	CH ₃ CN	No Reaction
13		<i>cis</i> -Pt(PhCN) ₂ Cl ₂	PhCN	No Reaction

Table 16: Screening of various gold catalyst for nitroalkynol cycloisomerization

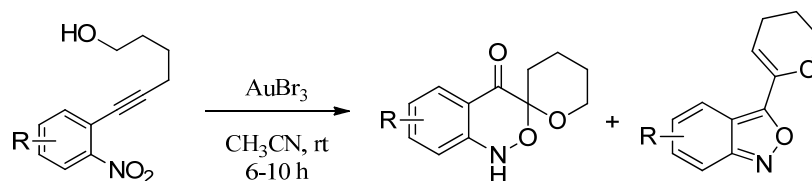
Changing the solvent had no effect on the outcome of this reaction. Next, the cycloisomerization of the hexynol derivative **47** (Table 16) with various gold complexes was examined. Table 16 shows the various complexes employed in this regard. With the three Au(III) salts, the outcome of the reaction was solvent dependent. With acetonitrile as the solvent, the cycloisomerization of **47** with AuBr₃

Protons/ Carbon			
Ha	2.48 (t, <i>J</i> = 6.4 Hz)	1.76–1.84 (m)	5.88 (t, <i>J</i> = 4.3 Hz)
Hb	1.66–1.76 (m)	1.58–1.74 (m)	2.28–2.32 (m)
Hd	3.68 (t, <i>J</i> = 5.8 Hz)	3.88–3.94 (m)	4.24 (t, <i>J</i> = 5.1 Hz)
Ca	31.6 (t)	24.5 (t)	
Cd	62.1 (t)	63.5 (t)	66.6 (t)
Aromatic protons	7.37 (ddd, 1H) 7.50 (dt, 1H) 7.56 (dd, 1H) 7.94 (dd, 1H)	6.85 (d, 1H) 7.05 (t, 1H) 7.43 (ddd, 1H) 7.94 (dd, 1H)	6.93 (dd, 1H) 7.25 (dd, 1H) 7.49 (d, 1H) 7.78(d, 1H)

Table 17: ¹H and ¹³C NMR chemical shift for compound xx, xx and xx

predominantly gave the spiorbenzoxazinone **51**, with anthranil **75** as a minor product. Under similar conditions, the reactions with AuCl₃ and HAuCl₄ in acetonitrile resulted in the immediate disappearance of alkynol and gave intractable polar

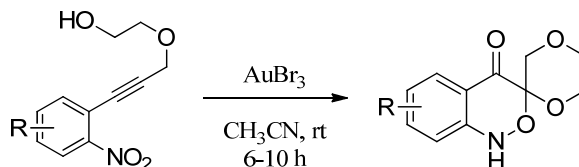
mixtures. When the solvent was changed to CH_2Cl_2 , a mixture of spirobenzoxazinone **51** and the anthranil compound **75** were obtained in moderate yields with AuCl_3 and HAuCl_4 . All the products were characterized by spectral and analytical data. Table 17 shows a brief comparison of NMR data of both the products with the starting compound.



Entry	Nitro-Alkynol (%)	Products/Yield (%)	
1	 47	 51 (57%)	 75 (10%)
2	 55	 76 (35%)	 77 (30%)
3	 56	 78 (40%)	 79 (35%)
4	 57	 80 (38%)	 81 (32%)

Table 18: [Au]-Catalyzed nitroalkynol cycloisomerization (0.5 mol% Pd (II) in acetonitrile at rt for 5-8 h)

Having been successful with the cycloisomerization of hexynol derivative **47** and considering the product divergence resulting from the catalyst employed, we have further explored the present cycloisomerization with the available hexynol derivatives. The reactions were facile and the benzoxazinones products were obtained in good to excellent yields (Table 18). The formation of substantial amounts of anthranil derivatives was noticed in the reactions of all the hexynols.



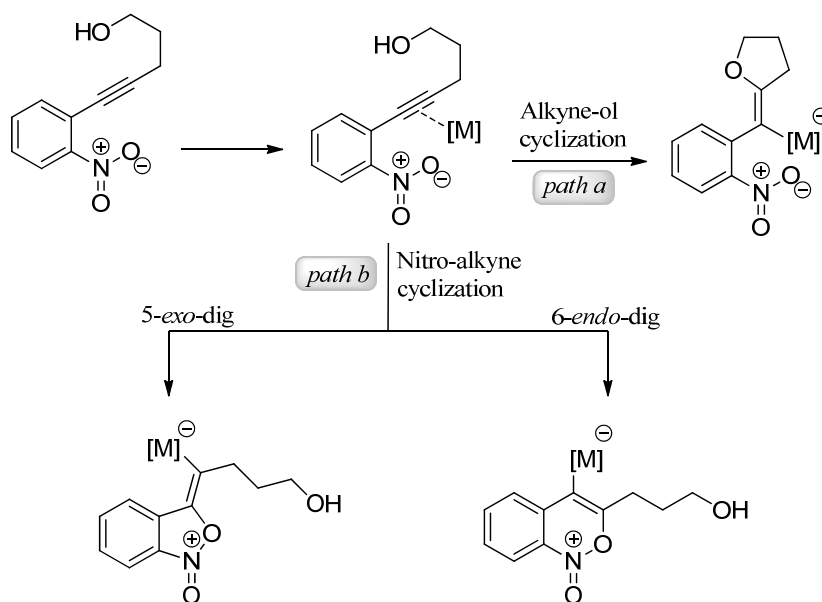
Entry	Nitro-Alkynol (%)	Products/Yield (%)
1	 58	 82 (51%)
2	 59	 83 (72%)
3	 60	 84 (85%)
4	 61	 85 (67%)

Table 19: Generalization of [Au]-catalyzed nitroalkynol cycloisomerization

Similarly, the gold mediated nitroalkynol cyclization of the available propargyl glycol derived nitroalkynols **58–61** were carried out under established conditions (Table 19). With all these substrates, the cyclizations led to the exclusive isolation of spirobenzoxazin-4-one derivatives. The structures of all the products were confirmed by spectral and analytical data.

2.3.3. Mechanism

The possible mechanism for the palladium/gold catalyzed nitroalkynol substrate involves initial formation of the palladium-alkyne coordinated complex. This can undergo further transformation through two possible pathways depending on the attack of the nucleophile on the alkyne complex. That is, the [M]-catalyzed cycloisomerization can take place through two competing pathways – a) the alkyne



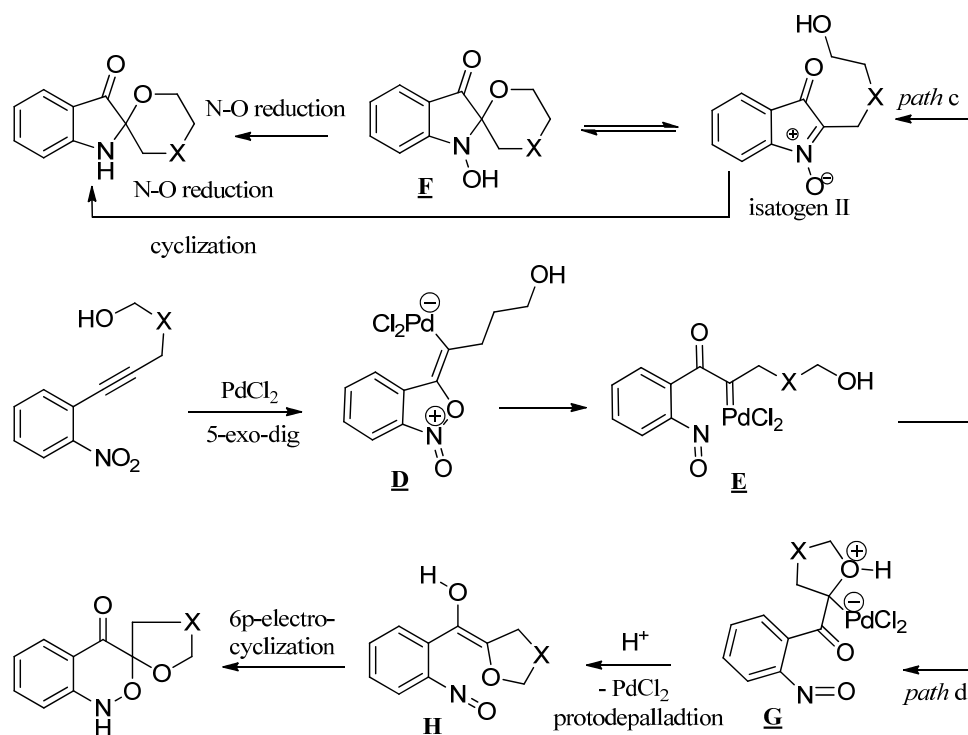
Scheme 62: Possible mode of cyclization in presence of Metal

cycloisomerization (path a; Scheme 62), where the hydroxy group acts as a nucleophile in competition with the nitro group and b) the internal redox *via* nitroalkyne cycloisomerization (path b; Scheme 62) leaving the hydroxy group as a spectator (Scheme 62). With the alkyne cycloisomerization, the formation of proto-demetalated intermediates such as *exo*-glycols as side products is expected.⁵⁹ However, no such side products were observed and we speculated that the reactions

were proceeding with the initial internal nitroalkyne redox. Next, the internal N–O bond redox could occur either by the 5-*exo*-dig or 6-*endo*-dig⁹⁴ mode of nitroalkyne cycloisomerization depending upon substrate and the metal complex employed.

2.3.3.1. [Pd]-Catalyzed cycloisomerization

As described in the previous section, for [Pd]-mediated cycloisomerization, the internal N–O bond redox could occur only by the 5-*exo*-dig mode of nitroalkyne cycloisomerization, as it is less energetic and more favourable than the 6-*endo*-dig mode. In the first case, when we extend the reaction to the Pd[II]-mediated cyclization,⁹⁵ a 5-*exo*-dig nitro-alkyne cyclization gives **D** which, upon internal N–O bond redox, leads to the intermediate metal carbene **E** (Scheme 63). This metal

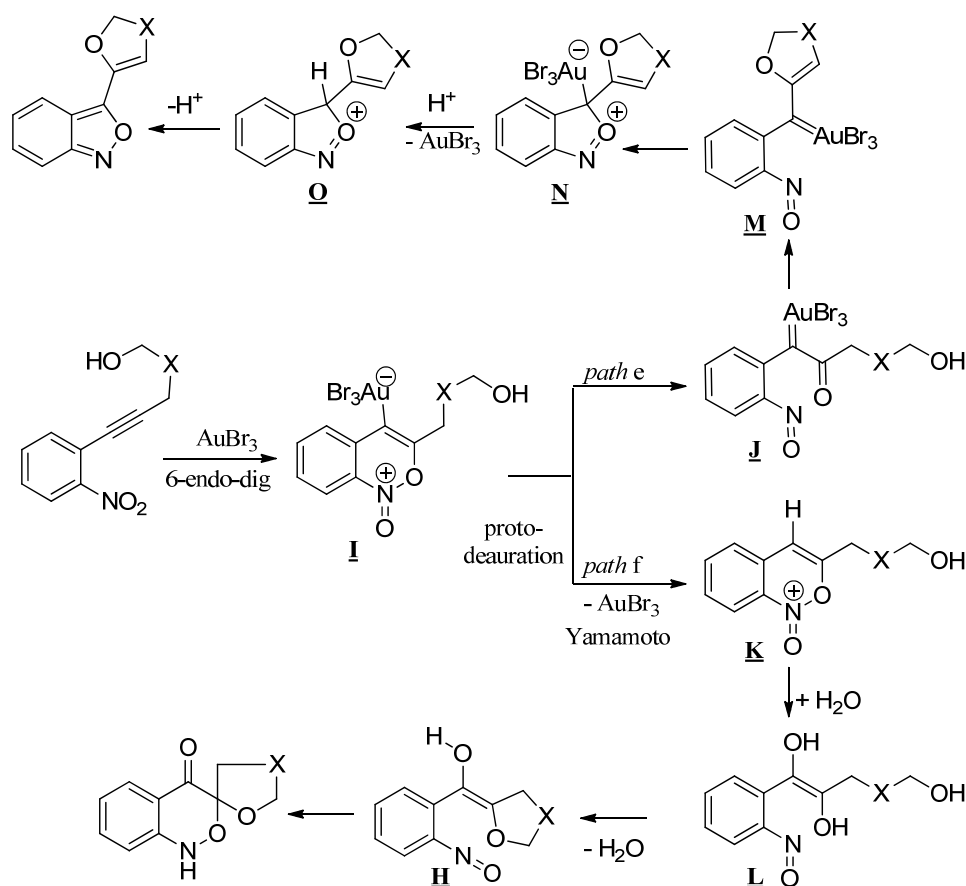


Scheme 63: Possible catalytic path way for the [Pd] mediated cycloisomerization

carbene **E** could undergo a nucleophilic addition either by the nitrogen of the nitroso-group or by the oxygen of the –OH group. With the pentynol substrates, where both these additions lead to a 5-membered heterocycle, both the cyclizations seem to be competing equally, leading to two different products in equal proportions. The addition of the nitrogen to the metal carbene (Scheme 63, *path c*) leads to the isatogen

II which subsequently undergoes an intramolecular addition of the –OH group to the imine carbon preceded or preceded by the N–O bond reduction and thus gives the indolinone. On the other hand, the addition of –OH to the metal carbene followed by the proto-depalladation (Scheme 63, *path d*) leads to the enol **H**, which subsequently undergoes a $6n$ -electrocyclization resulting in the benzoxazinone. When the addition of the –OH forms a 6-membered ring, which is the case with hexynols and propargyl glycols, the cyclization is energetically more demanding and the addition of nitrogen of the nitroso-group to the metal carbene is the exclusive pathway, thereby providing only the indolinones.

2.3.3.2. [Au]-Catalyzed cycloisomerization



Scheme 64: Possible catalytic path way for the gold mediated cycloisomerization

Next, considering available information, for the cyclizations with the Au[III]-complex, we extend the 6-*endo*-dig mode of nitroalkyne cycloisomerization and the formation of the alkenyl-Au[III] species **I**. The intermediate **I** can undergo either an

internal redox forming the regioisomeric metal carbene **J** (Scheme 64, *path f*) or a protodemetalation giving nitronate **K**. The intermediate **K** upon hydration gives the *nitroso-ene-diol* **L**. This path is in parallel with the mechanism that has been extended by Yamamoto²⁹ for nitroalkyne cycloisomerizations leading to isatogens and/or anthranils.³¹ The resulting ene-diol **L** could be trapped by the internal OH nucleophile to provide the intermediate **H**. The intermediate **H** should undergo a *6n*-electrocyclization to give the benzoxazinone. The formation of benzoxazinones either as the major or as exclusive products indicates that with AuBr₃, the protodemetalation seems to be more facile than the metallocarbene formation. The formation of anthranil side products could be explained by the internal addition of the oxygen of the nitroso group to the metal carbene **M** (formed *via* the dehydration of the metal carbene **J**) resulting in **N**, which upon proto-demetalation followed by deprotonation forms the anthranil (Scheme 64, *path e*).

2.4. Friedel-Craft alkylation of spiroindolin-3-ones: A sequential metal catalyzed approach for the central tricycle core structure of Isatisine A

The 2,2-disubstituted indolin-3-one (pseudo indoxyl) group is an important structural feature or an advanced intermediate for many important biologically active natural products. Like isatisine A, mersicarpine, austamide and notoamide O³² (Figure 19). Numerous efforts have been made by many groups for the development of a method for the synthesis of 2,2-disubstituted indolin-3-one derivatives. The first reliable method was reported by Kishi in 1978,⁹⁶ which was used as part of the total synthesis of austamide. But unfortunately, this method was limited to the creation of only spirocycles. A related method developed by McWhorter in 2003 involves Grignard addition to 2-arylidolone to generate 3*H*-indol-3-ol,⁹⁷ which, upon treatment with acid, undergoes pinacol-like rearrangement to give 2,2-disubstituted indolin-3-one. Another important and original method that needs a mention in this regard is the Smalley's rearrangement.⁹⁸

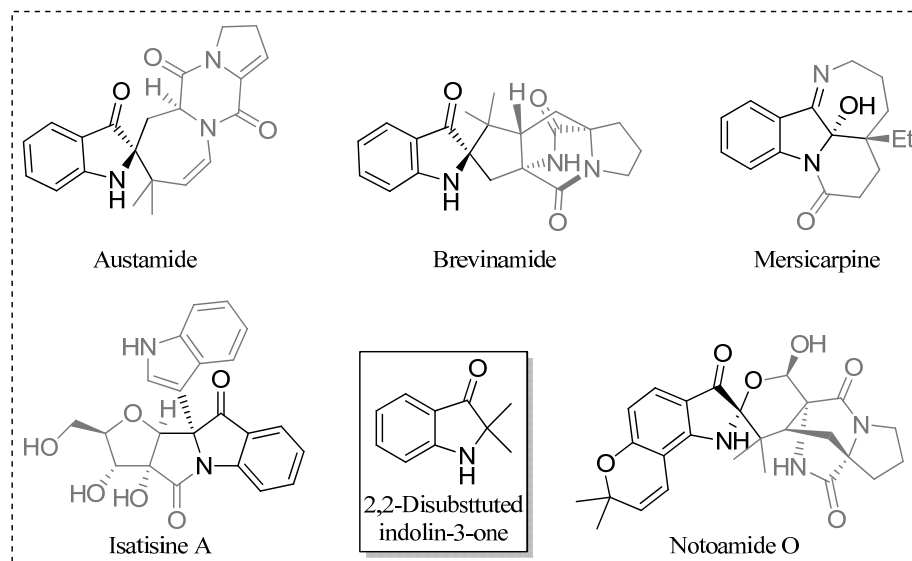


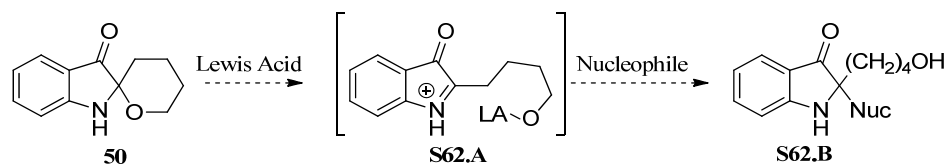
Figure 19: Natural products having a 2,2-disubstituted indolin-3-one structural unit

As discussed earlier, Isatisine A was taken as our prime target and we had already developed two separate methods to construct the central indolin-3-one unit. The first one was palladium catalyzed nitroalkyne cycloisomerization for the

synthesis of isatogens and the second was the palladium catalyzed nitroalkynol cycloisomerization leading to spiroindolin-3-one derivatives. According to our retro synthetic approach for Isatisine A, our next concern was to develop a method for addition of indole either to an isatogen or to a spiroindolin-3-one unit followed by metal catalyzed oxidative lactamization. In this context, prior to starting the synthesis of Isatisine A, we were interested in executing a model study for the core structure of the molecule by first developing methods for alkylation of spiroindolin-3-one followed by oxidative lactamization.

2.4.1. Our approach for core of Isatisine A

Our working hypothesis was based on Kobayashi's report of TiCl_4 mediated alkylation of spiroindolin-3-one. The opening of the *spiro-N,O*-ketal **50** with a Lewis acid to regenerate electrophilic indolone **A**, followed by addition of an external nucleophile, could allow the construction of the nitrogen-containing quaternary center of a 2,2-disubstituted indolin-3-one **50** through a Mannich-type reaction (Scheme 65). This means that the *spiro-N,O*-ketal **50** could serve as a masked, stable 2-alkylindolone, a moiety known to be highly unstable. Based on this concept, Yoshihisa Kobayashi *et al.* have reported the Lewis acid mediated addition of various



Scheme 65: Lewis acid mediated activation of a masked indolone

nucleophiles (not indole) on spiroindolin-3-one, to obtain 2,2-disubstituted indolinone. The main disadvantage of this method was the use of TiCl_4 , which may not be suitable in the context of our isatisine A total synthesis, as the intermediate involved would be endowed with the sensitive functional or protecting groups. To avoid the harsh conditions, we opted to search for a milder Lewis acid for this proposed C–C bond formation event.

After having a careful look at the above approach, we assumed that the C (3) carbon of indole can act as a nucleophile for the Friedelcraft alkylation of spiroindolin-3-one, in presence of metal salt/Lewis acid to form the desired indole addition product. If we can do so, then the oxidative coupling of the alcohol and indoline amine to form the lactam should give the core structure of Isatisine A. That means that the core of Isatisine A can be achieved starting from simple and commercially available starting compounds using four metal catalyzed transformations – namely i. a Pd-mediated Sonogashira coupling, ii. An in-house developed Pd-mediated nitroalkyne/nitroalkynol cyclisomerization, iii. a metal mediated Mannich type reaction which is yet to be developed and iv. scouting for a suitable metal-mediated oxidative cyclization of γ -aminoalcohols leading to the γ -lactams. Thus, starting with pentynol and 2-nitro iodobenzene and following the above-mentioned four reaction sequences can give the tricyclic core of Isatisine A (Figure 20). During these studies,

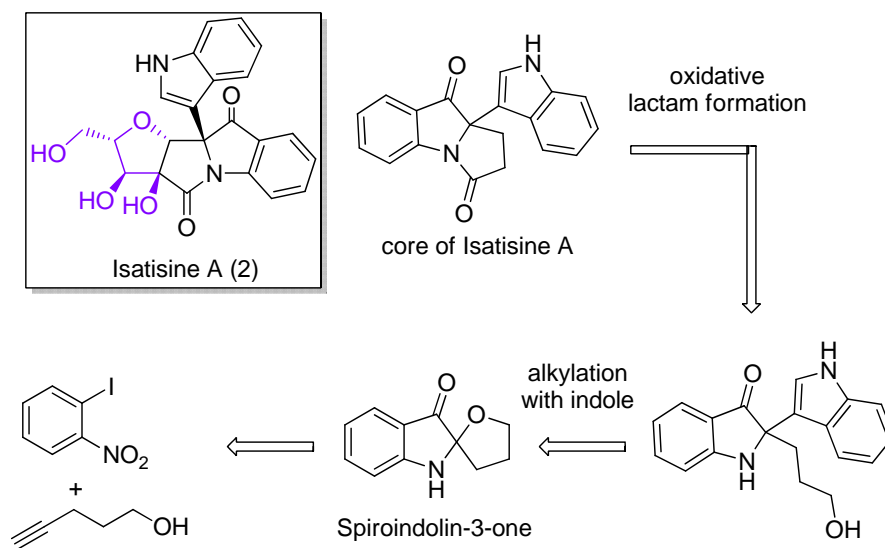
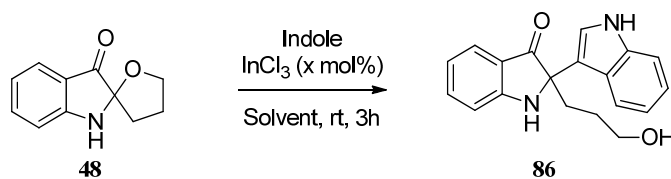


Figure 20: Retro synthetic approach for the core of Isatisine A

an InCl_3 mediated C(2)-alkylation of isatogen with indole was developed in our group. Following this, we planned to use the same InCl_3 as a Lewis acid for the alkylation of spiroindoline-3-one with indole.

2.4.2. Result and discussion

With this concept in mind, the spiroindolinones **48** prepared earlier was subjected for the alkylation reaction, by treatment with indole (1.3 eq.) in presence of InCl_3 (5 mol%) in acetonitrile as a solvent at room temperature (Scheme 66). After 3 h, the starting material was consumed completely and a single slower moving spot was observed on TLC. Control experiments revealed that the alkylation of **48** was feasible in the halogenated solvents such as CH_2Cl_2 , DCE (Table 20), while in other solvents such as acetone, toluene and THF, the starting spiroindolinone was found to be intact. Among all solvents, acetonitrile was found to be the best, resulting in



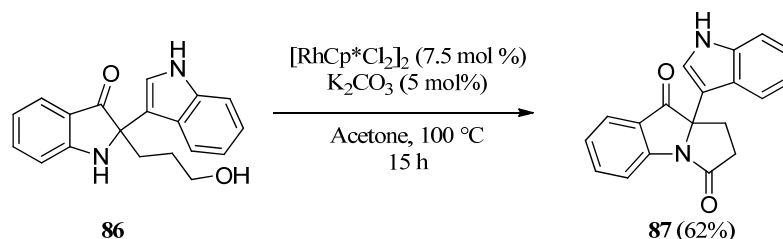
Scheme 66: Alkylation of spiroindolin-3-one with indole

Entry	Solvent	InCl_3 (mol %)	Time	Product (% yield)
1	CH_2Cl_2	1	3 h	45
2	DCE	1	3 h	37
3	THF	1	24 h	No reaction
4	CH_3CN	1	15 min	69–78
5		0.5	45 min	
6		0.1	2 h	
7		0.05	5 h	
8	Acetone	1	24 h	No reaction
9	Toluene	1	24 h	No reaction

Table 20: Screening of different condition for alkylation reaction

the isolation of the requisite addition product **86** in better yields. Furthermore, the reaction was carried out in acetonitrile by varying the amount of InCl_3 . When one equivalent of InCl_3 was employed, the reaction was complete within 15 minutes and compound **86** was obtained in excellent yields. The structure of compound **86** was established with the help of spectral and analytical data. For example, in the ^1H NMR spectrum of compound **86**, the appearance of an additional multiplet by the integration of five protons in the range of δ 6.74–7.55 indicated the presence of an indole unit. Similarly, the desired eight extra peaks in ^{13}C NMR of compound **86**, the presence of indole carbons signals in the range of δ 112.1–162.5 and the C(3) carbon of spiroindolin-3-one at δ 206 have further confirmed the proposed structure of **86**.

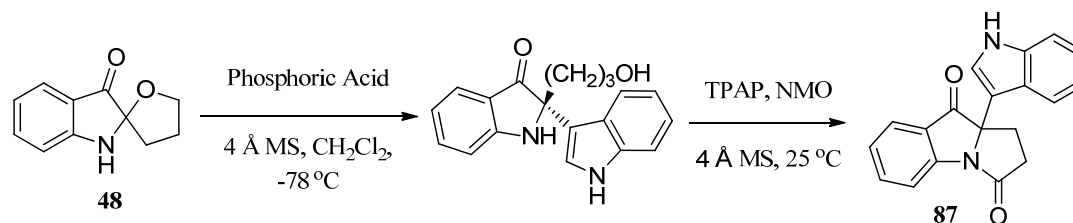
The next objective was the metal catalyzed oxidative lactamization of the γ -aminoalcohol **86**. It has been an old, routine literature procedure that the formation of amide pursued the path of oxidation of alcohol to acid followed by Lewis acid or base mediated cyclization leading to the lactams, which is also sometimes complicated when the intermediate is heavily functionalized. So, in order to avoid such difficulties, we sketched our plan to install the crucial lactam through a metal mediated oxidation. After screening various transition metal catalysts that have been prescribed for this



Scheme 67: Rhodium mediated oxidative coupling of amine alcohol

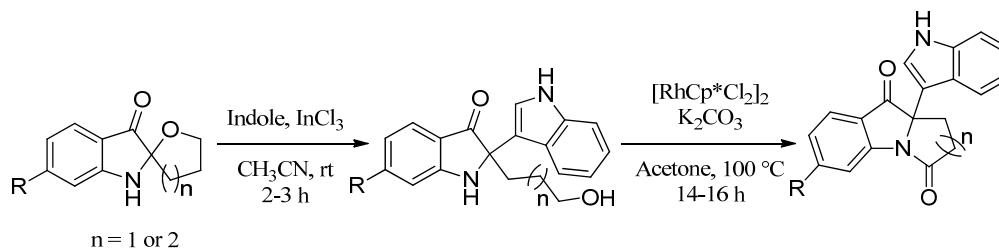
purpose,⁴² it was realized that the $[\text{Cp}^*\text{RhCl}_2]_2$ was the most fruitful catalyst in this regard. Thus, the treatment of aminoalcohol **86** with $[\text{Cp}^*\text{RhCl}_2]_2$ (8 mol%) and K_2CO_3 (5 mol%) in acetone at 100 °C for 15 hours in a sealed tube, provided the required benzo-fused lactam **87** in 62% yield (Scheme 67). The structure of the lactam **87** was confirmed by spectral and analytical data. While this work was in progress, You⁴¹ et al. reported the synthesis of this compound by using a phosphoric acid mediated addition of indole to the spiroindolin-3-one **48** and subsequent oxidative

cyclization by using TPAP and NMO as the oxidant in stoichiometric amounts (Scheme 68).



Scheme 68: *Asymmetric Friedel–Craft reaction of spiroindolin-3-one with indole*

To show the generality of this γ -lactam synthesis, we employed the other available spiroindolin-3-ones **62** and **64** the synthesis of which was described in the previous section (Table 13). The indole addition reactions with **62** and **64** were carried out using 1 eq. InCl_3 as a reagent to obtain the corresponding indole addition products **88** (79%) and **89** (86%) respectively. The spectral and analytical data were in accordance with the assigned structure. The oxidative cyclization of the resulting γ -amino alcohols **88** and **89** was facile under the above-mentioned conditions and resulted in the cyclized products **92** (63 %) and **93** (67%) in good yields. To extend the generality of this method, we have next proceeded for the synthesis of δ -lactams from the corresponding δ -amino alcohols. The hexynol derived spiroindolin-3-one **68** was prepared according to the established two-step catalytic sequence being both the steps catalyzed by palladium and was subjected for the [In]-mediated indole addition and subsequently the resulting amino alcohol for a [Rh]-catalyzed oxidative cyclization to obtain the δ -lactam **94**. In the CMR spectrum, absence of the one tertiary carbon and presence of quaternary carbon at δ 170 confirmed the lactam – C=O group. Other available hexynol derived spiroindolin-3-ones **69** have been also



Scheme 69: *Generalization of the approach*

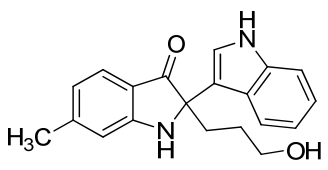
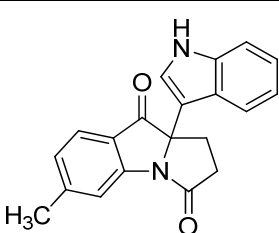
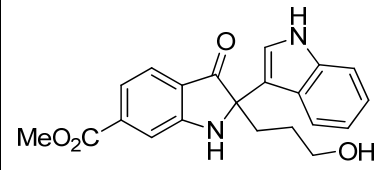
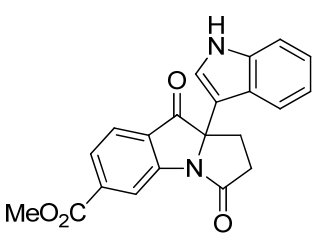
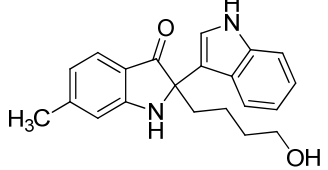
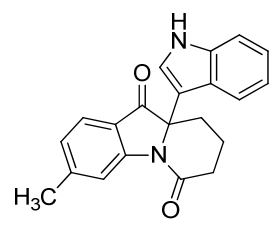
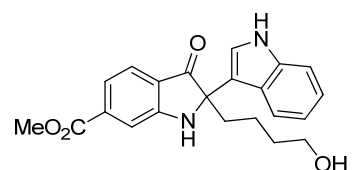
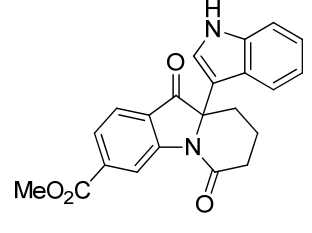
Entry	R	Alkylation product	Cyclized product
1	-CH ₃	 88 (79 %)	 92 (63 %)
2	-CO ₂ Me	 89 (86 %)	 93 (67 %)
3	-CH ₃	 90 (88 %)	 94 (58 %)
4	-CO ₂ Me	 91 (89 %)	 95 (64 %)

Table 21: Generalization of the sequential approach for γ - and δ -lactam derivative

employed for this purpose and the results are given in the in table 21. All the reactions were ensured in the usual manner under the same conditions and the nature aryl substituents (either electron donating or with drawing) seems to have less influence. Next, we examined the scope of these conditions with the available propargyl glycol derived spiroindolin-3-ones **71** and **72**. The [In]-mediated indole additions to **71** and **72** proceeded smoothly to provide the products **96** and **97** respectively in good yields.

Surprisingly, the [Rh]-catalyzed oxidative cyclization of **96** and **97** was sluggish and prolonging the reactions led mainly to the partial decomposition of the starting compounds. At the end, we could isolate the product in negligible amounts (only 1–5%) along with the substantial amounts of unreacted starting materials (Table 22). Even after altering all possible reaction conditions such as prolonged heating or varying the catalyst and carbonate amount etc., no substantial enhancement in yield or completion of the reaction could be achieved.

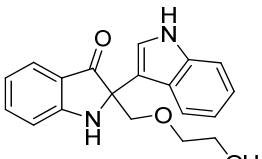
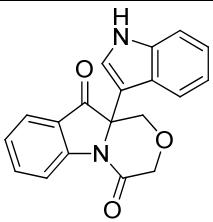
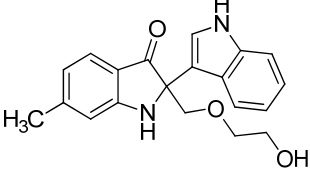
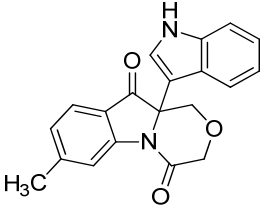
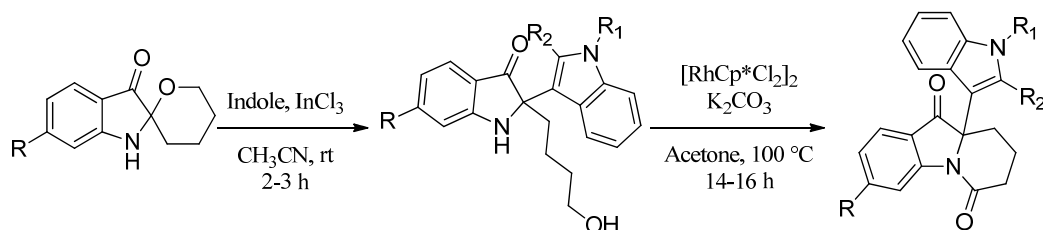
Entry	Spiroindolin-3-one	Alkylation product	Cyclized product
1	71	 96 (77 %)	 98 (5 %) + 96 (52%)
2	72	 97 (79 %)	 99 (3 %) + 97 (61%)

Table 22: Alkylation (1 mol% InCl_3 in CH_3CN solvent) Followed by lactamization (0.08 – 1 eq. $[\text{RhCp}^*\text{Cl}_2]_2$, 0.05 eq. K_2CO_3) of propargyl glycol derivative

After examining the possibility of changing substituents in the spiroindolin-3-one, we next examined the scope of this strategy with substituted indoles. The N–Me and C(2)–Me substituted indoles were chosen as nucleophiles in this regard. The [In]-mediated addition of 2-methyl indole with hexynol derived spiroindolinones **50** and **69** proceeded smoothly under standard conditions and the corresponding addition products **100** and **101** respectively were obtained in good yields (Table 23). The oxidative cyclization of these δ -aminoalcohol with cat. $[\text{Cp}^*\text{RhCl}_2]_2$ gave the benzo fused lactam products **103** and **104**. Similarly, the addition of N-methyl indole to **48** and subsequent oxidative lactamization of intermediate aminoalcohol **102** gave the benzo fused lactam **105** in 65% yield.



Scheme 70: Generalization of the sequential approach with substituted indole

Entry	R ₁ /R ₂	Spiro Comp.	Alkylated product (% yield)	Lactam product (% yield)
1	H/CH ₃	50	<p>100 (87 %)</p>	<p>103 (65 %)</p>
2	H/CH ₃	69	<p>101 (86 %)</p>	<p>104 (59 %)</p>
3	CH ₃ /H	48	<p>102 (89 %)</p>	<p>105 (65 %)</p>

Table 23: Generalization of the sequential approach with substituted indole

This exercise thus completed the development of the key tools that effectively address the construction of the fused-tricyclic core of isatisine A. All four reactions being [M]-catalyzed/mediated ones, they address the key C–C and C–hetero atom bond formation steps, applied one after the other in a four step sequence. Now a stage has been set for the execution of their applicability in the total synthesis of isatisine A - a risky proposition which is going to be realized in the final stages of the total synthesis.

2.5. Total Synthesis of Isatisine A

The total synthesis of complex natural products remains the challenging, educative, and continuously contemporary area in organic chemistry. As a part of our total synthesis program, we aim to develop new strategies and methods that make the process of synthesizing natural products as efficient and flexible as possible. Needless to say, the design of the overall synthetic plan of the total synthesis is an important aspect as is the development of new methods, especially the catalytic ones, which address the skeletal complexity of the targeted molecules. Our group has been actively engaged in developing a new philosophy for synthesizing molecules, which is rightly called the target cum flexible synthesis platform; wherein, we emphasize that that right selection of building blocks and reactions must enable *not* one single target molecule but should result in a collection of small molecules having a similar core. In this context, we have selected the total synthesis of Isatisine A wherein we intended to develop a highly modular strategy that involves mainly the catalytic transformations in the final stages.

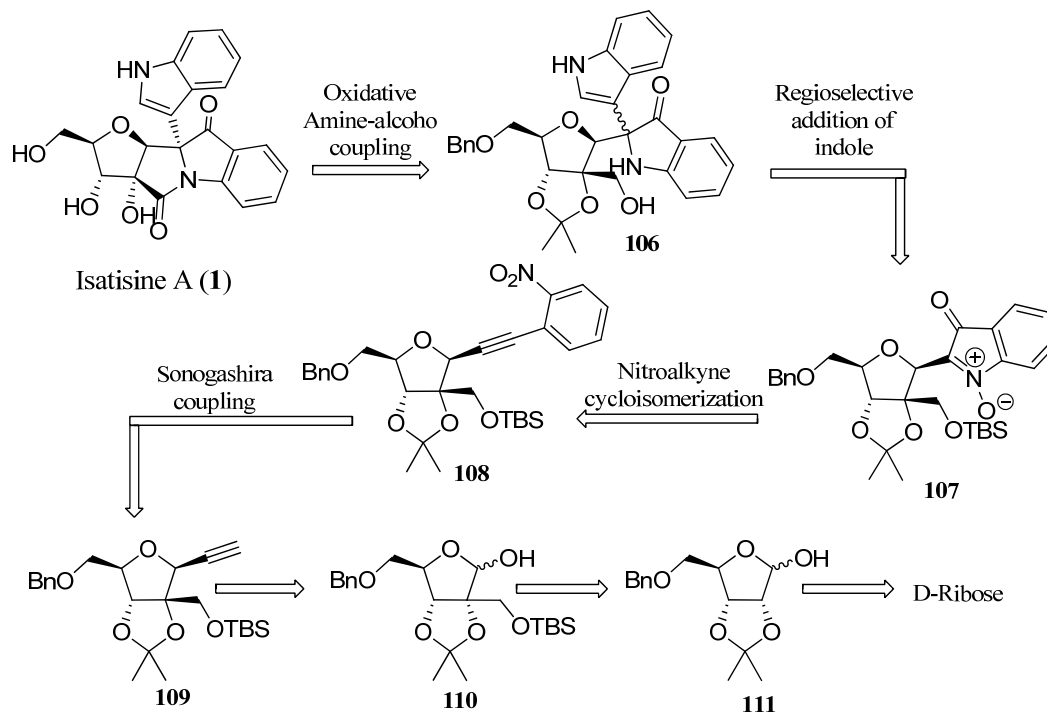
As mentioned in the previous sections, as part of our program on the total synthesis of Isatisine A, we have developed novel nitroalkyne/nitroalkynol cycloisomerization for the construction of the indolin-3-one group and also a model approach for the core structure of isatisine A. During this period, four groups have reported the total synthesis of Isatisine A,⁵¹ the details of which have been described briefly in the introduction.

2.5.2.1 Retrosynthetic disconnection for Isatisine A

As mentioned previously, our intention in this regard was to develop a modular strategy for the synthesis of Isatisine A and address the construction of key fused tetracyclic systems at the final stages by employing multiple penultimate catalytic reactions that address the key C–C and C–Hetero atom bond formations. The key retro synthetic disconnections are outlined in Scheme 71.

The construction of the central lactam ring has been planned as the final event in our total synthesis *via* a metal-mediated oxidative cyclization of a γ -aminolalcohol,

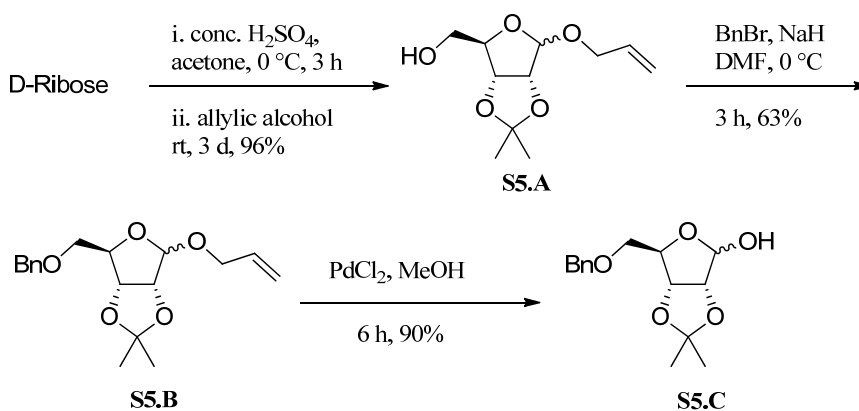
thus identifying **106** as the corresponding retron. The synthesis of **106** was planned *via* a metal/Lewis acid mediated addition of indole to the corresponding isatogen **107** which, in turn, was planned from a palladium catalyzed cycloisomerization of the nitroalkyne **108**. Considering the lack of selectivity in the cycloisomerization of pentynols to spiroindolinones, we have devised the route *via* isatogen. The synthesis of compound **108** will be through the Sonogashira coupling of 2-iodonitrobenzene with the fully TBS protected alkynol **109**. We have devised two approaches for the synthesis of key alkynol **109**. In one approach the addition of Grignard to the lactol **110** and selective mesylation of resulting propargyl-OH and subsequent cyclization was planned. Alternatively, alkynol **109** could be synthesized from the lactone using the Kishi's C-glycoside synthesis protocol that comprises a sequence of acetylene Grignard addition to a sugar lactone followed by the reduction of intermediate cyclic acetal using triethylsilane in the presence of borontrifluoride-etherate. The crossed aldol reaction of the known lactol **111** has been planned for the chiral pool synthesis of the lactol fragment **110**.



Scheme 71: Key retro synthetic disconnection for Isatisine A

2.5.2.2. Results and Discussion

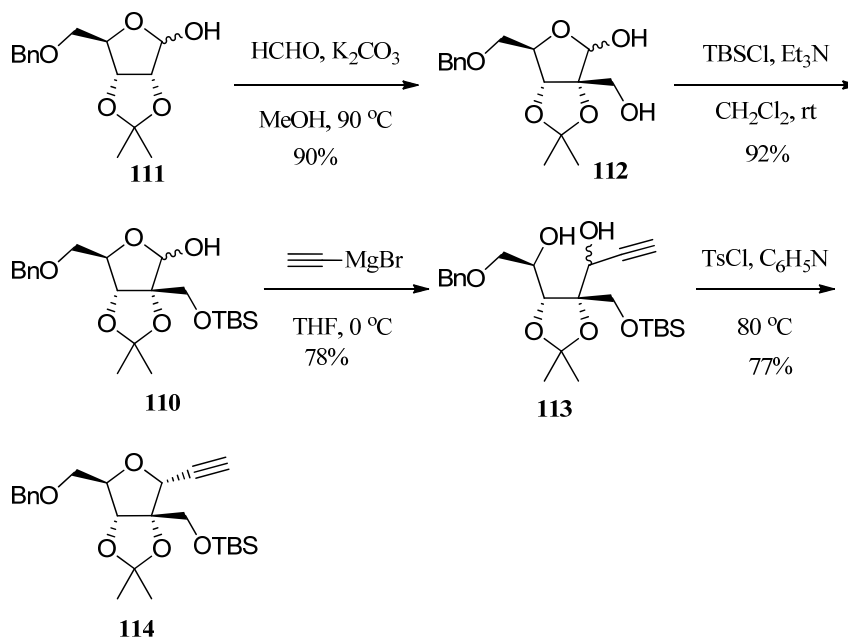
The synthesis of the lactol **110** commenced with the preparation of benzylated product **111** from the D-ribose following the known procedure.⁹⁹ Thus, the treatment of D-ribose with acetone in the presence of sulfuric acid at 0 °C followed by addition of allylic alcohol afforded, *via* a Fischer glycosidation reaction, the desired anomeric mixture of allyl 2,3-O-isopropylidene-β-D-ribofuranoside **S72.A** in 96% yield in a one-pot procedure. The anomeric proton appeared as a broad singlet at 5.12 ppm in the proton NMR spectrum, while the anomeric carbon was observed at 108.0 ppm in the corresponding ¹³C NMR spectrum. The free primary hydroxyl group compound **S72.A** was protected as its benzyl ether by treatment with benzyl bromide and sodium hydride in DMF at 0 °C to give **S72.B** in 63% yield. The anomeric *O*-deallylation was carried out in two steps¹⁰⁰ – i. isomerization of the allyl moiety to form the corresponding enol ether by employing potassium tert-butoxide in dimethyl sulfoxide at 100 °C; ii. deprotection of the enol ether group using mercuric oxide and mercuric chloride in acetone:water (9:1) which afforded the lactol **111** in 90% yield over the two steps. Alternatively, the same deallylation could be conducted under mild conditions by employing catalytic amounts of palladium chloride in methanol at rt to procure the lactol **111** in 72% yield, however the reaction was sluggish when attempted on large scales.



Scheme 71: Preparation of starting compound **111**

The key cross aldol reaction of the ribose derivative¹⁰¹ **111** for the hydroxymethylation at C(2) has been carried out with excess of 40% formaldehyde

solution and potassium carbonate in methanol at 90 °C for 30 hours to procure the lactol intermediate **112** in 90% yield. Selective protection of the primary hydroxy group in **112** by using one equivalent of TBSCl and triethylamine in dichloromethane as solvent at room temperature gave the key lactol **110** (2:1 anomeric mixture) in 92% yield. The ^1H NMR spectrum, the presence of two singlets at δ 0.0 (6H) and 0.03 (3H) and another two singlets at δ 0.86 (9H) and 0.89 (4.5 H) corresponding to the methyl and tertiary butyl protons of TBS group provides corroboration for the structure of **110** (Scheme 73).

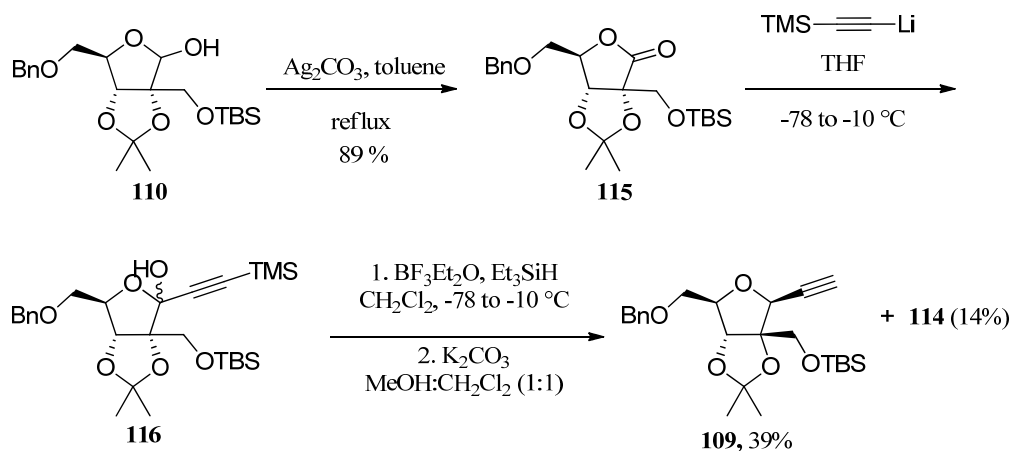


Scheme 73: Synthetic approach for the alkyne compound from D-ribose

After having successfully synthesized the key lactol **110**, our next concern was its conversion to the advanced intermediate **109**. Our initial approach involved the acetylene Grignard¹⁰² addition in THF at 0 °C to the lactol **110**. The treatment of the intermediate alkynol with *p*-toluene sulphonylchloride and pyridine at 80 °C gave the cyclic alkyne compound **114** in 77% yield as a single diastereomer. The stereochemistry of the newly generated center in **114** was investigated with the help of COSY and NOESY spectra. The connectivity of the ring-H has been deduced with the help of the COSY and the spatial proximity by NOESY. In the NOESY of compound **114**, a strong cross peak between the C(1)-H proton and two C(2')-2H was present and no correlation was observed between C(1)-H and C(4)-H. This

revealed 1,2-trans relation between the hydroxymethyl and alkyne groups and confirmed that compound **114** was the undesired α -anomer (Scheme 73).

This warranted an execution of the Kishi's¹⁰³ strategy as an alternative for the synthesis of the required β -alkyne isomer. The oxidation of lactol **110** using Ag_2CO_3 in toluene at refluxing temperature for 6 hours gave the lactone **115** in 89% yield. The structure of lactone **115** was confirmed by the spectral and analytical data. For instance, the absence of the anomeric CH-proton in PMR spectra of compound **115** along with the appearance of one quarternary carbon at δ 174 and the disappearance of one CH-carbon in the CMR spectra confirm the presence of the carbonyl carbon.



Scheme 74: Synthesis of β -alkyne fragment

Further, the presence of the carbonyl group was supported by the IR spectrum, with the band at 1710 cm^{-1} corresponding to the -C=O stretching. Other analytical data such as HRMS and ESI-MS were in accordance with the proposed structure (Scheme 74). The alkylation of lactone **115** with trimethylsilylethynyllithium in THF at $-78\text{ }^\circ\text{C}$ gave the hemiacetals **116**, which was subjected to deoxygenation¹⁰⁴ without further purification using Et_3SiH in the presence $\text{BF}_3\cdot\text{Et}_2\text{O}$ in a mixture of acetonitrile- CH_2Cl_2 at $0\text{ }^\circ\text{C}$. The resulting crude product was treated with K_2CO_3 in a 1:1 mixture of methanol and dichloromethane solvent to furnish the key alkynol **109** (39%) along

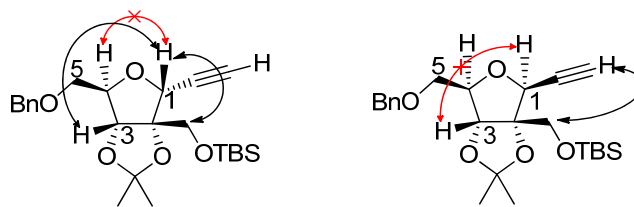


Figure 21

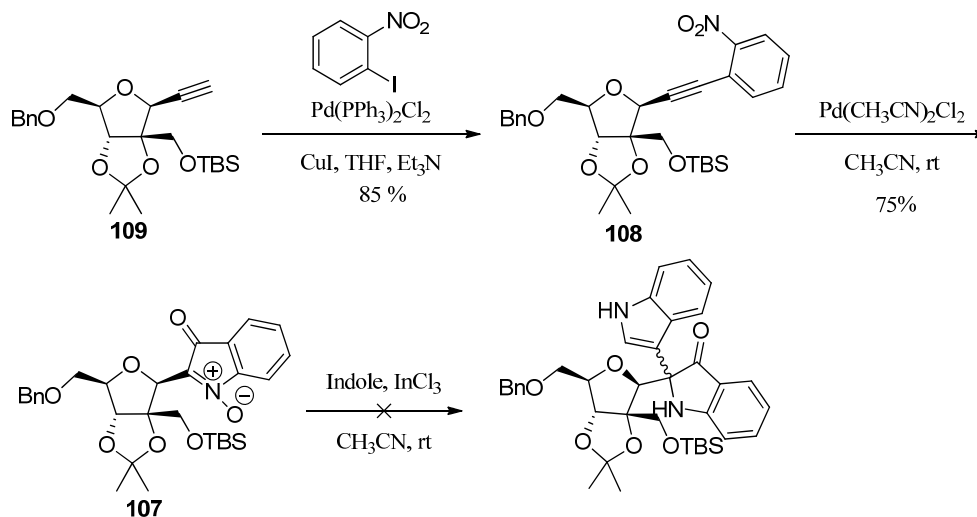
with the α -anomer **114** (14%) in a 3:1 ratio in (39% + 14%) yield over three steps. The β -anomeric configuration of the major isomer was deduced with the help of 2D NMR spectral analysis. For example, in the NOESY spectrum of the major isomer **109**, a characteristic strong cross peak between the C(1)–H and C(4)–H was noticed, which indicated the 1,4-*cis* configuration of the tetrahydrofuran unit. The alkyne and anomeric proton for the major compound resonate at δ 2.53 (d, J = 2.1 Hz, 1H) and 4.53 (d, J = 2.1 Hz, 1H) whereas for the minor isomer, the same protons resonate at δ 2.58 (d, J = 2.3 Hz, 1H) and 4.69 (br d, J = 2.3 Hz, 1H) (Table 24).

Proton(s)/ Carbon(s)		
H1	4.53 (d, J = 2.1 Hz, 1H)	4.69 (br d, J = 2.3 Hz, 1H)
H3	4.64 (d, J = 2.6 Hz, 1H)	4.62 (d, J = 1.4 Hz, 1H)
H4	4.21 (dt, J = 2.6, 5.2 Hz, 1H)	4.26–4.31 (m, 1H)
H5	3.55 (dd, J = 5.2, 10.1 Hz, 1H) 3.60 (dd, J = 5.2, 10.1 Hz, 1H)	3.5 (dd, J = 5.4, 10.2 Hz, 1H) 3.55 (dd, J = 5.4, 10.2 Hz, 1H)
C≡C-H	2.53 (d, J = 2.1 Hz, 1H)	2.58 (d, J = 2.3 Hz, 1H)
H2'	3.76 (d, J = 11.3 Hz, 1H) 4.02 (d, J = 11.3 Hz, 1H)	3.7 (br s, 2H)

Table 24: Comparison of the PMR data for both isomers

After having the requisite *cis*-alkynol **109** in hand, our next concern was the total synthesis of isatisine A from **109** by deploying the key catalytic transformations

that we have developed and/or executed earlier on the model substrates. The Sonogashira coupling of **109** with 2-iodonitrobenzene under standard conditions was facile and furnished the nitroalkyne **108** in 85% yield. The absence of alkyne protons at δ 2.53 ppm as well as the presence of four additional protons at δ 7.47 (ddd, $J = 1.5, 7.4, 7.5$ Hz, 1H), 7.56 (dt, $J = 1.5, 7.5$ Hz, 1H), 7.61 (dd, $J = 1.5, 7.6$ Hz, 1H), 8.03 (dd, $J = 1.3, 7.6$ Hz, 1H) in $^1\text{H-NMR}$ substantiated this result. The nitroalkyne

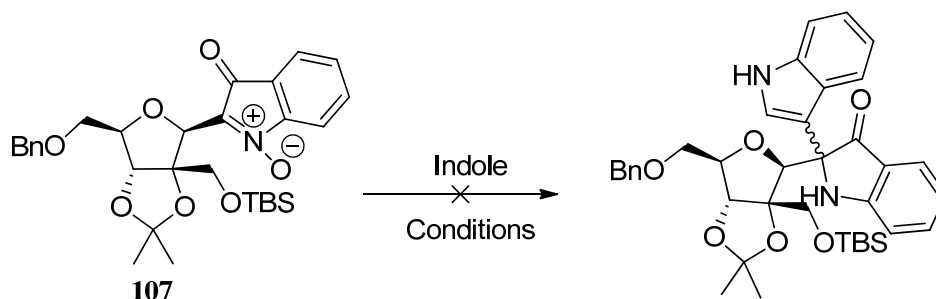


Scheme 75: Synthetic approach to Isatisine A.

cycloisomerization of **108** – the first key transformation in our total synthesis proceeded smoothly with 5 mol% of $\text{Pd}(\text{CH}_3\text{CN})_2\text{Cl}_2$ in acetonitrile at room temperature with the disappearance of the starting compound within 8 hours and afforded **107** as the exclusive product in 75% yield.¹⁰⁵ The formation of the isatogen compound was confirmed by spectral and analytical data. For instance, in the ^1H NMR spectrum of **107**, the isatogen ring protons appear at δ 7.52–7.64 as a multiplet and the anomeric proton appear at δ 5.41 which was deshielded by δ 0.59 due to the presence of the strong, electron withdrawing nitrone group. In the ^{13}C NMR spectrum, the peak at δ 184.5 confirmed the presence of a carbonyl group (Scheme 75).

Having the key isatogen **107** in hand, the next task was executing the alkylation of isatogen with indole and the subsequent N – O reduction by employing InCl_3 as a reagent. Accordingly, compound **107** was treated with indole in the presence of 20 mol% InCl_3 in acetonitrile solvent, which led to a complex reaction

mixture from which the isolation of any identifiable product was found to be a difficult task. Varying the temperature, solvent and the amounts of InCl_3 had no effect



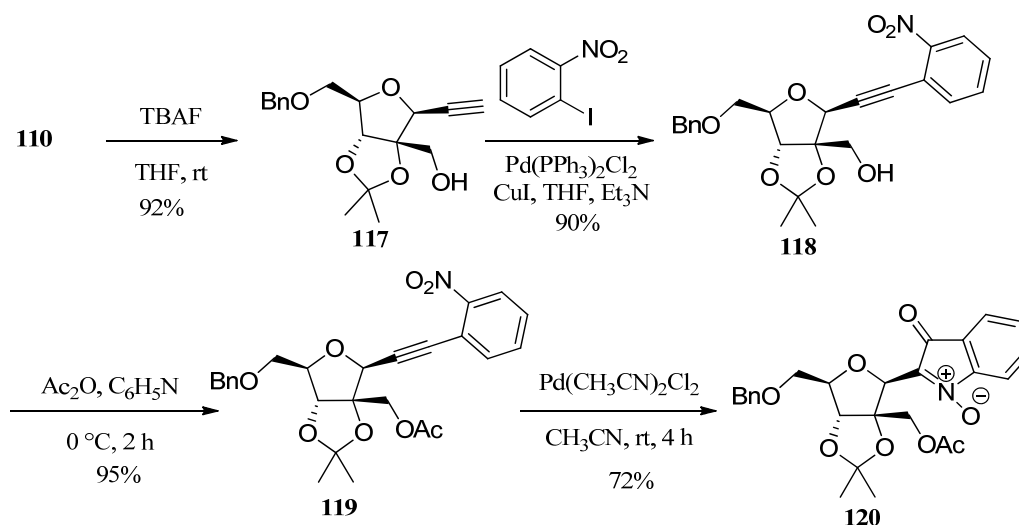
Serial no.	solvent	lewis acid	condition	product
1	CH_3CN	InCl_3	rt / heating	complex mixture
2	toluene	InCl_3	rt / heating	complex mixture
3	benzene	InCl_3	rt / heating	no reaction
4	$\text{C}_2\text{H}_4\text{Cl}_2$	InCl_3	rt / heating	complex mixture
5	CH_2Cl_2	InCl_3	rt / heating	no reaction
6	CH_3CN	TiCl_4	-10 °C	complex mixture
7	CH_3CN	$\text{BF}_3 \cdot \text{Et}_2\text{O}$	0 °C	complex mixture

Table 25: Alkylation of compound *xx* under different condition

on the reaction outcome and also the use of other Lewis acids did not lead to the desired product. In the majority of the cases, the reaction ended with either deprotection of the TBS group or of the complex reaction mixture. We reasoned that the presence of a bulky and acid labile TBS group might be a reason for the failures that we encountered during the Lewis acid mediated Friedel-Crafts type alkylation of the isatogen **107** (Table 25).

As the key intermediate **107** was found to be an unsuitable substrate for the key indole addition reaction, we resorted next to switching the protection group of the hydroxyl group from TBS to acetate. The desilylation of **110** with 1.2 equivalents of 1M TBAF solution in THF gave the alkynol **117**. The Sonogashira coupling of **117** with 2-iodonitrobenzene furnished the nitroalkynol **118** in 90% yield (Scheme 76). The appearance of the additional aromatic ring proton around δ 7.25 to 8.05 and the

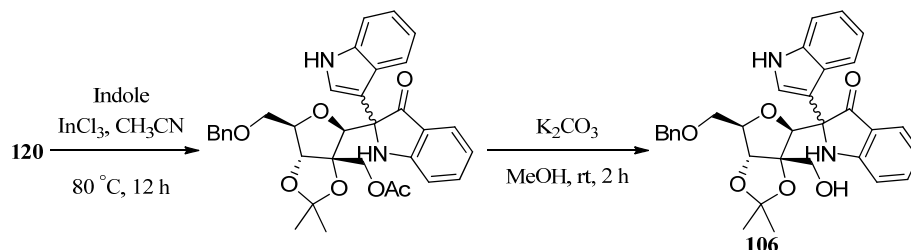
disappearance of the alkyne proton in PMR spectra confirmed the formation of **118**. Next, the hydroxyl group was protected as its acetate using acetic anhydride in presence of triethylamine in dichloromethane solvent at room temperature to give the acylated compound **119**. Nitroalkyne cyclization of compound **119** in presence of $\text{Pd}(\text{CH}_3\text{CN})_2\text{Cl}_2$ in acetonitrile as a solvent at room temperature for 7 hours gave the corresponding isatogen **120** in 72% yield. The spectral and analytical data of compound **120** are in accordance with the assigned structure.



Scheme 76: Synthesis of isatogen **120**

The key indole addition reaction with the isatogen **120** needed a substantial optimization. It was realized that the reaction in acetonitrile at rt in the presence of catalytic amounts of InCl_3 was sluggish. When carried out at 70 °C employing stoichiometric amounts InCl_3 , within 2 hours, the isatogen was found to completely disappear and the formation of two major compounds $[\text{ESI MS}: 605 ([\text{M}+\text{Na}]^+)$ and $621([\text{M}+\text{Na}]^+)$ was observed in the crude LCMS spectra of the reaction mixture. The observed MS data indicated the presence of the required indolin-3-one and the intermediate N–OH product. With this information, we continued the reaction further and after 14 hours, only one peak: $605 ([\text{M}+\text{Na}]^+)$ corresponding to the required alkylated product was observed. It was entirely surprising to find that the alkylation reaction proceeded when the hydroxyl was protected as its acetate, giving exclusively the desired indole addition product on over 300 mg scale. However, at this stage we failed to get a clean NMR spectrum due to the presence of traces of unidentified

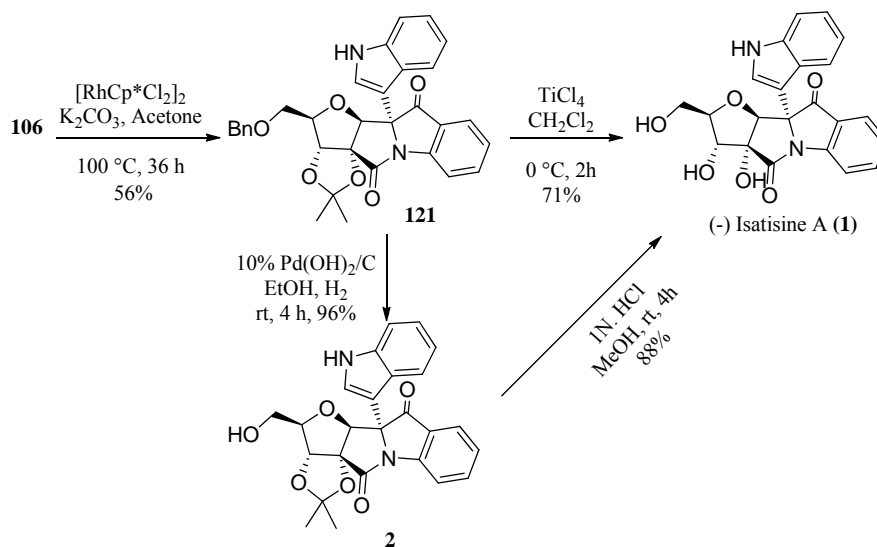
compounds which were found to be inseparable through column chromatography. The crude reaction mixture was treated with K_2CO_3 in methanol at room temperature for 2 hours and the key alcohol **106** was obtained in 65% yield over two steps (Scheme 77).



Scheme 77: Synthetic approach towards Isatisine A

After successful installation of the indole ring to isatogen to get the γ -amino alcohol substrate, we next proceed for the final key transformation to form the lactam by the metal-mediated oxidative lactamization. For this, compound **106** was treated with 20 mol% percentage of $[RhCp^*Cl_2]_2$ and catalytic potassium carbonate in acetone at $100\text{ }^\circ\text{C}$ for 36 hours to furnish lactam compound **121** in moderate yield. The spectral and analytical data were in agreement with the assigned structure and the proton chemical shifts/coupling constants noticed were comparable with that of the acetonide of the isatisine A.

Having the complete skeleton in hand, the stage was now set for the completion of the total synthesis of Isatisine A by deprotection of the benzyl and acetonide groups. To this end, the global deprotection of **121** using $TiCl_4$ ¹⁰⁶ resulted in the isolation of Isatisine A in 71% yield. The spectral and analytical data for Isatisine A was in accordance with the data reported by the other groups. The specific rotation of the synthetic isatisine A (**1**) was $[\alpha]_D^{25} = -276$ ($c = 0.21$, $MeOH$), which is essentially equal to that reported paper^{51a} ($[\alpha]_D^{14} = +274$). Alternatively, to have the access for the acetonide **2**, which shows promising anti HIV activity, we explored the possibility of selective debenzylation. This can be smoothly effected by hydrogenolysis of **121** with $Pd(OH)_2$ in ethanol at balloon pressure to furnish acetonide **2** in 96% yield. The specific rotation of the synthetic acetonide **2** was



Scheme 75: The total synthesis of Isatisine A

$[\alpha]_D^{25} = -270$ ($c = 0.56$, MeOH), which is essentially equal to that reported in the isolation paper ($[\alpha]_D^{14} = -283$ ($c=0.46$, MeOH)). Finally, hydrolysis of the acetonide following the reported procedure using 1N hydrochloric acid in methanol at room temperature affords Isatisine A in 88% yield. The spectral and analytical data was exactly matching with the previously synthesized Isatisine A. Table 26 and 27 shows the detailed comparisons of NMR data for the isolated and synthetic Isatisine A and its acetonide derivative.

In conclusion, we have developed a modular total synthesis of Isatisine A starting from the D-ribose derived known intermediate in 12 steps. The synthesis involved four consecutive metal catalyzed/mediated transformations addressing two of each C – C and C – hetero atom bond formations, to arrive at the known acetonide derivative of Isatisine A, which was ultimately hydrolyzed by acid catalysis to complete the total synthesis of naturally occurring isatisine A. In the context of this total synthesis, we have developed a mild and general method for the synthesis, hypothesized and executed a novel nitroalkynol cycloisomerization leading to the synthesis of spiroindolin-3-ones, established an InCl_3 mediated addition of indoles to isatogens and to the spiroindolin-3-ones, and documented the first application of a [Rh]-catalyzed oxidative γ -aminoalcohol cyclization leading to the γ -lactam in the synthesis of a complex natural product. Further improvements in yields, reduction of the synthetic steps, and the feasibility these penultimate events in a continuous flow

manner to synthesize a collection of small molecule libraries having the central fused tetracycli core of isatisine A are under progress in our lab and will be reported in due course.

Isolated Isatisine A	Synthetic Isatisine A
3.33 (dd, $J = 11.5, 4.5$ Hz, 1H)	3.33 (dd, $J = 12.0, 4.5$ Hz, 1H)
3.38 (dd, $J = 11.5, 4.5$ Hz, 1H)	3.38 (dd, $J = 12.0, 4.5$ Hz, 1H)
3.83 (m, 1H)	3.84 (m, 1H)
4.05 (d, $J = 4.0$ Hz, 1H)	4.06 (d, $J = 4.3$ Hz, 1H)
4.63 (s, 1H)	4.89 (s, 1H)
7.05 (dd, $J = 7.5, 7.5$ Hz, 1H)	7.05 (t, $J = 7.2$ Hz, 1H)
7.12 (dd, $J = 8.0, 7.0$ Hz, 1H)	7.12 (t, $J = 7.3$ Hz, 1H)
7.28 (s, 1H)	7.29 (s, 1H)
7.32 (dd, $J = 7.5, 7.5$ Hz, 1H)	7.3–7.35 (m, 2H)
7.33 (d, $J = 8.0$ Hz, 1H)	7.64 (d, $J = 7.3$ Hz, 1H)
7.63 (d, $J = 7.5$ Hz, 1H)	7.77 (br t, $J = 8.0$ Hz, 1H)
7.77 (dd, $J = 7.5, 7.5$ Hz, 1H)	7.93 (d, $J = 7.9$ Hz, 1H)
7.93 (d, $J = 8.0$ Hz, 1H)	7.99 (d, $J = 8.0$ Hz, 1H)
7.99 (d, $J = 8.5$ Hz, 1H)	

Table 26: Comparisons of ^1H NMR (CD_3OD , 500 MHz) data for synthetic and isolated Isatisine A

Isolated Isatisine A acetonide		Synthetic Isatisine A acetonide	
¹ H	¹³ C	¹ H	¹³ C
1.38 (s, 3 H)	26.3 (q),	1.36 (s, 3 H)	26.4 (q),
1.51 (s, 3H)	27.3 (q),	1.49 (s, 3 H)	27.4 (q),
3.44 (dd, <i>J</i> = 12.0, 4.4, 1H)	62.5 (t),	3.43 (dd, <i>J</i> = 11.9, 4.4, 1 H)	62.6 (t),
3.51 (dd, <i>J</i> = 12.0, 4.2, 1H)	76.3 (s),	3.49 (dd, <i>J</i> = 11.9, 4.2, 1H)	76.4 (s),
4.17 (m, 1H)	85.9 (d),	4.16 (dd, <i>J</i> = 7.7, 4.2, 1 H)	86.1 (d),
4.81 (d, <i>J</i> = 3.3, 1H)	87.1 (d),	4.79 (d, <i>J</i> = 3.4, 1 H)	87.2 (d),
4.91 (s, 1 H)	87.8 (d),	4.90 (s, 1 H)	87.9 (d),
7.09 (dd, <i>J</i> = 7.4, 7.4, 1H)	99.4 (s),	7.08 (t, <i>J</i> = 7.2, 1H)	99.6 (s),
7.17 (m, 1H)	111.0 (s),	7.14 (t, <i>J</i> = 7.2, 1H)	111.1 (s),
7.26 (s, 1H)	112.9 (d),	7.24 (s, 1H)	113.1 (d),
7.33 (dd, <i>J</i> = 7.6, 7.5, 1H)	117.4 (d),	7.31 (t, <i>J</i> = 7.5, 1H)	117.6 (d),
7.38 (br d, <i>J</i> = 8.2, 1H)	119.4 (s),	7.36 (d, <i>J</i> = 8.1, 1H)	119.6 (s),
7.65 (br d, <i>J</i> = 7.6, 1H)	120.7 (d),	7.63 (d, <i>J</i> = 7.6, 1H)	120.9 (d),
7.78 (dd, <i>J</i> = 8.1, 7.5, 1H)	121.2 (d),	7.80–7.74 (m, 1H)	121.4 (d),
7.94 (br d, <i>J</i> = 8.0, 1H)	123.3 (d),	7.93 (d, <i>J</i> = 8.0, 1H)	123.4 (d),
8.02 (br d, <i>J</i> = 8.1, 1H)	124.3 (d),	8.01 (d, <i>J</i> = 8.1, 1H)	124.4 (d),
	125.7 (s),		125.8 (s),
	126.2 (d),		126.3 (d),
	127.0 (d),		127.1 (d),
	127.3 (s),		127.4 (s),
	137.9 (d),		138.0 (d),
	139.1 (s),		139.2 (s),
	151.2 (s),		151.3 (s),
	171.4 (s),		171.6 (s),
	195.7 (s)		195.8 (s)

Table 27: ¹H NMR (CD₃OD, 500 MHz), ¹³C NMR (CD₃OD, 125 MHz) for both of the compound

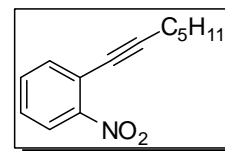
EXPERIMENTAL

3.1. Experimental Details for Nitroalkyne Cycloisomerization

General Procedure for the Sonogashira Coupling: To a solution of alkyne (1 mmol), aryl iodide (1.2 mmol) in Et₃N (8 mL) and DMF (4 mL), TPP (0.1 mmol) and Pd(PPh₃)₂Cl₂ (0.1 mmol), were added and degassed with argon for 30 min. CuI (0.1 mmol) was added and degassed with argon for 10 min and stirred at rt for 2-5 h. The reaction mixture was partitioned between ethyl acetate and water. Organic layer was separated, washed with brine, dried (Na₂SO₄), concentrated and the residue obtained was purified by column chromatography (ethyl acetate in petroleum ether) to afford the coupled product.

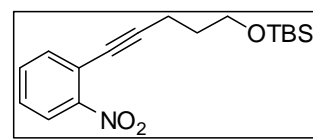
1-(hept-1-yn-1-yl)-2-nitrobenzene (3): Yellow oil, 70% yield.

IR (CHCl₃): ν 3022, 2958, 2922, 2860, 2233, 1608, 1568, 1527, 1480, 1466, 1345, 1216, 851, 757, 668 cm⁻¹. ¹H NMR (400 MHz, CDCl₃): δ 0.89 (t, J = 7.2 Hz, 3 H), 1.28–1.37 (m, 2 H), 1.38–1.45 (m, 2 H), 1.56–1.63 (m, 2 H), 2.42 (t, J = 7.2 Hz, 2 H), 7.33 (br. ddd, J = 1.6, 7.3, 8.2 Hz, 1 H), 7.46 (dt, J = 1.2, 7.7 Hz, 1 H), 7.51 (dd, J = 1.6, 7.8 Hz, 1 H), 7.90 (dd, J = 8.3, 1.2 Hz, 1 H) ppm. ¹³C NMR (125 MHz, CDCl₃): δ 13.9 (q), 19.7 (t), 22.1 (t), 27.9 (t), 30.9 (t), 75.9 (s), 99.2 (s), 119.3 (s), 124.2 (d), 127.7 (d), 132.3 (d), 134.6 (d), 150.0 (s) ppm. C₁₃H₁₅NO₂ (217.27): calcd. C 71.87, H 6.96, N 6.45; found C 71.76, H 6.91, N 6.40.

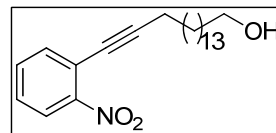


Tert-butyldimethyl((5-(2-nitrophenyl)pent-4-yn-1-

yl)oxy)silane (6): Yellow oil, 72% yield. IR (CHCl₃): ν 3032, 2954, 2885, 1684, 1634, 1557, 1520, 1471, 1465, 1445, 1345, 1276, 1255, 1180, 1143, 1101, 1006, 980, 836, 776 cm⁻¹. ¹H NMR (200 MHz, CDCl₃): δ 0.05 (s, 6H), 0.88 (s, 9H), 1.82 (quint, J = 6.6 Hz, 2H), 2.55 (d, J = 7.1 Hz, 2H), 3.76 (t, J = 6.0 Hz, 2 H), 7.37 (br. ddd, J = 2.2, 6.8, 8.2 Hz, 1 H), 7.50 (dt, J = 1.2, 7.7 Hz, 1H), 7.55 (dd, J = 2.2, 8.2 Hz, 1H), 7.94 (br. d, J = 8.2 Hz, 1H) ppm. ¹³C NMR (50 MHz, CDCl₃): δ -5.5 (q, 2 C), 16.1 (t), 18.2 (s), 25.8 (q, 3 C), 31.2 (t), 61.3 (t), 75.9 (s), 98.7 (s), 119.1 (s), 124.2 (d), 127.8 (d), 132.4 (d), 134.6 (d), 149.9 (s) ppm. C₁₇H₂₅NO₃Si (319.48): calcd. C 63.91, H 7.89, N 4.38; found C 63.81, H 7.72, N 4.32.

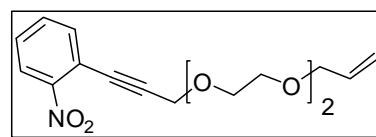


17-(2-Nitrophenyl)heptadec-16-yn-1-ol (7): Yellow oil, 68% yield. IR (CHCl₃): ν 3367, 2922, 2852, 2400, 1608, 1528, 1464, 1320, 1056, 755 cm⁻¹. ¹H NMR (200 MHz,



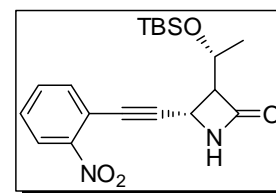
CDCl₃): δ 1.24 (br. s, 22 H), 1.52–1.68 (m, 5 H), 2.46 (t, J = 6.8 Hz, 2 H), 3.62 (t, J = 6.6 Hz, 2 H), 7.37 (br. ddd, J = 2.1, 7.1, 8.2 Hz, 1 H), 7.51 (dt, J = 1.2, 7.7 Hz, 1 H), 7.57 (dd, J = 2.1, 8.7 Hz, 1 H), 7.96 (dd, J = 1.2, 8.2 Hz, 1 H) ppm. ¹³C NMR (50 MHz, CDCl₃): δ 19.8 (t), 25.7 (t), 28.3 (t), 28.8 (t), 29.1 (t), 29.4 (t), 29.5 (t), 29.5 (t, 3 C), 29.6 (t, 3 C), 32.7 (t), 62.9 (t), 75.9 (s), 99.4 (s), 119.3 (s), 124.3 (d), 127.8 (d), 132.5 (d), 134.7 (d), 150.0 (s) ppm. C₂₃H₃₅NO₃ (373.53): calcd. C 73.96, H 9.44, N 3.75; found C 73.88, H 9.34, N 3.71.

1-(3-(2-(2-(allyloxy)ethoxy)ethoxy)prop-1-yn-1-yl)-2-nitrobenzene (8): Yellow liquid, 62% yield.



IR (CHCl₃): ν 2915, 2403, 1683, 1613, 1559, 1505, 1469, 1401, 1265, 1097, 1034, 933, 765 cm⁻¹. ¹H NMR (200 MHz, CDCl₃): δ 3.60–3.65 (m, 2H), 3.67–3.76 (m, 4H), 3.81–3.86 (m, 2H), 4.03 (dt, J = 5.7, 1.4 Hz, 2H), 4.50 (s, 2H), 5.18 (ddd, J = 10.4, 3.1, 1.3 Hz, 1H), 5.27 (ddd, J = 17.2, 3.1, 1.3 Hz, 1H), 5.92 (ddt, J = 17.2, 10.4, 5.7 Hz, 1H), 7.37 (br ddd, J = 1.8, 7.1, 8.0 Hz, 1H), 7.50 (dt, J = 1.4, 7.7 Hz, 1H), 7.55 (dd, J = 2.0, 7.7 Hz, 1H), 7.94 (d, J = 1.4, 8.0 Hz, 1H) ppm. ¹³C NMR (50MHz, CDCl₃): δ 59.0 (t), 69.2 (t), 69.3 (t), 70.4 (t), 70.6 (t), 72.1 (t), 81.5 (s), 93.4 (s), 116.9 (s), 117.9 (t), 124.5 (d), 128.8 (d), 132.7 (d), 134.7 (d), 134.8 (d), 149.7(s) ppm. ESI-MS: m/z 328.4 (100%, [M+Na]⁺). Anal. Calcd for C₁₆H₁₉NO₅: C, 62.94; H, 6.27;N, 4.59. Found: C, 62.82; H, 6.21;N, 4.49.

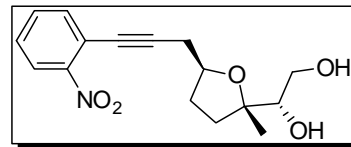
(4S)-3-((R)-1-((tert-butylidimethylsilyl)oxy)ethyl)-4-((2-nitrophenyl)ethynyl)azetidin-2-one (9): Light grey color solid, 67% yield. Mp. 119 °C. [α]_D²⁵ = +42.6 (c = 1, CHCl₃). IR (CHCl₃): ν 3414, 3019, 2956, 2930, 2885,



2400, 1770, 1672, 1609, 1570, 1529, 1472, 1377, 1346, 1215, 1144, 1065, 959, 756 cm⁻¹. ¹H NMR (200 MHz, CDCl₃): δ 0.07 (s, 6H), 0.87 (s, 9H), 1.28 (d, J = 6.3 Hz, 3H), 3.41–3.44 (m, 1H), 4.23–4.34 (m, 1H), 4.61 (d, J = 2.5 Hz, 1H), 6.32 (bs, 1H), 7.42–7.52 (m, 1H), 7.56–7.59 (m, 2H), 8.04 (dd, J = 1.1, 7.7 Hz, 1H) ppm. ¹³C NMR (125 MHz, CDCl₃): δ -5.2 (q), -4.4 (q), 17.8 (s), 22.2 (q), 25.6 (q, 3C), 39.3 (d), 64.4

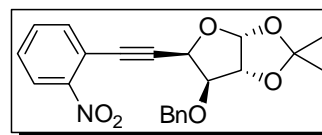
(d), 67.8 (d), 79.9 (s), 95.1 (s), 117.6 (s), 124.5 (d), 128.9 (d), 132.7 (d), 134.6 (d), 149.8 (s), 167.7 (s) ppm. ESI-MS: m/z 397.6 (100%, $[M+Na]^+$). Anal. Calcd for $C_{19}H_{26}N_2O_4Si$: C, 60.93; H, 7.0; N, 7.48. Found: C, 60.81; H, 7.2; N, 7.34.

Compound 10. Yellow liquid, 57% yield. IR (CHCl₃): ν 3390, 2975, 2742, 2235, 1608, 1595, 1527, 1476, 1380, 1280, 1069, 755 cm^{-1} . ¹H NMR



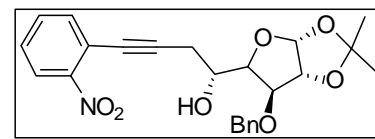
(200 MHz, CDCl₃): δ 1.16 (s, 3H), 1.58–1.66 (m, 1H), 1.88–1.96 (m, 1H), 2.04–2.16 (m, 2H), 2.71 (t, $J = 5.7$ Hz, 2H), 3.05 (bs, 1H), 3.31 (bs, 1H), 3.47–3.53 (m, 1H), 3.62–3.71 (m, 2H), 4.11–4.19 (m, 1H), 7.33–7.41 (m, 1H), 7.45–7.56 (m, 2H), 7.93 (d, $J = 7.8$ Hz, 1H) ppm. ¹³C NMR (50 MHz, CDCl₃): δ 23.7 (q), 26.8 (t), 30.9 (t), 32.7 (t), 63.1 (t), 76.7 (d), 77.3 (s), 78.0 (d), 85.0 (s), 95.2 (s), 118.7 (s), 124.3 (d), 128.1 (d), 132.6 (d), 134.7 (d), 149.8 (s) ppm. Anal. Calcd for $C_{16}H_{19}NO_5$: C, 62.94; H, 6.27; N, 4.59. Found: C, 62.79; H, 6.38; N, 4.48.

Compound 11. Yellow liquid, 73% yield. $[\alpha]_D^{25} = +88.8$ ($c = 1$, CHCl₃). IR (CHCl₃): ν 3020, 2960, 2400, 1608, 1575, 1530, 1481, 1437, 1385, 1347, 1215, 1163,



1075, 928, 758 cm^{-1} . ¹H NMR (200 MHz, CDCl₃): δ 1.32 (s, 3H), 1.50 (s, 3H), 4.14 (d, $J = 3.0$ Hz, 1H), 4.63 (d, $J = 3.8$ Hz, 1H), 4.80 (d, $J = 12.2$ Hz, 1H), 4.89 (d, $J = 12.2$ Hz, 1H), 5.14 (d, $J = 3.0$ Hz, 1H), 6.03 (d, $J = 3.8$ Hz, 1H), 7.26–7.39 (m, 5H), 7.52–7.61 (m, 2H), 7.67 (dd, $J = 7.6, 1.8$ Hz, 1H), 8.06 (dd, $J = 7.9, 1.4$ Hz, 1H) ppm. ¹³C NMR (50 MHz, CDCl₃): δ 26.1 (q), 26.8 (q), 71.5 (d), 72.8 (t), 82.7 (d), 82.9 (d), 83.0 (s), 91.0 (s), 104.7 (d), 112.1 (s), 117.7 (s), 124.5 (d), 127.7 (d, 2C), 127.8 (d), 128.4 (d, 2C), 129.1 (d), 132.8 (d), 135.2 (d), 137.3 (s), 149.5 (s) ppm. Anal. Calcd for $C_{22}H_{21}NO_6$: C, 66.83; H, 5.35; N, 3.54. Found: C, 66.85; H, 5.45; N, 3.47.

Compound 12. Yellow liquid, 75% yield. $[\alpha]_D^{25} = -42.2$ ($c = 1$, CHCl₃). IR (CHCl₃): ν 3678, 3020, 2950, 2934, 2400, 1676, 1612, 1569, 1528, 1454,



1375, 1345, 1215, 1120, 1076, 1025, 758 cm^{-1} . ¹H NMR (200 MHz, CDCl₃): δ 1.32 (s, 3H), 1.48 (s, 3H), 2.69 (bs, 1H), 2.85 (d, $J = 5.6$ Hz, 1H), 2.89 (t, $J = 2.0$ Hz, 1H), 4.14–4.29 (m, 3H), 4.63 (d, $J = 11.7$ Hz, 1H), 4.64 (d, $J = 3.7$ Hz, 1H), 4.75 (d, $J =$

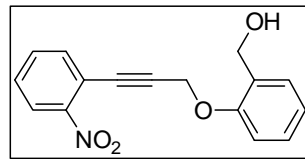
11.7 Hz, 1H), 5.95 (d, $J = 3.7$ Hz, 1H), 7.33–7.39 (m, 5H), 7.46–7.51 (m, 1H), 7.51–7.62 (m, 2H), 8.03 (dd, $J = 8.0, 0.9$ Hz, 1H) ppm. ^{13}C NMR (50 MHz, CDCl_3): δ 26.1 (t), 26.3 (q), 26.7 (q), 67.1 (d), 72.3 (t), 78.6 (s), 81.4 (d), 81.7 (d), 82.4 (d), 94.8 (s), 105.1 (d), 111.8 (s), 118.7 (s), 124.5 (d), 127.8 (d, 2C), 128.1 (d), 128.2 (d), 128.6 (d, 2C), 132.8 (d), 134.7 (d), 137.3 (s), 149.8(s) ppm. Anal. Calcd for $\text{C}_{24}\text{H}_{25}\text{NO}_7$: C, 65.59; H, 5.73; N, 3.19. Found: C, 65.41; H, 5.69; N, 3.14.

(2-((3-(2-nitrophenyl)prop-2-yn-1-

yl)oxy)phenyl)methanol (13): Yellow liquid, 68% yield.

IR (CHCl_3): ν 3372, 3019, 2953, 2400, 1656, 1616, 1587, 1531, 1487, 1456, 1291, 1230, 1119, 753 cm^{-1} . ^1H

NMR (200 MHz, CDCl_3): δ 2.42 (s, 1H), 4.74 (s, 2H), 5.03 (s, 2H), 6.97–7.12 (m, 2H), 7.26–7.36 (m, 2H), 7.42–7.52 (m, 1H), 7.55–7.61 (m, 2H), 8.03 (dd, $J = 7.7, 1.2$ Hz, 1H) ppm. ^{13}C NMR (50MHz, CDCl_3): δ 56.65 (t), 61.46 (t), 82.40 (s), 91.58 (s), 111.97 (d), 117.38 (s), 121.58 (d), 124.53 (d), 128.77 (d), 128.81 (d), 129.15 (d), 129.70 (s), 132.82 (d), 134.91 (d), 149.55 (s), 155.29 (s) ppm. Anal. Calcd for $\text{C}_{16}\text{H}_{13}\text{NO}_4$: C, 67.84; H, 4.63; N, 4.94. Found: C, 67.79; H, 4.69; N, 4.83.

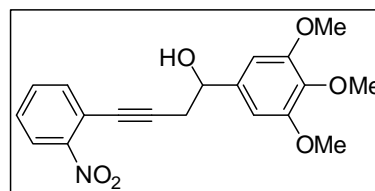


4-(2-nitrophenyl)-1-(3,4,5-trimethoxyphenyl)but-3-yn-1-ol (14): Grey color spongy

mass, 62% yield. IR (CHCl_3): ν 3352, 3010, 2939,

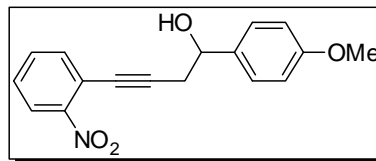
2400, 1694, 1593, 1505, 1463, 1328, 1236, 1126, 1004, 754 cm^{-1} . ^1H NMR (200 MHz, CDCl_3): δ 2.83 (d, $J = 6.2$ Hz, 2H), 3.19 (s, 1H), 3.72 (s, 3H),

3.74 (s, 6H), 4.84 (t, $J = 6.2$ Hz, 1H), 6.58 (s, 2H), 7.27–7.36 (m, 1H), 7.38–7.49 (m, 2H), 7.89 (d, $J = 8.1$ Hz, 1H) ppm. ^{13}C NMR (50 MHz, CDCl_3): δ 30.8 (t), 55.7 (q, 2C), 60.5 (q), 72.1 (d), 78.2 (s), 94.9 (s), 102.3 (d, 2C), 118.3 (s), 124.3 (d), 128.1 (d), 132.6 (d), 134.5 (d), 136.7 (s), 138.4 (s), 149.4 (s), 152.8 (s, 2C) ppm. Anal. Calcd for $\text{C}_{19}\text{H}_{19}\text{NO}_6$: C, 63.86; H, 5.36; N, 3.92. Found: C, 63.79; H, 5.31; N, 3.88.



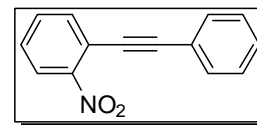
1-(4-methoxyphenyl)-4-(2-nitrophenyl)but-3-

yn-1-ol (15): Dark yellow colour liquid, 61% yield. IR (CHCl₃): ν 3410, 3019, 2936, 2834, 2400, 2223, 1611, 1527, 1514, 1465, 1441, 1345, 1250,



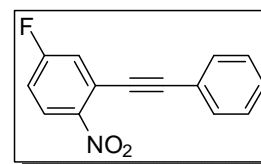
1215, 1111, 1035, 757 cm⁻¹. ¹H NMR (200 MHz, CDCl₃): δ 2.75 (bs, 1H), 2.89 (d, J = 6.3 Hz, 2H), 3.79 (s, 3H), 4.95 (t, J = 6.0 Hz, 1H), 6.89 (dt, J = 8.7, 2.3 Hz, 2H), 7.34–7.45 (m, 3H), 7.51–7.56 (m, 2H), 8.01 (d, J = 7.7 Hz, 1H) ppm. ¹³C NMR (50 MHz, CDCl₃): δ 30.8 (t), 55.1 (q), 71.8 (d), 78.3 (s), 95.2 (s), 113.7 (d, 2C), 113.8 (s), 118.6 (s), 124.4 (d), 126.9 (d, 2C), 128.2 (d), 128.5 (s), 132.7 (d), 134.6(d), 149.7 (s), 159.1 (s) ppm. Anal. Calcd for C₁₇H₁₅NO₄: C, 68.68; H, 5.09; N, 4.71. Found: C, 68.79; H, 5.23; N, 4.65.

1-nitro-2-(phenylethynyl)benzene (26): Orange color spongy mass, 67% yield. (*the sample also contains small amounts of isatogen*). IR (CHCl₃): ν 3019, 2410, 1605, 1567,



1514, 1465, 1345 cm⁻¹. ¹H NMR (200 MHz, CDCl₃): δ 7.35–7.40 (m, 3H), 7.44–7.50 (m, 1H), 7.56–7.62 (m, 3H), 7.66–7.72 (m, 1H), 8.07 (d, J = 1.2, 7.9 Hz, 1H) ppm. ¹³C NMR (100 MHz, CDCl₃): δ 84.8 (s), 97.1 (s), 113.9 (s), 122.3 (s), 124.5 (d), 128.3 (d, 2C), 128.3 (d), 129.1 (d), 131.9 (d, 2C), 132.6 (d), 134.4 (d), 149.5 (s) ppm. Anal. Calcd for C₁₄H₉NO₂: C, 75.33; H, 4.06; N, 6.27. Found: C, 75.53; H, 4.16; N, 6.13.

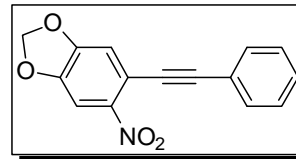
4-fluoro-1-nitro-2-(phenylethynyl)benzene (27): Dark orange color solid, 75% yield. Mp. 45 °C. IR (CHCl₃): ν 3054, 2936, 1652, 1610, 1578, 1520, 1477, 1447, 1385, 1357, 1260, 895, 780, 756, 688, 603 cm⁻¹. ¹H NMR (200



MHz, CDCl₃): δ 7.14 (ddd, J = 9.1, 6.4, 2.7 Hz, 1H), 7.36–7.43 (m, 4H), 7.57–7.63 (m, 2H), 8.15 (dd, J = 9.2, 5.1 Hz, 1H) ppm. ¹³C NMR (50 MHz, CDCl₃): δ 83.9 (s), 98.5 (s), 116.0 (d, $J_{\text{C}\beta\text{F}}$ = 24.1 Hz), 121.1(d, $J_{\text{C}\beta\text{F}}$ = 24.1 Hz), 121.4 (s, $J_{\text{C}\gamma\text{F}}$ = 10.7 Hz), 121.7 (s), 127.4 (d, $J_{\text{C}\gamma\text{F}}$ = 10.7 Hz), 128.4 (d, 2C), 129.5 (d), 132.0 (d, 2C), 145.6 (s, $J_{\text{C}\delta\text{F}}$ = 3.3 Hz), 164.3 (s, $J_{\text{C}\alpha\text{F}}$ = 257.2 Hz) ppm. Anal. Calcd for C₁₄H₈FN₂O₂: C, 69.71; H, 3.34; F, 7.88; N, 5.8. Found: C, 69.63; H, 3.41; F, 7.72; N, 5.78.

5-nitro-6-(phenylethynyl)benzo[d][1,3]dioxole (28):

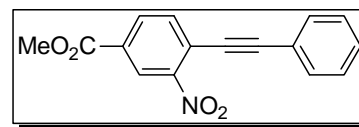
Pale brown color solid, 72% yield. Mp. 101 °C. IR (CHCl₃): ν 3077, 3022, 2400, 1614, 1557, 1522, 1493, 1443, 1341, 1297, 1210, 1073, 959, 754 cm⁻¹. ¹H NMR



(200 MHz, CDCl₃): δ 6.14 (s, 2H), 7.04 (s, 1H), 7.35–7.38 (m, 3H), 7.55–7.60 (m, 3H) ppm. ¹³C NMR (50 MHz, CDCl₃): δ 5.4 (s), 96.1 (s), 103.9 (t), 105.4 (d), 112.4(d), 114.7 (s), 122.5 (s), 128.4 (d, 2C), 129.0 (d), 131.9 (d, 2C), 144.4 (s), 147.8 (s), 151.5 (s) ppm. Anal. Calcd for C₁₅H₉NO₄: C, 67.42; H, 3.39; N, 5.24. Found: C, 67.37; H, 3.42; N, 5.20.

Methyl 3-nitro-4-(phenylethynyl)benzoate (29):

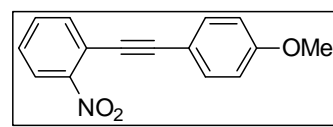
Orange color solid, 65% yield. Mp. 108 °C. IR (CHCl₃): ν 3022, 2924, 2400, 1728, 1617, 1557,



1532, 1437, 1345, 1286, 1115, 1026, 756 cm⁻¹. ¹H NMR (200 MHz, CDCl₃): δ 3.97 (s, 3H), 7.35–7.43 (m, 3H), 7.58 (dd J = 0.9, 3.4 Hz, 1H), 7.6 (br dd, J = 2.1, 7.7 Hz, 1H), 7.77 (d, J = 8.1 Hz, 1H), 8.22 (dd, J = 1.6, 8.1 Hz, 1H), 8.70 (d, J = 1.6 Hz, 1H) ppm. ¹³C NMR (50MHz, CDCl₃): δ 52.7 (q), 84.5 (s), 100.4 (s), 121.7 (s), 122.7 (s), 125.7 (d), 128.5 (d, 2C), 129.7 (d), 130.1 (s), 132.1 (d, 2C), 133.1 (d), 134.6 (d), 149.3 (s), 164.5 (s) ppm. Anal. Calcd for C₁₆H₁₁NO₄: C, 68.32; H, 3.94; N, 4.98. Found: C, 68.28; H, 3.81; N, 4.93.

1-((4-methoxyphenyl)ethynyl)-2-nitrobenzene (30):

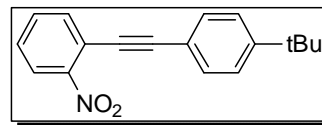
Brick red color spongy mass, 78% yield. Mp. 161 °C. IR (CHCl₃): ν 3019, 2936, 2400, 1720, 1611, 1600,



1567, 1523, 1464, 1439, 1342, 1288, 1251, 1080, 1029, 833, 756 cm⁻¹. ¹H NMR (200 MHz, CDCl₃): δ 3.84 (s, 3H), 6.89 (br dt, J = 9.1, 2.5 Hz, 2H), 7.42 (ddd, J = 1.6, 7.3, 8.2 Hz, 1H), 7.50–7.55 (m, 2H), 7.59 (dd, J = 7.3, 1.5Hz, 1H), 7.68 (dd, J = 7.7, 1.5 Hz, 1H), 8.07 (dd, J = 8.2, 1.2 Hz, 1H) ppm. ¹³C NMR (50 MHz, CDCl₃): δ 55.2 (q), 83.9 (s), 97.7 (s), 114.1 (d, 2C), 114.4 (s), 119.2 (s), 124.7 (d), 127.9 (d), 132.6 (d), 133.6 (d, 2C), 134.3 (d), 149.4 (s), 160.4 (s) ppm. Anal. Calcd for C₁₅H₁₁NO₃: C, 71.14; H, 4.38; N, 5.53. Found: C, 71.31; H, 4.31; N, 5.47.

1-((4-(tert-butyl)phenyl)ethynyl)-2-nitrobenzene (31):

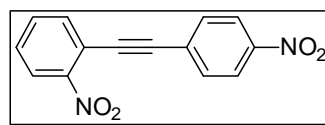
Red color spongy mass, 75% yield. IR (CHCl₃): ν 3020, 2960, 2400, 1603, 1568, 1526, 1476, 1346, 1293, 1215,



1105, 1022, 837, 757 cm⁻¹. ¹H NMR (200 MHz, CDCl₃): δ 1.33 (s, 9H), 7.38–7.45 (m, 3H), 7.48–7.63 (m, 3H), 7.72 (dd, J = 7.7, 1.6Hz, 1H), 8.08 (dd, J = 8.0, 1.3 Hz, 1H) ppm. ¹³C NMR (50 MHz, CDCl₃): δ 31.1 (q, 3C), 34.8 (s), 84.2 (s), 97.4 (s), 118.9 (s), 119.3 (s), 124.6 (d), 125.4 (d, 2C), 128.3 (d), 131.7 (d, 2C), 132.7 (d), 134.5 (d), 141.8 (s), 152.6 (s) ppm. Anal. Calcd for C₁₈H₁₇NO₂: C, 77.40; H, 6.13; N, 5.01. Found: C, 77.29; H, 6.24; N, 4.92.

1-nitro-2-((4-nitrophenyl)ethynyl)benzene (32):

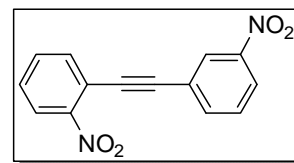
Orange color spongy mass, 65% yield. IR (CHCl₃): ν 2985, 2400, 1608, 1596, 1447, 1373, 1276, 1215, 1017,



909, 759 cm⁻¹. ¹H NMR (200 MHz, CDCl₃): δ 7.56 (ddd, J = 1.7, 7.3, 8.0 Hz, 1H), 7.67 (dt, J = 1.5, 7.7 Hz, 1H), 7.72–7.79 (m, 3H), 8.15 (dd, J = 8.1, 1.3Hz, 1H), 8.25 (dt, J = 9.0, 2.1Hz, 2H) ppm. ¹³C NMR (50MHz, CDCl₃): δ 89.4 (s), 94.3 (s), 117.5 (s), 123.6 (d, 2C), 124.9 (d), 128.1 (s), 129.1 (s), 129.6 (d), 132.7 (d, 2C), 133.1 (d), 134.7 (d), 147.5 (s) ppm. Anal. Calcd for C₁₄H₈N₂O₄: C, 62.69; H, 3.01; N, 10.44. Found: 62.62; H, 3.09; N, 10.39.

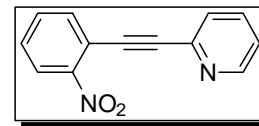
1-nitro-2-((3-nitrophenyl)ethynyl)benzene (33):

Orange color spongy mass, 62% yield. IR (CHCl₃): ν 3019, 2956, 2400, 1603, 1596, 1524, 1479, 1465, 1373, 1359, 1242, 1097, 1047, 938, 738 cm⁻¹. ¹H NMR (200 MHz, CDCl₃): δ



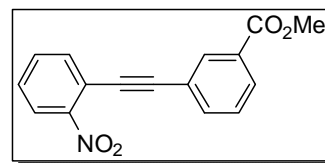
7.58 (dt, J = 7.9, 1.4 Hz, 2H), 7.69 (dd, J = 7.3, 1.4 Hz, 1H), 7.77 (dd, J = 7.7, 1.4 Hz, 1H), 7.91 (dt, J = 1.2, 7.7 Hz, 1H), 8.15 (dd, J = 1.1, 8.2 Hz, 1H), 8.25 (ddd, J = 1.0, 2.2, 8.3 Hz, 1H), 8.43 (t, J = 1.7 Hz, 1H) ppm. ¹³C NMR (50MHz, CDCl₃): δ 86.9 (s), 93.9 (s), 117.6 (s), 123.8 (d), 124.2 (s), 124.9 (d), 126.6 (d), 129.4(d), 129.5 (d), 133.1 (d), 134.7 (d), 137.7 (d), 148.1 (s), 149.6 (s) ppm. Anal. Calcd for C₁₄H₈N₂O₄: C, 62.69; H, 3.01; N, 10.44. Found: C 62.60; H, 3.11; N, 10.36.

2-((2-nitrophenyl)ethynyl)pyridine (34): Red color solid, 55% yield. Mp. 95 °C. IR (CHCl₃): ν 3032, 2958, 2233, 1632, 1608, 1568, 1527, 1480, 1467, 1345, 1216, 1145, 851,



757 cm⁻¹. ¹H NMR (200 MHz, CDCl₃): δ 7.28–7.32 (m, 1H), 7.53 (tt, J = 7.8, 1.5 Hz, 1H), 7.62–7.66 (m, 2H), 7.73 (tt, J = 7.7, 1.7 Hz, 1H), 7.80–7.82 (m, 1H), 8.12 (d, J = 8.0 Hz, 1H), 8.66 (d, J = 4.2 Hz, 1H) ppm. ¹³C NMR (100 MHz, CDCl₃): δ 84.1 (s), 95.5 (s), 117.7 (s), 123.5 (d), 124.7 (d), 127.9 (d), 129.3 (d), 132.9 (d), 134.9 (d), 136.2 (d), 142.6 (s), 149.7 (s), 150.1 (d) ppm. Anal. Calcd for C₁₃H₈N₂O₂: C, 69.64; H, 3.60; N, 12.49. Found: C, 69.69; H, 3.72; N, 12.41.

Methyl 3-((2-nitrophenyl)ethynyl)benzoate (35):

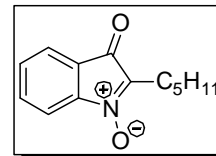


Orange color solid, 85% yield. IR (CHCl₃): ν 3021, 2953, 2400, 1743, 1610, 1527, 1438, 1345, 1296, 1262, 1215, 1152, 1083, 910, 756 cm⁻¹. ¹H NMR (200 MHz, CDCl₃): δ 3.93 (s, 3H), 7.45 (dt, J = 04, 7.8 Hz, 1H), 7.47 (ddd, J = 1.6, 7.3, 8.1 Hz, 1H), 7.61 (dt, J = 1.4, 7.7, Hz, 1H), 7.71 (ddd, J = 0.4, 1.6, 7.3 Hz, 1H), 7.76 (dd, J = 1.4, 7.7 Hz, 1H), 8.09 (dd, 1.2, 8.1 Hz, 1H), 8.03 (ddd, J = 1.2, 1.7, 7.8 Hz, 1H), 8.23 (dt, J = 1.7, 0.5Hz, 1H) ppm. ¹³C NMR (50 MHz, CDCl₃): δ 52.3 (q), 85.5 (s), 95.7 (s), 118.2 (s), 122.7 (s), 124.7 (d), 128.6 (d), 128.8 (d), 130.1 (d), 130.5 (s), 132.8 (d), 132.9 (d), 134.6 (d), 136.0 (d), 149.4 (s), 166.1 (s) ppm. Anal. Calcd for C₁₆H₁₁NO₄: C, 68.32; H, 3.94; N, 4.98. Found: C, 68.27; H, 3.84; N, 4.91.

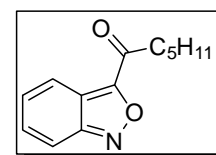
General Procedure for Cycloisomerization: To a solution of alkyne **3** (0.5 mmol) in CH₃CN (15 mL) was added Pd(CH₃CN)₂Cl₂ (0.025 mmol, 5 mol%), were added and stirred under argon for 4 h at rt. The reaction mixture was concentrated and the residue obtained was purified by column chromatography (ethyl acetate in petroleum ether) to afford the cyclised product.

3-oxo-2-pentyl-3H-indole 1-oxide (4): Yellow syrup, 69% yield.

IR (CHCl₃): ν 3019, 2958, 2930, 1711, 1695, 1607, 1588, 1528, 1466, 1353, 1322, 1297, 1216, 1180, 1056, 755 cm⁻¹. ¹H NMR (200 MHz, CDCl₃): δ 0.89 (t, J = 7.0 Hz, 3H), 1.31–1.40 (m, 4H), 1.63–1.71 (m, 2H), 2.67 (t, J = 7.4 Hz, 2H), 7.50–7.56 (m, 2H), 7.60–7.66 (m, 2H) ppm. ¹³C NMR (50 MHz, CDCl₃): δ 13.8 (q), 21.3 (t), 22.3 (t), 25.1 (t), 31.7 (t), 113.7 (d), 121.3 (d), 123.1 (s), 125.5 (s), 130.9 (d), 134.3 (d), 147.4 (s), 186.8 (s) ppm. Anal. Calcd for C₁₃H₁₅NO₂: C, 71.87; H, 6.96; N, 6.45. Found: C, 71.76; H, 6.91; N, 6.40.



1-(benzo[c]isoxazol-3-yl)hexan-1-one (5): To a solution of alkyne **3** (100 mg, 0.46 mmol) in CH₃CN (15 mL) was added AuBr₃ (10 mg, 0.023 mmol, 5 mol%), were added and stirred under argon for 4 h at rt. The reaction mixture was concentrated

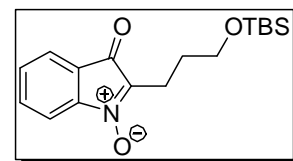


and the residue obtained was purified by column chromatography (5% → 10% ethyl acetate in petroleum ether) to afford **5** (75 mg, 75%) as yellow oil. IR (CHCl₃): ν 3022, 2958, 2932, 1732, 1608, 1568, 1527, 1480, 1480, 1345, 1216, 851, 757, 668 cm⁻¹. ¹H NMR (400 MHz, CDCl₃): δ 0.93 (t, J = 6.9 Hz, 3H), 1.36–1.45 (m, 4H), 1.76–1.90 (m, 2H), 3.17 (t, J = 7.4 Hz, 2H), 7.27 (ddd, J = 1.0, 6.4, 8.7 Hz, 1H), 7.40 (ddd, J = 1.0, 6.4, 8.9 Hz, 1H), 7.73 (dt, J = 1.0, 8.8 Hz, 1H), 8.05 (dt, J = 1.0, 8.8 Hz, 1H) ppm. ¹³C NMR (125 MHz, CDCl₃): δ 13.9 (q), 22.4 (t), 23.2 (t), 31.3 (t), 40.1 (t), 115.9 (d), 119.1 (s), 121.2 (d), 128.4 (d), 131.2 (d), 157.5 (s), 159.7 (s), 190.5 (s) ppm. Anal. Calcd for C₁₃H₁₅NO₂: C, 71.87; H, 6.96; N, 6.45. Found: C, 71.61; H, 7.08; N, 6.40.

2-(3-((tert-butyl)dimethylsilyloxy)propyl)-3-oxo-3H-

indole 1-oxide (16): Yellow liquid, 71% yield. IR

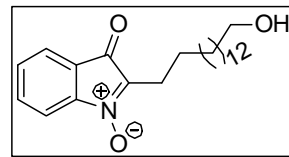
(CHCl₃): ν 2954, 2929, 2885, 1709, 1684, 1634, 1557, 1520, 1471, 1465, 1445, 1345, 1276, 1255, 1194, 1143, 1101, 1006, 980, 836, 776 cm⁻¹. ¹H NMR (200 MHz, CDCl₃): δ -0.05 (s, 6H), 0.80 (s, 9H), 1.81–1.94 (m, 2H), 2.71 (t, J = 7.4 Hz, 2H), 3.65 (t, J = 5.9 Hz, 2H), 7.44–7.51 (m, 2H), 7.55–7.60 (m, 2H) ppm. ¹³C NMR (50 MHz, CDCl₃): δ -5.5 (q, 2C), 18.2 (s), 18.6 (t), 25.8 (q, 3C), 28.3 (t), 62.8 (t), 113.6 (d), 121.3 (d), 123.2 (s), 125.5



(s), 130.8 (d), 134.2 (d), 147.5 (s), 186.7 (s) ppm. Anal. Calcd for $C_{17}H_{25}NO_3Si$: C, 63.91; H, 7.89; N, 4.38. Found: C, 63.81; H, 7.72; N, 4.32.

2-(15-hydroxypentadecyl)-3-oxo-3H-indole 1-oxide

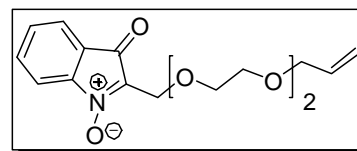
(17): Dark brown gum, 43% yield. IR ($CHCl_3$): ν 3381, 2920, 2851, 1705, 1607, 1531, 1475, 1385, 1185, 1058, 755 cm^{-1} . 1H NMR (200 MHz, $CDCl_3$): δ 1.25–1.35 (m,



22H), 1.50–1.69 (m, 5H), 2.66 (t, $J = 7.5$ Hz, 2H), 3.64 (t, $J = 6.6$ Hz, 2H), 7.51–7.66 (m, 4H), ppm. ^{13}C NMR (50 MHz, $CDCl_3$): δ 21.4 (t), 25.4 (t), 25.7 (t), 29.2 (t), 29.4 (t, 2C), 29.6 (t, 6C), 29.7 (t), 32.8 (t), 63.1 (t), 113.7 (d), 121.3 (d), 123.1 (s), 125.6 (s), 130.9 (d), 134.3 (d), 147.4 (s), 186.9 (s) ppm. Anal. Calcd for $C_{23}H_{35}NO_3$: C, 73.96; H, 9.44; N, 3.75. Found: C, 73.88; H, 9.34; N, 3.71.

2-((2-(2-(allyloxy)ethoxy)ethoxy)methyl)-3-oxo-

3H-indole 1-oxide (18): Dark brown spongy mass, 51% yield. IR ($CHCl_3$): ν 3079, 2919, 2856, 1707,

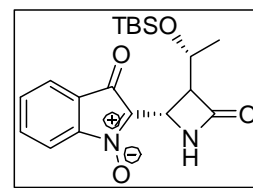


1608, 1568, 1526, 1475, 1459, 1345, 1262, 1180, 1098, 928, 747 cm^{-1} . 1H NMR (200 MHz, $CDCl_3$): δ 3.54–3.60 (m, 2H), 3.63–3.69 (m, 4H), 3.73–3.78 (m, 2H), 4.01 (dt, $J = 5.7, 1.4$ Hz, 2H), 4.58 (s, 2H), 5.18 (ddd, $J = 10.4, 3.1, 1.3$ Hz, 1H), 5.27 (ddd, $J = 17.2, 3.1, 1.3$ Hz, 1H), 5.90 (ddt, $J = 17.2, 10.4, 5.7$ Hz, 1H), 7.51–7.63 (m, 2H), 7.64–7.70 (m, 2H), ppm. ^{13}C NMR (125 MHz, $CDCl_3$): δ 58.9 (t), 69.4 (t), 70.3 (t), 70.5 (t), 71.4 (t), 72.2 (t), 112.2 (d), 117.1 (t), 119.0 (s), 123.5 (s), 123.9 (d), 125.8 (d), 134.8 (d), 138.6 (d), 149.1 (s), 182.9 (s) ppm. Anal. Calcd for $C_{16}H_{19}NO_5$: C, 62.94; H, 6.27; N, 4.59. Found: C, 62.82; H, 6.21; N, 4.49.

2-((2S)-3-((R)-1-((tert-butyl dimethylsilyl)oxy)ethyl)-4-

oxoazetidin-2-yl)-3-oxo-3H-indole 1-oxide (19): Yellow solid, 75% yield. Mp. 103 °C. $[\alpha]_D^{25} = +22.4$ ($c = 1, CHCl_3$).

IR ($CHCl_3$): ν 3414, 3019, 2956, 2930, 2885, 1770, 1712,

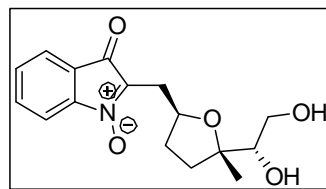


1672, 1609, 1570, 1529, 1472, 1377, 1346, 1215, 1180, 1144, 1065, 959, 756 cm^{-1} . 1H NMR (200 MHz, $CDCl_3$): δ 0.11 (d, $J = 1.3$ Hz, 6H), 0.89 (s, 9H), 1.27 (d, $J = 6.3$ Hz, 3H), 3.87–3.90 (m, 1H), 4.31–4.42 (m, 1H), 4.90 (d, $J = 2.5$ Hz, 1H), 6.16 (s, 1H), 7.57–7.69 (m, 4H) ppm. ^{13}C NMR (50 MHz, $CDCl_3$): δ -5.0 (q), -4.2 (q), 18.0

(s), 22.6 (q), 25.8 (q, 3C), 41.8 (d), 62.8 (d), 64.5 (d), 114.1 (d), 121.9 (d), 123.1 (s), 131.9 (d), 134.6 (d), 146.8 (s), 167.7 (s), 185.2 (s) ppm. Anal. Calcd for $C_{19}H_{26}N_2O_4Si$: C, 60.93; H, 7.0; N, 7.48; Si, 7.50. Found: C, 60.81; H, 7.2; N, 7.34; Si, 7.13.

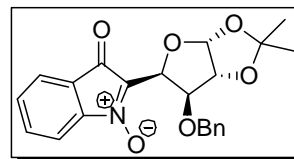
2-(((2S,5S)-5-((S)-1,2-dihydroxyethyl)-5-methyltetrahydrofuran-2-yl)methyl)-3-oxo-3H-indole 1-oxide (20): Orange oil. 65% yield. IR

($CHCl_3$): ν 3410, 2971, 2931, 1713, 1608, 1559, 1527, 1463, 1376, 1217, 1174, 1089, 755 cm^{-1} . 1H NMR (200 MHz, $CDCl_3$): δ 1.16 (s, 3H), 1.57–1.84 (m, 3H),



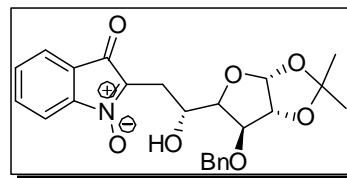
2.01–2.16 (m, 2H), 2.69 (br s, 1H), 2.82 (dd, $J = 5.8, 14.4$ Hz, 1H), 2.98 (dd, $J = 7.3, 14.4$ Hz, 1H), 3.43–3.53 (m, 1H), 3.60–3.69 (m, 2H), 4.39–4.53 (m, 1H), 7.47–7.76 (m, 4H) ppm. ^{13}C NMR (50MHz, $CDCl_3$): δ 24.0 (q), 29.7 (t), 32.2 (t), 32.4 (t), 63.1 (t), 76.0 (d), 76.6 (d), 85.0 (s), 113.9 (d), 121.5 (d), 123.0 (s), 127.6 (s), 132.2 (d), 134.4 (d), 147.3 (s), 186.6 (s) ppm. Anal. Calcd for $C_{16}H_{19}NO_5$: C, 62.99; H, 6.27; N, 4.59. Found: C, 62.79; H, 6.38; N, 4.48.

Compound 21. Brown syrup. 83% yield. $[\alpha]_D^{25} = -18.5$ ($c = 1, CHCl_3$). IR ($CHCl_3$): ν 3054, 2987, 2685, 1711, 1606, 1575, 1502, 1421, 1265, 1165, 1061, 896, 739, 705 cm^{-1} . 1H NMR (400 MHz, $CDCl_3$): δ 1.38 (s, 3H), 1.53 (s,



3H), 4.40 (d, $J = 4.5$ Hz, 1H), 4.43 (d, $J = 13.1$ Hz, 1H), 4.63 (d, $J = 12.1$ Hz, 1H), 4.77 (d, $J = 3.9$ Hz, 1H), 5.65 (d, $J = 4.5$ Hz, 1H), 6.21 (d, $J = 3.9$ Hz, 1H), 7.04–7.13 (m, 5H), 7.54–7.58 (m, 3H), 7.63 (dd, $J = 1.5, 7.7$ Hz, 1H) ppm. ^{13}C NMR (100 MHz, $CDCl_3$): δ 26.7 (q), 27.3 (q), 72.5 (t), 74.7 (d), 83.2 (d), 83.7 (d), 105.8 (d), 112.7 (s), 113.9 (d), 121.7 (d), 123.4 (s), 127.3 (d, 2C), 127.7 (d), 128.3 (d, 2C), 131.5 (d), 134.1 (d), 134.3 (s), 137.0 (s), 146.6 (s), 184.2 (s) ppm. Anal. Calcd for $C_{22}H_{21}NO_6$: C, 66.83; H, 5.35; N, 3.54. Found: C, 66.85; H, 5.45; N, 3.47.

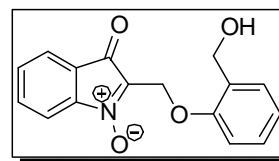
Compound 22. Yellow oil, 87% yield. $[\alpha]_D^{25} = -12.8$ ($c = 1, CHCl_3$). IR ($CHCl_3$): ν 3370, 3019, 2930, 1712, 1685, 1606, 1555, 1535, 1454, 1438, 1216, 1174, 1076, 1012, 756 cm^{-1} . 1H NMR (200 MHz,



CDCl₃): δ 1.31 (s, 3H), 1.45 (s, 3H), 2.95 (dd, $J = 15.3, 8.8$ Hz, 1H), 3.16 (dd, $J = 15.3, 3.6$ Hz, 1H), 3.58 (bs, 1H), 4.08 (dd, $J = 7.7, 3.2$ Hz, 1H), 4.16 (d, $J = 3.2$ Hz, 1H), 4.57–4.75 (m, 3H), 5.93 (d, $J = 6.6$ Hz, 1H), 7.31–7.38 (m, 5H), 7.51–7.66 (m, 4H) ppm. ¹³C NMR (50MHz, CDCl₃): δ 26.3 (q), 26.7 (q), 27.7 (t), 66.9 (d), 72.2 (t), 81.6 (d), 82.3 (d), 82.5 (d), 105.1 (d), 111.8 (s), 113.9 (d), 121.7 (d), 123.0 (s), 127.9 (d, 2C), 128.1 (d), 128.6 (d, 2C), 131.2 (d), 134.5 (d), 137.1 (s), 137.2 (s), 186.5 (s) ppm. Anal. Calcd for C₂₄H₂₅NO₇: C, 65.59; H, 5.73; N, 3.19. Found: C, 65.41; H, 5.69; N, 3.14.

2-((2-(hydroxymethyl)phenoxy)methyl)-3-oxo-3H-indole

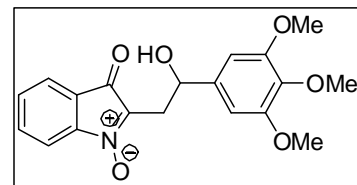
1-oxide (23): Yellow liquid, 67% yield. IR (CHCl₃): ν 3431, 2923, 2852, 1705, 1655, 1608, 1588, 1530, 1487, 1458, 1348, 1295, 1231, 1173, 1037, 756 cm⁻¹. ¹H NMR



(200 MHz, CDCl₃): δ 1.68 (br s, 1H), 4.66 (s, 2H), 5.19 (s, 2H), 6.93–7.06 (m, 2H), 7.24–7.28 (m, 2H), 7.56–7.71 (m, 4H) ppm. ¹³C NMR (50 MHz, CDCl₃): δ 56.2 (t), 61.9 (t), 111.5 (d), 114.4 (d), 121.8 (d), 122.0 (d), 122.8 (s), 129.0 (d), 129.5 (d), 130.1 (s), 132.1 (d), 133.5 (s), 134.7 (d), 146.8 (s), 155.6 (s), 185.4 (s) ppm. Anal. Calcd for C₁₆H₁₃NO₄: C, 67.84; H, 4.63; N, 4.94. Found: C, 67.79; H, 4.69; N, 4.83.

2-(2-hydroxy-2-(3,4,5-trimethoxyphenyl)ethyl)-3-

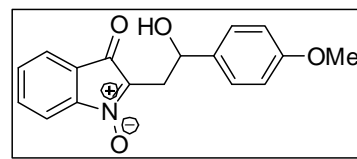
oxo-3H-indole 1-oxide (24): Dark brown gum, 67% yield. IR (CHCl₃): ν 3436, 2929, 2898, 1707, 1603, 1593, 1538, 1506, 1463, 1420, 1327, 1234, 1180,



1126, 769 cm⁻¹. ¹H NMR (200 MHz, CDCl₃): δ 3.08 (dd, $J = 15.0, 4.0$ Hz, 1H), 3.24, (dd, $J = 15.0, 8.0$ Hz, 1H), 3.84 (s, 9H), 5.14 (dd, $J = 8.0, 4.0$ Hz, 1H), 5.48 (s, 1H), 6.63 (s, 2H), 7.50–7.65 (m, 4H) ppm. ¹³C NMR (50MHz, CDCl₃): δ 31.8 (t), 56.1 (q, 2C), 60.8 (q), 71.4 (d), 102.0 (d, 2C), 114.0 (d), 121.9 (d), 122.8 (s), 131.4 (d), 134.7 (d), 136.8 (s), 137.1 (s), 138.8 (s), 147.2 (s), 153.2 (s, 2C), 186.5 (s) ppm. Anal. Calcd for C₁₉H₁₉NO₆: C, 63.86; H, 5.36; N, 3.92. Found: C, 63.79; H, 5.31; N, 3.88.

2-(2-hydroxy-2-(4-methoxyphenyl)ethyl)-3-oxo-

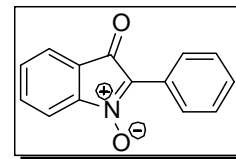
3H-indole 1-oxide (25): Pale grey color solid, 78% yield. IR (CHCl₃): ν 3350, 3019, 2928, 1712, 1664,



1611, 1514, 1494, 1464, 1345, 1215, 1174, 1056, 756 cm^{-1} . ^1H NMR (200 MHz, CDCl_3): δ 1.69 (s, 1H), 3.07 (dd, $J = 15.0, 4.1$ Hz, 1H), 3.21 (dd, $J = 15.0, 8.1$ Hz, 1H), 3.77 (s, 3H), 5.17 (dd, $J = 8.1, 4.1$ Hz, 1H), 6.83–6.90 (m, 2H), 7.31–7.38 (m, 2H), 7.53–7.59 (m, 2H), 7.62–7.67 (m, 2H) ppm. ^{13}C NMR (50 MHz, CDCl_3): δ 31.9 (t), 55.2 (q), 70.8 (d), 113.8 (d, 2C), 114.0 (d), 121.7 (d), 122.8 (s), 126.6 (d, 2C), 131.2 (d), 134.6 (d), 135.3 (s), 136.8 (s), 147.2 (s), 159.1 (s), 186.5 (s) ppm. Anal. Calcd for $\text{C}_{17}\text{H}_{15}\text{NO}_4$: C, 68.68; H, 5.09; N, 4.71. Found: C, 68.79; H, 5.23; N, 4.65.

3-oxo-2-phenyl-3H-indole 1-oxide (36): Dark orange colour

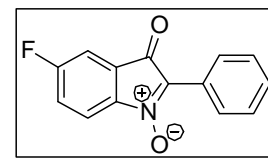
solid, 61% yield. Mp. 183 °C. IR (CHCl_3): ν 3054, 2986, 1702, 1601, 1569, 1527, 1512, 1496, 1422, 1374, 1265, 1178, 1046, 1029, 739, 705 cm^{-1} . ^1H NMR (200 MHz, CDCl_3): δ 7.45–7.50



(m, 3H), 7.53–7.57 (m, 1H), 7.61–7.65 (m, 1H), 7.67–7.70 (m, 2H), 8.61–8.66 (m, 2H) ppm. ^{13}C NMR (125 MHz, CDCl_3): δ 114.2 (d), 121.5 (d), 122.9 (s), 125.9 (s), 127.8 (d, 2C), 127.8 (s), 128.5 (d, 2C), 130.7 (d), 131.1 (d), 134.7 (d), 147.9 (s), 186.7 (s) ppm. Anal. Calcd for $\text{C}_{14}\text{H}_9\text{NO}_2$: C, 75.33; H, 4.06; N, 6.27. Found: C, 75.53; H, 4.16; N, 6.13.

5-fluoro-3-oxo-2-phenyl-3H-indole 1-oxide (37): Orange

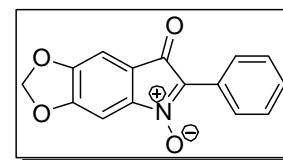
color solid, 91% yield. Mp. 143 °C. IR (CHCl_3): ν 3032, 2998, 1704, 1597, 1523, 1481, 1446, 1385, 1283, 1181, 1020, 875, 758, 685 cm^{-1} . ^1H NMR (200 MHz, CDCl_3): δ



7.29–7.35 (m, 2H), 7.48–7.51 (m, 3H), 7.67 (dd, $J = 9.0, 3.9$ Hz, 1H), 8.57–8.62 (m, 2H) ppm. ^{13}C NMR (50 MHz, CDCl_3): δ 109.66 (d, $J_{\text{C}\delta\text{F}} = 26.4$ Hz), 115.92 (d, $J_{\text{C}\gamma\text{F}} = 8.6$ Hz), 120.6 (d, $J_{\text{C}\delta\text{F}} = 26.4$ Hz), 124.8 (s, $J_{\text{C}\gamma\text{F}} = 8.6$ Hz), 125.6 (s), 127.5 (d, 2C), 128.5 (d, 2C), 128.5 (s), 130.8 (d), 143.2 (s, $J_{\text{C}\delta\text{F}} = 2.0$ Hz) 164.3 (s, $J = 253.9$ Hz), 185.4 (s, $J_{\text{C}\delta\text{F}} = 1.9$ Hz) ppm. Anal. Calcd for $\text{C}_{14}\text{H}_8\text{FNO}_2$: C, 69.71; H, 3.34; F, 7.88; N, 5.81. Found: C, 69.63; H, 3.41; F, 7.72; N, 5.78.

7-oxo-6-phenyl-7H-[1,3]dioxolo[4,5-f]indole 5-oxide (38): Red color solid, 67% yield. Mp. 176 °C. IR (CHCl_3):

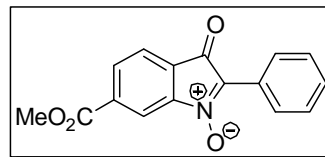
ν 3100, 3090, 2917, 1702, 1632, 1587, 1505, 1489, 1445, 1390, 1350, 1277, 1168, 1029, 919, 775 cm^{-1} . ^1H NMR



(200 MHz, CDCl₃): δ 6.14 (s, 2H), 7.02 (s, 1H), 7.16 (s, 1H), 7.43–7.51 (m, 3H), 8.57–7.61 (m, 2H) ppm. ¹³C NMR (50 MHz, CDCl₃): δ 97.3 (d), 102.1 (d), 103.1 (t), 116.5 (s), 125.9 (s), 127.4 (d, 2C), 128.4 (d, 2C), 128.6 (s), 130.3 (d), 144.6 (s), 149.6 (s), 152.7 (s), 185.8 (s) ppm. Anal. Calcd for C₁₅H₉NO₄: C, 67.42; H, 3.39; N, 5.24. Found: C, 67.37; H, 3.42; N, 5.20.

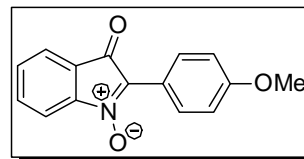
6-(methoxycarbonyl)-3-oxo-2-phenyl-3H-indole 1-oxide (39): Orange color solid, 87% yield. Mp. 150 °C.

IR (CHCl₃): ν 3084, 3031, 2955, 1746, 1709, 1596, 1577, 1475, 1460, 1379, 1352, 1284, 1185, 1068, 910, 807, 760 cm⁻¹. ¹H NMR (200 MHz, CDCl₃): δ 3.99 (s, 3H), 7.48–7.51 (m, 3H), 7.70 (d, J = 7.4 Hz, 1H), 8.26 (dd, J = 1.3, 7.6 Hz, 1H), 8.29 (br s, 1H), 8.60–8.64 (m, 2H) ppm. ¹³C NMR (50 MHz, CDCl₃): δ 52.9(q), 114.9 (d), 121.4 (d), 125.5 (s), 125.9 (s), 127.8 (d, 2C), 128.6 (d, 2C), 128.6 (s), 131.0 (d), 133.0 (d), 136.2 (s), 147.6 (s), 164.8 (s), 185.9 (s) ppm. Anal. Calcd for C₁₆H₁₁NO₄: C, 68.32; H, 3.94; N, 4.98. Found: C, 68.28; H, 3.81; N, 4.93.



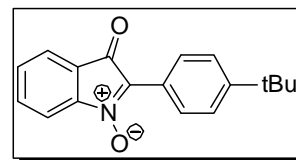
2-(4-methoxyphenyl)-3-oxo-3H-indole 1-oxide (40):

Red color solid, 67% yield. Mp. 160 °C. IR (CHCl₃): ν 3054, 2958, 1709, 1615, 1540, 1520, 1496, 1374, 1270, 1180, 1046, 745 cm⁻¹. ¹H NMR (400 MHz, CDCl₃): δ 3.86 (s, 3H), 7.00 (dt, J = 9.5, 2.3 Hz, 2H), 7.46–7.51 (m, 1H), 7.57–7.64 (m, 3H), 8.70 (dt, J = 9.5, 2.3 Hz, 2H) ppm. ¹³C NMR (400 MHz, CDCl₃): δ 55.3 (q), 113.9 (d), 114.1 (d, 2C), 118.8 (s), 121.5 (d), 122.8 (s), 124.8 (s), 129.7(d, 2C), 130.7(s), 134.8 (d), 148.0(d), 161.3 (s), 187.3 (s) ppm. Anal. Calcd for C₁₅H₁₁NO₃: C, 71.14; H, 4.38; N, 5.53. Found: C, 71.31; H, 4.31; N, 5.47.



2-(4-(tert-butyl)phenyl)-3-oxo-3H-indole 1-oxide (41):

Crimson red color solid, 91% yield. MP = 130 °C. IR (CHCl₃): ν 3065, 2951, 1702, 1596, 1529, 1494, 1461, 1377, 1320, 1284, 1184, 1024, 878, 839, 756 cm⁻¹. ¹H NMR (200 MHz, CDCl₃): δ 1.36 (s, 9H), 7.50–7.57 (m, 3H), 7.61–7.65 (m, 1H), 7.67–7.70 (m, 2H), 8.59 (dt, J = 8.8, 2.1 Hz, 2H) ppm. ¹³C NMR (50MHz, CDCl₃): δ

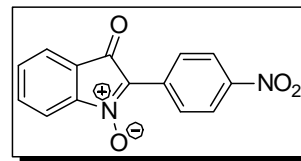


30.9 (q, 3C), 34.9 (s), 113.9 (d), 121.4 (d), 122.7 (s), 122.9 (s), 125.3 (s), 125.5 (d, 2C), 127.6 (d, 2C), 130.9 (d), 134.7 (d), 147.8 (s), 154.1(s), 186.9 (s) ppm. Anal. Calcd for C₁₈H₁₇NO₂: C, 77.40; H, 6.13; N, 5.01. Found: C, 77.29; H, 6.24; N, 4.92.

2-(4-nitrophenyl)-3-oxo-3H-indole 1-oxide (42):

Orange color solid, 69% yield. MP = 237 °C. IR (CHCl₃):

ν 3019, 3002, 1706, 1655, 1595, 1517, 1484, 1388, 1347, 1215, 1180, 1019, 756 cm⁻¹. ¹H NMR (200 MHz,

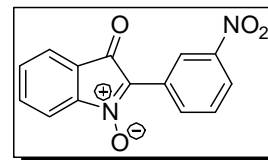


CDCl₃): δ 7.58–7.69 (m, 2H), 7.72–7.76 (m, 2H), 8.33 (dt, J = 8.3, 2.1 Hz, 2H), 8.89 (dt, J = 8.3, 2.1 Hz, 2H) ppm. ¹³C NMR (125 MHz, CDCl₃): δ 114.6 (d), 122.1 (d), 122.6(s), 123.7 (d, 2C), 123.9 (s), 128.2 (d, 2C), 131.6 (s), 132.2 (d), 135.3 (d), 147.7 (s), 147.9 (s), 186.2 (s) ppm. Anal. Calcd for C₁₄H₈N₂O₄: C, 62.69; H, 3.01; N, 10.44. Found: C, 62.60; H, 3.11; N, 10.36.

2-(3-nitrophenyl)-3-oxo-3H-indole 1-oxide (43): Dark

yellow solid, 56% yield. MP = 240 °C. IR (CHCl₃): ν 3020,

2927, 1711, 1619, 1595, 1529, 1469, 1317, 1216, 1175, 1093, 754 cm⁻¹. ¹H NMR (200 MHz, CDCl₃): δ 7.60–7.77

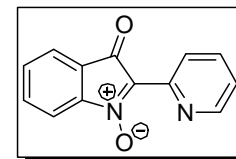


(m, 5H), 8.32 (ddd, J = 0.9, 2.1, 8.3 Hz, 1H), 9.0 (dd, J = 0.9, 1.5, 7.9 Hz, 1H), 9.61 (t, J = 1.9 Hz, 1H) ppm. ¹³C NMR (100 MHz, CDCl₃): δ 114.6(d), 122.1(d), 122.3 (d), 122.6 (s), 124.8 (d), 127.3 (s), 128.0 (s), 129.6 (d), 131.9 (d), 132.9 (d), 135.2 (d), 147.6 (s), 148.3 (s), 186.1 (s) (s) ppm. Anal. Calcd for C₁₄H₈N₂O₄: C, 62.69; H, 3.01; N, 10.44. Found: 62.60; H, 3.11; N, 10.36.

3-oxo-2-(pyridin-2-yl)-3H-indole 1-oxide (44): Red color

solid, 55% yield. Mp. 162 °C. IR (CHCl₃): ν 3084, 3031, 1708,

1596, 1519, 1485, 1459, 1376, 1272, 1184, 1091, 871, 751 cm⁻¹. ¹H NMR (500 MHz, CDCl₃): δ 7.35 (ddd, J = 0.4, 4.7, 7.5

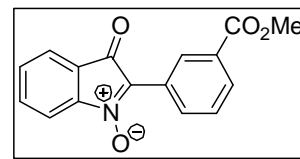


Hz, 1H), 7.61 (dt, J = 0.9, 7.3 Hz, 1H), 7.71 (d, J = 7.1 Hz, 2H), 7.73–7.76 (m, 1H), 7.86 (dt, J = 7.8, 1.7 Hz, 1H), 8.48 (d, J = 8.0 Hz, 1H), 8.88 (d, J = 4.1 Hz, 1H) ppm. ¹³C NMR (125 MHz, CDCl₃): δ 114.6 (d), 121.9 (d), 122.8 (s), 124.3 (d), 124.9 (d), 128.3 (s), 131.9 (d), 134.7 (d), 136.4 (d), 145.6 (s), 147.6 (s), 150.4 (d), 185.1 (s)

ppm. Anal. Calcd for $C_{13}H_8N_2O_2$: C, 69.64; H, 3.60; N, 12.49. Found: C, 69.69; H, 3.72; N, 12.41.

2-(3-(methoxycarbonyl)phenyl)-3-oxo-3H-indole 1-oxide (45): Yellow solid, 75% yield. Mp. 183 °C. IR

($CHCl_3$): ν 3084, 3031, 2955, 1746, 1709, 1596, 1577, 1519, 1485, 1434, 1376, 1298, 1272, 1184, 1091, 871,

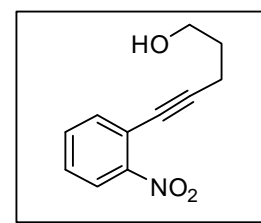


751 cm^{-1} . 1H NMR (200 MHz, $CDCl_3$): δ 3.97 (s, 3H), 7.55–7.61 (m, 2H), 7.63–7.65 (m, 1H), 7.68–7.73 (m, 2H), 8.14 (ddd, $J = 1.1, 1.6, 7.8$ Hz, 1H), 8.82 (ddd, $J = 1.1, 1.6, 8.1$ Hz, 1H), 9.30 (dt, $J = 1.7, 0.5$ Hz, 1H) ppm. ^{13}C NMR (50MHz, $CDCl_3$): δ 52.3 (q), 114.3 (d), 121.7 (d), 122.6 (s), 126.0 (s), 128.7 (d, 3C), 130.5 (s), 131.3 (s), 131.4 (d, 2C), 131.7 (d), 134.9 (d), 147.6 (s), 166.4 (s), 186.5 (s) ppm. Anal. Calcd for $C_{16}H_{11}NO_4$: C, 68.32; H, 3.94; N, 4.98. Found: C, 68.27; H, 3.84; N, 4.91.

3.2. Experimental data for nitroalkynol cycloisomerizations

General Procedure for Sonogashira Coupling: To a solution of alkyne (1 mmol), aryl iodide (1.2 mmol) in Et_3N (16 mL) and DMF (8 mL), TPP (0.1 mmol) and $Pd(PPh_3)_2Cl_2$ (0.05 mmol), were added and degassed with argon for 30 min. CuI (0.1 mmol) was added and degassed with argon for 10 min and stirred at rt for 5 h. The reaction mixture was partitioned between ethyl acetate and water. Organic layer was separated, washed with brine, dried (Na_2SO_4), concentrated and the residue obtained was purified by column chromatography (ethyl acetate in petroleum ether) to afford the coupled product.

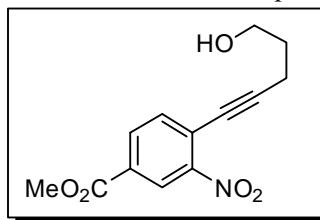
5-(2-nitrophenyl)pent-4-yn-1-ol (46): Yellow liquid, 83% yield. IR ($CHCl_3$): ν 3351, 2926, 2224, 1678, 1613, 1511, 1466, 1273, 1035 cm^{-1} . 1H NMR (200 MHz, $CDCl_3$): δ 1.87 (qui, $J = 6.4$ Hz, 2H), 1.87 (br s, 1H), 2.60 (t, $J = 6.8$ Hz, 2H), 3.83 (t, $J = 6.1$ Hz, 2H), 7.38 (ddd, $J = 2.1, 6.6,$



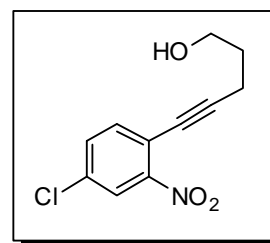
8.1 Hz, 1H), 7.51 (dt, $J = 1.4, 7.8$ Hz, 1H), 7.56 (dd, $J = 2.2, 7.6$ Hz, 1H), 7.95 (dd, $J = 1.3, 7.8$ Hz, 1H) ppm. ^{13}C NMR (50 MHz, $CDCl_3$): δ 16.2 (t), 30.7 (t), 61.2 (t), 76.3 (s), 98.3 (s), 118.9 (s), 124.3 (d), 127.9 (d), 132.6 (d), 134.6 (d), 149.8 (s) ppm. ESI-MS: m/z 206.4 (100%, $[M+H]^+$). Anal. Calcd for $C_{11}H_{11}NO_3$:

C, 64.38; H, 5.40; N, 6.83. Found: C, 64.47; H, 5.52; N, 6.62.

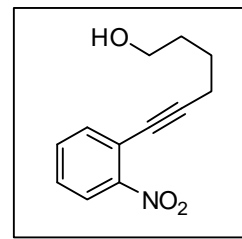
Methyl 4-(5-hydroxypent-1-yn-1-yl)-3-nitrobenzoate (53): Yellow liquid, 77% yield. IR (CHCl₃): ν 3365, 3017, 2954, 2230, 1719, 1619, 1534, 1437, 1289, 1090 cm⁻¹. ¹H NMR (200 MHz, CDCl₃): δ 1.85 (qui, J = 6.4 Hz, 2H), 2.34 (br s, 1H), 2.60 (t, J = 6.9 Hz, 2H), 3.79 (t, J = 6.1 Hz, 2H), 3.91 (s, 3H), 7.58 (dd, J = 8.1 Hz, 1H), 8.10 (dd, J = 1.7, 8.1 Hz, 1H), 8.55 (d, J = 1.7 Hz, 1H) ppm. ¹³C NMR (50 MHz, CDCl₃): δ 16.4 (t), 30.6 (t), 52.7 (q), 61.0 (t), 76.1 (s), 102.2 (s), 123.1 (s), 125.4 (d), 129.6 (s), 132.9 (d), 134.9 (d), 149.6 (s), 164.5 (s) ppm. ESI-MS: m/z 264.5 (100%, [M+H]⁺). Anal. Calcd for C₁₃H₁₃NO₅: C, 59.31; H, 4.98; N, 5.32. Found: C, 59.32; H, 5.00; N, 5.33.



5-(4-chloro-2-nitrophenyl)pent-4-yn-1-ol (54): Yellow liquid, 81% yield. IR (CHCl₃): ν 3368, 2949, 2230, 1605, 1555, 1530, 1478, 1345, 1259, 1110, 1058, cm⁻¹. ¹H NMR (200 MHz, CDCl₃): δ 1.76 (br s, 1H), 1.87 (qui, J = 6.5 Hz, 2H), 2.60 (t, J = 6.9 Hz, 2H), 3.82 (t, J = 6.1 Hz, 2H), 7.49 (d, J = 1.3 Hz, 2H), 7.97 (t, J = 1.3 Hz, 1H) ppm. ¹³C NMR (50 MHz, CDCl₃): δ 16.3 (t), 30.7 (t), 61.2 (t), 75.5 (s), 99.6 (s), 117.6 (s), 124.6 (d), 132.8 (d), 133.7 (s), 135.6 (d), 150.1 (s) ppm. ESI-MS: m/z 240.4 (100%, [M+H]⁺). Anal. Calcd for C₁₁H₁₀ClNO₃: C, 55.13; H, 4.21; Cl, 14.79; N, 5.84. Found: C, 55.22; H, 4.29; Cl, 14.62; N, 5.67.

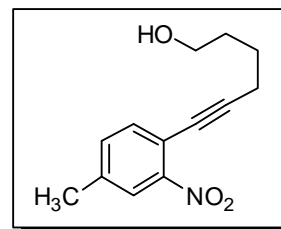


6-(2-nitrophenyl)hex-5-yn-1-ol (47): Yellow liquid, 71% yield. IR (CHCl₃): ν 3351, 2936, 2225, 1682, 1613, 1503, 1466, 1299, 1035 cm⁻¹. ¹H NMR (200 MHz, CDCl₃): δ 1.66–1.79 (m, 5H), 2.51 (t, J = 6.4 Hz, 2H), 3.69 (t, J = 6.0 Hz, 2H), 7.37 (ddd, J = 2.1, 6.8, 8.2 Hz, 1H), 7.50 (dt, J = 1.4, 7.7 Hz, 1H), 7.56 (dd, J = 2.1, 7.7 Hz, 1H), 7.94 (dd, J = 1.3, 7.8 Hz, 1H) ppm. ¹³C NMR (50 MHz, CDCl₃): δ 19.4 (t), 24.5 (t), 31.6 (t), 62.1 (t), 76.2 (s), 98.8 (s), 119.0 (s), 124.2 (d), 127.8 (d), 132.5 (d), 134.6 (d), 149.8 (s) ppm. ESI-MS: m/z 220.3 (100%, [M+H]⁺). Anal. Calcd for C₁₂H₁₃NO₃: C, 65.74; H, 5.98; N, 6.39. Found: C, 65.59; H, 5.91; N, 6.52.

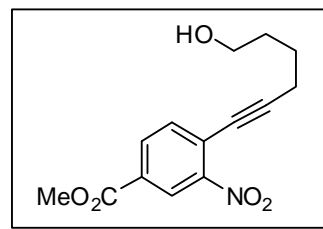


6-(4-methyl-2-nitrophenyl)hex-5-yn-1-ol (55):

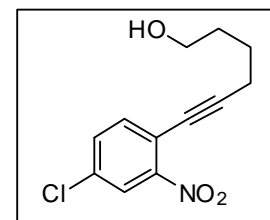
Yellow liquid, 70% yield. IR (CHCl₃): ν 3368, 3086, 2949, 2230, 1605, 1555, 1530, 1478, 1345, 1152, 1058 cm⁻¹. ¹H NMR (200 MHz, CDCl₃): δ 1.66–1.76 (m, 4H), 2.01 (br s, 1H), 2.38 (s, 3H), 2.48 (t, J = 6.4 Hz, 2H), 3.68 (t, J = 5.8 Hz, 2H), 7.29 (dd, J = 1.1, 7.9 Hz, 1H), 7.41 (d, J = 7.9 Hz, 1H), 7.73 (s, 1H) ppm. ¹³C NMR (50 MHz, CDCl₃): δ 19.4 (t), 20.9 (q), 24.5 (t), 31.6 (t), 62.1 (t), 76.1 (s), 97.6 (s), 116.1 (s), 124.5 (d), 133.3 (d), 134.3 (d), 138.7 (s), 149.7 (s) ppm. ESI-MS: m/z 234.5 (100%, [M+H]⁺). Anal. Calcd for C₁₃H₁₅NO₃: C, 66.94; H, 6.48; N, 6.00. Found: C, 67.04; H, 6.53; N, 5.89.

**Methyl 4-(6-hydroxyhex-1-yn-1-yl)-3-nitrobenzoate (56):**

Yellow liquid, 83% yield. IR (CHCl₃): ν 3377, 3017, 2952, 2228, 1728, 1621, 1533, 1437, 1234, 1098 cm⁻¹. ¹H NMR (200 MHz, CDCl₃): δ 1.66–1.77 (m, 4H), 2.04 (br s, 1H), 2.52 (t, J = 6.5 Hz, 2H), 3.68 (t, J = 6.0 Hz, 2H), 3.92 (s, 3H), 7.59 (dd, J = 8.1 Hz, 1H), 8.11 (dd, J = 1.6, 8.1 Hz, 1H), 8.56 (d, J = 1.6 Hz, 1H) ppm. ¹³C NMR (50 MHz, CDCl₃): δ 19.6 (t), 24.3 (t), 31.5 (t), 52.7 (q), 62.0 (t), 76.0 (s), 102.7 (s), 123.2 (s), 125.4 (d), 129.5 (s), 132.8 (d), 134.9 (d), 149.7 (s), 164.5 (s) ppm. ESI-MS: m/z 278.4 (100%, [M+H]⁺). Anal. Calcd for C₁₄H₁₅NO₅: C, 60.64; H, 5.45; N, 5.05. Found: C, 60.75; H, 5.39; N, 5.22.

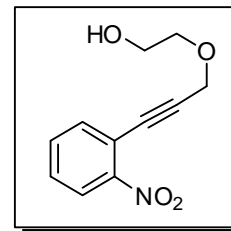
**6-(4-chloro-2-nitrophenyl)hex-5-yn-1-ol (57):**

Yellow liquid, 73% yield. IR (CHCl₃): ν 3387, 3018, 2952, 2230, 1605, 1545, 1528, 1478, 1346, 1258, 1110, 1051 cm⁻¹. ¹H NMR (200 MHz, CDCl₃): δ 1.62–1.79 (m, 4H), 2.12 (br s, 1H), 2.49 (t, J = 6.5 Hz, 2H), 3.68 (t, J = 6.0 Hz, 2H), 7.47 (d, J = 1.3 Hz, 2H), 7.94 (t, J = 1.3 Hz, 1H) ppm. ¹³C NMR (50 MHz, CDCl₃): δ 19.6 (t), 24.4 (t), 31.6 (t), 62.2 (t), 75.4 (s), 100.1 (s), 117.7 (s), 124.6 (d), 132.8 (d), 133.6 (s), 135.6 (d), 150.1 (s) ppm. ESI-MS: m/z 254.7 (100%, [M+H]⁺). Anal. Calcd for C₁₂H₁₂ClNO₃: C, 56.81; H, 4.77; Cl, 13.98; N, 5.52. Found: C, 56.79; H, 4.71; Cl, 13.71; N, 5.39.

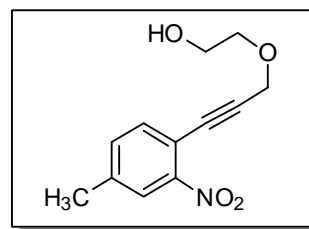


2-((3-(2-nitrophenyl)prop-2-yn-1-yl)oxy)ethanol (58):

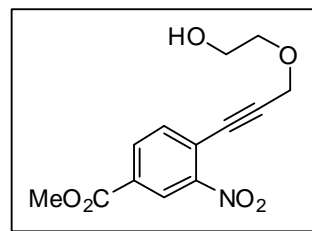
Yellow liquid, 70% yield. IR (CHCl₃): ν 3020, 2918, 2223, 1608, 1578, 1480, 1345, 1216, 1068 cm⁻¹. ¹H NMR (200 MHz, CDCl₃): δ 2.29 (br s, 1H), 3.71–3.81 (m, 4H), 4.47 (s, 2H), 7.37 (ddd, J = 2.1, 6.9, 8.1 Hz, 1H), 7.50 (dt, J = 1.3, 7.8 Hz, 1H), 7.56 (dd, J = 1.9, 7.7 Hz, 1H), 7.94 (dd, J = 1.1, 7.8 Hz, 1H) ppm. ¹³C NMR (50 MHz, CDCl₃): δ 58.9 (t), 61.5 (t), 71.3 (t), 81.6 (s), 93.0 (s), 117.7 (s), 124.4 (d), 128.8 (d), 132.8 (d), 134.7 (d), 149.5 (s) ppm. ESI-MS: m/z 221.4 (100%, [M]⁺). Anal. Calcd for C₁₁H₁₁NO₃: C, 59.73; H, 5.01; N, 6.33. Found: C, 59.59; H, 5.25; N, 6.18.

**2-((3-(4-methyl-2-nitrophenyl)prop-2-yn-1-**

yl)oxy)ethanol (59): Off white solid, 70% yield. Mp. 79 °C. IR (CHCl₃): ν 3327, 3021, 2952, 2219, 1609, 1595, 1525, 1434, 1344, 1216, 1084 cm⁻¹. ¹H NMR (200 MHz, CDCl₃): δ 2.23 (br s, 1H), 2.41 (s, 3H), 3.71–3.81 (m, 4H), 4.45 (s, 2H), 7.35 (dd, J = 1.0, 7.9 Hz, 1H), 7.48 (d, J = 7.9 Hz, 1H), 7.73 (s, 1H) ppm. ¹³C NMR (50 MHz, CDCl₃): δ 21.1 (q), 59.1 (t), 61.7 (t), 71.3 (t), 81.7 (s), 92.0 (s), 114.9 (s), 124.9 (d), 133.6 (d), 134.5 (d), 139.9 (s), 149.5 (s) ppm. ESI-MS: m/z 236.2 (100%, [M+H]⁺). Anal. Calcd for C₁₂H₁₃NO₄: C, 61.27; H, 5.57; N, 5.95. Found: C, 61.09; H, 5.63; N, 5.81.

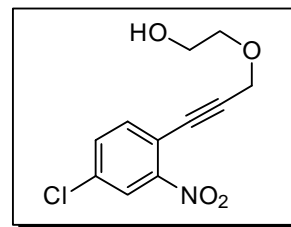
**Methyl 4-(3-(2-hydroxyethoxy)prop-1-yn-1-yl)-3-**

nitrobenzoate (60): Yellow liquid, 74% yield. IR (CHCl₃): ν 3325, 2927, 2220, 1754, 1608, 1526, 1345, 1250, 1120, 1056 cm⁻¹. ¹H NMR (200 MHz, CDCl₃): δ 2.30 (br s, 1H), 3.71–3.83 (m, 4H), 3.95 (s, 3H), 4.49 (s, 2H), 7.68 (d, J = 8.1 Hz, 1H), 8.18 (dd, J = 1.5, 8.1 Hz, 1H), 8.65 (d, J = 1.5 Hz, 1H) ppm. ¹³C NMR (50 MHz, CDCl₃): δ 52.8 (q), 59.1 (t), 61.4 (t), 71.5 (t), 81.3 (s), 96.6 (s), 121.8 (s), 125.6 (d), 130.6 (s), 133.1 (d), 135.0 (d), 149.5 (s), 164.4 (s) ppm. ESI-MS: m/z 280.3 (100%, [M+H]⁺). Anal. Calcd for C₁₃H₁₃NO₆: C, 55.91; H, 4.69; N, 5.02. Found: C, 55.77; H, 4.52; N, 4.95.



2-((3-(4-chloro-2-nitrophenyl)prop-2-yn-1-

yl)oxy)ethanol (61): Yellow liquid, 82% yield. IR (CHCl₃): ν 3421, 2974, 2932, 2229, 1605, 1556, 1533, 1478, 1345, 1261, 1110, 882, 833, 759, 656 cm⁻¹. ¹H NMR (200 MHz, CDCl₃): δ 2.15 (br s, 1H), 3.72–3.83



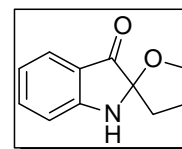
(m, 4H), 4.47 (s, 2H), 7.54 (d, $J = 1.3$ Hz, 1H), 7.55 (s, 1H), 8.03 (t, $J = 1.3$ Hz, 1H) ppm. ¹³C NMR (50 MHz, CDCl₃): δ 59.1 (t), 61.7 (t), 71.4 (t), 80.8 (s), 94.2 (s), 116.3 (s), 124.9 (d), 133.1 (d), 134.9 (s), 135.7 (d), 149.9 (s) ppm. ESI-MS: m/z 256.6 (100%, [M+H]⁺). Anal. Calcd for C₁₁H₁₀ClNO₃: C, 51.68; H, 3.94; Cl, 13.87; N, 5.48. Found: C, 51.51; H, 3.78; Cl, 13.61; N, 5.39.

General procedure for nitroalkynol cycloisomerization with Pd[CH₃CN]₂Cl₂:

To a degassed solution of alkynol (0.5 mmol) in CH₃CN (15 mL) was added Pd(CH₃CN)₂Cl₂ (5 mol%) and the contents stirred under argon for 4 h to 6 h at rt (monitor by TLC). The reaction mixture was concentrated and the residue obtained was purified by column chromatography (ethyl acetate in petroleum ether) to afford the desired product.

4,5-dihydro-3H-spiro[furan-2,2'-indolin]-3'-one (48): Yellow

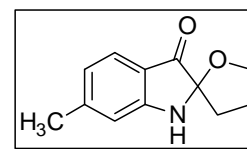
liquid, 29% yield. IR (CHCl₃): ν 3022, 2926, 1717, 1608, 1526, 1469, 1348, 1235, 1048 cm⁻¹. ¹H NMR (200 MHz, CDCl₃): δ 1.93–2.16 (m, 2H), 2.21–2.32 (m, 2H), 4.02–4.18 (m, 2H), 4.83



(br s, 1H), 6.74 (d, $J = 8.1$ Hz, 1H), 6.81 (t, $J = 7.4$ Hz, 1H), 7.41 (ddd, $J = 1.3, 7.3, 8.4$ Hz, 1H), 7.56 (d, $J = 7.7$ Hz, 1H), ppm. ¹³C NMR (50 MHz, CDCl₃): δ 25.7 (t), 33.9 (t), 69.2 (t), 95.0 (s), 112.1 (d), 119.0 (s), 119.6 (d), 125.0 (d), 137.8 (d), 159.6 (s), 200.9 (s) ppm. ESI-MS: m/z 190.2 (100%, [M+H]⁺). HRMS: Found: 190.0856 ([M+H]⁺); Calcd.: 190.0868 ([M+H]⁺). Anal. Calcd for C₁₁H₁₁NO₂: C, 69.83; H, 5.86; N, 7.40. Found: C, 69.67; H, 5.82; N, 7.35.

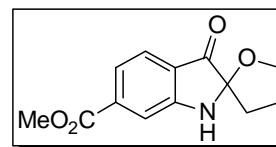
6'-methyl-4,5-dihydro-3H-spiro[furan-2,2'-indolin]-3'-

one (62): Orange colour solid, 36% yield. Mp. 133 °C. IR (CHCl₃): ν 3017, 2915, 2888, 1712, 1616, 1587, 1459, 1324,



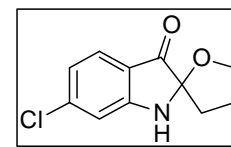
1216, 1111, 1021, 755 cm^{-1} . ^1H NMR (200 MHz, CDCl_3): δ 1.91–2.12 (m, 2H), 2.20–2.34 (m, 2H), 2.28 (s, 3H), 4.05–4.13 (m, 2H), 4.91 (br s, 1H), 6.51 (s, 1H), 6.60 (d, $J = 7.9$ Hz, 1H), 7.43 (d, $J = 7.9$ Hz, 1H) ppm. ^{13}C NMR (50 MHz, CDCl_3): δ 22.3 (q), 25.6 (t), 33.9 (t), 69.1 (t), 95.2 (s), 112.3 (d), 116.6 (s), 121.0 (d), 124.6 (d), 149.5 (s), 160.1 (s), 200.1 (s) ppm. ESI-MS: m/z 202.1 (100%, $[\text{M}-\text{H}]^+$), 204.1 (50%, $[\text{M}+\text{H}]^+$). HRMS: Found: 204.1039 ($[\text{M}+\text{H}]^+$), Calcd.: 204.1025 ($[\text{M}+\text{H}]^+$). Anal. Calcd for $\text{C}_{12}\text{H}_{13}\text{NO}_2$: C, 70.92; H, 6.45; N, 6.89. Found: C, 70.85; H, 6.33; N, 6.67.

Methyl 3'-oxo-4,5-dihydro-3H-spiro[furan-2,2'-indoline]-6'-carboxylate (64): Yellow liquid, 38% yield.



IR (CHCl_3): ν 3012, 2998, 1715, 1702, 1608, 1568, 1508, 1474, 1466, 1316, 1263, cm^{-1} . ^1H NMR (200 MHz, CDCl_3): δ 1.99–2.14 (m, 2H), 2.23–2.33 (m, 2H), 3.91 (s, 3H), 4.05–4.15 (m, 2H), 4.93 (br s, 1H), 7.39 (br s, 1H), 7.46 (dd, $J = 1.3, 7.9$ Hz, 1H), 7.60 (d, $J = 7.9$ Hz, 1H) ppm. ^{13}C NMR (100 MHz, CDCl_3): δ 25.7 (t), 33.9 (t), 52.5 (q), 69.3 (t), 95.3 (s), 113.1 (d), 120.5 (d), 122.1 (s), 124.9 (d), 138.1 (s), 159.1 (s), 166.3 (s), 200.7 (s) ppm. ESI-MS: m/z 270.1 (100%, $[\text{M}+\text{Na}]^+$). HRMS: Found: 246.0317 ($[\text{M}-\text{H}]^+$), Calcd.: 246.0202 ($[\text{M}-\text{H}]^+$). Anal. Calcd for $\text{C}_{13}\text{H}_{13}\text{NO}_4$: C, 63.15; H, 5.30; N, 5.67. Found: C, 63.01; H, 5.17; N, 5.52.

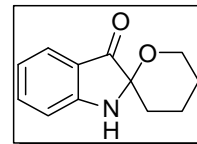
6'-chloro-4,5-dihydro-3H-spiro[furan-2,2'-indolin]-3'-one (66): Yellow solid, 32% yield. Mp. 136 $^\circ\text{C}$.



IR (CHCl_3): ν 3019, 2985, 1714, 1610, 1580, 1454, 1316, 1215, 1066, 928, 755 cm^{-1} . ^1H NMR (200 MHz, CDCl_3): δ 1.96–2.09 (m, 2H), 2.21–2.31 (m, 2H), 4.00–4.15 (m, 2H), 5.06 (br s, 1H), 6.69 (d, $J = 1.6$ Hz, 1H), 6.75 (dd, $J = 1.6, 8.1$ Hz, 1H), 7.45 (d, $J = 8.2$ Hz, 1H) ppm. ^{13}C NMR (50 MHz, CDCl_3): δ 25.6 (t), 33.9 (t), 69.3 (t), 95.3 (s), 112.0 (d), 117.3 (s), 120.2 (d), 126.0 (d), 144.3 (s), 160.0 (s), 199.5 (s) ppm. ESI-MS: m/z 246.2 (100%, $[\text{M}+\text{Na}]^+$). HRMS: Found: 222.0321 ($[\text{M}-\text{H}]^+$), Calcd.: 222.0322 ($[\text{M}-\text{H}]^+$). Anal. Calcd for $\text{C}_{11}\text{H}_{10}\text{ClNO}_2$: C, 59.07; H, 4.51; Cl, 15.85; N, 6.26. Found: C, 59.20; H, 4.63; Cl, 15.69; N, 6.09.

3',4',5',6'-tetrahydrospiro[indoline-2,2'-pyran]-3-one (50):

Yellow Solid, 55% yield, Mp. 112 °C. IR (CHCl₃): ν 2985, 2924, 1713, 1625, 1489, 1455, 1307, 1268, 1118, 1077 cm⁻¹. ¹H

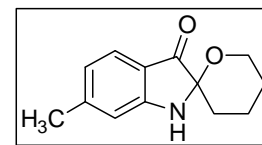


NMR (200 MHz, CDCl₃): δ 1.50–1.85 (m, 4H), 1.94–2.11 (m, 2H), 3.74–3.86 (m, 1H), 4.05–4.15 (m, 1H), 5.13 (br s, 1H), 6.08–6.87 (m, 2H), 7.44 (dt, J = 1.22, 8.2 Hz, 1H), 7.59 (dd, J = 1.1, 7.9 Hz, 1H), ppm. ¹³C NMR (50 MHz, CDCl₃): δ 19.2 (t), 24.7 (t), 30.5 (t), 63.7 (t), 87.5 (s), 112.7 (d), 119.8 (s), 120.0 (d), 125.4 (d), 137.8 (d), 159.4 (s), 198.9 (s) ppm. ESI-MS: m/z 226.3 (100%, [M+Na]⁺). HRMS: Found: 226.0904 ([M+Na]⁺), Calcd.: 226.0844 ([M+Na]⁺). Anal. Calcd for C₁₂H₁₃NO₂: C, 70.92; H, 6.45; N, 6.89. Found: C, 70.77; H, 6.39; N, 6.72.

6-methyl-3',4',5',6'-tetrahydrospiro[indoline-2,2'-

pyran]-3-one (68): Brown colour solid, 79% yield. Mp.

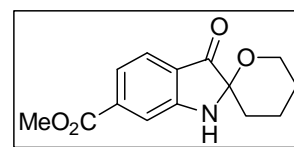
128 °C. IR (CHCl₃): ν 3015, 1711, 1616, 1570, 1459,



1323, 1289, 1021, 756 cm⁻¹. ¹H NMR (200 MHz, CDCl₃): δ 1.47–1.83 (m, 4H), 1.93–2.11 (m, 2H), 2.32 (s, 3H), 3.72–3.84 (m, 1H), 4.03–4.13 (m, 1H), 5.12 (br s, 1H), 6.62 (s, 1H), 6.64 (d, J = 8.0 Hz, 1H), 7.46 (d, J = 8.0 Hz, 1H), ppm. ¹³C NMR (50 MHz, CDCl₃): δ 19.2 (t), 22.4 (q), 24.7 (t), 30.6 (t), 63.7 (t), 87.8 (s), 112.8 (d), 117.4 (s), 121.5 (d), 125.1 (d), 149.5 (s), 159.9 (s), 198.2 (s) ppm. ESI-MS: m/z 218.2 (100%, [M+Na]⁺). HRMS: Found: 218.1168 ([M+H]⁺), Calcd.: 218.1181 ([M+H]⁺). Anal. Calcd for C₁₃H₁₅NO₂: C, 71.87; H, 6.96; N, 6.45. Found: C, 71.79; H, 6.82; N, 6.33.

Methyl 3-oxo-3',4',5',6'-tetrahydrospiro[indoline-2,2'-pyran]-6-carboxylate (69):

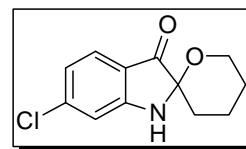
Yellow solid, Mp. 162 °C, 84% yield. IR (CHCl₃): ν 3032, 2945, 1715, 1702, 1615, 1568, 1527, 1480, 1466, 1345, 1210, 1018 cm⁻¹.



¹H NMR (200 MHz, CDCl₃): δ 1.52–1.84 (m, 4H), 1.94–2.17 (m, 2H), 3.73–3.85 (m, 1H), 3.90 (s, 3H), 4.05–4.15 (m, 1H), 5.30 (br s, 1H), 7.44–7.48 (m, 2H), 7.62 (d, J = 8.3 Hz, 1H) ppm. ¹³C NMR (50 MHz, CDCl₃): δ 19.0 (t), 24.6 (t), 30.4 (t), 52.5 (q), 63.7 (t), 87.7 (s), 113.7 (d), 120.5 (d), 122.7 (s), 125.2 (d), 138.0 (s), 158.9 (s), 166.2 (s), 198.73 (s) ppm. ESI-MS: m/z 284.2 (100%, [M+Na]⁺). HRMS: Found: 284.3364 ([M+Na]⁺); Calcd: 284.0899 ([M+Na]⁺). Anal. Calcd for C₁₄H₁₅NO₄: C, 64.36; H, 5.79; N, 5.36. Found: C, 64.22; H, 5.58; N, 5.29.

6-chloro-3',4',5',6'-tetrahydrospiro[indoline-2,2'-**pyran]-3-one (70):** Low melting solid, 82% yield. IR(CHCl₃): ν 3018, 3945, 1718, 1604, 1457, 1314, 1215,1045 cm⁻¹. ¹H NMR (200 MHz, CDCl₃): δ 1.50–1.85 (m, 4H), 1.94–2.16 (m, 2H),3.71–3.83 (m, 1H), 4.06–4.16 (m, 1H), 5.20 (br s, 1H), 6.79 (dd, $J = 1.6, 8.2$ Hz,1H), 6.82 (s, 1H), 7.51 (dd, $J = 1.6, 7.2$ Hz, 1H), ppm. ¹³C NMR (50 MHz, CDCl₃): δ 19.1 (t), 24.6 (t), 30.5 (t), 63.8 (t), 87.7 (s), 112.5 (d), 118.1 (s), 120.6 (d), 126.4(d), 144.1 (s), 159.7 (s), 197.4 (s) ppm. ESI-MS: m/z 240.3 (100%, [M+Na]⁺).HRMS: Found: 260.0871 ([M+Na]⁺), Calcd.: 260.0454 ([M+Na]⁺). Anal. Calcdfor C₁₂H₁₂ClNO₂: C, 60.64; H, 5.09; Cl, 14.92; N, 5.89. Found: C, 60.58; H, 5.20;

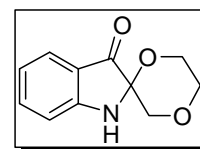
Cl, 14.77; N, 5.71.

**spiro[[1,4]dioxane-2,2'-indolin]-3'-one (71):** Yellow liquid,64% yield. IR (CHCl₃): ν 3016, 2964, 2925, 1709, 1619, 1486,1471, 1321, 1234, 1121, 1081 cm⁻¹. ¹H NMR (200 MHz,CDCl₃): δ 3.61 (d, $J = 11.5$ Hz, 1H), 3.78–3.99 (m, 3H), 3.89 (d, $J = 11.5$ Hz, 1H),4.03–4.16 (m, 1H), 5.53 (br s, 1H), 6.85–6.92 (m, 2H), 7.50 (dt, $J = 1.3, 7.2$ Hz,1H), 7.6 (d, $J = 7.7$ Hz, 1H) ppm. ¹³C NMR (50 MHz, CDCl₃): δ 62.4 (t), 66.5 (t),

71.0 (t), 86.6 (s), 113.2 (d), 120.2 (s), 120.6 (d), 125.4 (d), 138.2 (d), 159.6 (s),

195.9 (s) ppm. ESI-MS: m/z 228.1 (100%, [M+Na]⁺). HRMS: Found: 228.0598([M+Na]⁺), Calcd.: 228.0637 ([M+Na]⁺). Anal. Calcd for C₁₁H₁₁NO₃: C, 64.38; H,

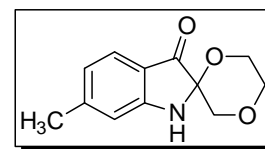
5.40; N, 6.83. Found: C, 64.21; H, 5.29; N, 6.71.

**6'-methylspiro[[1,4]dioxane-2,2'-indolin]-3'-one (72):**Yellow liquid, 80% yield. IR (CHCl₃): ν 3018, 2947, 1718,1611, 1581, 1452, 1314, 1215, 1066 cm⁻¹. ¹H NMR (200MHz, CDCl₃): δ 2.36 (s, 3H), 3.59 (d, $J = 11.5$ Hz, 1H), 3.83–3.98 (m, 3H), 3.88(d, $J = 11.5$ Hz, 1H), 4.01–4.15 (m, 1H), 5.48 (br s, 1H), 6.69 (s, 1H), 6.71 (d, $J =$ 8.5 Hz, 1H), 7.49 (d, $J = 8.5$ Hz, 1H) ppm. ¹³C NMR (50 MHz, CDCl₃): δ 22.5 (q),

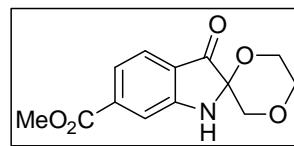
62.4 (t), 66.4 (t), 71.1 (t), 86.9 (s), 113.3 (d), 118.0 (s), 122.2 (d), 125.1 (d), 150.2

(s), 160.1 (s), 195.1 (s) ppm. ESI-MS: m/z 242.1 (100%, [M+Na]⁺). HRMS: Found:242.2808 ([M+Na]⁺), Calcd. 242.0793 ([M+Na]⁺). Anal. Calcd for C₁₂H₁₃NO₃: C,

65.74; H, 5.98; N, 6.39. Found: C, 65.68; H, 5.78; N, 6.22.

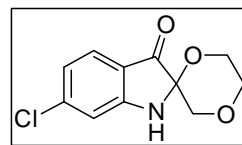


Methyl 3'-oxospiro[[1,4]dioxane-2,2'-indoline]-6'-carboxylate (73): Yellow colour solid, Mp. 171 °C, 82% yield. IR (CHCl₃): ν 3018, 2951, 1727, 1715,



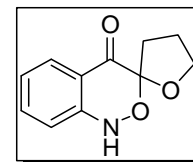
1624, 1587, 1495, 1454, 1322, 1263, 1161, 1002 cm⁻¹. ¹H NMR (200 MHz, CDCl₃): δ 3.61 (d, J = 11.5 Hz, 1H), 3.84–3.98 (m, 3H), 3.89 (d, J = 11.5 Hz, 1H), 3.93 (s, 3H), 4.02–4.15 (m, 1H), 5.66 (br s, 1H), 7.52 (dd, J = 1.2, 8.7 Hz, 1H), 7.56 (s, 1H), 7.65 (d, J = 8.7 Hz, 1H) ppm. ¹³C NMR (50 MHz, CDCl₃): δ 52.6 (q), 62.4 (t), 66.4 (t), 70.7 (t), 86.7 (s), 114.2 (d), 121.2 (d), 123.1 (s), 125.3 (d), 138.5 (s), 159.1 (s), 166.1 (s), 195.8 (s) ppm. ESI-MS: m/z 279.4 (100%, [M+Na]⁺). HRMS: Found: 263.1181 ([M]⁺), Calcd.: 263.0794 ([M]⁺). Anal. Calcd for C₁₃H₁₃NO₅: C, 59.31; H, 4.98; N, 5.32. Found: C, 59.20; H, 4.85; N, 5.23.

6'-chlorospiro[[1,4]dioxane-2,2'-indolin]-3'-one (74):



Yellow liquid, 78% yield. IR (CHCl₃): ν 2946, 2895, 1718, 1604, 1550, 1439, 1314, 1212, 1067 cm⁻¹. ¹H NMR (200 MHz, CDCl₃): δ 3.60 (d, J = 11.5 Hz, 1H), 3.80–3.97 (m, 3H), 3.87 (d, J = 11.5 Hz, 1H), 3.99–4.11 (m, 1H), 5.74 (br s, 1H), 6.84 (dd, J = 1.6, 8.2 Hz, 1H), 6.88 (d, J = 1.6 Hz, 1H), 7.52 (d, J = 8.2 Hz, 1H) ppm. ¹³C NMR (50 MHz, CDCl₃): δ 62.4 (t), 66.4 (t), 70.8 (t), 86.8 (s), 113.1 (d), 118.4 (s), 121.2 (d), 126.4 (d), 144.7 (s), 159.9 (s), 194.5 (s) ppm. ESI-MS: m/z 262.2 (100%, [M+Na]⁺). HRMS: Found: 240.0542 ([M+H]⁺), Calcd.: 240.0427 ([M+H]⁺). Anal. Calcd for C₁₁H₁₀ClNO₃: C, 55.13; H, 4.21; Cl, 14.79; N, 5.84. Found: C, 55.23; H, 4.18; Cl, 14.57; N, 5.71.

4',5'-dihydro-3'H-spiro[benzo[c][1,2]oxazine-3,2'-furan]-

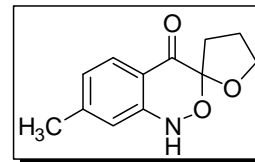


4(1H)-one (49): Yellow liquid, 27% yield. IR (CHCl₃): ν 3019, 1695, 1645, 1599, 1448, 1215, 1078 cm⁻¹. ¹H NMR (200 MHz, CDCl₃): δ 1.93–2.19 (m, 3H), 2.70–2.85 (m, 1H), 4.05–4.24 (m, 2H), 6.85 (d, J = 8.2 Hz, 1H), 7.05 (t, J = 7.5 Hz, 1H), 7.43 (ddd, J = 1.4, 7.3, 8.3 Hz, 1H), 7.94 (dd, J = 1.4, 7.9 Hz, 1H) ppm (The N–H proton is missing in the Spectrum). ¹³C NMR (50 MHz, CDCl₃): δ 24.7 (t), 31.2 (t), 71.0 (t), 107.5 (s), 114.7 (d), 117.7 (s), 122.4 (d), 127.7 (d), 134.8 (d), 150.4 (s), 185.1 (s) ppm. ESI-MS: m/z 228.2 (100%, [M+Na]⁺). HRMS: Found: 228.0597 ([M+Na]⁺), Calcd.: 228.0637 ([M+Na]⁺). Anal. Calcd for C₁₁H₁₁NO₃: C, 64.38; H, 5.40; N, 6.83.

Found: C, 64.42; H, 5.31; N, 6.72.

7-methyl-4',5'-dihydro-3'H-spiro[benzo[c][1,2]oxazine-3,2'-furan]-4(1H)-one (63): Brown colour solid, Mp. 118

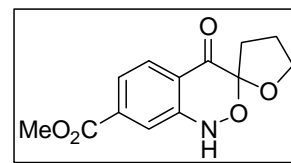
°C, 34% yield. IR (CHCl₃): ν 3012, 2981, 1685, 1613, 1459, 1340, 1294, 1019 cm⁻¹. ¹H NMR (200 MHz, CDCl₃):



δ 1.92–2.17 (m, 3H), 2.32 (s, 3H), 2.69–2.83 (m, 1H), 4.04–4.22 (m, 2H), 6.63 (s, 1H), 6.85 (dd, J = 0.7, 8.1 Hz, 1H), 7.41 (br s, 1H), 7.82 (d, J = 8.1 Hz, 1H) ppm.

¹³C NMR (50 MHz, CDCl₃): δ 22.0 (q), 24.7 (t), 31.2 (t), 71.0 (t), 107.6 (s), 114.6 (d), 115.6 (s), 123.9 (d), 127.7 (d), 146.2 (s), 150.5 (s), 184.9 (s) ppm. ESI-MS: m/z 242.2 (100%, [M+Na]⁺). HRMS: Found: 220.0960 ([M+H]⁺), Calcd.: 220.0974 ([M+H]⁺). Anal. Calcd for C₁₂H₁₃NO₃: C, 65.74; H, 5.98; N, 6.39. Found: C, 65.79; H, 5.79; N, 6.27.

4-oxo-1,4,4',5'-tetrahydro-3'H-spiro[benzo[c][1,2]oxazine-3,2'-furan]-7-yl acetate (65): Yellow colour solid, Mp. 123 °C. 34% yield. IR



(CHCl₃): ν 3020, 1729, 1684, 1618, 1590, 1435, 1301, 1215, 1090 cm⁻¹. ¹H NMR (400 MHz, CDCl₃): δ 1.99–2.05 (m, 1H), 2.10–2.21 (m, 2H), 2.73–2.81 (m, 1H), 3.91 (s, 3H), 4.08–4.14 (m, 1H), 4.16–4.22 (m, 1H), 7.55 (s, 1H), 7.57 (br s, 1H), 7.65 (dd, J = 1.4, 8.1 Hz, 1H), 7.98 (d, J = 8.1 Hz, 1H) ppm. ¹³C NMR (100 MHz, CDCl₃): δ 24.7 (t), 31.2 (t), 52.6 (q), 71.3 (t), 107.4 (s), 116.4 (d), 120.3 (s), 122.6 (d), 128.1 (d), 135.3 (s), 150.2 (s), 165.8 (s), 184.6 (s) ppm. ESI-MS: m/z 270.1 (100%, [M+Na]⁺). HRMS: Found: 263.0849 ([M]⁺), Calcd.: 263.0794 ([M]⁺). Anal. Calcd for C₁₃H₁₃NO₅: C, 59.31; H, 4.98; N, 5.32. Found: C, 59.27; H, 4.89; N, 5.22.

X-Ray crystallographic data: X-ray intensity data of compound **66** was collected on a Bruker SMART APEX CCD diffractometer with graphite-monochromatized (Mo K α =0.71073 Å) radiation at room temperature. Data were collected with ω scan width of 0.3° and with four different settings of φ (0°, 90°, 180° and 270°) keeping the sample-to-detector distance fixed at 6.145 cm and the detector position (2θ) fixed at -28°. The X-ray data collection was monitored by SMART program (Bruker, 2003). All the data were corrected for Lorentzian, polarization

and absorption effects using Bruker's SAINT and SADABS programs. SHELX-97 was used for structure solution and full-matrix least-squares refinement on F^2 . Hydrogen atoms were included in the refinement as per the riding model. The overall quality of the diffraction data was very poor due to the poor quality of the crystals which is reflected in its high R-value.

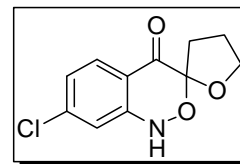
Crystal data for **66** ($C_{13}H_{13}N_1O_5$): $M = 263.24$, crystal dimensions $0.22 \times 0.16 \times 0.06 \text{ mm}^3$, monoclinic, space group $P2_1/n$, $a = 14.478(8)$, $b = 5.258(3)$, $c = 17.353(10) \text{ \AA}$, $V = 1315.8(13) \text{ \AA}^3$, $Z = 4$; $\rho_{\text{calcd}} = 1.329 \text{ gcm}^{-3}$, $\mu (\text{Mo-K}\alpha) = 0.103 \text{ mm}^{-1}$, $F(000) = 552$, $2\theta_{\text{max}} = 50.00^\circ$, 7556 reflections collected, 1815 unique, 1346 observed ($I > 2\sigma(I)$) reflections, 173 refined parameters, R value 0.1249, $wR2 = 0.3022$ (all data $R = 0.1520$, $wR2 = 0.3159$), $S = 1.241$, minimum and maximum transmission 0.9780 and 0.9934 respectively, maximum and minimum residual electron densities $+0.495$ and $-0.374 \text{ e \AA}^{-3}$.

7-chloro-4',5'-dihydro-3'H-spiro[benzo[c][1,2]oxazine-

3,2'-furan]-4(1H)-one (67): Orange colour solid, Mp. 118

$^\circ\text{C}$, 31% yield. IR (CHCl_3): ν 2923, 1682, 1613, 1452, 1313, 1270, 1056 cm^{-1} . $^1\text{H NMR}$ (200 MHz, CDCl_3): δ 1.92–2.23

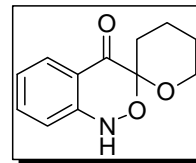
(m, 3H), 2.68–2.83 (m, 1H), 4.04–4.23 (m, 2H), 6.85 (d, $J = 1.8 \text{ Hz}$, 1H), 6.99 (dd, $J = 1.8, 8.6 \text{ Hz}$, 1H), 7.55 (s, 1H), 7.85 (d, $J = 8.6 \text{ Hz}$, 1H) ppm. $^{13}\text{C NMR}$ (50 MHz, CDCl_3): δ 24.6 (t), 31.1 (t), 71.1 (t), 107.5 (s), 114.3 (d), 115.9 (s), 122.9 (d), 129.3 (d), 141.0 (s), 151.1 (s), 184.2 (s) ppm. ESI-MS: m/z 240.2 (100%, $[\text{M}+\text{H}]^+$). HRMS: Found: 240.0420 ($[\text{M}+\text{H}]^+$), Calcd.: 240.0427 ($[\text{M}+\text{H}]^+$). Anal. Calcd for $C_{11}H_{10}ClNO_3$: C, 55.13; H, 4.21; Cl, 14.79; N, 5.84. Found: C, 55.01; H, 4.09; Cl, 14.58; N, 5.79.



General procedure for nitroalkynol cycloisomerization with AuBr_3 : To a degassed solution of alkynol (0.5 mmol) in CH_3CN (15 mL) was added AuBr_3 (5 mol%) and the contents stirred under argon for 2 h to 4 h at rt (monitor by TLC). The reaction mixture was concentrated and the residue obtained was purified by column chromatography (ethyl acetate in petroleum ether) to afford the desired product.

3',4',5',6'-tetrahydrospiro[benzo[c][1,2]oxazine-3,2'-pyran]-

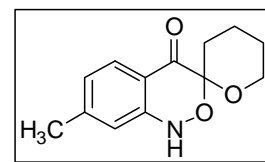
4(1H)-one (51): Yellow solid, Mp. 121 °C, 57% yield. IR (CHCl₃): ν 3020, 2930, 1725, 1605, 1550, 1461, 1302, 1217, 1108, 1080, 756 cm⁻¹. ¹H NMR (200 MHz, CDCl₃): δ 1.61–1.75



(m, 2H), 1.80–1.87 (m, 3H), 2.33–2.42 (m, 1H), 3.87–3.97 (m, 2H), 6.86 (d, J = 8.2 Hz, 1H), 7.04 (ddd, J = 1.0, 7.3, 8.0 Hz, 1H), 7.27 (s, 1H), 7.43 (ddd, J = 1.5, 7.3, 8.5 Hz, 1H), 7.95 (dd, J = 1.0, 8.0 Hz, 1H) ppm. ¹³C NMR (50 MHz, CDCl₃): δ 17.9 (t), 24.4 (t), 25.6 (t), 63.5 (t), 98.8 (s), 114.0 (d), 116.9 (s), 122.2 (d), 128.1 (d), 134.5 (d), 150.5 (s), 185.2 (s) ppm. ESI-MS: m/z 242.2 (100%, [M+Na]⁺). HRMS: Found: 220.1017 ([M+H]⁺), Calcd.: 220.0974 ([M+H]⁺). Anal. Calcd for C₁₂H₁₃NO₃: C, 65.74; H, 5.98; N, 6.39. Found: : C, 65.85; H, 5.76; N, 6.25.

7-methyl-3',4',5',6'-tetrahydrospiro[benzo[c][1,2]oxazine-3,2'-pyran]-4(1H)-

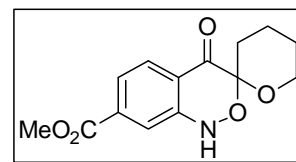
one (76): Sticky liquid, 35% yield. IR (CHCl₃): ν 3019, 2948, 2855, 1686, 1614, 1580, 1454, 1310, 1270, 1215, 1045 cm⁻¹. ¹H NMR (200 MHz, CDCl₃): δ 1.58–1.74 (m,



2H), 1.76–1.84 (m, 3H), 2.28–2.51 (m, 1H), 2.33 (s, 3H), 3.88–3.94 (m, 2H), 6.64 (s, 1H), 6.85 (dd, J = 0.8, 8.1 Hz, 1H), 7.83 (d, J = 8.1 Hz, 1H) ppm. ¹³C NMR (50 MHz, CDCl₃): δ 17.9 (t), 22.0 (q), 24.5 (t), 25.6 (t), 63.5 (t), 98.7 (s), 114.0 (d), 114.9 (s), 123.7 (d), 128.1 (d), 145.9 (s), 150.6 (s), 185.0 (s) ppm. ESI-MS: m/z 256.3 (100%, [M+Na]⁺). Anal. Calcd for C₁₃H₁₅NO₃: C, 66.94; H, 6.48; N, 6.00. Found: C, 66.74; H, 6.32; N, 5.87.

4-oxo-1,3',4,4',5',6'-hexahydrospiro[benzo[c][1,2]oxazine-3,2'-pyran]-7-yl

acetate (78): Yellow solid, 40% yield. Mp. 153 °C. IR (CHCl₃): ν 2951, 1727, 1703, 1615, 1580, 1438, 1286, 1229, 1092, 752 cm⁻¹. ¹H NMR (200 MHz, CDCl₃): δ 1.62–1.86 (m, 5H), 2.27–2.43 (m, 1H), 3.90–4.00 (m,

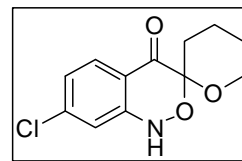


2H), 3.91 (s, 3H), 7.36 (br s, 1H), 7.54 (d, J = 1.3 Hz, 1H), 7.63 (dd, J = 1.3, 8.2 Hz, 1H), 7.99 (d, J = 8.2 Hz, 1H) ppm. ¹³C NMR (50 MHz, CDCl₃): δ 17.9 (t), 24.4 (t), 25.4 (t), 52.6 (q), 63.6 (t), 98.7 (s), 115.6 (d), 119.5 (s), 122.3 (d), 128.4 (d), 135.0 (s), 150.2 (s), 165.9 (s), 184.6 (s) ppm. ESI-MS: m/z 278.2 (100%, [M+H]⁺). HRMS: Found: 278.1007 ([M+H]⁺), Calcd.: 278.1028 ([M+H]⁺). Anal. Calcd for C₁₄H₁₅NO₅: C, 60.64; H, 5.45; N, 5.05. Found: C, 60.52; H, 5.28; N,

4.88.

7-chloro-3',4',5',6'-tetrahydrospiro[benzo[c][1,2]oxazine-3,2'-pyran]-4(1H)-

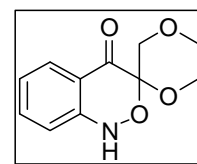
one (80): Low melting solid, 38% yield. IR (CHCl₃): δ 3020, 1683, 1614, 1453, 1314, 1216, 1058, 919 cm⁻¹. ¹H NMR (200 MHz, CDCl₃): δ 1.62–1.73 (m, 2H), 1.78–1.86 (m, 3H), 2.27–2.43 (m, 1H), 3.88–3.92 (m, 2H), 6.87 (d, J =



1.8 Hz, 1H), 6.99 (dd, J = 1.8, 8.5 Hz, 1H), 7.26 (s, 1H), 7.87 (d, J = 8.5 Hz, 1H) ppm. ¹³C NMR (50 MHz, CDCl₃): δ 17.8 (t), 24.4 (t), 25.4 (t), 63.6 (t), 98.8 (s), 113.76 (d), 115.2 (s), 122.7 (d), 129.7 (d), 140.8 (s), 151.1 (s), 184.2 (s) ppm. ESI-MS: m/z 276.1 (100%, [M+H]⁺). Anal. Calcd for C₁₂H₁₂ClNO₃: C, 56.81; H, 4.77; Cl, 13.98; N, 5.52. Found: C, 56.99; H, 4.71; Cl, 13.75; N, 5.41.

spiro[benzo[c][1,2]oxazine-3,2'-[1,4]dioxan]-4(1H)-one (82):

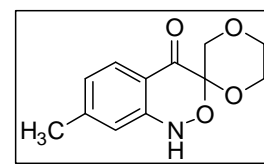
Yellow liquid, 51% yield. IR (CHCl₃): ν 2927, 2857, 1682, 1605, 1478, 1348, 1086, 1057, 918, 752 cm⁻¹. ¹H NMR (200 MHz, CDCl₃): δ 3.72 (d, J = 11.1 Hz, 1H), 3.81–3.87 (m, 2H),



3.84 (d, J = 12.6 Hz, 1H), 4.18–4.36 (m, 1H), 4.30 (d, J = 12.6 Hz, 1H), 6.85 (d, J = 8.3 Hz, 1H), 6.98–7.06 (m, 1H), 7.44 (ddd, J = 1.5, 7.2, 8.3 Hz, 1H), 7.61 (br s, 1H), 7.91 (dd, J = 1.5, 7.9 Hz, 1H) ppm. ¹³C NMR (50 MHz, CDCl₃): δ 61.3 (t), 65.6 (t, 2C), 95.4 (s), 113.6 (d), 116.5 (s), 122.1 (d), 127.9 (d), 135.0 (d), 150.5 (s), 183.7 (s) ppm. ESI-MS: m/z 244.3 (100%, [M+Na]⁺). HRMS: Found: 221.0753 ([M]⁺), Calcd.: 221.0688 ([M]⁺). Anal. Calcd for C₁₁H₁₁NO₄: C, 59.73; H, 5.01; N, 6.33. Found: C, 59.59; H, 4.95; N, 6.19.

7-methylspiro[benzo[c][1,2]oxazine-3,2'-[1,4]dioxan]-

4(1H)-one (83): Yellow liquid, 72% yield. IR (CHCl₃): ν 3019, 2980, 2928, 1687, 1615, 1453, 1381, 1321, 1215, 1115, 1068 cm⁻¹. ¹H NMR (200 MHz, CDCl₃): δ 2.30 (s,



3H), 3.69 (d, J = 11.2 Hz, 1H), 3.79–3.90 (m, 2H), 3.83 (d, J = 12.6 Hz, 1H), 4.16–4.34 (m, 1H), 4.27 (d, J = 12.6 Hz, 1H), 6.62 (s, 1H), 6.81 (dd, J = 0.7, 8.1 Hz, 1H), 7.77 (d, J = 8.1 Hz, 1H) ppm. ¹³C NMR (50 MHz, CDCl₃): δ 22.0 (q), 61.2 (t), 65.6 (t, 2C), 95.3 (s), 113.3 (d), 114.2 (s), 123.5 (d), 127.7 (d), 146.5 (s), 150.6 (s), 183.5 (s) ppm. ESI-MS: m/z 236.2 (100%, [M+H]⁺). Anal. Calcd for

C₁₂H₁₃NO₄: C, 61.27; H, 5.57; N, 5.95. Found: C, 61.30; H, 5.41; N, 5.76.

4-oxo-1,4-dihydrospiro[benzo[c][1,2]oxazine-3,2'-

[1,4]dioxan]-7-yl acetate (84): Yellow colour solid,

Mp. 168 °C, 85% yield. IR (CHCl₃): ν 2924, 1726,

1693, 1619, 1506, 1438, 1298, 1228, 1094, 1055, 918,

752 cm⁻¹. ¹H NMR (200 MHz, CDCl₃): δ 3.69 (d, J = 10.9 Hz, 1H), 3.81–3.97 (m,

2H), 3.85 (d, J = 12.7 Hz, 1H), 3.92 (s, 3H), 4.17–4.36 (m, 1H), 4.31 (d, J = 12.7

Hz, 1H), 7.58 (d, J = 1.4 Hz, 1H), 7.62 (dd, J = 1.4, 8.2 Hz, 1H), 7.84 (br s, 1H),

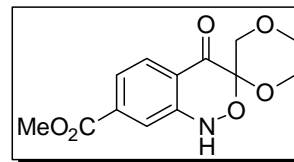
7.95 (d, J = 8.2 Hz, 1H) ppm. ¹³C NMR (50 MHz, CDCl₃): δ 52.7 (q), 61.3 (t),

65.4 (t), 65.6 (t), 95.2 (s), 115.3 (d), 119.0 (s), 122.2 (d), 128.2 (d), 135.5 (s),

150.2 (s), 165.8 (s), 183.2 (s) ppm. ESI-MS: m/z 279.4 (100%, [M]⁺). HRMS:

Found: 279.0936 ([M]⁺), Calcd.: 279.0743 ([M]⁺). Anal. Calcd for C₁₃H₁₃NO₆: C,

55.91; H, 4.69; N, 5.02. Found: C, 55.85; H, 4.73; N, 5.12.



7-chlorospiro[benzo[c][1,2]oxazine-3,2'-[1,4]dioxan]-

4(1H)-one (85): Yellow liquid, 67% yield. IR (CHCl₃): ν

3019, 2927, 2855, 1694, 1600, 1442, 1215, 1045, 758, 668

cm⁻¹. ¹H NMR (200 MHz, CDCl₃): δ 3.72 (d, J = 11.1 Hz,

1H), 3.80–3.87 (m, 2H), 3.84 (d, J = 12.7 Hz, 1H), 4.16–4.37 (m, 1H), 4.29 (d, J =

12.7 Hz, 1H), 6.88 (d, J = 1.6 Hz, 1H), 6.99 (dd, J = 1.6, 8.5 Hz, 1H), 7.62 (br s,

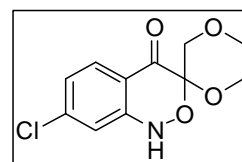
1H), 7.84 (d, J = 8.5 Hz, 1H) ppm. ¹³C NMR (50 MHz, CDCl₃): δ 61.3 (t), 65.4

(t), 65.6 (t), 95.3 (s), 113.3 (d), 114.8 (s), 122.7 (d), 129.5 (d), 141.4 (s), 151.0 (s),

182.8 (s) ppm. ESI-MS: m/z 256.3 (100%, [M+H]⁺). HRMS: Found: 256.0373

([M+H]⁺), Calcd.: 256.0377 ([M+H]⁺). Anal. Calcd for C₁₁H₁₀ClNO₄: C, 51.68; H,

3.94; Cl, 13.87; N, 5.48. Found: C, 51.55; H, 3.89; Cl, 13.62; N, 5.39.



3-(3,4-dihydro-2H-pyran-6-yl)benzo[c]isoxazole (75): Yellow

liquid, 10% yield. IR (CHCl₃): ν 3021, 2915, 1722, 1626, 1557,

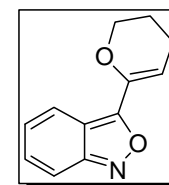
1440, 1290, 1215, 1045, 759 cm⁻¹. ¹H NMR (200 MHz, CDCl₃):

δ 1.93–2.04 (m, 2H), 2.27–2.35 (m, 2H), 4.25 (t, J = 5.1 Hz, 2H),

5.93 (t, J = 4.3 Hz, 1H), 6.93 (dd, J = 6.4, 8.7, Hz, 1H), 7.25 (dd, J = 6.4, 9.1 Hz, 1H),

7.49 (d, J = 9.1 Hz, 1H), 7.78 (d, J = 8.7 Hz, 1H) ppm. ¹³C NMR (50 MHz, CDCl₃): δ

20.4 (t), 22.0 (t), 66.6 (t), 104.9 (d), 114.2 (s), 114.6 (d), 122.0 (d), 123.7 (d), 130.8

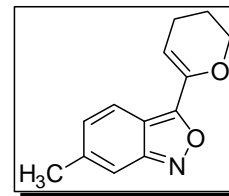


(s), 144.4 (s), 157.3 (s), 160.3 (s) ppm. ESI-MS: m/z 202.2 (100%, $[M+H]^+$). Anal. Calcd for $C_{12}H_{11}NO_2$: C, 71.63; H, 5.51; N, 6.96. Found: C, 71.59; H, 5.48; N, 6.75.

3-(3,4-dihydro-2H-pyran-6-yl)-6-methylbenzo[c]isoxazole

(77): Yellow liquid, 30% yield. IR ($CHCl_3$): ν 3019, 2927, 2855, 1729, 1626, 1557, 1440, 1300, 1215, 1045, 759 cm^{-1} .

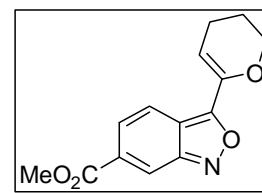
1H NMR (400 MHz, $CDCl_3$): δ 1.96–2.00 (m, 2H), 2.28–2.32 (m, 2H), 2.35 (s, 3H), 4.24 (t, $J = 5.1$ Hz, 2H), 5.88 (t, $J = 4.3$



Hz, 1H), 6.75 (d, $J = 9.1$ Hz, 1H), 7.20 (s, 1H), 7.65 (d, $J = 9.1$ Hz, 1H) ppm. ^{13}C NMR (100 MHz, $CDCl_3$): δ 20.4 (t), 22.0 (t), 22.4 (q), 66.6 (t), 104.7 (d), 112.1 (d), 113.1 (s), 121.4 (d), 127.2 (d), 141.2 (s), 144.4 (s), 158.0 (s), 159.8 (s) ppm. ESI-MS: m/z 216.2 (100%, $[M+H]^+$). HRMS: Found: 216.1022 ($[M+H]^+$), Calcd. 216.1025 ($[M+H]^+$). Anal. Calcd for $C_{13}H_{13}NO_2$: C, 72.54; H, 6.09; N, 6.51. Found: C, 72.59; H, 6.23; N, 6.45.

Methyl 3-(3,4-dihydro-2H-pyran-6-yl)benzo[c]isoxazole-6-carboxylate (79):

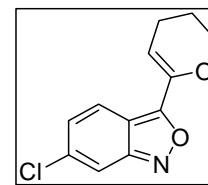
Off white solid, Mp. 131 °C 35% yield. IR ($CHCl_3$): ν 3022, 2958, 2922, 1710, 1695, 1608, 1568, 1527, 1480, 1466, 1345, 1216 cm^{-1} . 1H NMR (200 MHz, $CDCl_3$): δ 1.94–2.05 (m, 2H), 2.28–2.37 (m, 2H), 3.94 (s, 3H), 4.27



(t, $J = 5.1$ Hz, 2H), 5.97 (t, $J = 4.3$ Hz, 1H), 7.49 (dd, $J = 1.1, 9.1$ Hz, 1H), 7.83 (dd, $J = 1.1, 9.1$ Hz, 1H), 8.28 (t, $J = 1.1$ Hz, 1H) ppm. ^{13}C NMR (50 MHz, $CDCl_3$): δ 20.4 (t), 22.0 (t), 52.6 (q), 66.7 (t), 105.7 (d), 115.2 (s), 118.7 (d), 122.6 (d), 122.8 (d), 132.8 (s), 144.2 (s), 157.1 (s), 161.2 (s), 166.3 (s) ppm. ESI-MS: m/z 282.3 (100%, $[M+H]^+$). Found: 260.0508 ($[M+H]^+$), Calcd. 260.0923 ($[M+H]^+$). Anal. Calcd for $C_{14}H_{13}NO_4$: C, 64.86; H, 5.05; N, 5.40. Found: C, 64.72; H, 5.19; N, 5.29.

6-chloro-3-(3,4-dihydro-2H-pyran-6-yl)benzo[c]isoxazole

(81): Colourless liquid, 32% yield. IR ($CHCl_3$): ν 3018, 2926, 1723, 1609, 1506, 1461, 1323, 1217, 1117, 756, 666 cm^{-1} . 1H NMR (200 MHz, $CDCl_3$): δ 1.93–2.04 (m, 2H), 2.27–2.36 (m,



2H), 4.25 (t, $J = 5.1$ Hz, 2H), 5.95 (t, $J = 4.3$ Hz, 1H), 6.85 (dd, $J = 1.6, 9.2$ Hz, 1H), 7.49 (dd, $J = 0.9, 1.6$ Hz, 1H), 7.74 (dd, $J = 0.9, 9.2$ Hz, 1H) ppm. ^{13}C NMR

(50 MHz, CDCl₃): δ 20.4 (t), 21.9 (t), 66.7 (t), 105.8 (d), 112.8 (s), 113.2 (d), 123.7 (d), 125.6 (d), 137.3 (s), 144.1 (s), 157.5 (s), 161.1 (s) ppm. ESI-MS: m/z 236.0 (100%, [M+H]⁺). HRMS: Found: 236.0461 ([M+H]⁺), Calcd. 236.0478 ([M+H]⁺). Anal. Calcd for C₁₂H₁₀ClNO₂: C, 61.16; H, 4.28; Cl, 15.04; N, 5.94. Found: C, 61.21; H, 4.19; Cl, 14.94; N, 5.77.

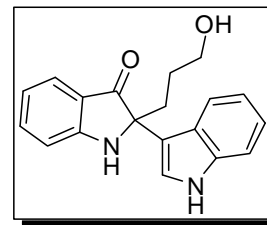
3.3. Experimental data of Sequential Approach for Isatisine A core

General Procedure for Indole Addition: To a solution of spiroindolin-3-one (2 mmol), indole (2.5 mmol) in CH₃CN (2 mL), anhydrous InCl₃ (5 mol %) was added under argon atmosphere and stirred for 30–50 min. After completion of the reaction as indicated by TLC, the reaction mixture was concentrated under reduced pressure and the residue obtained was purified by column chromatography (ethyl acetate in petroleum ether) to afford desired alkylated product.

2-(3-hydroxypropyl)-2-(1H-indol-3-yl)indolin-3-one (86):

Yellow solid, M.P. 130 °C. 78% yield. IR (CHCl₃): ν 3325, 2927, 2220, 1690, 1608, 1526, 1345, 1250, 1120, 1056 cm⁻¹.

¹H NMR (200 MHz, CDCl₃): δ 1.33-1.49 (m, 1H), 1.53-1.68 (m, 1H), 2.14-2.43 (m, 2H), 3.53 (t, J = 6.4 Hz, 2H), 6.74 (t, J



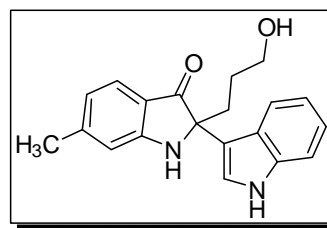
= 7.3 Hz, 1H), 6.87–6.94 (m, 2H), 7.05 (t, J = 7.2 Hz, 1H), 7.24 (s, 1H), 7.30 (d, J = 8.1 Hz, 1H), 7.42-7.55 (m, 3H) ppm. ¹³C NMR (50 MHz, CDCl₃): δ 27.2 (t), 34.0 (t), 62.6 (t), 67.0 (s), 112.1 (d), 112.7 (d), 114.2 (s), 118.6 (d), 119.6 (d), 120.1 (s), 120.6 (d), 122.2 (d), 123.5 (d), 125.2 (d), 125.6 (s), 137.9 (s), 138.6 (d), 162.5 (s), 206.0 (s) ppm. ESI-MS: m/z 329.3 (100%, [M+Na]⁺).

2-(3-hydroxypropyl)-2-(1H-indol-3-yl)-6-methylindolin-3-one (88):

Yellow solid, M.P. 145 °C. 79% yield. IR (CHCl₃): ν 3370, 3266,

2990, 2816, 1679, 1611, 1462, 1251, 1149, 933, 744 cm⁻¹. ¹H NMR (400 MHz, CDCl₃): δ 1.42–1.49 (m, 1H), 1.60–1.69 (m, 1H), 2.21–2.28 (m, 1H), 2.33–2.40

(m, 1H), 2.93 (s, 3H), 3.56 (d, J = 5.4 Hz, 2H), 6.61 (d, J = 7.8 Hz, 1H), 6.80 (br s, 1H), 6.85 (s, 1H), 6.92 (t, J = 7.3 Hz, 1H), 7.07 (t, J = 7.5 Hz, 1H), 7.37 (d, J = 8.4 Hz, 1H), 7.38 (d, J = 7.5 Hz, 1H), 7.65 (d, J = 8.1 Hz, 1H),



10.19 (br s, 1H), ppm. ^{13}C NMR (100 MHz, CDCl_3): δ 22.4 (q), 28.1 (t), 34.7 (t), 62.7 (t), 70.1 (s), 112.3 (d), 112.7 (d), 115.9 (s), 118.7 (s), 119.6 (d), 120.1 (d), 121.6 (d), 122.2 (d), 123.6 (d), 124.8 (d), 126.4 (s), 138.3 (s), 149.1 (s), 162.5 (s), 202.4 (s) ppm. ESI-MS: m/z 343.15 (100%, $[\text{M}+\text{Na}]^+$). HRMS: Found: 343.1389 ($[\text{M}+\text{Na}]^+$), 359.1359 ($[\text{M}+\text{K}]^+$), Calcd.: 343.1423 ($[\text{M}+\text{H}]^+$) 359.1162 ($[\text{M}+\text{Na}]^+$).

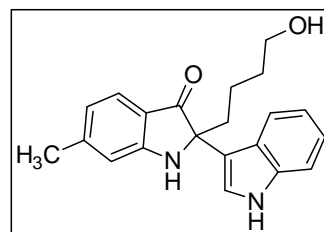
Methyl 2-(3-hydroxypropyl)-2-(1H-indol-3-yl)-3-oxoindoline-6-carboxylate (89):

Due to poor solubility of the compound in most of the solvent we are not able to obtain a clean spectra. Our effort to obtain the spectra is still in progress.

2-(4-hydroxybutyl)-2-(1H-indol-3-yl)-6-

Methylindolin-3-one (90): Yellow liquid, 88% yield.

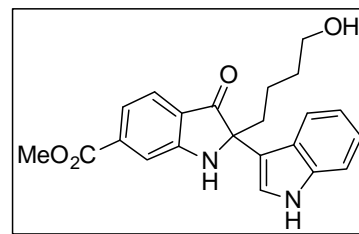
IR (CHCl_3): ν 3370, 3266, 3058, 2908, 2816, 1698, 1651, 1611, 1462, 1251, 1149, 857, 767 cm^{-1} . ^1H NMR (500 MHz, CDCl_3): δ 2.01–2.06 (m, 1H), 2.17–2.23 (m, 1H), 2.25–2.33 (m, 2H), 2.38 (s, 3H), 3.40 (t, $J = 6.4$ Hz, 2H), 4.60 (br s, 2H), 6.59 (d, $J = 8.1$ Hz, 1H), 6.78 (s, 1H), 6.86 (t, $J = 7.6$ Hz, 1H), 7.03 (t, $J = 7.4$ Hz, 1H), 7.27 (s, 1H), 7.31 (d, $J = 8.2$ Hz, 1H), 7.39 (d, $J = 7.9$ Hz, 1H), 7.42 (br d, $J = 8.2$ Hz, 1H) ppm. ^{13}C NMR (125 MHz, CDCl_3): δ 22.6 (q), 23.7 (t), 33.9 (t), 38.0 (t), 62.8 (t), 71.1 (s), 112.4 (d), 112.7 (d), 114.7 (s), 115.3 (s), 118.3 (s), 119.9 (d), 120.6 (d), 121.2 (d), 122.5 (d), 123.9 (d), 125.2 (d), 126.5 (s), 138.7 (s), 140.2 (s), 151.2 (s), 164.1 (s), 206.2 (s) ppm. ESI-MS: m/z 357.2 (100%, $[\text{M}+\text{Na}]^+$).



Methyl 2-(4-hydroxybutyl)-2-(1H-indol-3-yl)-3-

oxoindoline-6-carboxylate (91): Yellow solid, M.P.

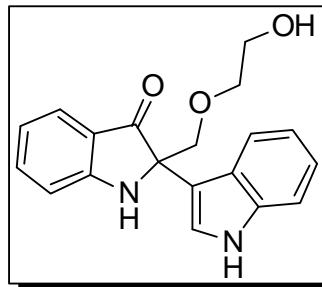
167 °C. 89% yield. IR (CHCl_3): ν 3358, 2925, 2854, 1916, 1710, 1622, 1458, 1282, 1089, 750 cm^{-1} . ^1H NMR (200 MHz, CDCl_3): δ 1.47–1.60 (m, 2H), 2.23–2.44 (m, 2H), 3.50 (t, $J = 6.0$ Hz, 2H), 3.93 (s, 3H), 6.94 (ddd, $J = 1.0, 7.1, 7.9$ Hz, 1H), 7.04–7.12 (m, 1H), 7.21 (br s, 1H), 7.34–7.44 (m, 3H), 7.69 (d, $J = 8.1$ Hz, 1H), 7.65 (d, $J = 7.1$ Hz, 1H), 7.67 (s, 1H), 10.3 (br s, 1H) ppm. ^{13}C NMR (50 MHz, CDCl_3): δ 21.1 (t), 33.9 (t), 37.9 (t), 52.7 (q), 62.2 (t), 71.0 (s), 112.4 (d), 113.8 (d), 115.1 (s), 118.7 (d), 119.8 (d), 121.4 (d), 122.3 (d), 123.6 (s), 123.7 (s), 125.1 (d), 126.2 (s), 138.3 (s), 138.5 (s), 161.5 (s), 167.0 (s), 206.0 (s), 206.4 (s). ppm. HRMS:



Found: 401.1479 ($[M+Na]^+$), 417.1198 ($[M+K]^+$); Calcd.: 401.1478 ($[M+Na]^+$), 417.1217 ($[M+K]^+$).

2-((2-hydroxyethoxy)methyl)-2-(1H-indol-3-

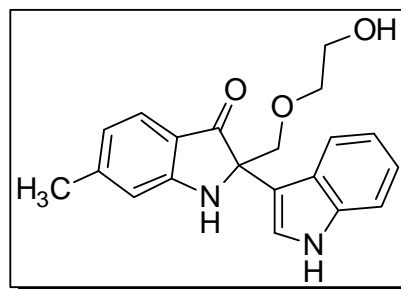
yl)indolin-3-one (96): Yellow liquid, 77% yield. IR ($CHCl_3$): ν 3345, 2925, 2855, 1701, 1614, 1492, 1459, 1246, 1120, 1064, 748 cm^{-1} . 1H NMR (500 MHz, $CDCl_3$): δ 3.06–3.65 (m, 4H), 4.04 (d, $J = 9.8$ Hz, 1H), 4.21 (d, $J = 9.8$ Hz, 1H), 5.36 (br s, 1H), 6.88 (t, $J = 7.3$



Hz, 1H), 6.96 (d, $J = 8.2$ Hz, 1H), 7.06 (t, $J = 7.6$ Hz, 1H), 7.17 (t, $J = 7.3$ Hz, 1H), 7.29 (s, 1H), 7.35 (d, $J = 8.2$ Hz, 1H), 7.50 (t, $J = 7.8$ Hz, 1H), 7.58 (d, $J = 8.2$ Hz, 1H), 7.67 (d, $J = 7.8$ Hz, 1H), 8.19 (br s, 1H) ppm. ^{13}C NMR (125 MHz, $CDCl_3$): δ 61.6 (t), 69.9 (s), 72.9 (t), 74.6 (t), 111.6 (d), 111.9 (s), 113.1 (d), 113.9 (s), 119.6 (d), 119.8 (d), 120.2 (d), 121.0 (s), 122.5 (d), 122.9 (d), 125.0 (d), 125.3 (s), 125.8 (s), 128.7 (s), 137.6 (s), 146.4 (s), 161.1 (s), 204.8 (s) ppm. ESI-MS: m/z 359.1 (100%, $[M+K]^+$). HRMS: Found: 345.1208 ($[M+Na]^+$), Calcd.: 345.1215 ($[M+Na]^+$).

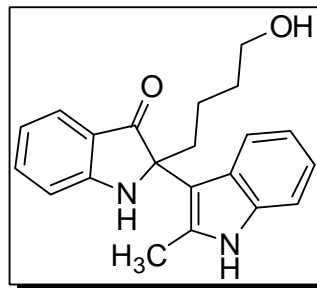
2-((2-hydroxyethoxy)methyl)-2-(1H-indol-3-

yl)-6-methylindolin-3-one (97): Yellow liquid, 79% yield. IR ($CHCl_3$): ν 3393, 3361, 2925, 1680, 1621, 1462, 1365, 1115, 745 cm^{-1} . 1H NMR (500 MHz, $CDCl_3$): δ 2.37 (s, 3H), 3.58–3.63 (m, 4H), 4.0



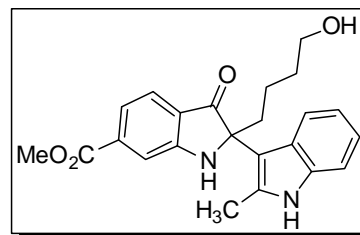
(d, $J = 9.8$ Hz, 1H), 4.19 (d, $J = 9.8$ Hz, 1H), 5.30 (br s, 1H), 6.7 (d, $J = 7.9$ Hz, 1H), 6.73 (s, 1H), 7.04 (t, $J = 7.6$ Hz, 1H), 7.15 (t, $J = 7.3$ Hz, 1H), 7.22 (s, 1H), 7.32 (d, $J = 7.9$ Hz, 1H), 7.53 (t, $J = 7.9$ Hz, 1H), 7.55 (d, $J = 7.9$ Hz, 1H), 8.26 (br s, 1H) ppm. ^{13}C NMR (125 MHz, $CDCl_3$): δ 22.5 (q), 61.5 (t), 70.0 (s), 72.9 (t), 74.5 (t), 111.7 (d), 111.9 (s), 113.1 (d), 118.7 (s), 119.7 (d), 120.1 (d), 121.4 (d), 122.4 (d), 123.1 (d), 124.7 (d), 136.6 (s), 149.3 (s), 161.6 (s), 200.7 (s) ppm. ESI-MS: m/z 359.3 (100%, $[M+Na]^+$).

2-(4-hydroxybutyl)-2-(2-methyl-1H-indol-3-yl)indolin-3-one (100): Yellow liquid, 87% yield. IR (CHCl₃): ν 3393, 3012, 2932, 1682, 1619, 1462, 1323, 1216, 1020, 755 cm⁻¹. ¹H NMR (500 MHz, CDCl₃): δ 1.26–1.31 (m, 2H), 1.55–1.60 (m, 2H), 2.23–2.29 (m, 1H), 2.44–2.53 (m, 1H), 2.45 (s, 3H), 3.59 (t, *J* = 6.3 Hz, 2H), 5.12 (br s, 1H), 6.81–6.84 (m, 1H), 6.88 (d, *J* = 8.2 Hz, 1H), 7.0–7.03 (m, 1H), 7.06–7.09 (m, 1H), 7.22 (d, *J* = 7.9 Hz, 1H), 7.47 (ddd, *J* = 1.2, 7.2, 8.2 Hz, 1H), 7.63 (br d, *J* = 7.6 Hz, 1H), 7.67 (d, *J* = 8.0 Hz, 1H), 7.82 (br s, 1H) ppm. ¹³C NMR (125 MHz, CDCl₃): δ 14.9 (q), 20.1 (t), 32.8 (t), 37.4 (t), 62.5 (t), 70.7 (s), 109.2 (s), 110.5 (d), 112.2 (d), 118.9 (d), 119.7 (d), 119.9 (d), 121.1 (d), 121.3 (d), 125.0 (d), 127.4 (s), 131.8 (s), 134.9 (s), 137.3 (d), 160.2 (s), 203.4 (s) ppm. ESI-MS: *m/z* 357.11 (100%, [M+Na]⁺). HRMS: Found: 357.1570 ([M+Na]⁺), Calcd.: 357.1579 ([M+Na]⁺).



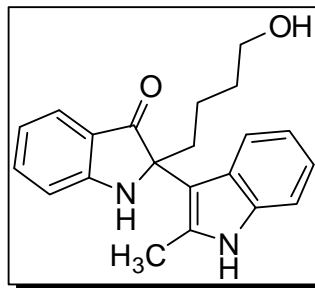
Methyl 2-(4-hydroxybutyl)-2-(2-methyl-1H-indol-3-yl)-3-oxoindoline-6-carboxylate (101): Yellow liquid, 86% yield. IR (CHCl₃): ν 3368, 2929, 2857, 1707, 1682, 1622, 1458, 1322, 1290, 1090, 752 cm⁻¹.

¹H NMR (500 MHz, CDCl₃): δ 1.35–1.40 (m, 2H), 1.53–1.58 (m, 2H), 2.56 (s, 3H), 3.5 (t, *J* = 6.3 Hz, 2H), 3.93 (s, 3H), 6.91 (ddd, *J* = 1.1, 7.1, 8.0 Hz, 1H), 6.99 (ddd, *J* = 1.1, 7.1, 8.0 Hz, 1H), 7.21 (s, 1H), 7.26 (d, *J* = 7.9 Hz, 1H), 7.34–7.36 (m, 1H), 7.57 (d, *J* = 8.2 Hz, 2H), 7.67 (s, 1H), 7.81 (d, *J* = 8.2 Hz, 1H) ppm. ¹³C NMR (125 MHz, CDCl₃): δ 14.8 (q), 21.4 (t), 29.8 (s), 33.9 (t), 38.4 (t), 52.7 (q), 62.3 (t), 72.3 (s), 108.8 (s), 111.3 (d), 113.5 (d), 118.6 (d), 119.6 (d), 121.3 (d), 121.5 (d), 123.9 (s), 125.2 (d), 128.4 (s), 133.4 (s), 136.4 (s), 138.6 (s), 160.8 (s), 167.1 (s), 203.4 (s) ppm. ESI-MS: *m/z* 415.06 (100%, [M+H]⁺). HRMS: Found: 415.1603 ([M+Na]⁺), 431.1536 ([M+K]⁺); Calcd.: 415.1634 ([M+Na]⁺), 431.1373 ([M+K]⁺).



2-(4-hydroxybutyl)-2-(2-methyl-1H-indol-3-yl)indolin-3-one (102): Yellow liquid, 89% yield. IR (CHCl₃): ν 3393, 3012, 2932, 1682, 1619, 1462, 1323, 1216, 1020, 755 cm⁻¹. ¹H NMR (500 MHz, CDCl₃): δ 1.26–1.31 (m, 2H), 1.55–1.60 (m, 2H), 2.23–2.29 (m, 1H), 2.44–2.53 (m, 1H), 2.45 (s, 3H), 3.59 (t, *J* = 6.3 Hz, 2H), 5.12 (br s, 1H), 6.81–6.84 (m, 1H), 6.88 (d, *J* = 8.2 Hz, 1H), 7.0–7.03 (m, 1H), 7.06–7.09 (m,

1H), 7.22 (d, $J = 7.9$ Hz, 1H), 7.47 (ddd, $J = 1.2, 7.2, 8.2$ Hz, 1H), 7.63 (br d, $J = 7.6$ Hz, 1H), 7.67 (d, $J = 8.0$ Hz, 1H), 7.82 (br s, 1H) ppm. ^{13}C NMR (125 MHz, CDCl_3): δ 14.9 (q), 20.1 (t), 32.8 (t), 37.4 (t), 62.5 (t), 70.7 (s), 109.2 (s), 110.5 (d), 112.2 (d), 118.9 (d), 119.7 (d), 119.9 (s), 121.1 (d), 121.3 (d), 125.0 (d), 127.4 (s), 131.8

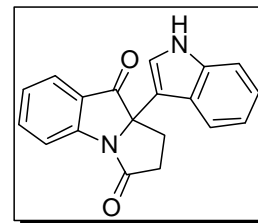


(s), 134.9 (s), 137.3 (d), 160.2 (s), 203.4 (s) ppm. ESI-MS: m/z 357.11 (100%, $[\text{M}+\text{Na}]^+$). HRMS: Found: 357.1570 ($[\text{M}+\text{Na}]^+$), Calcd.: 357.1579 ($[\text{M}+\text{Na}]^+$).

General Procedure for oxidative amide formation: Under an atmosphere of argon in a glass shield tube, substrate (1 mmol), $[\text{Cp}^*\text{RhCl}_2]_2$ (0.025 mmol, 5.0%Rh), K_2CO_3 (0.1 mmol, 10%), and acetone (8 mL) were placed and the cap was sealed. The mixture was stirred at 100 °C (oil bath temp.) for 12 h. After evaporation of the solvent, the products were isolated by column chromatography of the residue (using ethylacetate and petroleum ether as elutant) afford the desired product.

9a-(1H-indol-3-yl)-1H-pyrrolo[1,2-a]indole-3,9(2H,9aH)-

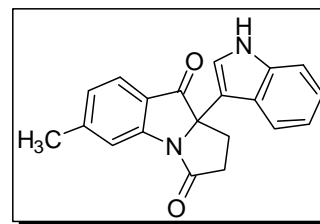
dione (87): Yellow liquid, 62% yield. IR (CHCl_3): ν 3342, 2926, 2854, 1727, 1675, 1608, 1458, 1378, 1291, 1086, 745 cm^{-1} . ^1H NMR (500 MHz, CDCl_3): δ 2.49–2.63 (m, 2H), 2.86 (dd, $J = 7.9, 11.9$ Hz, 1H), 2.90–2.97 (m, 1H), 7.15–7.21 (m,



4H), 7.33 (d, $J = 7.6$ Hz, 1H), 7.66 (dt, $J = 1.5, 8.2$ Hz, 1H), 7.96 (d, $J = 8.2$ Hz, 1H), 8.0 (d, $J = 7.6$ Hz, 1H), 8.53 (br s, 1H) ppm. ^{13}C NMR (125 MHz, CDCl_3): δ 29.2 (t), 34.6 (t), 73.9 (s), 77.0 (s), 111.7 (d), 112.2 (s), 116.4 (d), 120.3 (d), 120.6 (d), 122.1 (d), 122.7 (d), 124.5 (s), 124.9 (s), 125.1 (d), 125.4 (d), 136.8 (d), 137.3 (s), 149.3 (s), 173.8 (s), 198.8 (s) ppm. ESI-MS: m/z 325.4 (100%, $[\text{M}+\text{Na}]^+$).

9a-(1H-indol-3-yl)-6-methyl-1H-pyrrolo[1,2-a]indole-

3,9(2H,9aH)-dione (92): Yellow liquid, 63% yield. IR (CHCl_3): ν 3368, 2955, 2856, 1707, 1682, 1608, 1471, 1361, 1254, 745 cm^{-1} . ^1H NMR (500 MHz, $(\text{CD}_3)_2\text{CO}$): δ 2.57 (dd, $J = 7.6, 15.9$ Hz, 1H), 2.63–2.69 (m, 1H),

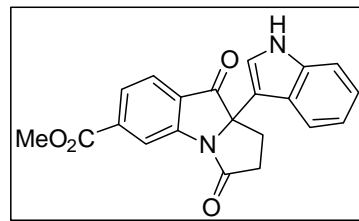


2.83 (dd, $J = 7.3, 11.6$ Hz, 1H) 2.89–2.96 (m, 1H), 7.06 (ddd, $J = 0.9, 7.0, 7.9$ Hz, 1H), 7.06 (ddd, $J = 0.9, 7.0, 7.9$ Hz, 1H), 7.42–7.44 (m, 2H), 7.51 (d, $J = 7.9$ Hz, 1H),

7.76 (s, 1H), 7.87 (d, $J = 7.9$ Hz, 1H), ppm. ^{13}C NMR (125 MHz, $(\text{CD}_3)_2\text{CO}$): δ 22.4 (q), 29.8 (t), 35.1 (t), 74.9 (s), 112.7 (d), 113.2 (s), 117.5 (s), 121.5 (s), 120.2 (d), 122.8 (d), 123.6 (d), 123.6 (s), 125.4 (d), 125.8 (d), 126.8 (d), 138.8 (s), 149.2 (d), 151.3 (s), 174.2 (s), 199.6 (s) ppm. ESI-MS: m/z 339.05 (100%, $[\text{M}+\text{Na}]^+$). HRMS: Found: 317.1288 ($[\text{M}+\text{H}]^+$), 339.1113 ($[\text{M}+\text{Na}]^+$), Calcd.: 317.129 ($[\text{M}+\text{H}]^+$) 339.111 ($[\text{M}+\text{Na}]^+$).

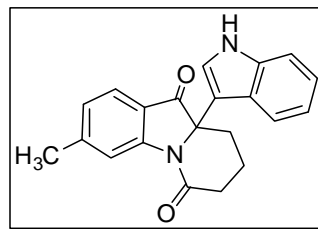
Methyl 9a-(1H-indol-3-yl)-3,9-dioxo-2,3,9a-tetrahydro-1H-pyrrolo[1,2-a]indole-6-carboxylate

(93): Yellow solid, M.P. 138 °C. 67% yield. IR (CHCl_3): ν 3358, 2952, 1726, 1675, 1608, 1430, 1380, 1294, 1087, 746 cm^{-1} . ^1H NMR (400 MHz, CDCl_3): δ 1.88–2.01 (m, 2H), 2.49–2.64 (m, 2H), 3.94 (s, 3H), 7.10–7.15 (m, 2H), 7.19 (dt, $J = 1.1, 8.0$ Hz, 1H), 7.34 (d, $J = 8.0$ Hz, 1H), 7.7 (d, $J = 8.0$ Hz, 1H), 7.84–7.88 (m, 2H), 8.42 (br s, 1H), 9.15 (br s, 1H) ppm. ^{13}C NMR (100 MHz, CDCl_3): δ 28.3 (t), 31.4 (t), 52.7 (q), 71.7 (s), 111.7 (d), 111.9 (s), 119.1 (d), 120.5 (d), 122.9 (d), 123.0 (d), 124.0 (s), 124.7 (d), 125.2 (s), 125.9 (d), 137.2 (s), 137.6 (s), 150.9 (s), 166.1 (s), 169.8 (s), 197.3 (s) ppm. ESI-MS: m/z 339.05 (100%, $[\text{M}+\text{Na}]^+$).



9a-(1H-indol-3-yl)-3-methyl-7,8,9a-tetrahydropyrido[1,2-a]indole-6,10-dione (94)

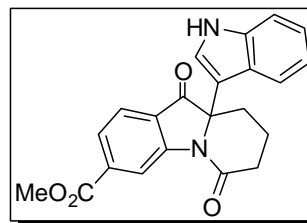
(94): Off white solid, Mp. 112 °C, 58% yield. IR (CHCl_3): ν 3422, 3276, 2927, 2834, 1909, 1648, 1603, 1457, 1424, 1377, 1024, 742 cm^{-1} . ^1H NMR (400 MHz, CDCl_3): δ 1.83–



2.04 (m, 4H), 2.46–2.50 (m, 2H), 2.52 (s, 3H), 7.01 (d, $J = 7.5$ Hz, 1H), 7.10–7.14 (m, 2H), 7.34 (d, $J = 2.3$ Hz, 1H), 7.42 (d, $J = 8.2$ Hz, 1H), 7.55 (d, $J = 7.8$ Hz, 1H), 7.72 (d, $J = 8.0$ Hz, 1H), 8.43 (s, 1H), 10.47 (br s, 1H) ppm. ^{13}C NMR (100 MHz, CDCl_3): δ 18.0 (t), 22.6 (q), 28.8 (t), 29.3 (d), 29.8 (d), 31.9 (t), 72.1 (s), 112.8 (d), 118.9 (d), 120.3 (d), 120.8 (s), 121.1 (d), 122.7 (d), 124.5 (s), 124.9 (d), 125.3 (s), 126.5 (d), 138.5 (s), 149.4 (s), 152.9 (s), 169.9 (s), 197.9 (s) ppm. ESI-MS: m/z 353.04 (100%, $[\text{M}+\text{Na}]^+$). HRMS: Found: 353.1246 ($[\text{M}+\text{Na}]^+$), Calcd.: 353.1266 ($[\text{M}+\text{Na}]^+$).

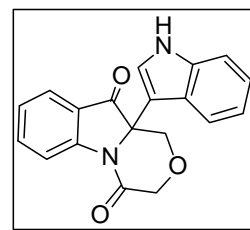
Methyl 9a-(1H-indol-3-yl)-6,10-dioxo-6,7,8,9a,10-hexahydropyrido[1,2-a]indole-3-carboxylate (95):

Yellow solid, M.P. 87 °C. 64% yield. IR (CHCl₃): ν 3379, 3019, 2953, 1720, 1705, 1614, 1578, 1438, 1292, 1214, 754 cm⁻¹. ¹H NMR (200 MHz, CDCl₃): δ 1.81–2.01 (m, 4H), 2.53–2.60 (m, 2H), 3.94 (s, 3H), 7.09–7.23 (m, 3H), 7.35 (dd, *J* = 1.8, 7.2 Hz, 1H), 7.7 (d, *J* = 7.9 Hz, 1H), 7.84–7.89 (m, 2H), 8.42 (br s, 1H), 8.16 (s, 1H), ppm. ¹³C NMR (50 MHz, CDCl₃): δ 21.1 (t), 33.9 (t), 38.0 (t), 52.7 (q), 62.2 (s), 71.0 (s), 112.4 (d), 113.8 (d), 115.1 (s), 118.7 (d), 119.7 (d), 121.4 (d), 122.3 (d), 123.6 (s), 123.7 (d), 125.1 (d), 126.2 (s), 138.3 (s), 138.5 (s), 161.5 (s), 167.0 (s), 203.1 (s) ppm. ESI-MS: *m/z* 280.3 (100%, [M+H]⁺). HRMS: Found: 397.1127 ([M+Na]⁺), Calcd.: 397.1165 ([M+Na]⁺).



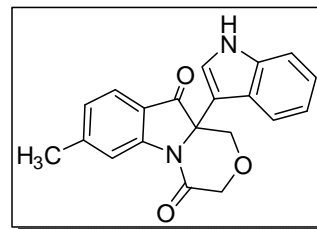
10a-(1H-indol-3-yl)-1H-[1,4]oxazino[4,3-a]indole-

4,10(3H,10aH)-dione (98): Yellow liquid, 5% yield. IR (CHCl₃): ν 3452, 2924, 1716, 1657, 1599, 1458, 1378, 1124, 856 cm⁻¹. ¹H NMR (500 MHz, CDCl₃): δ 3.95 (d, *J* = 11.3 Hz, 1H), 4.30 (d, *J* = 17.4 Hz, 1H), 4.43 (d, *J* = 17.4 Hz, 1H), 4.92 (d, *J* = 11.3 Hz, 1H), 7.14 (dt, *J* = 0.9, 7.0 Hz, 1H), 7.19 (dt, *J* = 1.2, 8.2 Hz, 1H), 7.23 (d, *J* = 2.7 Hz, 1H), 7.28 (dt, *J* = 0.7, 7.2 Hz, 1H), 7.34 (d, *J* = 8.2 Hz, 1H), 7.69–7.75 (m, 2H), 7.85 (d, *J* = 8.0 Hz, 1H), 8.26 (br s, 1H), 8.47 (d, *J* = 8.2 Hz, 1H) ppm. ¹³C NMR (125 MHz, CDCl₃): δ 66.9 (t), 67.6 (t), 69.7 (s), 111.3 (s), 111.8 (d), 118.4 (d), 120.3 (d), 120.7 (d), 122.7 (s), 122.9 (d), 123.3 (d), 124.2 (s), 125.0 (d), 125.7 (d), 137.0 (s), 137.3 (d), 150.9 (s), 166.1 (s), 195.2 (s) ppm.



10a-(1H-indol-3-yl)-7-methyl-1H-[1,4]oxazino[4,3-a]indole-4,10(3H,10aH)-dione (99):

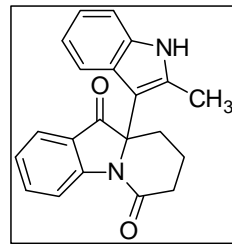
Yellow liquid, 3% yield. IR (CHCl₃): ν 3378, 2972, 2928, 2858, 1719, 1699, 1619, 1458, 1425, 1113, 823, 744 cm⁻¹. ¹H NMR (500 MHz, CDCl₃): δ 2.51 (s, 3H), 3.93 (d, *J* = 11.6 Hz, 1H), 4.28 (d, *J* = 17.4 Hz, 1H), 4.41 (d, *J* = 17.4 Hz, 1H), 4.89 (d, *J* = 11.6 Hz, 1H), 7.10 (d, *J* = 7.9 Hz, 1H), 7.11–7.14 (m, 1H), 7.18 (dt, *J* = 0.9, 7.9 Hz, 1H), 7.23 (d, *J* = 2.7 Hz, 1H), 7.33 (d, *J* = 7.9 Hz, 1H), 7.59 (d, *J* = 7.6 Hz, 1H), 7.82 (d, *J* = 8.2 Hz, 1H), 8.29 (br s, 2H), ppm. ¹³C NMR (125 MHz, CDCl₃): δ 22.7 (q), 66.8 (t), 67.7 (t), 69.9 (s),



111.6 (s), 111.7 (d), 118.6 (d), 120.3 (d), 120.5 (s), 120.6 (s), 122.8 (d), 123.2 (d), 124.3 (s), 124.7 (d), 127.0 (d), 137.0 (d), 149.4 (s), 151.3 (s), 166.2 (s), 194.7 (s)ppm.

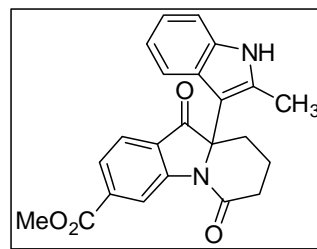
9a-(2-methyl-1H-indol-3-yl)-7,8,9a-tetrahydropyrido[1,2-a]indole-6,10-dione (103): Yellow liquid, 65% yield. IR

(CHCl₃): ν 3334, 2956, 2927, 1726, 1682, 1619, 1462, 1378, 1293, 1123, 743 cm⁻¹. ¹H NMR (500 MHz, CDCl₃): δ 1.77–1.88 (m, 2H), 1.90–1.96 (m, 1H), 2.38 (s, 3H), 2.53 (t, *J* = 6.9 Hz, 2H), 3.17–3.21 (m, 1H), 7.04–7.1 (M, 2H), 7.19–7.23 (M, 2H), 7.68–7.72 (M, 2H), 7.84 (d, *J* = 6.2 Hz, 1H), 8.14 (s, 1H), 8.60 (d, *J* = 8.4 Hz, 1H), ppm. ¹³C NMR (125 MHz, CDCl₃): δ 13.9 (q), 17.2 (t), 28.7 (t), 31.5 (t), 71.7 (s), 109.1 (s), 110.5 (d), 112.2 (d), 118.9 (d), 119.7 (d), 119.9 (d), 120.1 (s), 121.3 (d), 124.7 (s), 124.8 (d), 127.4 (s), 131.7 (s), 135.0 (s), 137.3 (d), 151.0 (s), 170.1 (s), 197.8 (s) ppm. ESI-MS: *m/z* 353.02 (100%, [M+Na]⁺). HRMS: Found: 331.1458 ([M+H]⁺), 353.1085 ([M+Na]⁺), Calcd.: 331.1446 ([M+H]⁺) 353.0693 ([M+Na]⁺).



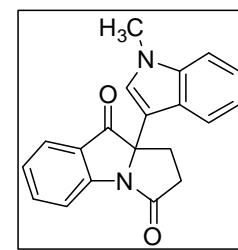
Methyl 9a-(2-methyl-1H-indol-3-yl)-6,10-dioxo-6,7,8,9,9a,10-hexahydropyrido[1,2-a]indole-3-carboxylate (104): Yellow liquid, 59% yield. IR

(CHCl₃): ν 3325, 2927, 2220, 1754, 1608, 1526, 1345, 1250, 1120, 1056 cm⁻¹. ¹H NMR (500 MHz, CDCl₃): δ 1.79–1.86 (m, 1H), 1.88–1.97 (m, 2H), 2.39 (s, 3H), 2.55–2.58 (m, 2H), 3.97 (s, 3H), 7.07–7.03 (m, 2H), 7.22–7.24 (m, 1H), 7.74 (d, *J* = 7.9 Hz, 1H), 7.83 (br s, 1H), 7.89 (dd, *J* = 1.2, 7.9 Hz, 1H), 7.79 (s, 1H), 9.20 (s, 1H), ppm. ¹³C NMR (125 MHz, CDCl₃): δ 14.1 (q), 17.2 (t), 28.7 (t), 31.6 (t), 52.7 (q), 72.3 (s), 105.2 (s), 110.6 (d), 119.3 (d), 120.1 (s), 120.5 (d), 121.8 (d), 124.7 (d), 125.9 (d), 126.2 (s), 126.4 (s), 132.8 (s), 135.1 (s), 137.6 (s), 150.8 (s), 166.1 (s), 169.9 (s), 197.1 (s) ppm. ESI-MS: *m/z* 411.07 (100%, [M+Na]⁺). HRMS: Found: 388.1424 ([M]⁺), 411.1308 ([M+Na]⁺), Calcd.: 388.1423 ([M]⁺) 411.1321 ([M+Na]⁺).



9a-(1-methyl-1H-indol-3-yl)-1H-pyrrolo[1,2-a]indole-

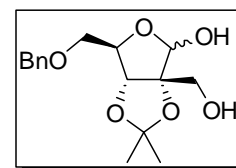
3,9(2H,9aH)-dione (105): Yellow liquid, 65% yield. IR (CHCl₃): ν 3379, 3019, 2953, 1720, 1705, 1614, 1578, 1438, 1292, 1214, 754 cm⁻¹. ¹H NMR (200 MHz, CDCl₃): δ 2.50–2.63



(m, 2H), 2.83–2.87 (m, 1H), 2.93–3.0 (m, 1H), 3.70 (s, 3H), 7.18 (ddd, $J = 1.2, 6.7, 7.9$ Hz, 1H), 7.22 (dt, $J = 0.8, 7.6$ Hz, 1H), 7.26–7.30 (m, 2H), 7.63 (d, $J = 7.6$ Hz, 1H), 7.68 (ddd, $J = 1.2, 7.5, 8.2$ Hz, 1H), 7.97 (d, $J = 8.2$ Hz, 1H), 7.98 (d, $J = 7.9$ Hz, 1H) ppm. ^{13}C NMR (125 MHz, CDCl_3): δ 29.4 (t), 32.9 (q), 34.7 (t), 74.0 (s), 109.7 (d), 110.6 (s), 116.5 (d), 120.0 (d), 120.8 (d), 122.4 (d), 125.0 (s), 125.1 (d), 125.5 (d), 126.6 (d), 136.8 (d), 138.0 (s), 149.3 (s), 173.8 (s), 198.7 (s) ppm. ESI-MS: m/z 329.3 (100%, $[\text{M}+\text{Na}]^+$).

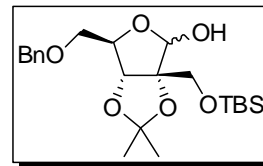
3.4. Experimental detail for Total synthesis of Isatisine A.

5-*O*-benzyl-2-*C*-(Hydroxymethyl)-2,3-*O*-isopropylidene-*D*-ribofuranose (112): A suspension of lactol **111** (20 gm, 71.35 mmol) and K_2CO_3 (14.8 g, 107 mmol) in MeOH (150 mL) was treated with 37% aqueous formaldehyde (150 ml) and stirred for 18 h at 85 °C. After completion of the reaction as indicated by TLC, the reaction mixture was cooled in ice bath and neutralized with 10% aqueous HCl. The reaction mixture was concentrated and extracted with ethyl acetate. The combined organic layer was dried (Na_2SO_4), concentrated and purified by column chromatography to afford the diol **112** (19.9 gm, 90%) as a colourless liquid. R_f (50% ethyl acetate/pet. ether) 0.3; $[\alpha]_D^{25} = 10.6$ (c 2.77, CHCl_3). IR (CHCl_3): ν 3428, 2989, 2936, 2870, 1715, 1496, 1455, 1372, 1216, 1075, 860, 755 cm^{-1} . ^1H NMR (200 MHz, CDCl_3): δ 1.43 (s, 3H, major), 1.47 (s, 2.3H, minor), 1.5 (s, 3H, major), 1.58 (s, 1.52.3H, minor), 2.18–2.24 (m, 0.7H, minor), 2.33–2.39 (m, 1H, major), 3.58–3.68 (m, 3.3H), 3.7–3.83 (m, 4H), 4.23–4.27 (m, 0.8H, minor), 4.34–4.37 (m, 1H, major), 4.51–4.61 (m, 4.7H), 4.64–4.68 (m, 1.4H), 4.73 (s, 0.7H), 5.24 (d, $J = 10.3$ Hz, 1H, minor), 5.31 (d, $J = 10.9$ Hz, 1H, major), 7.28–7.4 (m, 8.8H) ppm. ^{13}C NMR (50 MHz, CDCl_3): δ 27.1 (q, minor), 27.3 (d, q, minor), 27.5 (q, major), 28.1 (q, major), 62.6 (t, major), 62.9 (t, minor), 70.9 (t, major), 71.5 (t, minor), 73.7 (t, minor), 74.1 (t, major), 80.9 (d, minor), 83.9 (d, minor), 84.6 (d, major), 85.8 (d, major), 91.4 (s, minor), 94.8 (s, major), 98.8 (d, minor), 104.6 (d, major), 113.3 (ds, major), 114.1 (s, minor), 127.8 (d, minor), 127.9 (d, minor), 128.2 (d, major), 128.5 (d, minor), 128.6 (d, major), 128.8 (d, major), 135.9 (s, major), 137.2 (s, minor) ppm. ESI-MS: m/z 333.2 (100%, $[\text{M}+\text{Na}]^+$).



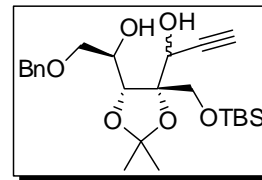
5-O-benzyl-2-C-(((tert-butyldimethylsilyl)oxy)methyl)-

2,3-O-isopropylidene-D-ribofuranose (110): At 0 °C, a solution of alcohol **112** (15 g, 48.3 mmol) in CH₂Cl₂ (30 mL) was treated with triethylamine (13.5 mL, 96.7 mmol)



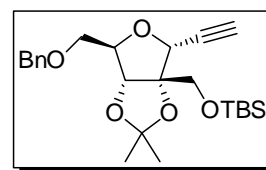
followed by TBDMSCl (7.28 g, 48.3 mmol). The reaction mixture was slowly allowed to reach room temperature and was stirred for 8 h. After the completion of the reaction, ice was added to the reaction mixture and stirred for 5 min. The contents were diluted with CH₂Cl₂ (60 mL) and the resulting layers were separated. The aqueous layer was extracted with CH₂Cl₂ (2 x 50 mL). The combined organic layer was washed with brine, dried over MgSO₄, concentrated. The crude product was purified by flash column chromatography to afford lactols **110** (18.88 g, 92%) as colorless oil. R_f (15% ethyl acetate/pet. ether) 0.3; $[\alpha]_D^{25} = 14.1$ (c 3.24, CHCl₃). IR (CHCl₃): ν 3432, 2931, 2858, 1725, 1496, 1457, 1381, 1251, 1212, 1090, 838, 777 cm⁻¹. ¹H NMR (200 MHz, CDCl₃): δ 0.0 (s, 6H, major), 0.03 (s, 3H, minor), 0.86 (s, 9H, major), 0.89 (s, 4.5H, minor), 1.42 (s, 1.5H, minor), 1.45 (s, 3H, major), 1.47 (s, 1.5H, minor), 1.55 (s, 3H, major), 3.55 (d, $J = 4.3$ Hz, 2H, major), 3.62 (d, $J = 3.0$ Hz, 1H, minor), 3.5 (dd, $J = 5.4, 10.2$ Hz, 1H), 3.55 (dd, $J = 5.4, 10.2$ Hz, 1H), 3.7 (br s, 2H), 4.2–4.25 (m, 1H), 4.23 (dt, $J = 1.3, 4.3$ Hz, 1H, major), 4.32 (dt, $J = 1.1, 4.33.0$ Hz, 0.5H, minor), 4.55 (d, $J = 12.0$ Hz, 1H), 4.62 (d, $J = 1.4$ Hz, 1H), 5.14 (d, $J = 10.7$ Hz, 1H, major), 5.22 (d, $J = 11.4$ Hz, 0.5H, minor), 7.27–2.37 (m, 7.5H) ppm. ¹³C NMR (50 MHz, CDCl₃): δ -5.7 (q), -5.5 (q), 18.3 (s, major), 18.4 (s, minor), 25.8 (q, major), 25.9 (q, minor), 27.3 (q, major), 27.6 (q, major), 27.9 (q, minor), 27.9 (q, minor), 62.3 (t, minor), 62.8 (t, major), 70.8 (t, major), 71.2 (t, minor), 73.6 (t, major), 74.1 (t, minor), 81.0 (d, major), 83.7 (d, major), 84.4 (d, minor), 85.8 (d, minor), 91.4 (s, major), 95.0 (s, minor), 98.4 (d, major), 105.1 (d, minor), 113.4 (s, minor), 114.1 (s, major), 127.7 (d, major), 127.8 (d, minor), 128.2 (d, minor), 128.4 (d, major), 128.7 (d, minor), 136.2 (s, minor), 137.6 (s, major) ppm. ESI-MS: m/z 447.2 (100%, $[M+Na]^+$). HRMS: for C₂₂H₃₆O₆Si; Found: 401.1479 ($[M+Na]^+$), 417.1198 ($[M+K]^+$); Calcd.: 401.1478 ($[M+Na]^+$), 417.1217 ($[M+K]^+$).

Compound 113: Flame dried Mg (86 mg, 3.53 mmol) was treated with dry THF (4 mL) and few crystals of iodine. To it *n*-BuCl (327 mg, 3.53 mmol) was added and the contents were refluxed till the generation of Grignard reagent. Heating



was removed and stirring was continued at room temperature till all the magnesium was consumed. Then the reaction mixture was cooled to 0 °C and acetylene gas was bubbled into it for 15 min. At the same temperature, a solution of lactol **110** (300 mg, 0.706 mmol) in THF (3 mL) was added and stirred for 30 min at 0 °C. The reaction was quenched with saturated NH₄Cl solution, diluted with water and extracted with ethyl acetate. The combined organic layer was dried over Na₂SO₄, concentrated and purified on silica gel chromatography to give the diol **113** (340 mg, 78%) as colorless oil. *R_f* (15% ethyl acetate/pet. ether) 0.4; [α]_D²⁵ = -2.3 (*c* 1.2, CHCl₃). IR (CHCl₃): ν 3447, 2988, 2931, 2861, 1725, 1603, 1496, 1454, 1381, 1217, 1071, 757 cm⁻¹. ¹H NMR (200 MHz, CDCl₃): δ 0.09 (s, 3H), 0.09 (s, 3H), 0.90 (s, 9H), 1.37 (s, 3H), 1.46 (s, 3H), 2.46 (d, *J* = 2.3 Hz, 1H), 3.54–3.68 (m, 3H), 3.77 (dd, *J* = 2.4, 10.1 Hz, 1H), 3.87 (d, *J* = 10.6 Hz, 1H), 4.07 (d, *J* = 10.6 Hz, 1H), 4.58–4.65 (m, 3H), 7.29–7.36 (m, 5H) ppm. ¹³C NMR (50 MHz, CDCl₃): δ -5.7 (q), -5.5 (q), 18.3 (s), 25.9 (q, 3C), 26.1 (q), 27.7 (q), 63.8 (d), 64.0 (t), 68.5 (d), 71.9 (t), 73.4 (t), 74.3 (s), 77.8 (d), 82.5 (s), 84.6 (d), 108.8 (s), 127.6 (d), 127.7 (d, 2C), 128.3 (d, 2C), 138.1 (s) ppm. ESI-MS: *m/z* 473.1 (100%, [M+Na]⁺).

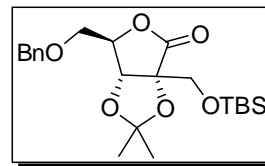
Compound 114: To a solution of diol **113** (200 mg, 0.444 mmol) in dry pyridine (2 mL) was added tosyl chloride (169 mg, 0.887 mmol) and the resulting solution was heated at 50–60 °C for 3 h. To this water was added and the contents were



extracted with CH₂Cl₂. The combined organic phase was dried with MgSO₄ and concentrated to dryness under reduced pressure. The crude was purified by silica gel column chromatography to procure alkyne **114** (148 mg, 77% yield) as colorless oil. *R_f* (10% ethyl acetate/pet. ether) 0.5; [α]_D²⁵ = -12.1 (*c* 4.03, CHCl₃). IR (CHCl₃): ν 3306, 2931, 2858, 2118, 1727, 1496, 1455, 1381, 1253, 1218, 1060, 839, 756 cm⁻¹. ¹H NMR (200 MHz, CDCl₃): δ 0.03 (s, 6H), 0.87 (s, 9H), 1.43 (s, 3H), 1.58 (s, 3H), 2.58 (d, *J* = 2.3 Hz, 1H), 3.5 (dd, *J* = 5.4, 10.2 Hz, 1H), 3.55 (dd, *J* = 5.4, 10.2 Hz, 1H), 3.7 (br s, 2H), 4.26–4.31 (m, 1H), 4.58 (d, *J* = 12.0 Hz, 1H), 4.55 (d, *J* = 12.0 Hz, 1H), 4.62 (d, *J* = 1.4 Hz, 1H), 4.69 (br d, *J* = 2.3 Hz, 1H), 7.26–7.34 (m, 5H)

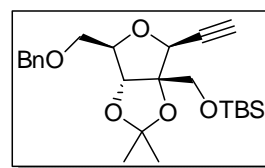
ppm. ^{13}C NMR (50 MHz, CDCl_3): δ -5.7 (q), -5.5 (q), 18.3 (s), 25.8 (q, 3C), 27.3 (q), 27.9 (q), 63.2 (t), 69.4 (t), 72.9 (d), 73.4 (t), 76.2 (d), 78.5 (s), 83.6 (d), 85.2 (d), 93.5 (s), 114.2 (s), 127.7 (d, 2C), 127.8 (d), 128.4 (d, 2C), 137.7 (s) ppm. ESI-MS: m/z 455.2 (100%, $[\text{M}+\text{Na}]^+$).

Compound 115: A suspension of TBS lactol **110** (5 g, 16.1 mmol) and Ag_2CO_3 impregnated on celite (36.7 g, 64.4 mmol, contains 1 mmol of Ag_2CO_3 per 0.57 g of prepared reagent) in dry toluene (50 mL) was reflux for 6 h. After



completion of reaction as indicated by TLC, the contents were cooled to room temperature and filtered through a pad of Celite. The celite pad was washed with toluene and the combined filtrate was concentrated in vacuo. The crude product was purified by silica gel column chromatography to procure lactone **115** (4.43 g, 89% yield) as crystalline solid. R_f (5% ethyl acetate/pet. ether) 0.2, MP: 83 °C.; $[\alpha]_D^{25} = -12$ (c 1.27, CHCl_3). IR (CHCl_3): ν 2931, 2858, 1789, 1727, 1496, 1463, 1383, 1253, 1214, 1108, 1080, 838, 780 cm^{-1} . ^1H NMR (200 MHz, CDCl_3): δ 0.0 (s, 3H), 0.02 (s, 3H), 0.86 (s, 9H), 1.40 (s, 3H), 1.44 (s, 3H), 3.67 (d, $J = 4.5$ Hz, 2H), 3.80 (d, $J = 10.6$ Hz, 1H), 3.97 (d, $J = 10.6$ Hz, 1H), 4.5 (d, $J = 12.2$ Hz, 1H), 4.56 (d, $J = 12.2$ Hz, 1H), 4.6 (t, $J = 4.5$ Hz, 1H), 4.72 (s, 1H), 7.26–7.38 (m, 5H) ppm. ^{13}C NMR (50 MHz, CDCl_3): δ -5.7 (q), -5.5 (q), 18.3 (s), 25.8 (q, 3C), 26.7 (q), 27.1 (q), 61.8 (t), 69.0 (t), 73.7 (t), 79.7 (d), 82.5 (d), 86.0 (s), 113.4 (s), 127.8 (d, 2C), 128.0 (d), 128.5 (d, 2C), 137.1 (s), 174.7 (s) ppm. ESI-MS: m/z 445.1 (100%, $[\text{M}+\text{Na}]^+$). HRMS: Found: 401.1479 ($[\text{M}+\text{Na}]^+$), 417.1198 ($[\text{M}+\text{K}]^+$); Calcd.: 401.1478 ($[\text{M}+\text{Na}]^+$), 417.1217 ($[\text{M}+\text{K}]^+$).

Compound 109: A solution of trimethylsilyl acetylene (3.23 mL, 22.7 mmol) in THF (15 mL) was cooled to -78 °C under argon and treated with $n\text{-BuLi}$ (13.6 mL, 1.6 M in hexane) and stirred at -78 °C for 45 min. To this was introduced a



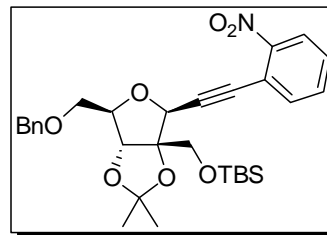
solution of lactone **115** (4.0 g, 9.47 mmol) in THF (15 mol) was added drop wise and stirring was continued for another 5 min at -78 °C and then at -10 °C for 30 min. The reaction mixture was quenched with saturated aq. NH_4Cl solution and partitioned between ethyl acetate and water. The organic layer was washed with brine, dried over

Na₂SO₄ and concentrated. The resulting crude product was used for the next step without any further purification.

To a cooled (-78 °C) solution of the 500 mg of crude hemiacetal and triethylsilane (1.6 mL, 9.6 mmol) in anhydrous CH₂Cl₂ (20 mL) BF₃·OEt₂ (0.57 mL, 4.8 mmol) was added drop wise and stirring was continued at the same temperature for 30 min. When all the starting material was completely consumed as indicated by TLC, the reaction mixture was neutralized with triethylamine and extracted with dichloromethane. The combined organic layer was dried (Na₂SO₄), filtered and concentrated to obtain 600 mg of crude product. The crude was subjected for next step without further purification.

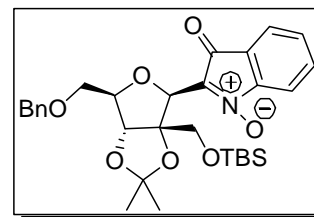
Potassium carbonate (0.6 g, 3.44 mmol) was added to a stirred solution of crude compound (0.5 g) in a 1 : 1 mixture of methanol-CH₂Cl₂ (30 mL) at room temperature, and the reaction mixture was stirred for 4 h. The reaction mixture was concentrated and then extracted with dichloromethane. The combined organic layer was dried (Na₂SO₄) and concentrated under reduced pressure. The crude product was subjected to column chromatography purification to afford **109** (190 mg, 39%) and **114** (72 mg); **109** as colorless liquid; *R_f* (10% ethyl acetate/pet. ether) 0.6; [α]_D²⁵ = -34.5 (*c* 1.55, CHCl₃). IR (CHCl₃): ν 3932, 2858, 2139, 1722, 1612, 1586, 1513, 1463, 1370, 1250, 1104, 1006, 838, 758 cm⁻¹. ¹H NMR (200 MHz, CDCl₃): δ 0.05 (s, 3H), 0.06 (s, 3H), 0.90 (s, 9H), 1.41 (s, 3H), 1.52 (s, 3H), 2.53 (d, *J* = 2.1 Hz, 1H), 3.55 (dd, *J* = 5.2, 10.1 Hz, 1H), 3.60 (dd, *J* = 5.2, 10.1 Hz, 1H), 3.76 (d, *J* = 11.3 Hz, 1H), 4.02 (d, *J* = 11.3 Hz, 1H), 4.21 (dt, *J* = 2.6, 5.2 Hz, 1H), 4.53 (d, *J* = 2.1 Hz, 1H), 4.55 (d, *J* = 12.2 Hz, 1H), 4.59 (d, *J* = 12.2 Hz, 1H), 4.64 (d, *J* = 2.6 Hz, 1H), 7.26–2.33 (m, 5H) ppm. ¹³C NMR (50 MHz, CDCl₃): δ -5.6 (q), -5.4 (q), 18.4 (s), 25.9 (q, 3C), 26.8 (q), 28.3 (q), 61.7 (t), 69.7 (t), 73.5 (t), 75.5 (d), 76.6 (d), 77.6 (s), 82.0 (d), 83.3 (d), 92.0 (s), 114.8 (s), 127.7 (d), 127.8 (d, 2C), 128.4 (d, 2C), 137.9 (s) ppm. ESI-MS: *m/z* 433.1 (100%, [M+H]⁺). HRMS (ESI) Calcd for C₂₄H₃₆O₅SiNa [M+Na]⁺ 455.223, found: 455.2236.

Compound 108: To a solution of alkyne **109** (500 mg, 1.16 mmol), aryl iodide (345 mg, 1.39 mmol) in $\text{Et}_3\text{N}:\text{THF}$ (2:1, 9 mL) were added TPP (30 mg, 0.115 mmol) and $\text{Pd}(\text{PPh}_3)_2\text{Cl}_2$ (80 mg, 0.115 mmol) and the suspension was degassed with argon for 10 min. To this CuI (22 mg, 0.115 mmol) was



introduced and the degassed with argon for 10 min and stirred at room temperature for 2 h. The reaction mixture was filtered through a Celite pad and the filtrate was concentrated under reduced pressure. The residue obtained was purified by column chromatography to afford the nitroalkyne **108** (547 mg, 85% yield) as yellow oil. R_f (15% ethyl acetate/pet. ether) 0.4; $[\alpha]_{\text{D}}^{25} = -90.5$ (c 0.34, CHCl_3). IR (CHCl_3): ν 2996, 2912, 2857, 1645, 1496, 1412, 1380, 1256, 1120, 1070, 838, 757 cm^{-1} . ^1H NMR (500 MHz, CDCl_3): δ 0.09 (s, 6H), 0.90 (s, 9H), 1.44 (s, 3H), 1.56 (s, 3H), 3.59 (dd, $J = 5.2, 10.4$ Hz, 1H), 3.64 (dd, $J = 5.2, 10.4$ Hz, 1H), 3.88 (d, $J = 11.6$ Hz, 1H), 4.18 (d, $J = 11.6$ Hz, 1H), 4.28 (dt, $J = 2.4, 5.2$ Hz, 1H), 4.57 (d, $J = 12.2$ Hz, 1H), 4.60 (d, $J = 12.2$ Hz, 1H), 4.7 (d, $J = 2.4$ Hz, 1H), 4.82 (s, 1H), 7.24–7.34 (m, 5H), 7.47 (ddd, $J = 1.5, 7.4, 7.5$ Hz, 1H), 7.56 (dt, $J = 1.5, 7.5$ Hz, 1H), 7.61 (dd, $J = 1.5, 7.6$ Hz, 1H), 8.03 (dd, $J = 1.3, 7.6$ Hz, 1H) ppm. ^{13}C NMR (125 MHz, CDCl_3): δ –5.67 (q), –5.4 (q), 18.4 (s), 25.9 (q, 3C), 26.9 (q), 28.4 (q), 61.9 (t), 69.7 (t), 73.5 (t), 76.4 (d), 82.2 (d), 83.0 (s), 83.6 (d), 91.0 (s), 93.1 (s), 114.8 (s), 117.6 (s), 124.6 (d), 127.7 (d), 127.8 (d, 2C), 128.4 (d, 2C), 129.2 (d), 132.7 (d), 135.2 (d), 137.9 (s), 149.7 (s) ppm. ESI-MS: m/z 576.2 (100%, $[\text{M}+\text{Na}]^+$). HRMS (ESI) Calcd for $\text{C}_{30}\text{H}_{39}\text{NO}_7\text{SiNa}$ $[\text{M}+\text{Na}]^+$ 576.2394, found: 576.2389.

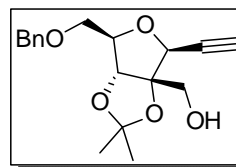
Compound 107: The compound **108** (500 mg, 0.9 mmol) was dissolved in acetonitrile (50 mL) and degassed under argon atmosphere for 10 min and $\text{Pd}(\text{CH}_3\text{CN})_2\text{Cl}_2$ (12 mg, 5 mol%) was introduced and stirred for 8 h at room temperature. The reaction mixture was concentrated



under reduced pressure. The crude was subjected to column chromatography purification to procure isatogen **107** (375 mg, 75 %) as yellow oil. R_f (20% ethyl acetate/pet. ether) 0.5; $[\alpha]_{\text{D}}^{25} = -120$ (c 0.42, CHCl_3). IR (CHCl_3): ν 3283, 3104, 2929, 2857, 1689, 1600, 1451, 1307, 1264, 1235, 917, 757 cm^{-1} . ^1H NMR (500 MHz, CDCl_3): δ –0.2 (s, 3H), –0.15 (s, 3H), 0.65 (s, 9H), 1.40 (s, 3H), 1.67 (s, 3H), 3.7 (dd,

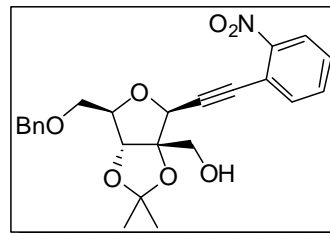
$J = 5.2, 10.4$ Hz, 1H), 3.76 (dd, $J = 5.2, 10.4$ Hz, 1H), 3.78 (d, $J = 11.3$ Hz, 1H), 3.92 (d, $J = 11.3$ Hz, 1H), 4.31–4.33 (m, 1H), 4.45 (d, $J = 3.4$ Hz, 1H), 4.64 (d, $J = 12.2$ Hz, 1H), 4.7 (d, $J = 12.2$ Hz, 1H), 5.41 (s, 1H), 7.27 (br d, $J = 7.1$ Hz, 1H), 7.34 (t, $J = 7.3$ Hz, 2H), 7.40 (br d, $J = 7.6$ Hz, 2H), 7.51–7.64 (m, 4H) ppm. ^{13}C NMR (125 MHz, CDCl_3): δ -5.9 (q), -5.6 (q), 18.2 (s), 25.6 (q, 3H), 27.5 (q), 28.5 (q), 64.2 (t), 69.9 (t), 73.6 (t), 78.0 (d), 83.7 (d), 83.9 (d), 94.9 (s), 114.1 (d), 115.2 (s), 121.5 (d), 123.4 (s), 127.6 (d), 127.8 (d, 2C), 128.3 (d, 2C), 131.4 (d), 134.2 (d), 134.6 (s), 138.0 (s), 146.9 (s), 184.5 (s) ppm. ESI-MS: m/z 576.2 (100%, $[\text{M}+\text{Na}]^+$). HRMS (ESI) Calcd for $\text{C}_{30}\text{H}_{39}\text{NO}_7\text{SiNa}$ $[\text{M}+\text{Na}]^+$ 576.2394, found: 576.2390.

Compound 117: At 0 °C, to a solution of compound **109** (1 g, 2.31 mmol) in THF (10 mL) 1M TBAF solution in THF (2.54 mL, 2.54 mmol) was added and stirred for 4 h at the same temperature. After completion, the reaction mixture was



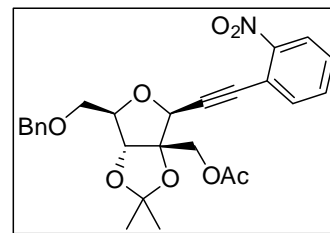
quenched with sat. NH_4Cl (20 mL) and the contents were partitioned between ethyl acetate and water. The organic layer was separated and the aqueous layer was extracted with ethyl acetate (20 mL x 3). The combined organic layer was dried (Na_2SO_4) and concentrated under reduced pressure. The residue obtained was purified by column chromatography to afford alkynol **117** (677 mg, 92% yield) as colorless oil. R_f (40% ethyl acetate/pet. ether) 0.5; $[\alpha]_D^{25} = -26$ (c 1.37, CHCl_3). IR (CHCl_3): ν 3479, 3291, 2990, 2936, 2862, 2121, 1723, 1496, 1455, 1382, 1217, 1152, 1072, 755 cm^{-1} . ^1H NMR (400 MHz, CDCl_3): δ 1.42 (s, 3H), 1.55 (s, 3H), 2.12 (br s, 1H), 2.61 (d, $J = 2.2$ Hz, 1H), 3.65 (br d, $J = 4.5$ Hz, 2H), 3.86 (d, $J = 12.3$ Hz, 1H), 4.01 (d, $J = 12.3$ Hz, 1H), 4.26 (dt, $J = 2.0, 4.5$ Hz, 1H), 4.55 (d, $J = 12.1$ Hz, 1H), 4.6 (d, $J = 12.1$ Hz, 1H), 4.62 (d, $J = 2.2$ Hz, 1H), 4.64 (d, $J = 2.0$ Hz, 1H), 7.28–2.35 (m, 5H) ppm. ^{13}C NMR (100 MHz, CDCl_3): δ 26.9 (q), 28.1 (q), 61.9 (t), 69.7 (t), 73.6 (t), 75.3 (d), 77.1 (d), 78.0 (s), 83.1 (d), 83.2 (d), 91.9 (s), 114.5 (s), 127.8 (d, 3C), 128.4 (d, 2C), 137.6 (s) ppm. ESI-MS: m/z 341.3 (100%, $[\text{M}+\text{Na}]^+$).

Compound 118: The Sonogashira coupling of alkynol **117** (200 mg, 0.32 mmol) and 2-nitroiodobenzene (187 mg, 0.753 mmol) was carried out according to the procedure used for the preparation of **108**. Purification of the crude by column chromatography (5% ethyl



acetate in petroleum ether) gave the nitroalkynol **118** (249 mg, 90%) as yellow syrup. $R_f = 0.6$ (Petether/EtOAc 7:3), $[\alpha]_D^{25} = -154$ ($c = 0.5$, CHCl_3). IR (CHCl_3): ν 3453, 2990, 2935, 2862, 2839, 1667, 1611, 1516, 1463, 1345, 1248, 1162, 1075, 853, 754 cm^{-1} . $^1\text{H NMR}$ (200 MHz, CDCl_3): δ 1.45 (s, 3H), 1.58 (s, 3H), 2.26 (br s, 1H), 3.69 (d, $J = 5.2$ Hz, 2H), 3.98 (br d, $J = 12.2$ Hz, 1H), 4.12 (br d, $J = 12.2$ Hz, 1H), 4.34 (dt, $J = 2.2, 5.1$ Hz, 1H), 4.56 (d, $J = 12.2$ Hz, 1H), 4.62 (d, $J = 12.2$ Hz, 1H), 4.7 (d, $J = 2.0$ Hz, 1H), 4.94 (s, 1H), 7.25–7.35 (m, 5H), 7.44–7.66 (m, 3H), 8.06 (dd, $J = 1.3, 7.7$ Hz, 1H) ppm. $^{13}\text{C NMR}$ (50 MHz, CDCl_3): δ 27.0 (q), 28.0 (q), 62.3 (t), 69.6 (t), 73.5 (t), 76.4 (d), 83.5 (s), 83.7 (d, 2C), 91.5 (s), 92.9 (s), 114.5 (s), 117.5 (s), 124.7 (d), 127.7 (d), 127.7 (d, 2C), 128.3 (d, 2C), 129.3 (d), 132.9 (d), 135.2 (d), 137.6 (s), 149.4 (s) ppm. ESI-MS: m/z 462.1 (100%, $[\text{M}+\text{Na}]^+$).

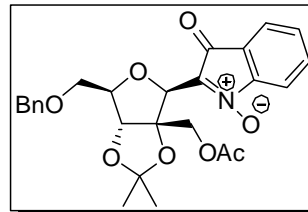
Compound 119: To a stirred solution of nitroalkynol **118** (300 mg, 0.68 mmol) in pyridene (1 mL) and Ac_2O (1.5 mL) was added cat. DMAP at room temperature and stirred for 9 h at rt. The reaction was diluted with ethyl acetate (30 mL). The organic layer was separated,



washed with saturated CuSO_4 solution, brine, dried (Na_2SO_4) and concentrated under reduced pressure. The crude was purified by silica gel column chromatography to afford the compound **119** (313 mg, 95%) as a yellow liquid. $R_f = 0.5$ (Petether/EtOAc 7:3), $[\alpha]_D^{25} = -144$ ($c = 0.35$, CHCl_3). IR (CHCl_3): ν 3358, 2925, 2854, 1916, 1720, 1622, 1458, 1282, 1089, 750 cm^{-1} . $^1\text{H NMR}$ (200 MHz, CDCl_3): δ 1.43 (s, 3H), 1.58 (s, 3H), 2.07 (s, 3H), 3.68 (dd, $J = 5.2, 10.5$ Hz, 1H), 3.71 (dd, $J = 5.2, 10.5$ Hz, 1H), 4.33 (dt, $J = 2.0, 5.2$ Hz, 1H), 3.41 (d, $J = 12.3$ Hz, 1H), 4.55 (d, $J = 12.1$ Hz, 1H), 4.60 (d, $J = 12.1$ Hz, 1H), 4.67 (d, $J = 2.0$ Hz, 1H), 4.75 (d, $J = 12.3$ Hz, 1H), 4.93 (s, 1H), 7.25–7.32 (m, 5H), 7.47–7.51 (m, 1H), 7.58 (dt, $J = 1.3, 7.8$ Hz, 1H), 7.61 (dd, $J = 1.7, 7.8$ Hz, 1H), 8.06 (dd, $J = 1.2, 8.2$ Hz, 1H) ppm. $^{13}\text{C NMR}$ (50 MHz, CDCl_3): δ 20.8 (q), 26.7 (q), 28.1 (q), 62.9 (t), 69.5 (d), 73.5 (d), 76.5 (t), 83.4 (d), 83.7 (d), 90.7 (s), 91.4 (s), 114.9 (s), 117.3 (s), 124.7 (d), 127.7 (d, 3C), 128.3 (d, 2C), 128.5 (s),

129.3 (d), 132.9 (d), 135.1 (d), 137.7 (s), 149.5 (s), 170.4 (s) ppm. ESI-MS: m/z 482.1 (100%, $[M+H]^+$). HRMS (ESI) Calcd for $C_{26}H_{27}NO_8Na$ $[M+Na]^+$ 504.1635, found: 504.1640.

Compound 120: The cycloisomerization of nitroalkyne **119** (300 mg, 0.42 mmol) using $Pd(CH_3CN)_2Cl_2$ (5 mol%) was carried out according to the procedure used for the preparation of **107**. Purification of the crude by column chromatography (5% ethyl acetate in petroleum

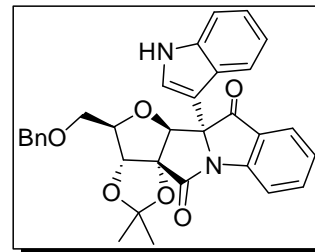


ether) gave **120** (216 mg, 72%) as yellow syrup. $R_f = 0.5$ (Petether/EtOAc 7:3), $[\alpha]_D^{25} = -162$ ($c = 0.87$, $CHCl_3$). IR ($CHCl_3$): ν 3394, 2927, 2850, 1746, 1690, 1606, 1527, 1457, 1382, 1233, 1086, 755 cm^{-1} . 1H NMR (200 MHz, $CDCl_3$): δ 1.40 (s, 3H), 1.68 (s, 3H), 1.79 (s, 3H), 3.68 (dd, $J = 4.6, 10.7$ Hz, 1H), 3.71 (dd, $J = 4.9, 10.7$ Hz, 1H), 4.32–4.38 (m, 3H), 4.62 (d, $J = 12.2$ Hz, 1H), 4.67 (d, $J = 3.0$ Hz, 1H), 4.71 (d, $J = 12.2$ Hz, 1H), 5.41 (s, 1H), 7.30–7.38 (m, 5H), 7.57–7.68 (m, 4H) ppm. ^{13}C NMR (50 MHz, $CDCl_3$): δ 20.5 (q), 27.0 (q), 28.4 (q), 63.6 (t), 69.7 (t), 73.7 (t), 77.7 (d), 83.5 (d), 84.0 (d), 92.3 (s), 114.3 (d), 115.6 (s), 121.7 (d), 123.1 (s), 127.7 (d), 127.8 (d, 2C), 128.4 (d, 2C), 131.9 (d), 133.3 (s), 134.5 (d), 137.9 (s), 146.8 (s), 170.1 (s), 184.6 (s) ppm. ESI-MS: m/z 482.1 (100%, $[M+H]^+$). HRMS (ESI) Calcd for $C_{26}H_{27}NO_8Na$ $[M+Na]^+$ 504.1635, found: 504.1641.

Compound 106: To a solution of compound **120** (100 mg, 0.122 mmol) and indole (22 mg, 0.182 mmol) in acetonitrile (2 mL) was added anhy. $InCl_3$ (40 mg, 0.182 mmol) degassed under argon atmosphere for 5 min. Reaction mixture was allowed to stir at 60 °C for 12 h. After completion of the reaction, acetonitrile was evaporated under reduced pressure and the crude was used for the next step without any further purification.

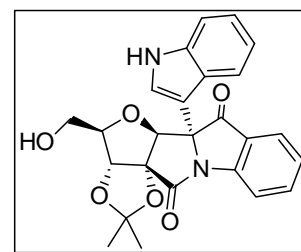
To a solution of the above crude product (130 mg) in methanol (3 mL) was added K_2CO_3 (0.5 equiv. of the crude mass) and the mixture was stirred for 30 min at room temperature. After completion of reaction, methanol was removed and the residue was purified by column chromatography to afford alcohol **106** (mg, 65% over two steps) as yellow oil. R_f (20% ethyl acetate/pet. ether) 0.5 (due to presence of a unseparable we were not able to take clean spectra for this compound).

Compound 121: Under argon an atmosphere of in a glass seal tube, compound **106** (20 mg, 0.037 mmol), $[\text{Cp}^*\text{RhCl}_2]_2$ (7.0%Rh), K_2CO_3 (5 mol %), and acetone (3 mL) were placed. The tube was sealed and was heated at 110 °C (oil bath temp.) for 26 h. The reaction mixture was concentrated and the resulting crude was purified by



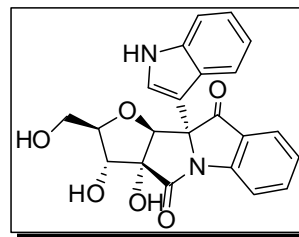
column chromatography to obtain the lactam **121** (11 mg, 56% yield) as yellow foam. R_f (20% ethyl acetate/pet. ether) 0.5; $[\alpha]_D^{25} = -132$ (c 0.16, CHCl_3). IR (CHCl_3): ν 3363, 2929, 2868, 1794, 1620, 1487, 1456, 1372, 1321, 12156, 1080, 750 cm^{-1} . ^1H NMR (500 MHz, CDCl_3) δ 1.39 (s, 3H), 1.52 (s, 3H), 3.33 (dd, $J = 2.7, 10.7$ Hz, 1H), 3.36 (dd, $J = 3.3, 10.7$ Hz, 1H), 3.81 (d, $J = 12.8$ Hz, 1H), 3.92 (d, $J = 12.8$ Hz, 1H), 4.32–4.33 (m, 1H), 4.86 (d, $J = 2.4$ Hz, 1H), 4.91 (s, 1H), 6.96 (br dd, $J = 1.8, 7.9$ Hz, 2H), 7.17–7.26 (m, 7H), 7.33–7.35 (m, 1H), 7.58 (br t, $J = 7.4$ Hz, 1H), 7.65 (d, $J = 7.4$, 1H), 7.99 (d, $J = 8.2$ Hz, 1H), 8.16–8.17 (m, 2H) ppm; ^{13}C NMR (125 MHz, CDCl_3) δ 25.6 (q), 27.0 (q), 68.9 (t), 73.0 (t), 75.0 (s), 84.6 (d), 85.6 (d), 87.2 (d), 98.2 (s), 111.5 (d), 111.8 (s), 116.4 (d), 117.7 (s), 120.6 (d), 121.0 (d), 122.5 (d), 122.9 (d), 124.5 (s), 125.4 (d), 125.5 (d), 126.1 (s), 127.5 (d), 127.6 (d, 2C), 128.2 (d, 2C), 136.2 (d), 137.2 (s), 137.5 (s), 149.9 (s), 169.9 (s), 194.0 (s) ppm. ESI-MS: m/z 559.2 (100%, $[\text{M}+\text{H}]^+$). HRMS (ESI) Calcd for $\text{C}_{32}\text{H}_{28}\text{N}_2\text{O}_6\text{Na}$ $[\text{M}+\text{Na}]^+$ 559.1845, found: 559.1849

(–)-Isatisine A acetonide (2): A suspension of compound **121** (10 mg, 0.019 mmol) and 10% $\text{Pd}(\text{OH})_2/\text{C}$ in ethanol (1.5 mL) was flushed with hydrogen gas and stirred under hydrogen (20 psi) atmosphere at rt for 3 h. The reaction mixture was filtered through a plug of filter aid, washed with ethyl acetate thoroughly (3×10 mL) and concentrated. Purification of crude product by column chromatography (30% ethyl acetate in petroleum ether) yielded product **2** (7.9 mg, 96%) as a yellow solid. $R_f = 0.2$ (Petether/EtOAc 5:2); $[\alpha]_D^{25} = -278$ (c 0.21, CH_3OH). IR (CHCl_3): ν 3425, 2989, 2915, 2859, 2830, 1720, 1615, 1470, 1376, 1265, 1246, 1215, 1148, 1087, 1055, 875 cm^{-1} . ^1H NMR (500 MHz, MeOD) δ 1.36 (s, 3H), 1.49 (s, 3H), 3.43 (dd, $J = 11.9, 4.4$ Hz, 1H), 3.49 (dd, $J = 11.9, 4.2$ Hz, 1H), 4.16 (dd, $J = 7.7, 4.2$ Hz, 1H), 4.79 (d, $J = 3.4$ Hz, 1H), 4.90 (s,



1H), 7.08 (t, $J = 7.2$ Hz, 1H), 7.14 (t, $J = 7.2$ Hz, 1H), 7.24 (s, 1H), 7.31 (t, $J = 7.5$ Hz, 1H), 7.36 (d, $J = 8.1$ Hz, 1H), 7.63 (d, $J = 7.6$ Hz, 1H), 7.80–7.74 (m, 1H), 7.93 (d, $J = 8.0$ Hz, 1H), 8.01 (d, $J = 8.1$ Hz, 1H) ppm; ^{13}C NMR (125 MHz, MeOD) $\delta = 26.4$ (q), 27.4 (q), 62.6 (t), 76.4 (s), 86.1 (d), 87.2 (d), 87.9 (d), 99.6 (s), 111.1 (s), 113.1 (d), 117.6 (d), 119.6 (s), 120.9 (d), 121.4 (d), 123.4 (d), 124.4 (d), 125.8 (s), 126.3 (d), 127.1 (d), 127.4 (s), 138.0 (d), 139.2 (s), 151.3 (s), 171.6 (s), 195.8 (s) ppm. ESI-MS: m/z 469.1 (100%, $[\text{M}+\text{H}]^+$).

(–)-Isatisine A (1); Path A: To a ice cooled solution of **121** (5 mg, 0.009 mmol) in CH_2Cl_2 (1 mL), was added solution of TiCl_4 (1 drop) in CH_2Cl_2 and stirred for 2 hour at the same temperature. The reaction was quenched with ice and extracted with CH_2Cl_2 (20 mL x 3); the combine organic lalery was dried over Na_2SO_4 , concentrated and the crude was subjected for column chromatography to procure Isatisine A (2.3 mg, 71%) as yellow solid.



Path B: To an ice cooled solution of compound **2** (10 mg, 0.022 mmol) in MeOH (1.5 mL), 2N HCl was added drop wise at the same temperature and allowed to stir for 2 h. The solvent was removed under reduced pressure and the crude product was subjected for column chromatography to obtain Isatisine A (8 mg, 88%) as yellow solid. R_f (Methanol/dichloromethane 1:9) 0.5; $[\alpha]_{\text{D}}^{25} = -275$ (c 0.21, CH_3OH). IR (CHCl_3): ν 3432, 2913, 2879, 1712, 1635, 1466, 1458, 1386, 1315, , 1282, 1089, 750 cm^{-1} . ^1H NMR (500 MHz, MeOD): δ 3.33 (dd, $J = 4.9, 11.8$ Hz, 1H), 3.4 (dd, $J = 4.9, 11.8$ Hz, 1H), 3.83–3.86 (m, 1H), 4.07 (d, $J = 4.3$ Hz, 1H), 4.89 (s, 1H), 7.05 (t, $J = 7.5$ Hz, 1H), 7.12 (t, $J = 7.3$ Hz, 1H), 7.29 (s, 1H), 7.3–7.35 (m, 2H), 7.64 (d, $J = 7.3$ Hz, 1H), 7.77 (br t, $J = 8.0$ Hz, 1H), 7.93 (d, $J = 7.9$ Hz, 1H), 7.99 (d, $J = 8.0$ Hz, 1H) ppm. ^{13}C NMR (100 MHz, MeOD): δ 63.2 (t), 74.4 (d), 76.8 (s), 84.7 (d), 89.0 (d), 99.0 (s), 110.7 (s), 112.9 (d), 117.8 (d), 120.7 (d), 121.6 (d), 123.2 (d), 124.6 (d), 126.1 (s), 126.3 (d), 127.0 (d), 127.4 (s), 138.0 (d), 139.1 (s), 151.9 (s), 174.7 (s), 196.8 (s) ppm. ESI-MS: m/z 429.01 (100%, $[\text{M}+\text{Na}]^+$).

REFERENCE

REFERENCES

1. a) Nicolaou, K. C.; Pfefferkorn, J. A.; Mitchell, H. J.; Roecker, A. J.; Barluenga, S.; Cao, G.-Q.; Affleck, R. L.; Lillig, J. E. *J. Am. Chem. Soc.* **2000**, *122*, 9954. b) Walsh, C. T. *Nature Chem. Biol.* **2005**, *1*, 122. c) Piggott, A. M.; Karuso, P. *Combinatorial Chemistry & High Throughput Screening* **2004**, *7*, 607. d) Grabowski, K.; Gisbert, S. *Curr. Chem. Biol.* **2007**, *1*, 115.
2. Newman, D. J. *J. Nat. Prod.* **2007**, *70*, 461.
3. For leading reviews on various approaches for small molecule library synthesis see: a) Thompson, L. A.; Ellman, J. A. *Chem. Rev.* **1996**, *96*, 555. b) Arya, P.; Joseph, R.; Gan, Z.; Rakic, B. *Chem. Biol.* **2005**, *12*, 163. c) Beeler, A. B.; Schaus, S. E.; Porco, J. A., Jr. *Curr. Opin. Chem. Biol.* **2005**, *9*, 277. d) Tan, D. S. *Nat. Chem. Biol.* **2005**, *1*, 74. e) Wilson, R. M.; Danishefsky, S. J. *J. Org. Chem.* **2007**, *72*, 4293. f) Schreiber, S. L. *Nature* **2009**, *457*, 153; (g) Kumar, K.; Waldmann, H. *Angew. Chem., Int. Ed.* **2009**, *48*, 3224. h) Schreiber, S. L. *Nature Chem. Biol.* **2009**, *457*, 153.
4. a) Nicolaou, K. C.; Vourloumis, D.; Winssinger, N.; Baran, P. S. *Angew. Chem. Int. Ed.* **2000**, *39*, 44. b) Nicolaou, K. C.; Sorensen, J. E. *Classics in Total Synthesis: Targets, Strategies, Methods*, Wiley-VCH **1996**.
5. a) Ramana, C. V.; Salian, S. R.; Gonnade, R. G. *Eur. J. Org. Chem.* **2007**, 5483. b) Ramana, C. V.; Reddy, C. N.; Gonnade, R. G. *Chem. Commun.* **2008**, 3151. c) Ramana, C. V.; Pandey, S. K. *Tetrahedron* **2010**, *66*, 390.
6. a) Ramana, C. V.; Suryawanshi, S. B. *Tetrahedron Lett.* **2008**, *49*, 445. b) Suryawanshi S. B.; Dushing M. P.; Ramana C. V. *Tetrahedron*, **2010**, *66*, 6085. c) Ramana, C. V.; Dushing, M. P.; Mohapatra, S.; Mallik, R.; Gonnade, R. G. *Tetrahedron Lett.* **2011**, *52*, 38.
7. J.-F. Liu, Z.-Y. Jiang, R.-R. Wang, Y.-T. Zeng, J.-J. Chen, X.-M. Zhang, Y.-B. Ma, *Org. Lett.* **2007**, *9*, 4127.
8. Pantanowitz, L.; Michelow, P. *Diagn Cytopathol.* **2011**, *39*, 65.
9. a) El Kouni M. H. *Curr Pharm Des.* **2002**, *8*, 581. b) Girard, M. P.; Osmanov, S. K.; Kieny, M. P. *Vaccine* **2006**, *25*, 1567.

10. a) Jung, M.; Lee, S.; Kim, H. *Curr. Med. Chem.* **2000**, *7*, 649. b) Asres, K.; Seyoum, A.; Veeresham, C.; Bucar, F.; Gibbons, S. *Phytother. Res.* **2005**, *19*, 557. c) Jung, M.; Lee, S.; Kim, H.; Kim, H. *Curr. Med. Chem.* **2000**, *7*, 649. d) Yu, D.; Suzuki, M.; Morris-Natschke, S. L.; Lee, K. H. *Med. Res. Rev.* **2003**, *23*, 322. e) Cos, P.; Mees, L.; Berghe, D. V.; Hermans, N.; Pieters, L.; Vlietinck, A. *J. Nat. Prod.* **2004**, *67*, 284.
11. a) Huang, Q.; Yoshihira, K.; Natori, S. *Planta Med.* **1981**, *42*, 308. b) Sha, J. M. *Yao Xue Tong Bao* **1983**, *18*, 27.
12. Liu, J. F.; Zhang, X. M.; Xue, D. Q.; Jiang, Z. Y.; Gu, Q.; Chen, J. J. *Zhongguo Zhongyao Zazhi.* **2006**, *31*, 1961.
13. For reviews on the preparation of isatogens, see: a) Hiremath, S. P.; Hooper, M. *Adv. Heterocycl. Chem.* **1978**, *22*, 123. b) Preston, P. N.; Tennant, G. *Chem. Rev.* **1972**, *72*, 627.
14. a) Baeyer, A. *Ber. Deut. Chem. Ges.* **1881**, *14*, 1741. b) Baeyer, A. *Ber. Deut. Chem. Ges.* **1881**, *15*, 50.
15. Castro, E. R.; Stephens, R. D. *J. Org. Chem.* **1963**, *28*, 2163.
16. Ruggli, P.; Disler, A. *Helv. Chim. Acta* **1927**, *10*, 938. b) Ruggli, P.; Preuss, R. *Helv. Chim. Acta* **1941**, *24*, 1345. c) Beak, E. K.; Chae, Y. S.; Shim, S. C. *Bull. Kor. Chem. Soc.* **1996**, *17*, 993. d) Krohnke, F.; Meyer-Delius, M. *Chem. Ber.* **1951**, *84*, 932. e) Splitter, J. S.; Calvin, M. *J. Org. Chem.* **1955**, *20*, 1086. f) Hooper, M.; Wibberley, D. G. *J. Chem. Soc. C* **1969**, 1596. g) Bond, C. C.; Hooper, M. *J. Chem. Soc. C: Org.* **1969**, 2453. h) Bond, C. C.; Hooper, M. *Synthesis* **1974**, 443.
17. Kröhnke, F.; Vogt, I. *Chem. Ber.* **1953**, *86*, 1500. b) Boyer, J.; Bernardes-Genisson, V.; Farines, V.; Souchard, J.-P.; Nepveu, F. *Free Radical Res.* **2004**, *38*, 459.
18. Ruggli, P.; Hegedu:s, B. *Helv. Chim. Acta* **1939**, *22*, 147.
19. Green, A. P.; Hooper, M.; Sweetman, A. J. *Biochem. Biophys. Res. Commun.* **1974**, *58*, 337.
20. Huisgen, R. *Angew. Chem. Int. Ed. Engl.* **1963**, *2*, 565.
21. a) Alessandri, L. *Gazz. Chim. Ital.* **1928**, *58*, 551. b) Alessandri, L. *Gazz. Chim. Ital.* **1928**, *58*, 738.
22. Castro, E. R.; Stephens, R. D. *J. Org. Chem.* **1963**, *28*, 2163.

23. a) Needham, E. R.; Perkin, W. H. *J. Chem. Soc.* **1904**, 148. b) Hooper, M.; Wibberley, D. *G. J. Chem. Soc. C* **1969**, 1596.
24. Beak, E. K.; Chae, Y. S.; Shim, S. C. *Bull. Kor. Chem. Soc.* **1996**, *17*, 993.
25. a) Ruggli, P.; Disler, A. *Helv. Chim. Acta* **1927**, *10*, 938. b) Ruggli, P.; Zimmerman, A. *Helv. Chim. Acta* **1932**, *15*, 865. c) Ruggli, P.; Preuss, R. *Helv. Chim. Acta* **1941**, *24*, 1345.
26. a) Krohnke, F.; Vogt, I. *Chem. Ber.* **1952**, *85*, 376. b) Kröhnke, F.; Vogt, I. *Chem. Ber.* **1953**, *86*, 1500. c) Génisson, V. B.; Bouniol, A.-V.; Nepveu, F. *Synlett* **2001**, 700. d) Slatt, J.; Bergman, J. *Tetrahedron* **2002**, *58*, 9187. e) Boyer, J.; Bernardes-Genisson, V.; Farines, V.; Souchard, J.-P.; Nepveu, F. *Free Radical Res.* **2004**, *38*, 459. e) Pudziuelyte, E.; Ríos-Luci, C.; León, L. G.; Cikotiene, I.; Padrón, J. M. *Bioorg. Med. Chem.* **2009**, *17*, 4955.
27. Ruggli, P.; Hegedus, B. *Helv. Chim. Acta* **1939**, *22*, 147.
28. Rosen, G. M.; Tsai, P.; Barth, E. D.; Dorey, G. D.; Casara, P.; Spedding, M.; Halpern, H. *J. J. Org. Chem.* **2000**, *65*, 4460.
29. Asao, N.; Sato, K.; Yamamoto, Y. *Tetrahedron Lett.* **2003**, *44*, 5675.
30. a) Söderberg, B. C. G.; Gorugantula, S. P.; Howerton, C. R.; Petersen, J. L.; Dantale, S. W. *Tetrahedron* **2009**, *65*, 7357. b) Nepveu, F.; Kim, S.; Boyer, J.; Chatriant, O.; Ibrahim, H.; Reybier, K.; Monje, M.-C.; Chevalley, S.; Perio, P.; Lajoie, B. H.; Bouajila, J.; Deharo, E.; Sauvain, M.; Tahar, R.; Basco, L.; Pantaleo, A.; Turini, F.; Arese, P.; Valentin, A.; Thompson, E.; Vivas, L.; Petit, S.; Nallet, J.-P. *J. Med. Chem.* **2010**, *53*, 699.
31. Li, X.; Incarvito, C. D.; Vogel, T.; Crabtree, R. H. *Organometallics* **2005**, *24*, 3066.
32. a) Bhakuni, D. S.; Silva, M.; Matlin, S. A.; Sammes, P. G. *Phytochemistry* **1976**, *15*, 574. b) Hutchison, A. J.; Kishi, Y. *J. Am. Chem. Soc.* **1979**, *101*, 6786. c) Williams, R. M.; Glinka, T.; Kwast, E.; Coffman, H.; Stille, J. K. *J. Am. Chem. Soc.* **1990**, *112*, 808. d) Baran, P. S.; Corey, E. J. *J. Am. Chem. Soc.* **2002**, *124*, 7904. e) Kam, T.-S.; Subramaniam, G.; Lim, K.-H.; Choo, Y.-M. *Tetrahedron Lett.* **2004**, *45*, 5995. e) Magolan, J.; Carson, C. A.; A., K. M. *Org. Lett.* **2008**, *10*, 1437. f) Tsukamoto, S.; Umaoka, H.; Yoshikawa, K.; Ikeda, T.; H., H. *J. Nat. Prod.* **2010**, *73*, 1438.

33. Mérour, J.-Y.; Gadonneix, P.; Malapel-Andrieu, B.; Desarbre, E. *Tetrahedron* **2001**, *57*, 1995.
34. Kawasaki, T.; Tang, C.-Y.; Nakanishi, H.; Hirai, S.; Ohshita, T.; Tanizawa, M.; Himori, M.; Satoh, H.; Sakamoto, M.; Miura, K.; Nakano, F. *J. Chem. Soc., Perkin Trans. 1* **1999**, 327.
35. Söderberg, B. C. G.; Gorugantula, S. P.; Howerton, C. R.; Petersen, J. L.; Dantale, S. W. *Tetrahedron* **2009**, *65*, 7357.
36. Košmrlj, J.; Kafka, S.; Leban, I.; M., G. *Magn. Reson. Chem.* **2007**, *45*, 700.
37. Buller, M. J.; Cook, T. G.; Kobayashi, Y. *Heterocycles*, **2007**, *72*, 163.
38. a) Patterson, D. A.; Wibberley, D. G. *J. Chem. Soc.* **1965**, 1706. b) Hooper, M.; Robertson, J. W. *Tetrahedron Lett.* **1971**, 2137.
39. a) Berti, C.; Greci, L.; Marchetti, L. *J. Chem. Soc. Perkin Trans. 2* **1979**, 233. b) Tommasi, G.; Bruni, P.; Greci, L.; Sgarabotto, P.; Righi, L. *J. Chem. Soc. Perkin Trans. 1* **1999**, 681. c) Liu, Y.; McWhorter, W. W. *J. Org. Chem.* **2003**, *68*, 2618.
40. a) Denis, J. N.; Mauger, H.; Vallee, Y. *Tetrahedron Lett.* **1997**, *38*, 8515. b) Chalaye-Mauger, H.; Denis, J. N.; Averbuch-Pouchot, M. T.; Vallee, Y. *Tetrahedron* **2000**, *56*, 791. c) Berini, C.; Minassian, F.; Pelloux-Leon, N.; Vallee, Y. *Tetrahedron Lett.* **2005**, *46*, 8653. d) Suneel Kumar, C. V.; Ramana, C. V. *Chem. Eur. J.* **2012**, accepted.
41. Yin, Q.; You, S.-L. *Chem. Sci.* **2011**, *2*, 1344.
42. Chen, C.; Hong, S. H. *Org. Biomol. Chem.* **2011**, *9*, 20.
43. a) Dobereiner, G. E.; Crabtree, R. H. *Chem. Rev.* **2010**, *110*, 681. b) Watanabe, Y.; Morisaki, Y.; Kondo, T.; Mitsudo, T. *J. Org. Chem.* **1996**, *61*, 4214. c) Fujita, K.; Enoki, Y.; Yamaguchi, R. *Tetrahedron* **2008**, *64*, 1943. d) Hamid, M.; Allen, C. L.; Lamb, G. W.; Maxwell, A. C.; Maytum, H. C.; Watson, A. J. A.; Williams, J. M. J. *J. Am. Chem. Soc.* **2009**, *131*, 1766.
44. Naota, T.; Murahashi, S.-I. *Synlett* **1991**, 693.
45. Gunanathan, C.; Ben-David, Y.; Milstein, D. *Science* **2007**, *317*, 790.
46. Ghosh, S. C.; Muthaiah, S.; Zhang, Y.; Xu, X.; Hong, S. H. *Adv. Synth. Catal.* **2009**, *351*, 2643.
47. Zhang, Y.; Chen, C.; Ghosh, S. C.; Li, Y.; Hong, S. H. *Organometallics* **2010**, *29*, 1374.
48. Shimizu, K.; Ohshima, K.; Satsuma, A. *Chem. Eur. J.* **2009**, *15*, 9977.

49. a) Fujita, K.; Takahashi, Y.; Owaki, M.; Yamamoto, K.; Yamaguchi, R. *Org. Lett.* **2004**, *6*, 2785. b) Fujita, K.; Yamamoto, K.; Yamaguchi, R. *Org. Lett.* **2002**, *4*, 2691.
50. Zweifel, T.; Naubron, J. V.; Grutzmacher, H. *Angew. Chem., Int. Ed.* **2009**, *48*, 559.
51. a) Karadeolian, A.; Kerr, M. A. *Angew. Chem. Int. Ed.* **2010**, *49*, 1133. b) Karadeolian, A.; Kerr, M. A. *J. Org. Chem.* **2010**, *75*, 6830. c) Lee, J.; Panek, J. S. *Org. Lett.* **2011**, *13*, 502. d) Zhang, X.; Mu, T.; Zhan, F.; Ma, L.; Liang, G. *Angew. Chem. Int. Ed.* **2011**, *50*, 1. e) Wu, W.; Xiao, M.; Wang, J.; Li, Y.; Xie, Z. *Org. Lett.* **2012**, *14*, 1624.
52. Pohlhaus, P. D.; Sanders, S. D.; Parsons, A. T.; Li, W.; Johnson, J. S. *J. Am. Chem. Soc.* **2008**, *130*, 8642.
53. a) (a) Qian, H.; Han, X.; Widenhofer, R. A. *J. Am. Chem. Soc.* **2004**, *126*, 9536. (b) Antoniotti, S.; Genin, E.; Michelet, V.; Geneêt, J.-P. *J. Am. Chem. Soc.* **2005**, *127*, 9976. (c) Trost, B. M.; Rudd, M. T. *J. Am. Chem. Soc.* **2005**, *127*, 4763. (d) Trost, B. M.; Rhee, Y. H. *J. Am. Chem. Soc.* **2003**, *125*, 7482. (e) Trost, B. M.; Rhee, Y. H. *J. Am. Chem. Soc.* **2002**, *124*, 2528. (f) Wipf, P.; Graham, T. H. *J. Org. Chem.* **2003**, *68*, 8798. g) Hartwig, J. F. *Nature* **2008**, *455*, 314.
54. a) Zeni, G.; Larock, R. C. *Chem. Rev.* **2004**, *104*, 2285. (b) Alonso, F.; Yus, M.; Beletskaya, I. P. *Chem. Rev.* **2004**, *104*, 3079. (c) Beller, M.; Seayad, J.; Tillack, A.; Jiao, H. *Angew. Chem., Int. Ed.* **2004**, *43*, 3368. (d) Xu, C.; Negishi, E.-C. *In Handbook of Organopalladium Chemistry for Organic Synthesis*; Negishi, E.-C., Ed.; John Wiley & Sons, **2002**, *1*, 2289. (e) Li, J. J.; Gribble, G. W. *Palladium in Heterocyclic Chemistry*, **2000**; (f) Poli, G.; Giambastiani, G.; Heumann, A. *Tetrahedron* **2000**, *56*, 5959 (g) Cacchi, S. *J. Organomet. Chem.* **1999**, *576*, 42.
55. Larock, R.C. *Top Organomet Chem* **2005** *14*, 147.
56. a) Vlaar, T.; Ruijter, E.; Orru, R. V. A. *Adv. Synth. Catal.* **2011**, *353*, 809. b) Egle M. Beccalli, E. M.; Broggini, G.; Fasana, A.; Rigamonti, M. *J. Org. Met. Chem.* **2011**, *696*, 277.
57. a) Ramana, C.V.; Mallik, R.; Gonnade, R. G.; Gurjar, M.K. *Tetrahedron Lett.* **2006**, *47*, 3649. b) Ramana, C. V.; Patel, P.; Gonnade, R. G. *Tetrahedron Lett.* **2007**, *48*, 4771. c) Ramana, C.V.; Mallik, R.; Gonnade, R. G. *Tetrahedron* **2008**, *64*, 219.
58. a) Kaneda, K.; Uchiyama, T.; Fujiwara, Y.; Imanaka, T.; Teranishi, S. *J. Org. Chem.* **1979**, *44*, 55. b) Zhu, G.; Zhang, Z. *J. Org. Chem.* **2005**, *70*, 3339. c) Hoye, T. R.; Wang,

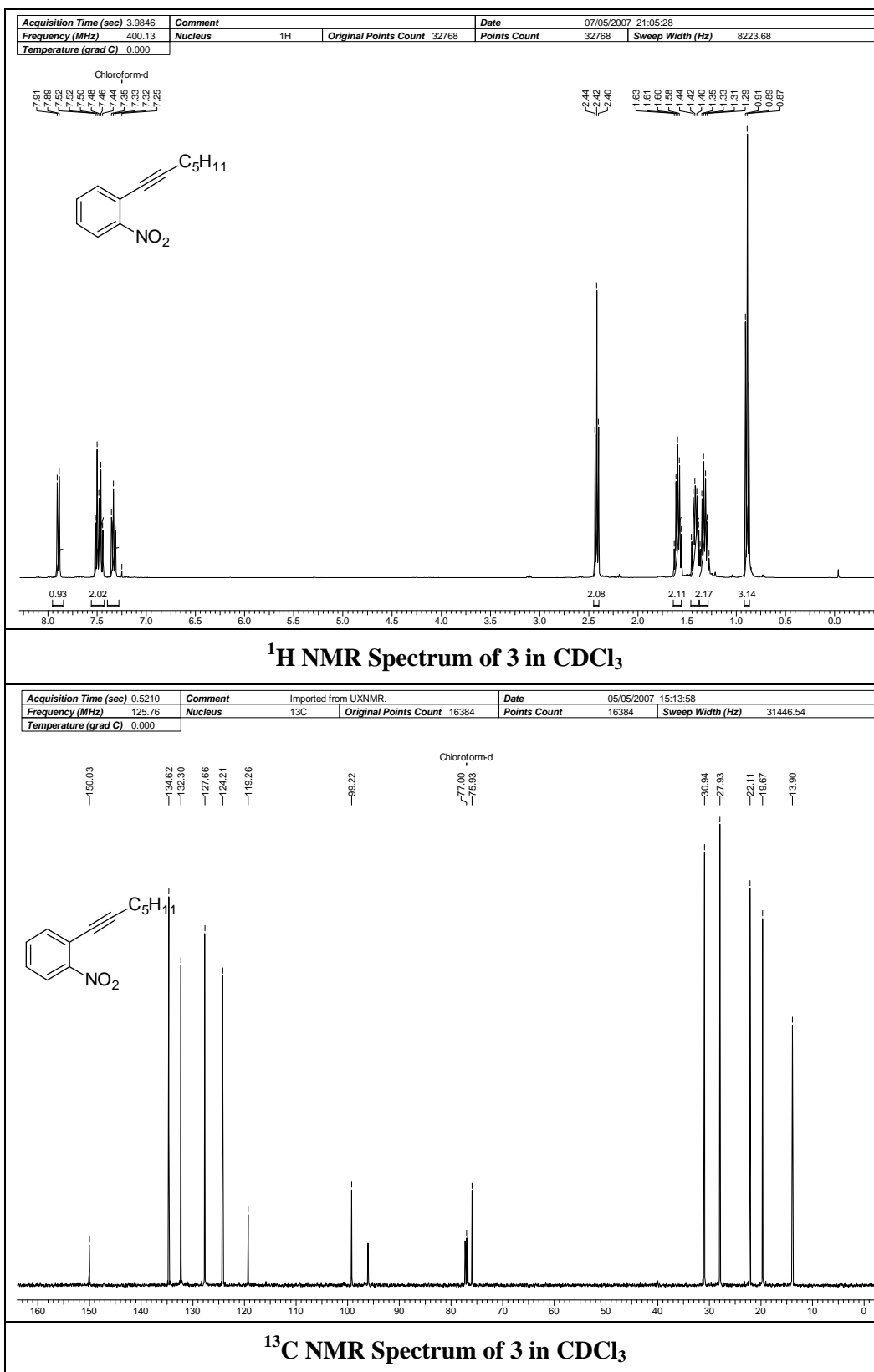
- J. *J. Am. Chem. Soc.* **2005**, *127*, 6950. d) Huang, X.-C.; Wang, F.; Liang, Y.; Li, J.-H. *Org. Lett.* **2009**, *11*, 1139.
59. a) Padwa, A.; Krumpke, E. K.; Weingarten, M. D. *J. Org. Chem.* **1995**, *60*, 5595. b) Woon, E. C. Y.; Dhimi, A.; Mahonb, M. F.; Threadgill, M. D. *Tetrahedron* **2006**, *62*, 4829. c) Ramana, C. V.; Mallik, R.; Gonnade, R. G. *Tetrahedron* **2008**, *64*, 219.
60. For the preparation of specific alkynes; a) Chattopadhyay, A. *J. Org. Chem.* **1996**, *61*, 6104. b) Sakya, S. M.; Strohmeyer, T. W.; Lang, S. A.; Lin, Y.-I. *Tetrahedron Lett.* **1997**, *38*, 5913. c) Han, Y.; Chi, Z.; Huang, Y.-Z. *Synth. Commun.* **1999**, *29*, 1287. d) Gurjar, M. K.; Ravindranadh, S. V.; Kumar, P. *Chem. Commun.* **2001**, 917. e) Ramana, C. V.; Salián, S. R.; Gonnade, R. G. *Eur. J. Org. Chem.* **2007**, 5483. f) Ramana, C. V.; Induvadana, B. *Tetrahedron Lett.* **2009**, *50*, 271.
61. Sonogashira, K.; Tohda, Y.; Hagihara, N. *Tetrahedron Lett.* **1975**, *16*, 4467.
62. Hooper, M.; Patterson, D. A.; Wibberley, D. G. *J. Pharm. Pharmacol.* **1965**, *17*, 734.
63. Sahasrabudhe, A. B.; Kamath, H. V.; Bapat, B. V.; Kullarni, S. N. *Indian J. Chem.* **1980**, *19B*, 230.
64. Helmut, H.; Rolf-Dieter, K.; Ernst-Heinrich, P. *Chem. Abs.* **1982**, *97*, 216185q.
65. Menton, K.; Spedding, M.; Gressens, P.; Villa, P.; Williamson, T.; Markham, A. *Eur. J. Pharmacol.* **2002**, *444*, 53.
66. Fiers, W.; Beyaert, R.; Declercq, W.; Vandenabeele, P. *Oncogene* **1999**, *18*, 7719.
67. a) Sweetman, A. P.; Hooper, G. M. *Biochem. Biophys. Res. Commun.* **1974**, *58*, 337. b) Nepveu, F.; Souchar, J.-P.; Rolland, Y.; Dorey, G.; Spedding, M. *Biochem. Biophys. Res. Commun.* **1998**, *242*, 272. c) Spedding, M.; Menton, K.; Markham, A.; Weetman, D. F. *J. Auton. Nerv. Syst.* **2000**, *81*, 225. d) Menton, K.; Spedding, M.; Gressens, P.; Villa, P.; Williamson, T.; Markham, A. *Eur. J. Pharmacol.* **2002**, *444*, 53.
68. Fiers, W.; Beyaert, R.; Declercq, W.; Vandenabeele, P. *Oncogene* **1999**, *18*, 7719.
69. Cramer, C. J. *Essentials of Computational Chemistry: Theories and Models* **2004**, Wiley-VCH, Weinheim.
70. Jensen, F. *Introduction to Computational Chemistry* **2006**, Wiley-VCH, Weinheim.
71. a) Becke, A. D. *J. Chem. Phys.* **1993**, *98*, 5648. b) Becke, A. D. *J. Chem. Phys.* **1993**, *98*, 1372.
72. Ramos, M. J.; Sousa, S. F.; Fernandes, P. A. *J. Phys. Chem. A* **2007**, *111*, 10439.

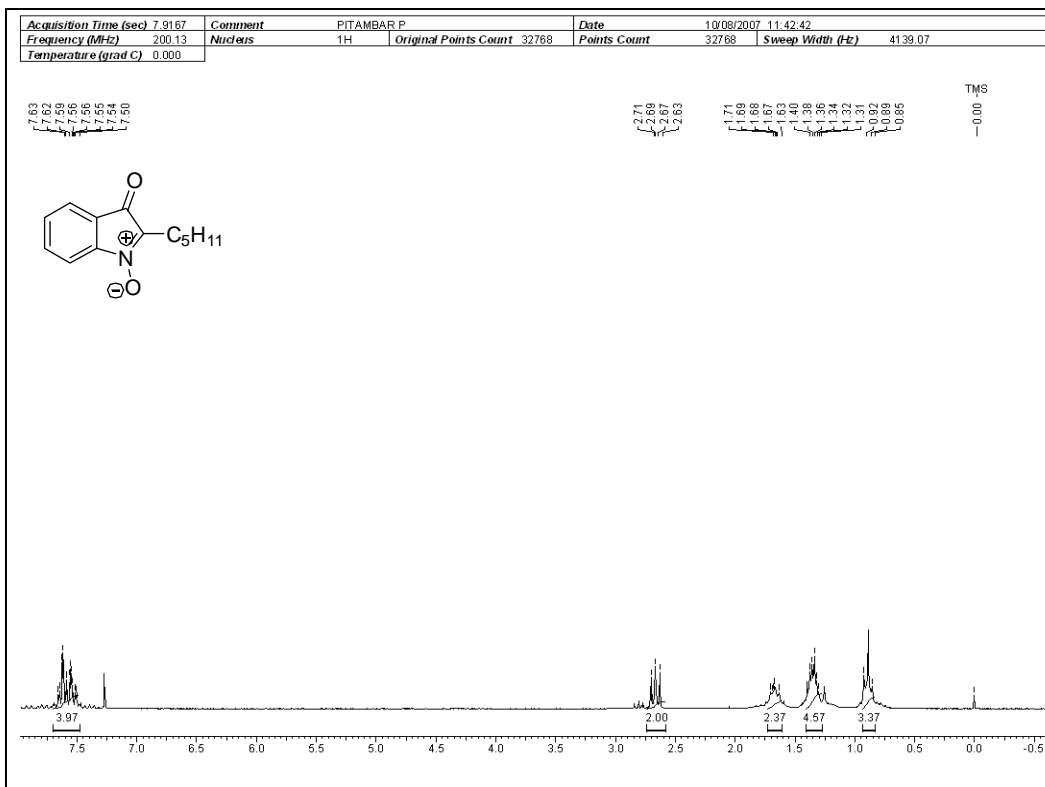
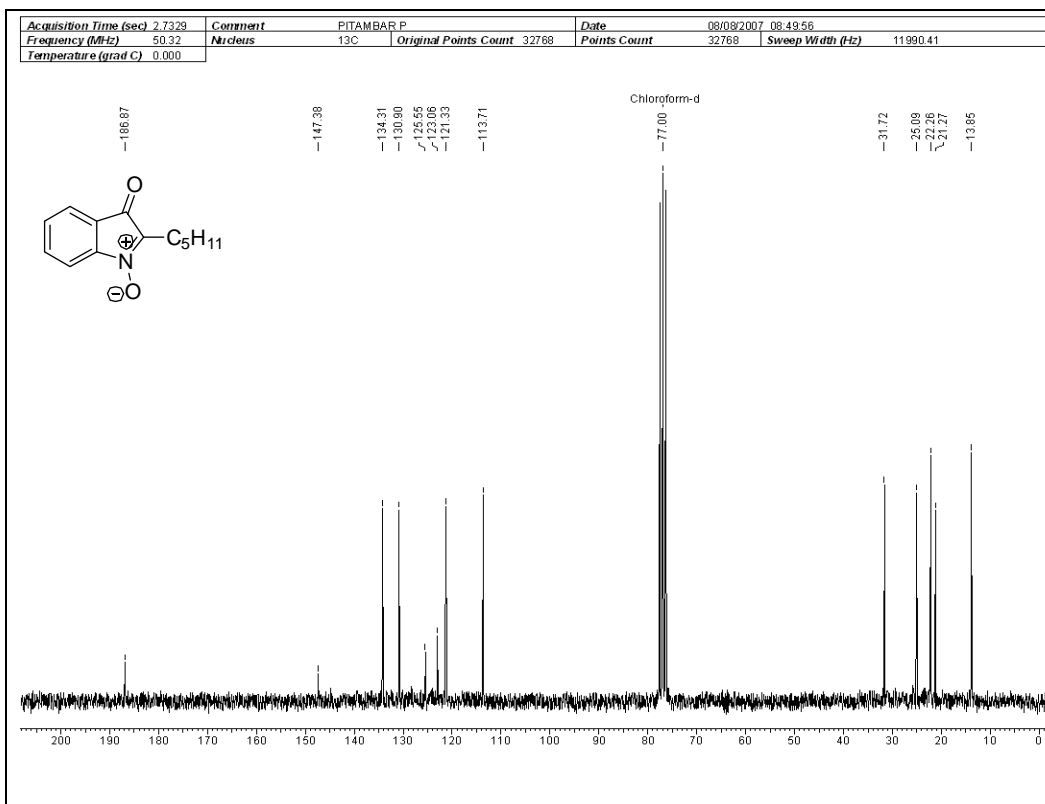
73. a) Lee, C. T.; Yang, W. T.; Parr, R. G. *Phys. Rev. B* **1988**, *37*, 785. b) Stephens, P. J.; Devlin, F. J.; Chabalowski, C. F.; Frisch, M. J. *J. Phys. Chem.* **1994**, *98*, 11623.
74. Zhao, Y.; Truhlar, D. G. *Acc. Chem. Res.* **2008**, *41*, 157.
75. Grimme, S.; Antony, J.; Ehrlich, S.; Krieg, H. *J. Chem. Phys.* **2010**, *132*, 154104.
76. Hay, P. J.; Wadt, W. R. *J. Chem. Phys.* **1985**, *82*, 299.
77. Tomasi, J.; Mennucci, B.; Cammi, R. *Chem. Rev.* **2005**, *105*, 2999.
78. a) Tannor, D. J.; Marten, B.; Murphy, R.; Friesner, R. A.; Sitkoff, D.; Nicholls, A.; Ringnalda, M.; Goddard, W. A.; Honig, B. *J. Am. Chem. Soc.* **1994**, *116*, 11875. b) Marten, B.; Kim, K.; Cortis, C.; Friesner, R. A.; Murphy, R. B.; Ringnalda, M. N.; Sitkoff, D.; Honig, B. *J. Phys. Chem. Rev.* **1996**, *100*, 11775.
79. Kozuch, S.; Shaik, S. *Acc. Chem. Res.* **2011**, *44*, 101.
80. Maskill, H. *The Physical Basis of Organic Chemistry* **1985**, Oxford University Press, Oxford.
81. a) Ahlrichs, R.; Bär, M.; Häser, M.; Horn, H.; Kölmel, C. *Chem. Phys. Lett.* **1989**, *162*, 165. b) Häser, M.; Ahlrichs, R.; Baron, H. P.; Weis, P.; Horn, H. *Theor. Chim. Acta* **1992**, *83*, 455.
82. Schäfer, A.; Huber, C.; Ahlrichs, R. *J. Chem. Phys.* **1994**, *100*, 5829.
83. a) Perdew, J. P. *Phys. Rev. B* **1986**, *33*, 8822. b) Becke, A. D. *Phys. Rev. A* **1998**, *38*, 3098.
84. a) Yukawa, T.; Tsutsumi, S. *Inorg. Chem.* **1968**, *7*, 1458. b) Mann, B. E. *J. Am. Chem. Soc.* **1975**, *97*, 1275. c) Bäckvall, J.-E.; Nilsson, Y. I. M.; Gatti, R. G. P. *Organometallics* **1995**, *14*, 4242. d) Lan, Y.; Deng, L.; Liu, J.; Wang, C.; Wiest, O.; Yang, Z.; Wu, Y. D. *J. Org. Chem.* **2009**, *74*, 5049.
85. a) Andrews, M. A.; Cheng, C.-W. F. *J. Am. Chem. Soc.* **1982**, *104*, 4268. b) Andrews, M. A.; Chang, T. C.-T.; Cheng, C.-W. F.; Kelly, K. P. *Organometallics* **1984**, *3*, 1777. c) Muzart, J. *J. Mol. Catal. A* **2007**, *276*, 62.
86. a) Landis, C. R.; Morales, C. M.; Stahl, S. S. *J. Am. Chem. Soc.* **2004**, *126*, 16302. b) Keith, J. M.; Nielsen, R. J.; Oxgaard, J.; Goddard III, W. A. *J. Am. Chem. Soc.* **2005**, *127*, 13172. c) Privalow, T.; Linde, C.; Zetterberg, K.; Moberg, C. *Organometallics* **2005**, *24*, 885. d) Popp, B. V.; Wendlandt, J. E.; Landis, C. R.; Stahl, S. S. *Angew. Chem. Int. Ed.* **2007**, *46*, 4410. e) Popp, B. V.; Stahl, S. S. *J. Am. Chem. Soc.* **2007**, *129*, 4410. f)

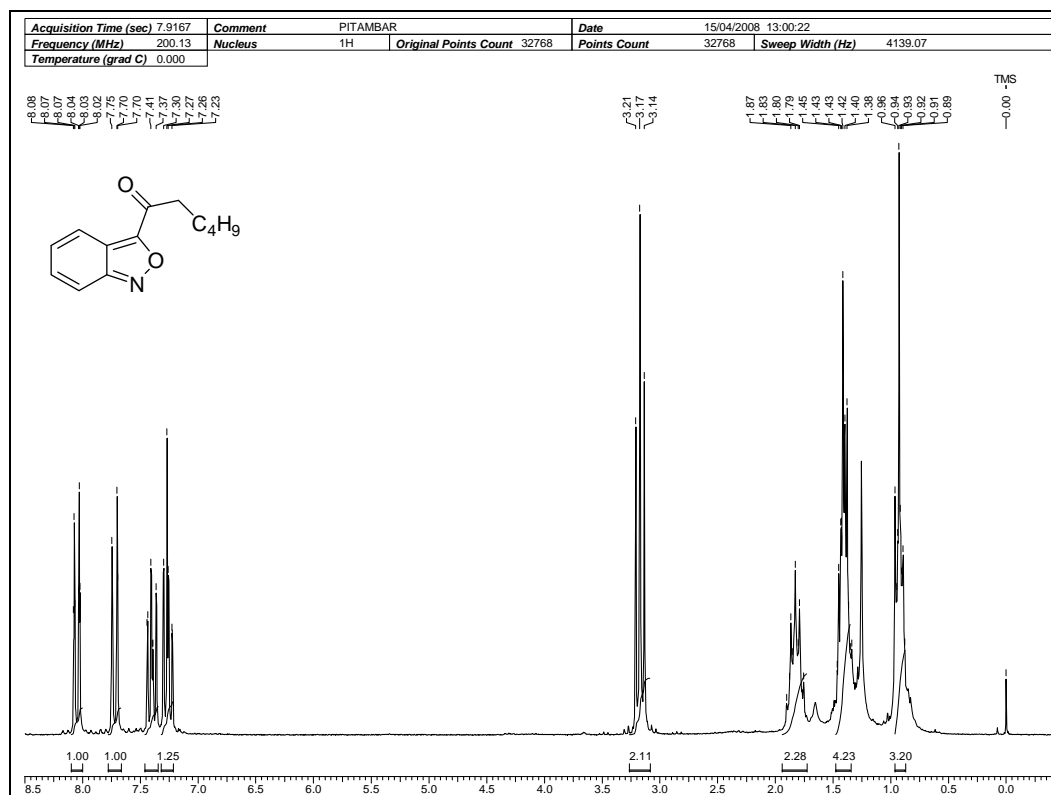
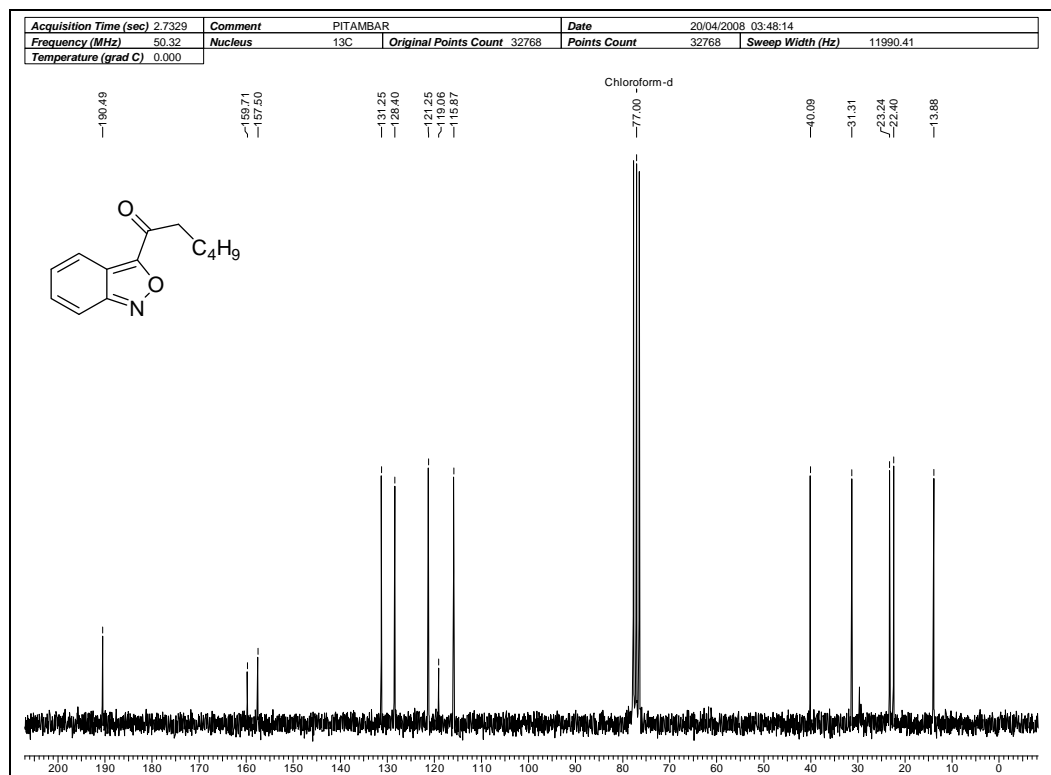
- Chowdhury, S.; Rivalta, I.; Russo, N.; Sicilia, E. *J. Chem. Theory Comput.* **2008**, *4*, 1283.
- g) Popp, B. V.; Stahl, S. S. *Chem. Eur. J.* **2009**, *15*, 2915.
87. a) Richter-Addo, G. B.; Legzdins, P. *Chem. Rev.* **1988**, *88*, 991. b) Cameron, M.; Gowenlock, B. G.; Vasapollo, G. *Chem. Soc. Rev.* **1990**, *19*, 355.
88. a) Rautenstrauch, V. *J. Org. Chem.* **1984**, *49*, 950. b) Caruana, P. A.; Frontier, A. J. *Tetrahedron* **2007**, *63*, 10646.
89. a) Alonso, F.; Yus, M.; Beletskaya, I. P. *Chem. Rev.* **2004**, *104*, 3079. b) Zeni, G.; Larock, R. C. *Chem. Rev.* **2004**, *104*, 2285. c) Hashmi, A. S. K. *Chem. Rev.* **2007**, *107*, 3180. d) Li, Z.; Brouwer, C.; He, C. *Chem. Rev.* **2008**, *108*, 3239.
90. a) Wróbel, Z.; Ma, Kosza, M. *Tetrahedron* **1997**, *53*, 5501. b) Leach, A. G.; Houk, K. N.; Davies, I. W. *Synthesis* **2005**, 3463. c) Attanasi, O. A.; Favi, G.; Filippone, P.; Giorgi, G.; Lillini, S.; Mantellini, F.; Perrulli, F. R. *Synlett* **2006**, 2731.
91. a) Hiroya, K.; Itoh, S.; Ozawa, M.; Kanamori, Y.; Sakamoto, T. *Tetrahedron Lett.* **2002**, *43*, 1277. b) Hiroya, K.; Itoh, S.; Sakamoto, T. *J. Org. Chem.* **2004**, *69*, 1126.
92. a) Patterson, D. A.; Wibberley, D. G. *J. Chem. Soc.* **1965**, 1706. b) Fakhretdinov, R. N.; G., T. A.; Dzhemilev, U. M. *Bull. Acad. Sci. USSR, Div. Chem. Sci.* **1986**, *35*, 2059. c) Bokach, N. A.; Krokhin, A. A.; Nazarov, A. A.; Kukushkin, V. Y.; Haukka, M.; Fraflsto da Silva, J. J. R.; Pombeiro, A. J. L. *Eur. J. Inorg. Chem.* **2005**, 3042. d) Luzyanin, K. V.; Tskhovrebov, A. G.; da Silva, M.; Haukka, M.; Pombeiro, A. J. L.; Kukushkin, V. Y. *Chem. Eur. J.* **2009**, *15*, 5969.
93. a) Clawson, R. W.; Deavers III, J., R. E. ; Akhmedov, N. G.; Söderberg, B. C. G. *Tetrahedron* **2006**, *62*, 10829.
94. a) Yeom, H.-S.; Lee, J.-E.; Shin, S. *Angew. Chem. Int. Ed.* **2008**, *47*, 7040. b) Yeom, H.-S.; Lee, Y.; Lee, J.-E.; Shin, S. *Org. Biomol. Chem.* **2009**, *7*, 4744. c) Shapiro, N. D.; Toste, F. D. *J. Am. Chem. Soc.* **2007**, *129*, 4160. d) Li, G.; Zhang, L. *Angew. Chem. Int. Ed.* **2007**, *46*, 5156. e) Davies, P. W.; Albrecht, S. J.-C. *Angew. Chem. Int. Ed.* **2009**, *48*, 8372.
95. During the revision of this manuscript, gold mediated cycloisomerization of 2-(ynol)aryl carbonyl compounds was reported: Liu, L.-P.; Hammond, G. B. *Org. Lett.* **2010**, *12*, 4640.

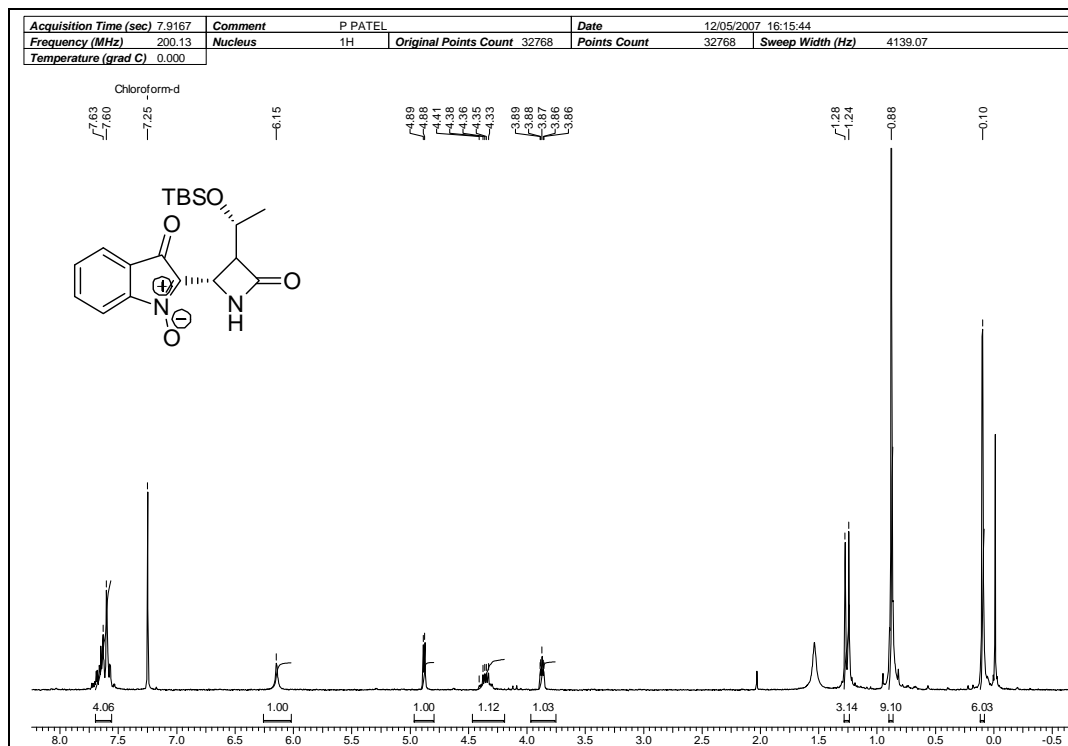
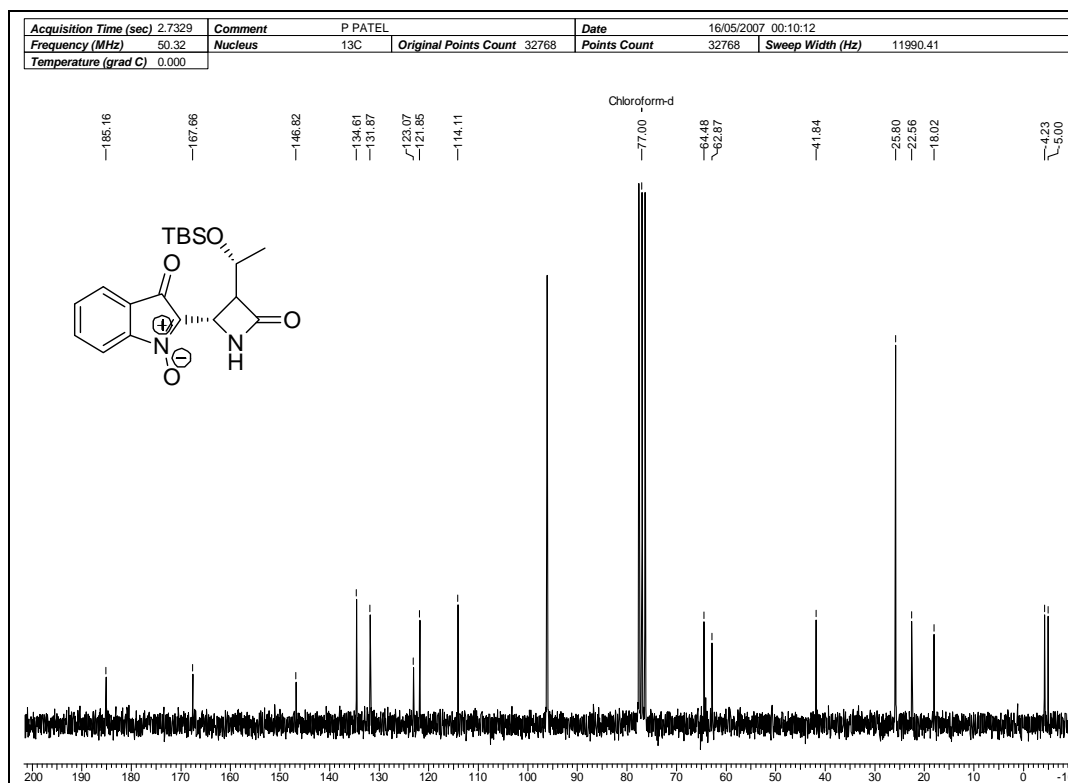
96. a) Hutchison, A. J.; Kishi, Y. *Tetrahedron Lett.* **1978**, *100*, 539. b) Hutchison, A. J.; Kishi, Y. *J. Am. Chem. Soc.* **1979**, *101*, 6786.
97. Liu, Y.; McWhorter, W. W., Jr. *J. Am. Chem. Soc.* **2003**, *125*, 4240.
98. Barker, A. J.; Paterson, T. McC.; Smalley, R. K.; Suschitzky, H. *J. Chem. Soc. Perkin I* **1986**, 1107.
99. Elhalem, E.; Comin, M. J.; Leitofuter, J.; Garca-Liñares, G.; Rodriguez, J. B. *Tetrahedron: Asymmetry* **2005**, *16* 425.
100. a) Gigg, R.; Warren, C. D. J. *Chem. Soc. C.* **1968**, 1903. b) Rosenberg, H. J.; Riñey, A. M.; Correa, V.; Taylor, C. W.; Potter, B. V. L. *Carbohydr. Res.* **2000**, *329*, 7.
101. a) Ho, P. T. *Can. J. Chem.* **1979**, *57*, 381. b) Wxzak, I.; Whistler, R. L. *Carbohydr. Res.* **1984**, *133*, 235.
102. a) Horton, D.; Hughes, J. B.; Tronchet, J. M. J. *Chem. Comm.* **1965**, 481. b) Grant Buchanan, J.; Edgar, A. R.; J., P. M. *J. Chem. Soc., Perkin Trans I* **1974**, 1943. c) Dolle, R. E.; Nicolaou, K. C. *J. Chem. Soc., Chem. Commun.* **1985**, 1016.
103. Lewis, M. D.; Cha, J. K.; Kishi, Y. *J. Am. Chem. Soc.* **1982**, *104*, 4911.
104. a) Calzada, E.; Clarke, C. A.; Roussin-Bouchard, C.; Wightman, R. H. *J. Chem. Soc. Perkin Trans. I* **1995**, 517. b) Aslam, T.; Fuchs, M. G. G.; Formal, A. L.; Wightman, R. H. *Tetrahedron Lett.* **2005** *46*, 3249.
105. Ramana, C. V.; Patel, P.; Vanka, K.; Miao, B.; Degterev, A. *Eur. J. Org. Chem.* **2010**, 5955.
106. Gurjar, M. K.; Nagaprasad, R.; Ramana, C. V. *Tetrahedron Letters* **2003**, *44*, 2873.

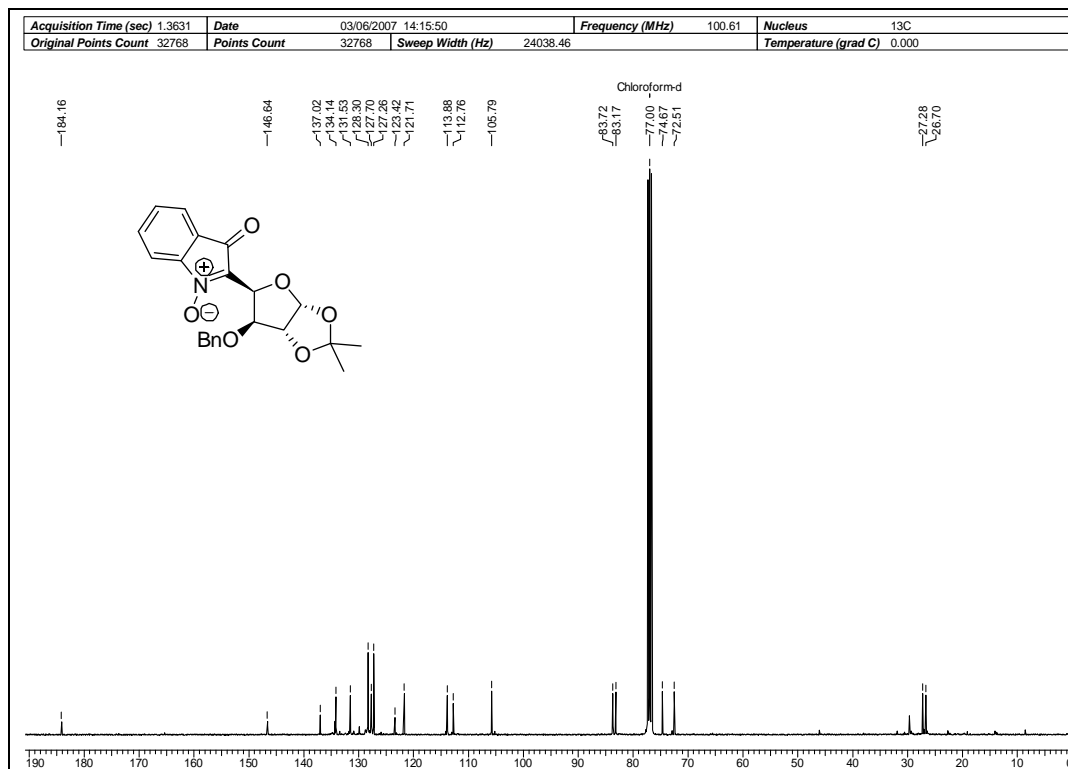
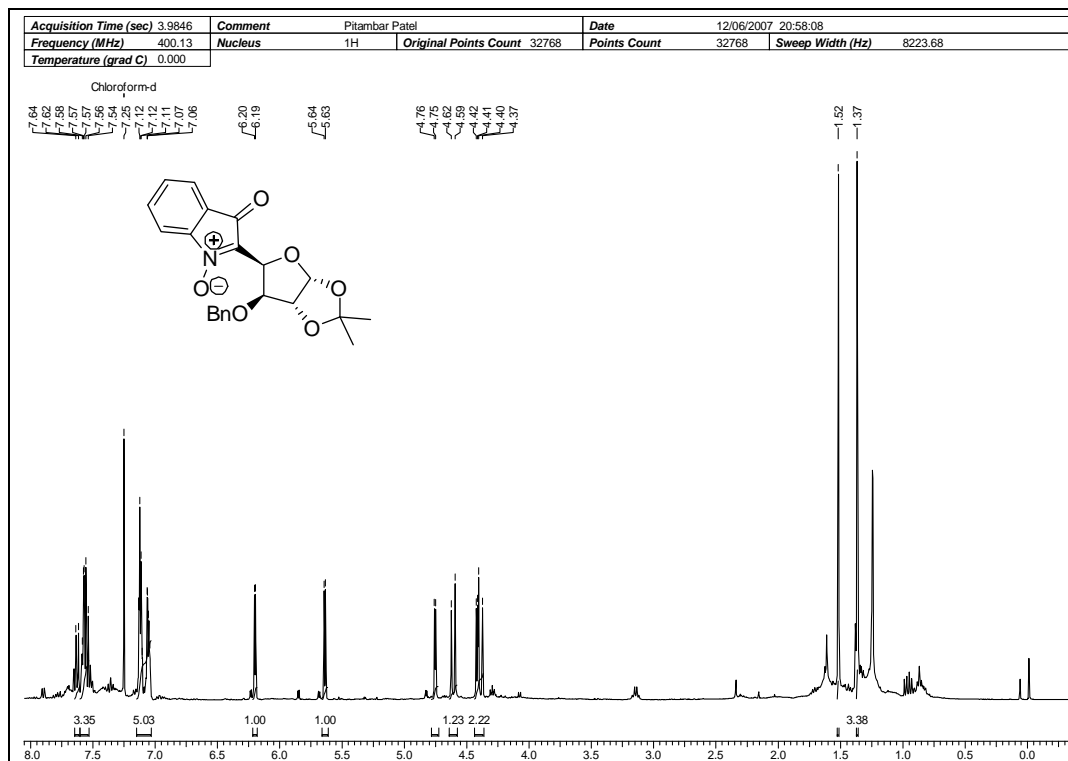
SPECTRA

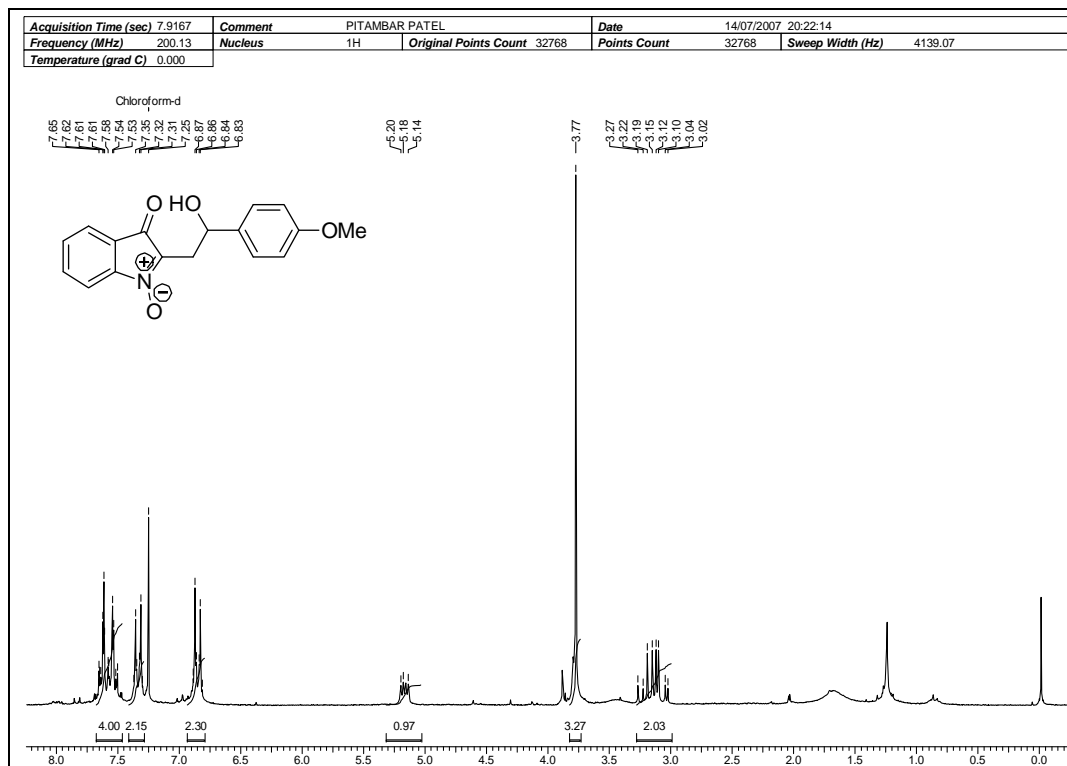
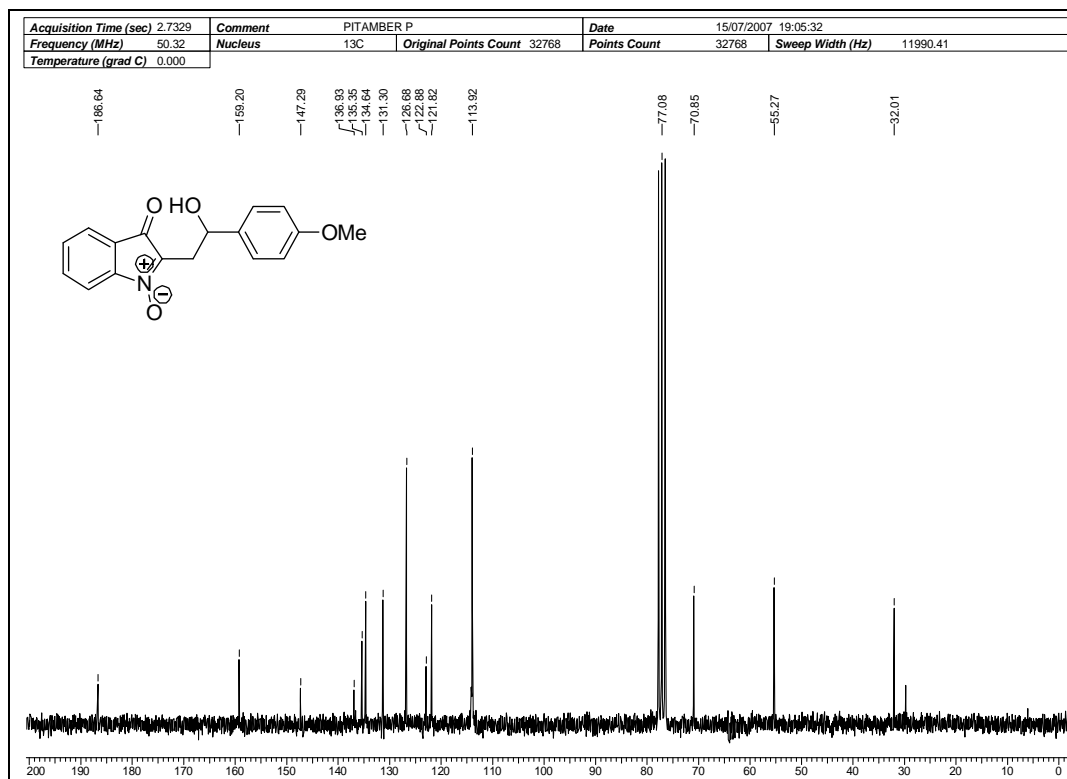


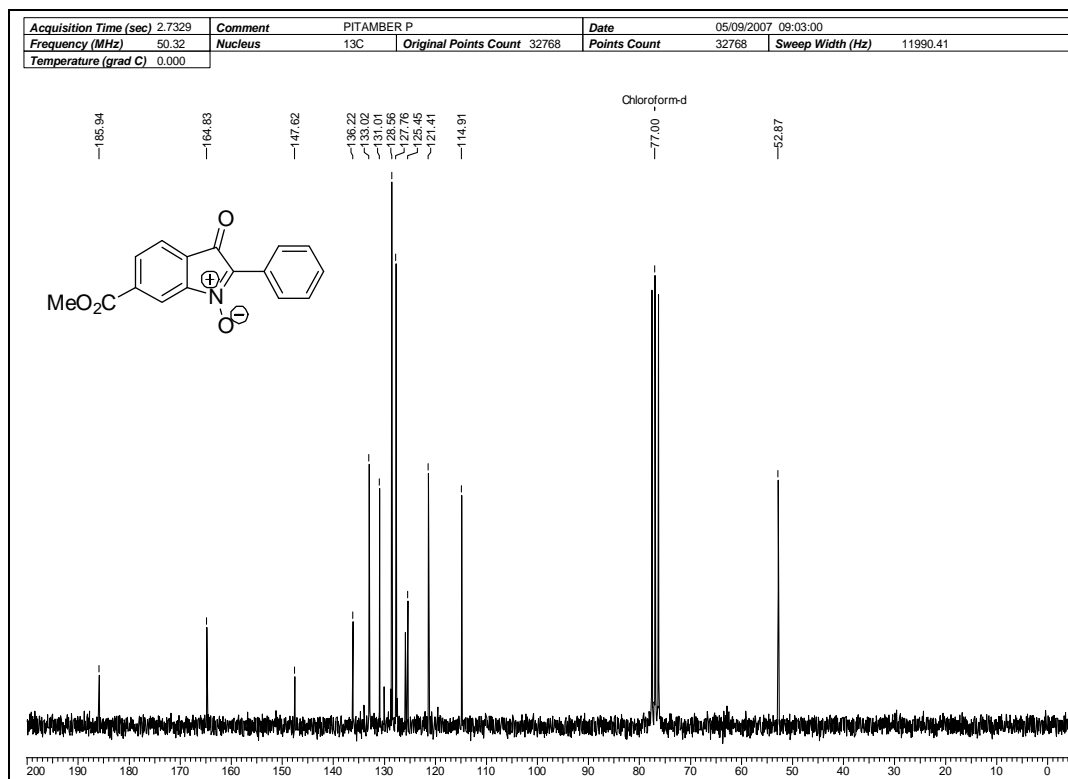
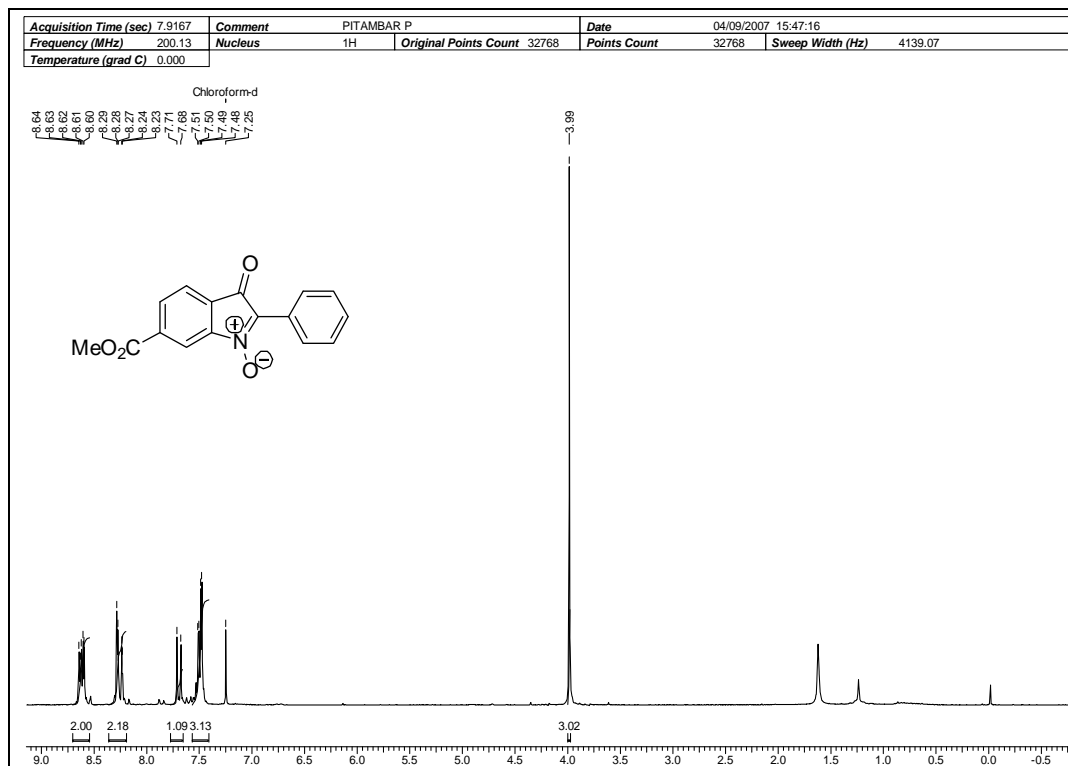
¹H NMR Spectrum of 4 in CDCl₃¹³C NMR Spectrum of 4 in CDCl₃

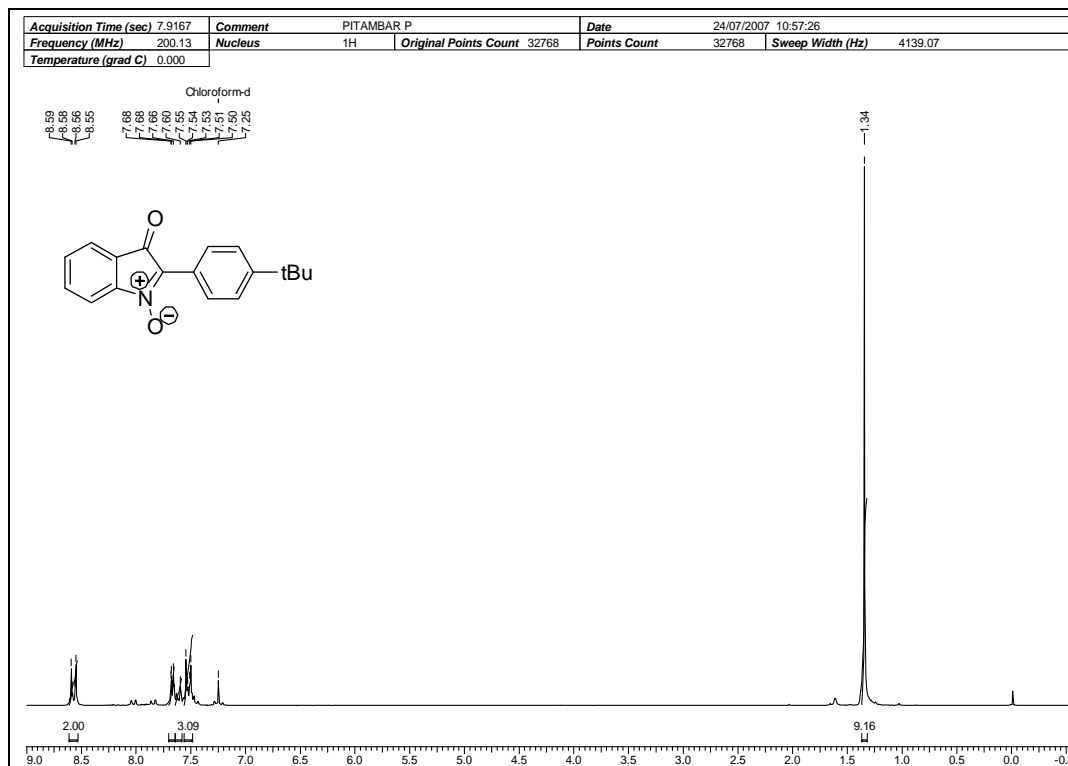
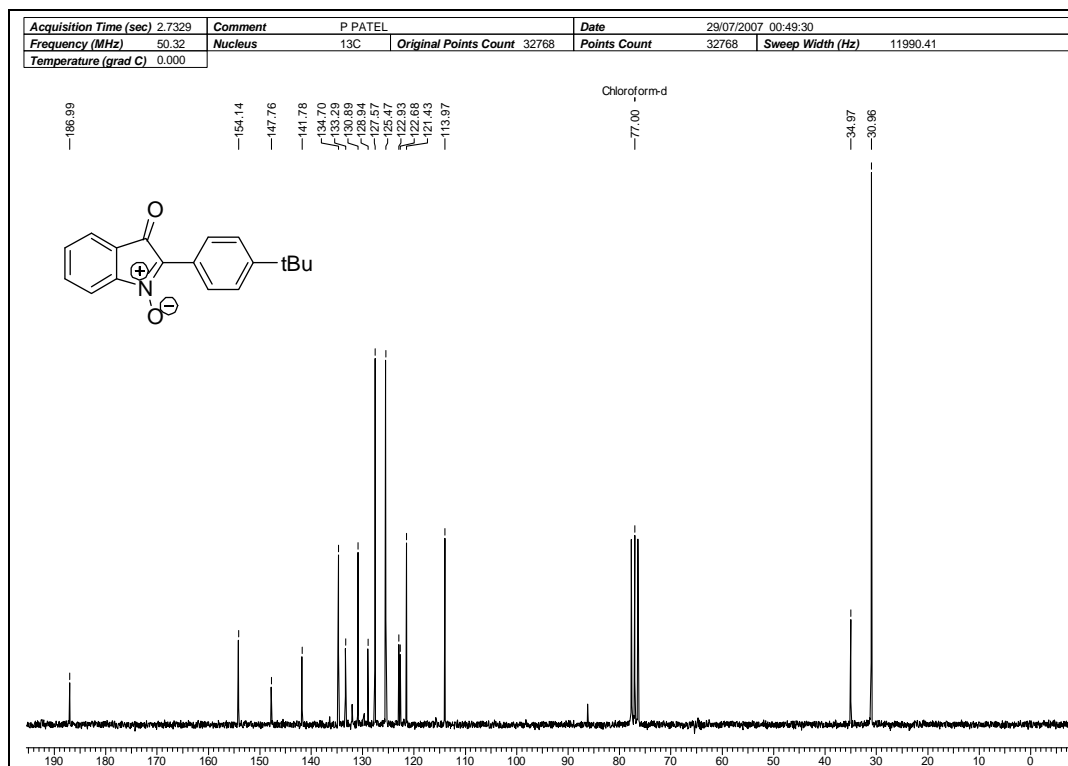
¹H NMR Spectrum of 5 in CDCl₃¹³C NMR Spectrum of 5 in CDCl₃

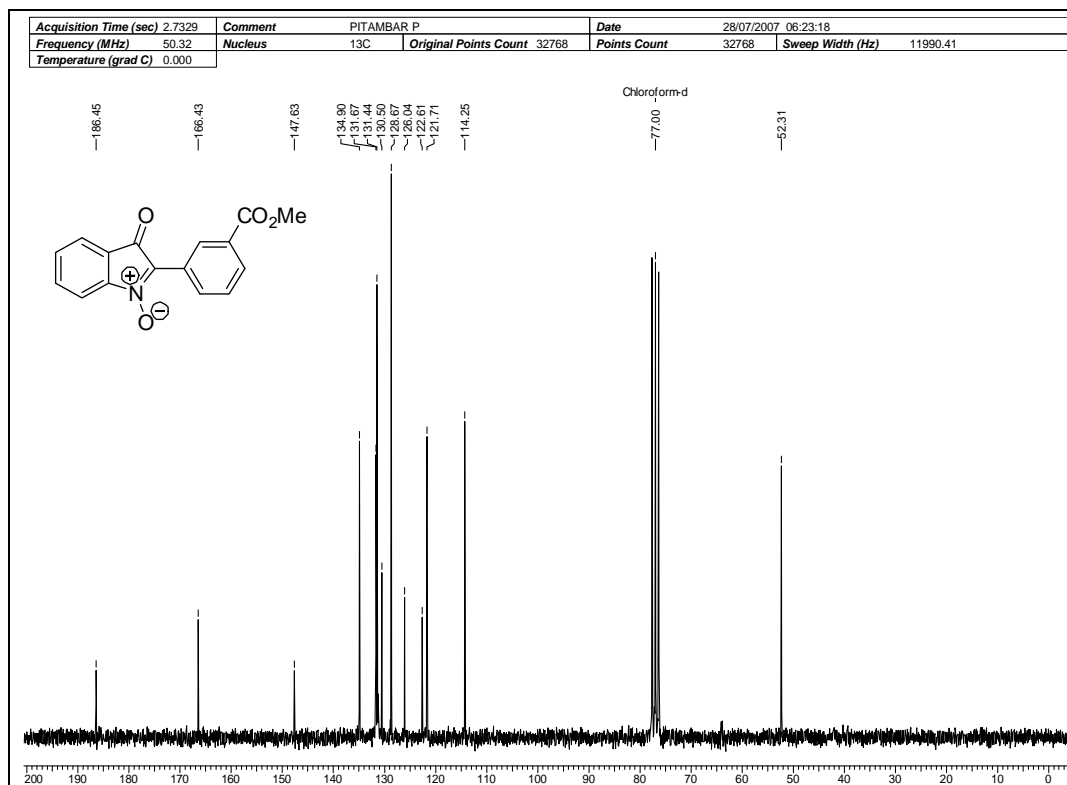
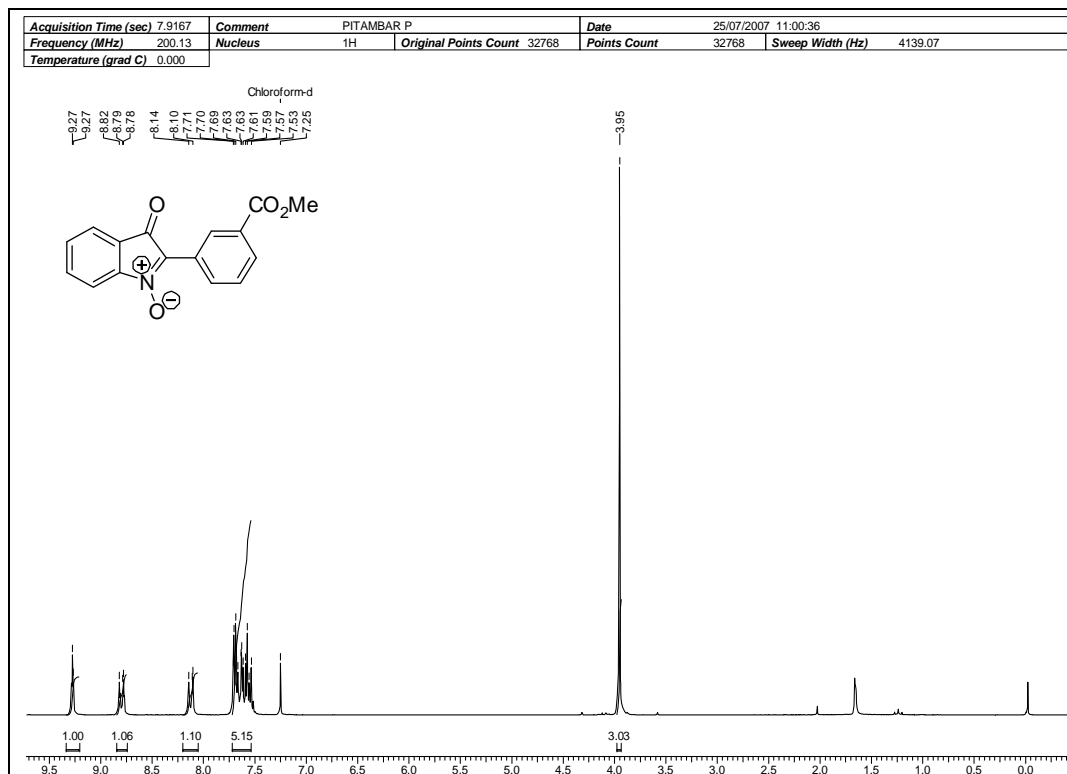
¹H NMR Spectrum of 19 in CDCl₃¹³C NMR Spectrum of 19 in CDCl₃

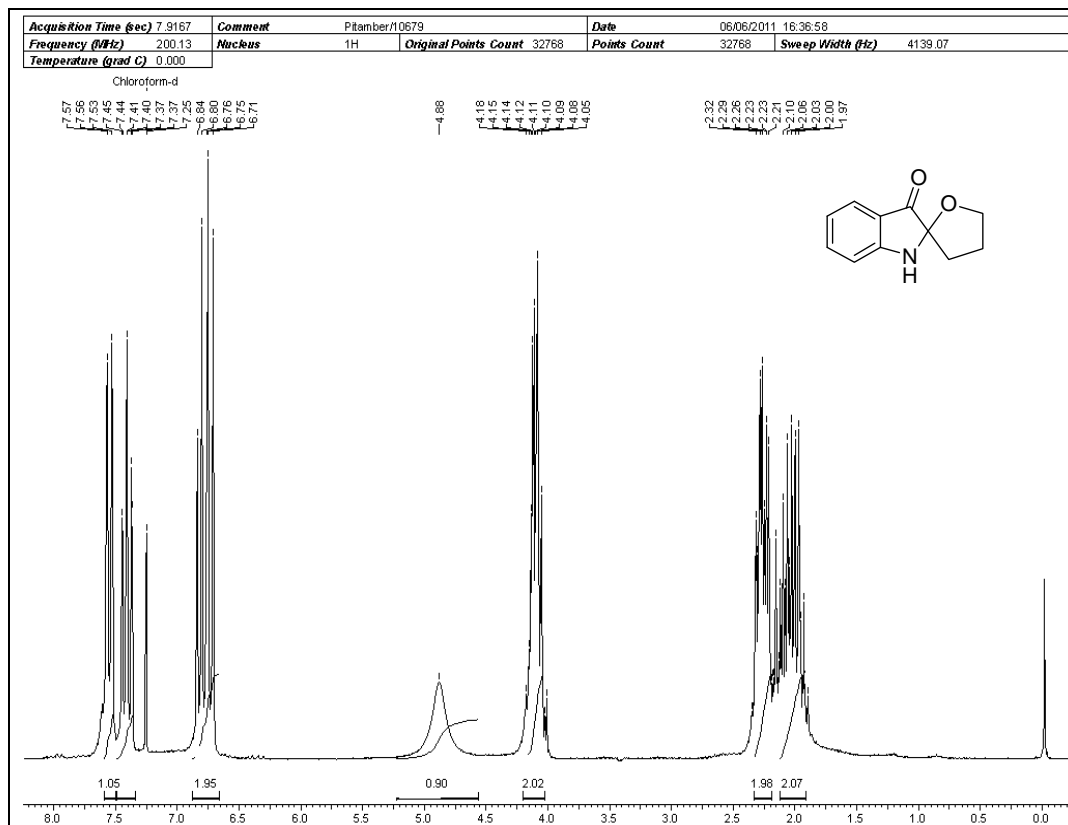
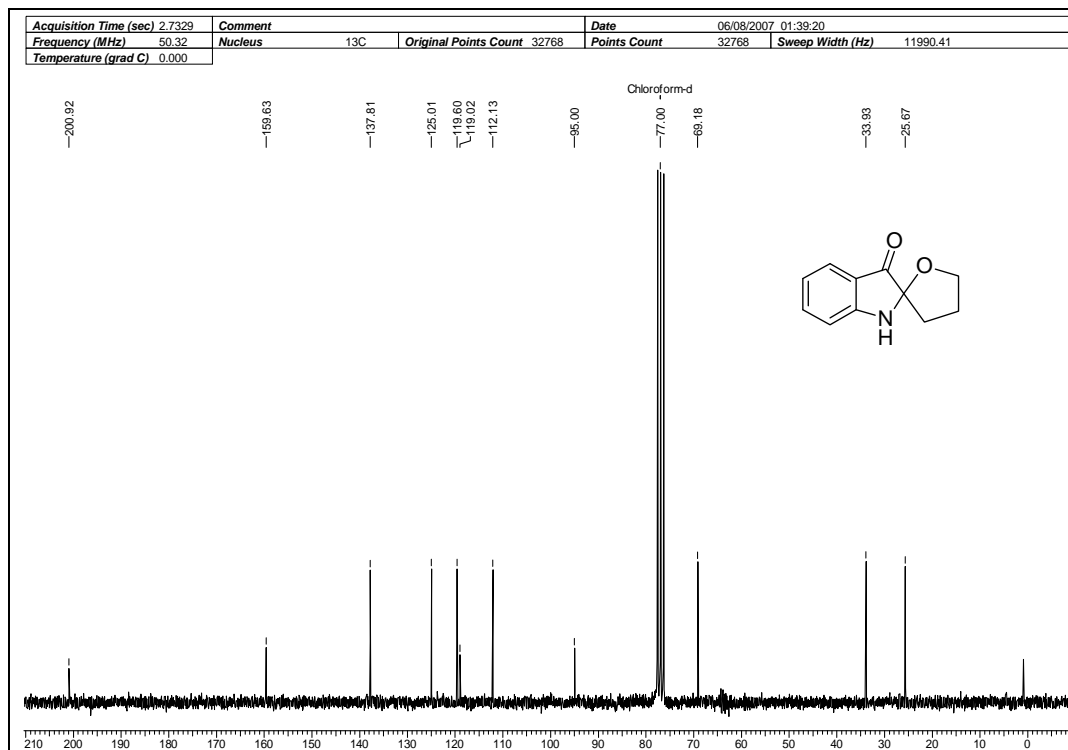


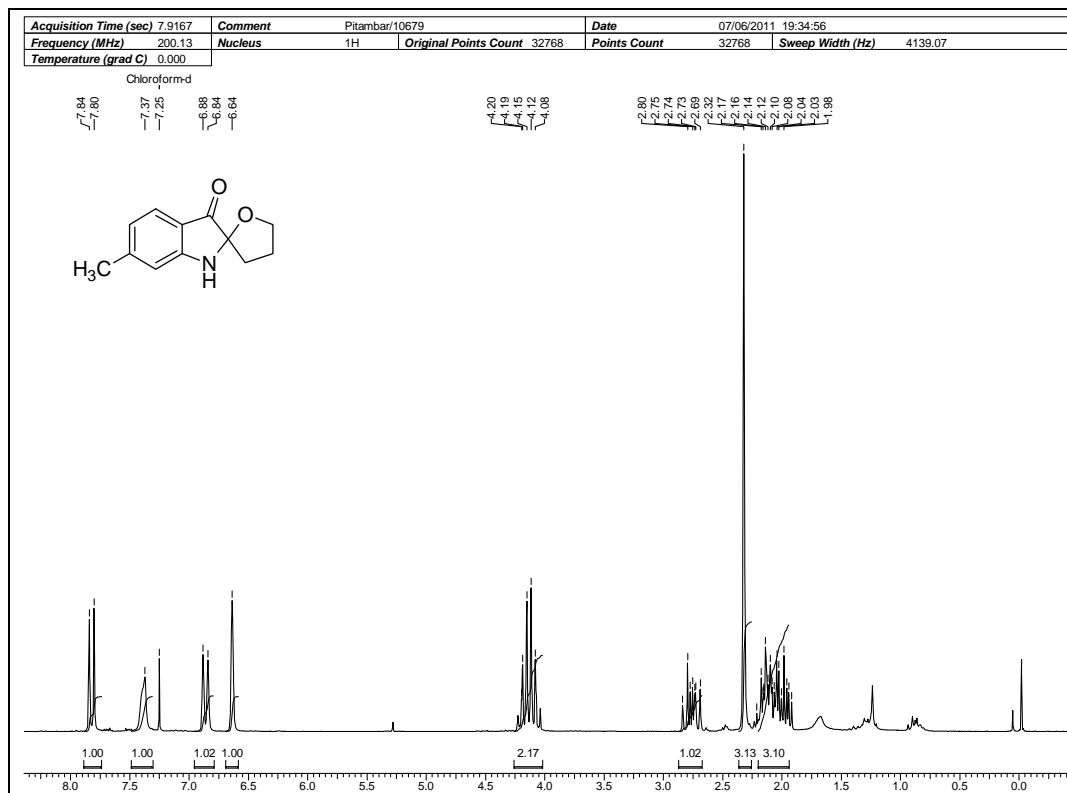
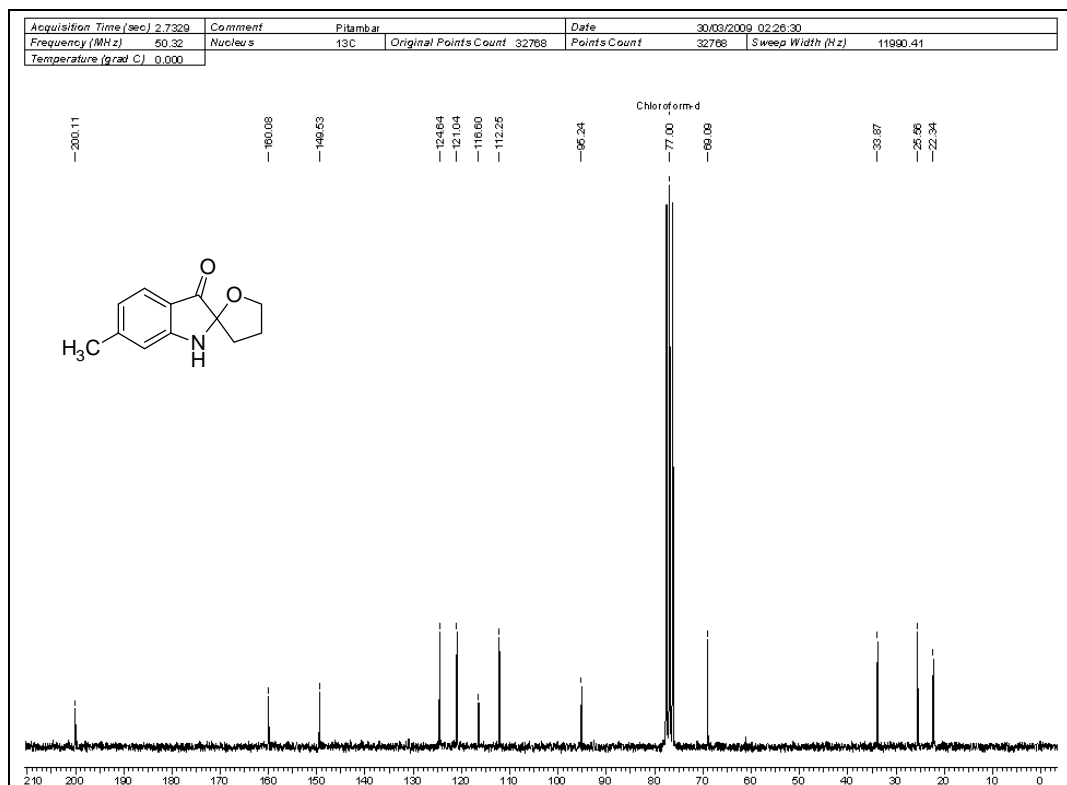
**¹H NMR Spectrum of 25 in CDCl₃****¹³C NMR Spectrum of 25 in CDCl₃**

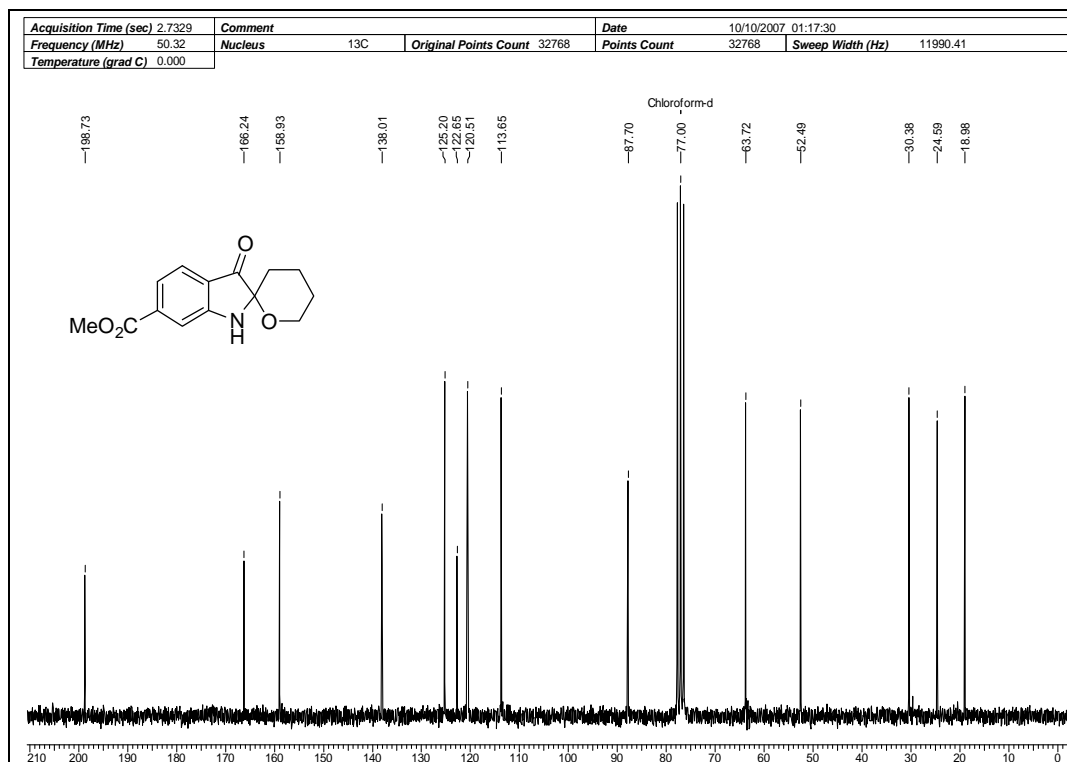
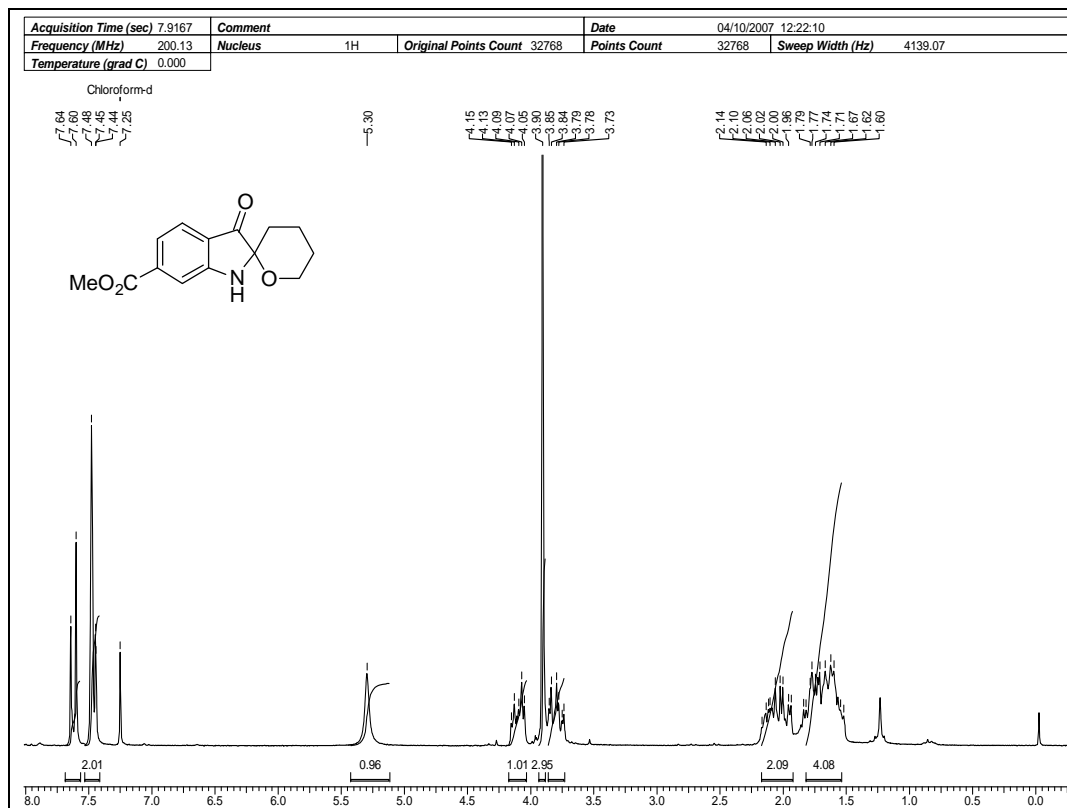


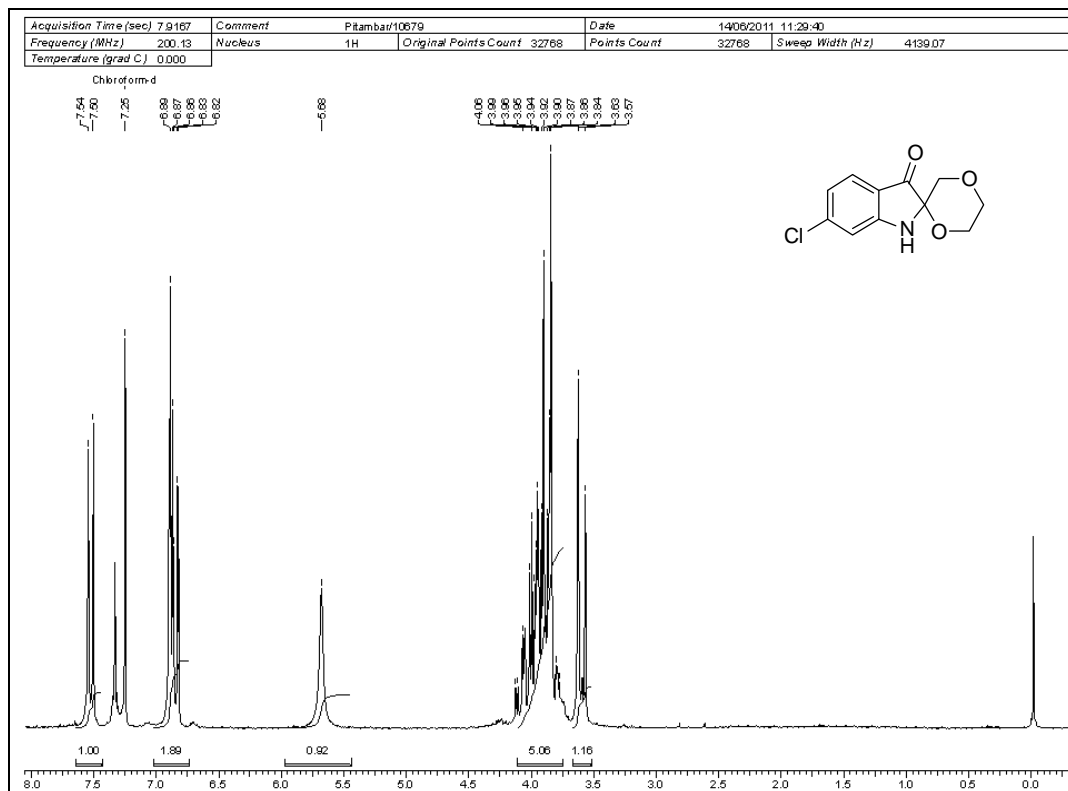
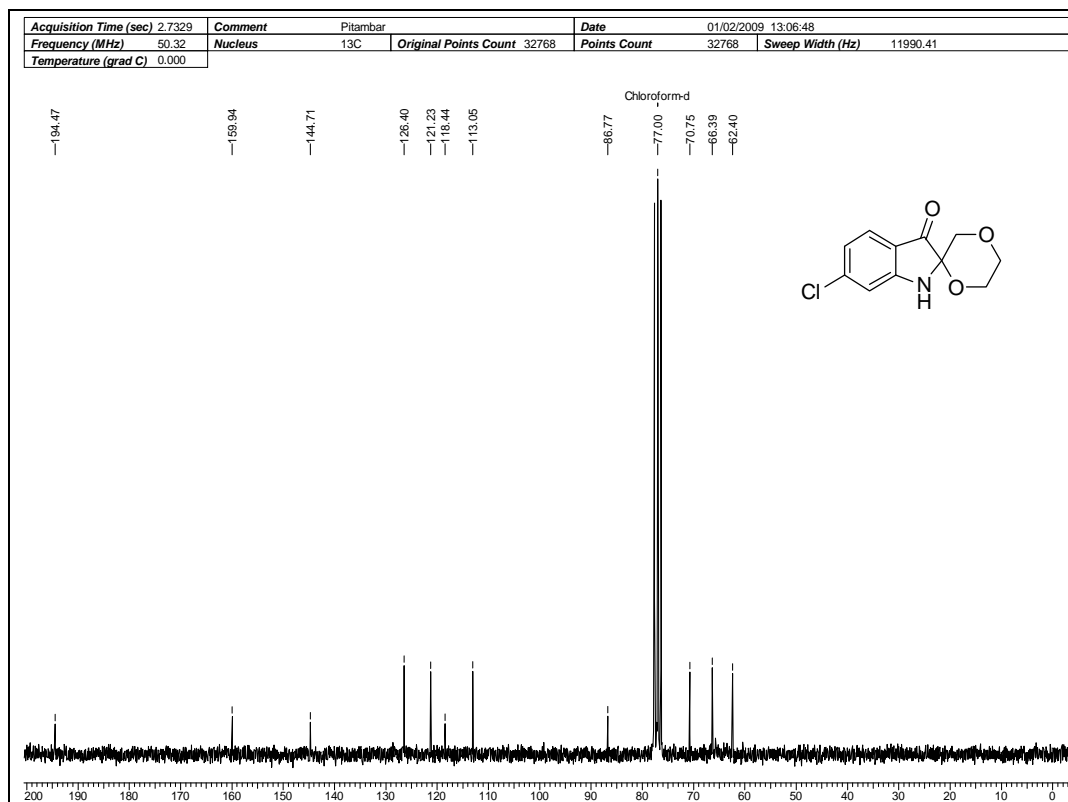
**¹H NMR Spectrum of 41 in CDCl₃****¹³C NMR Spectrum of 41 in CDCl₃**

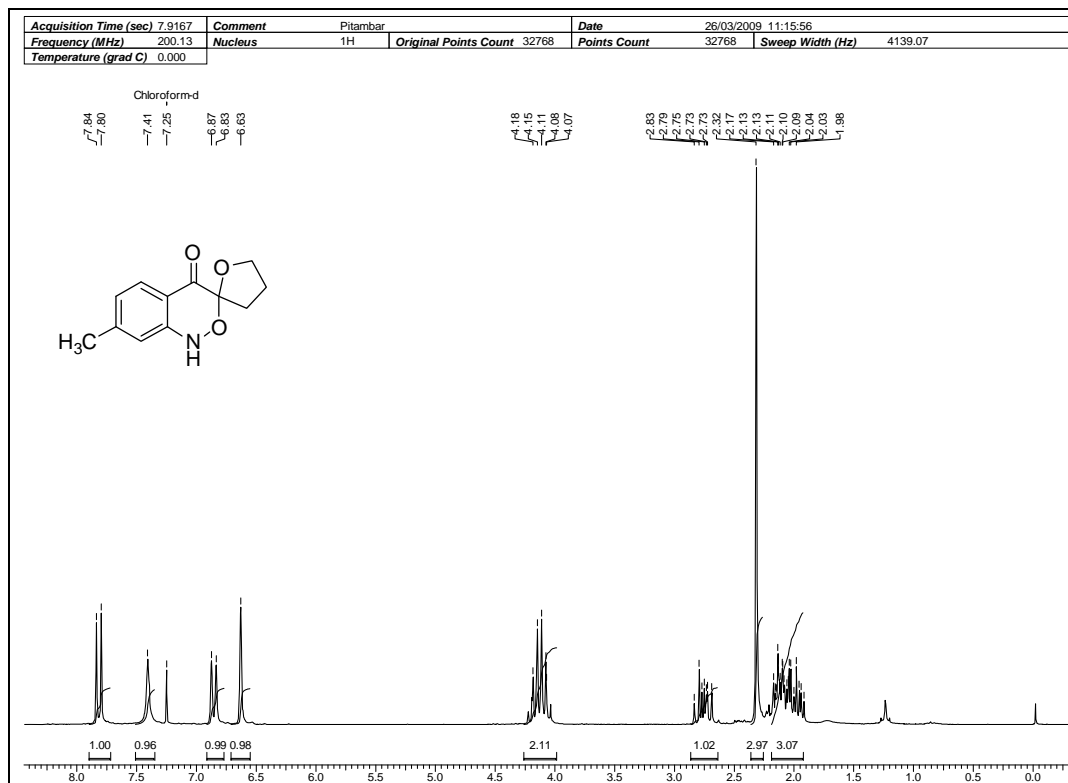
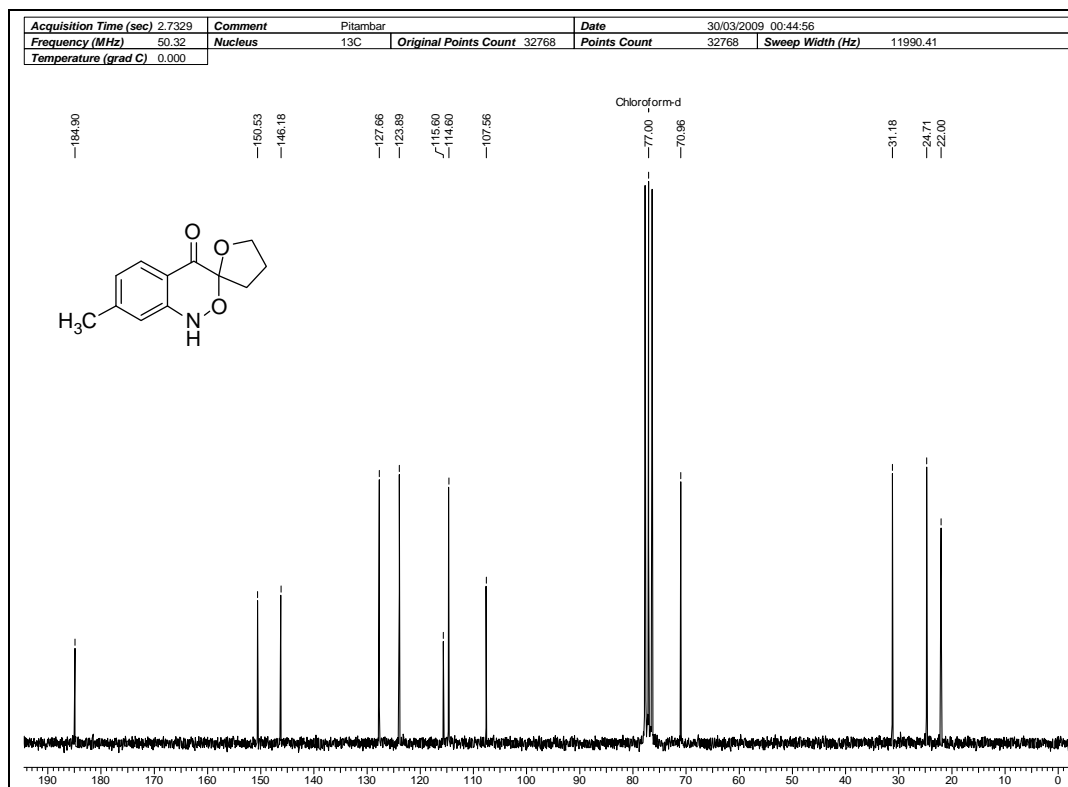


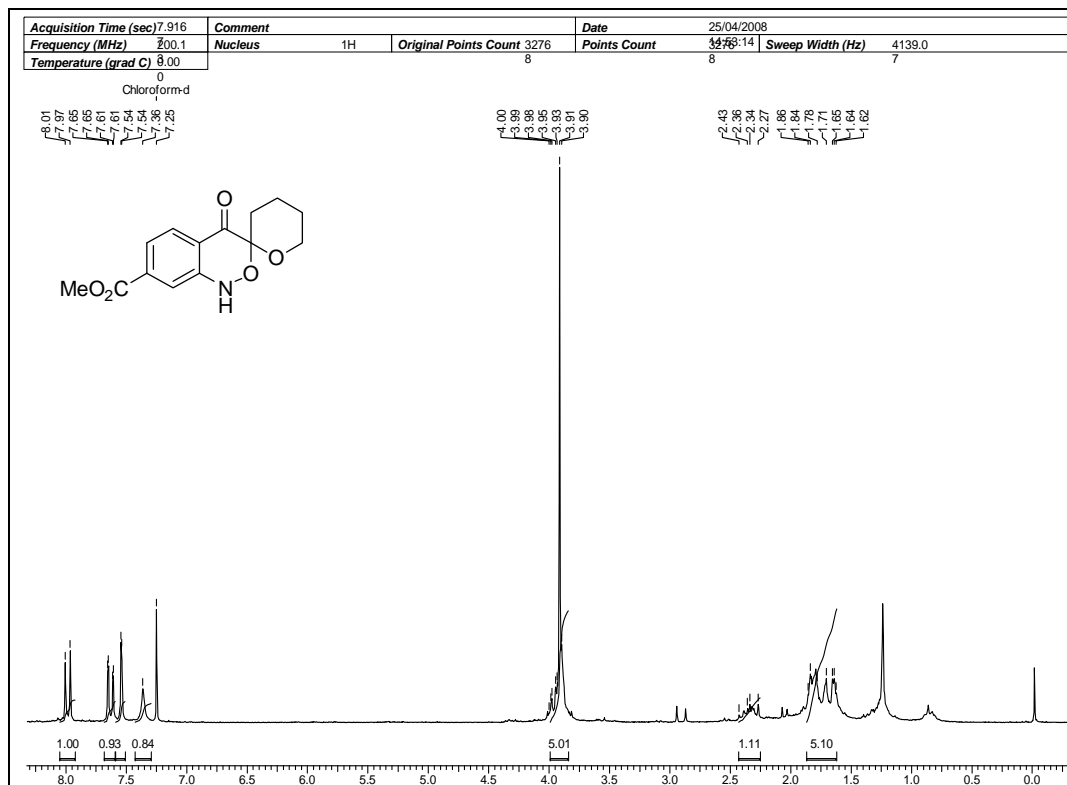
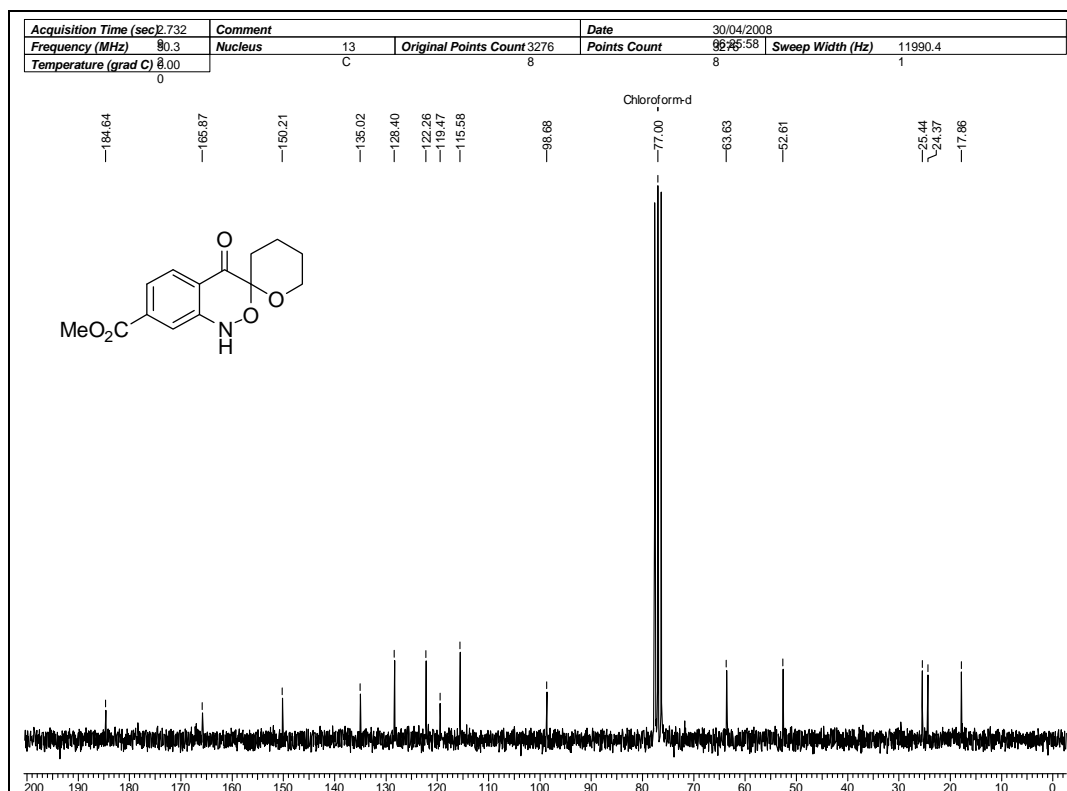
¹H NMR Spectrum of 48 in CDCl₃¹³C NMR Spectrum of 48 in CDCl₃

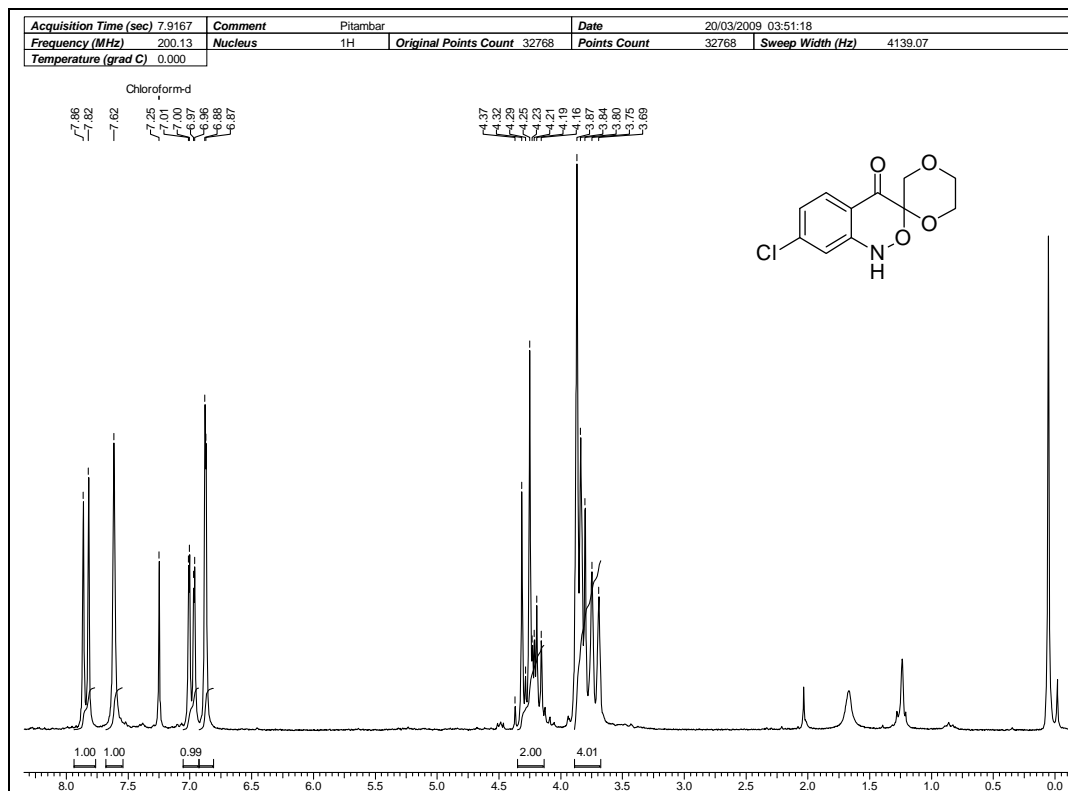
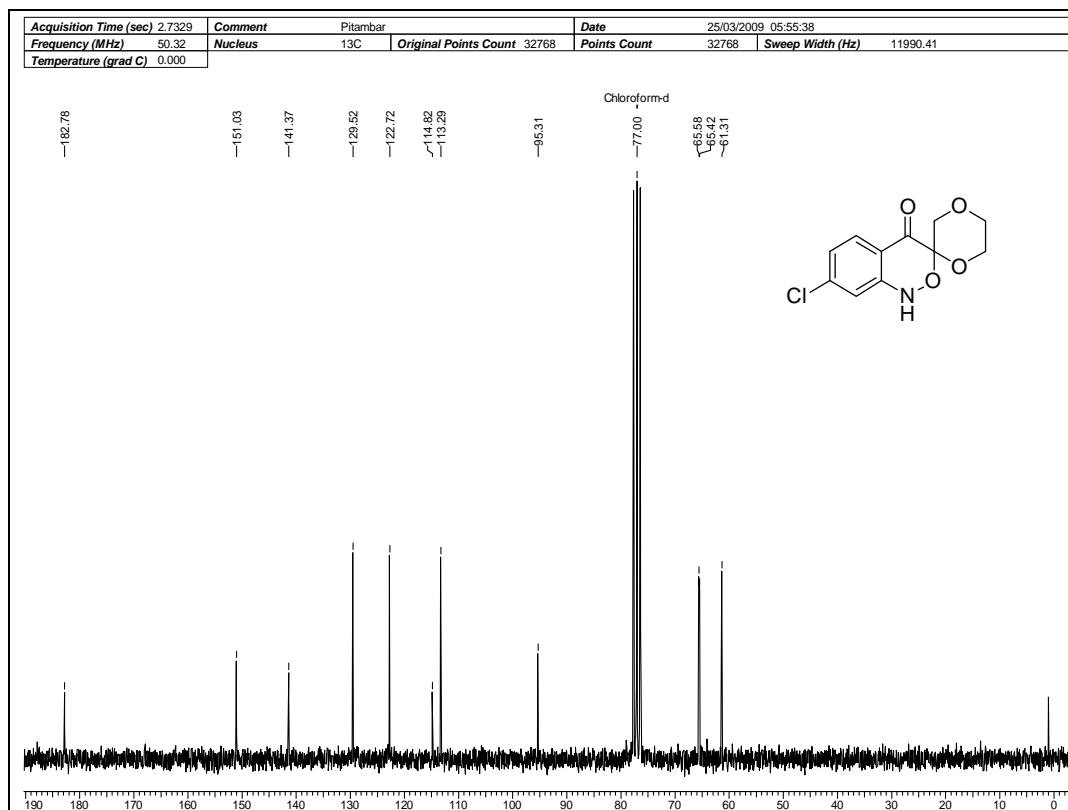
**¹H NMR Spectrum of 62 in CDCl₃****¹³C NMR Spectrum of 62 in CDCl₃**

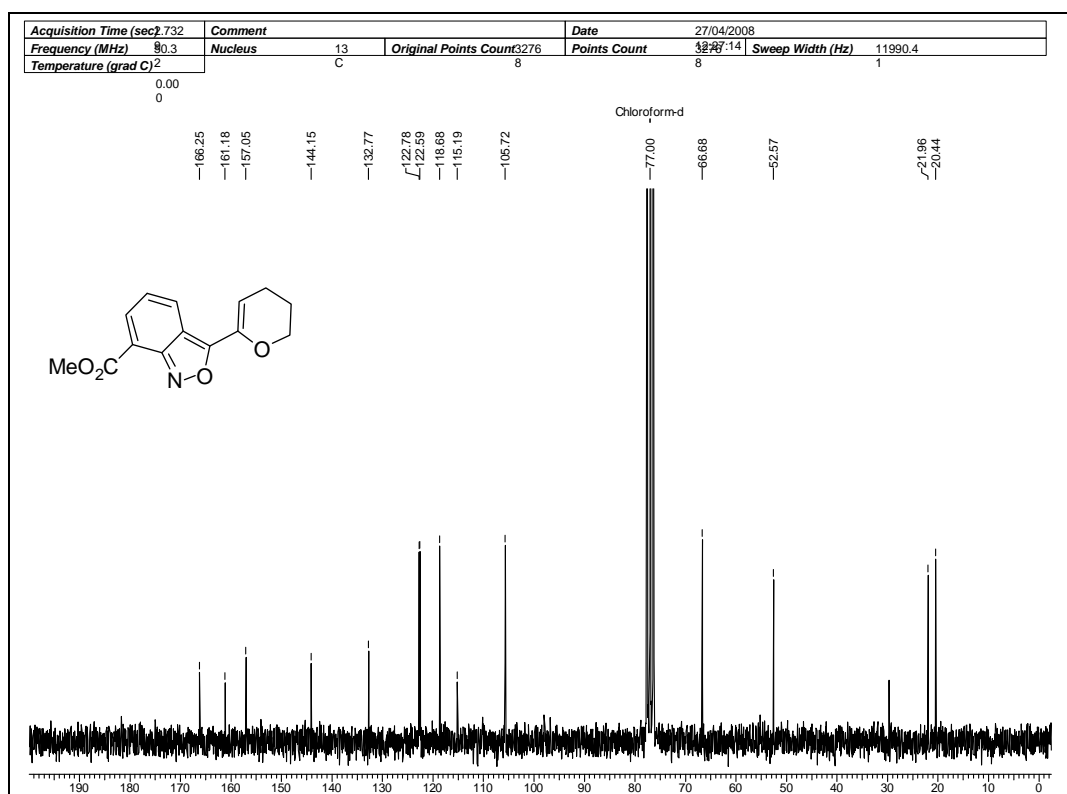
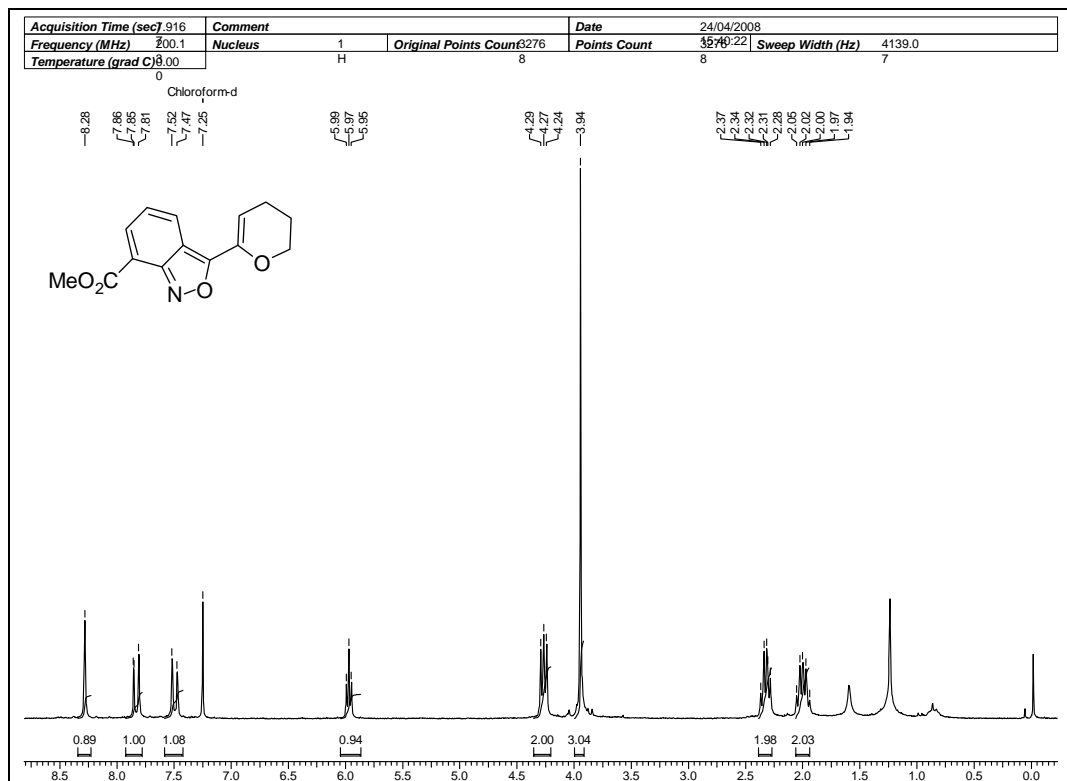


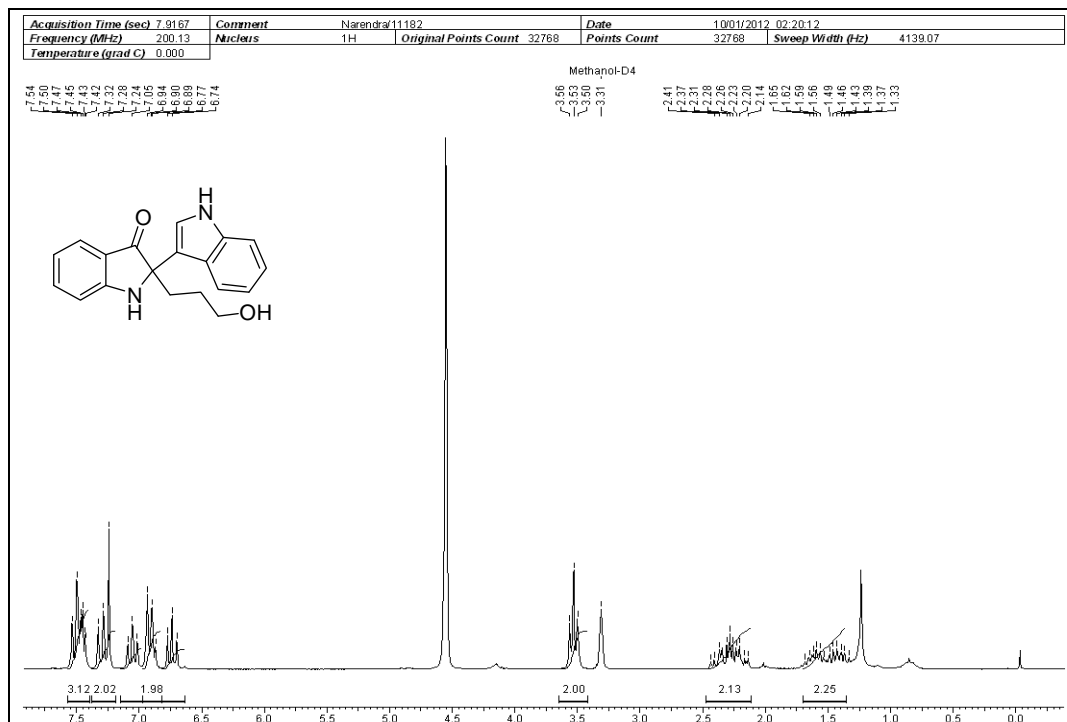
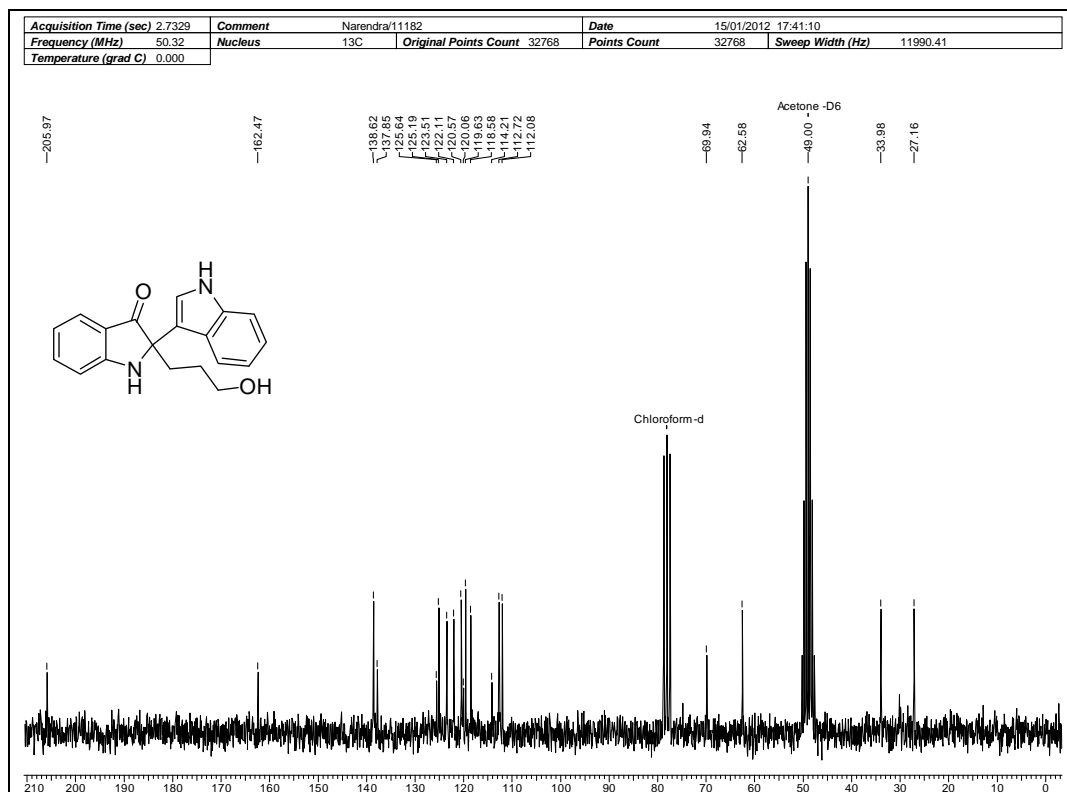
**¹H NMR Spectrum of 74 in CDCl₃****¹³C NMR Spectrum of 74 in CDCl₃**

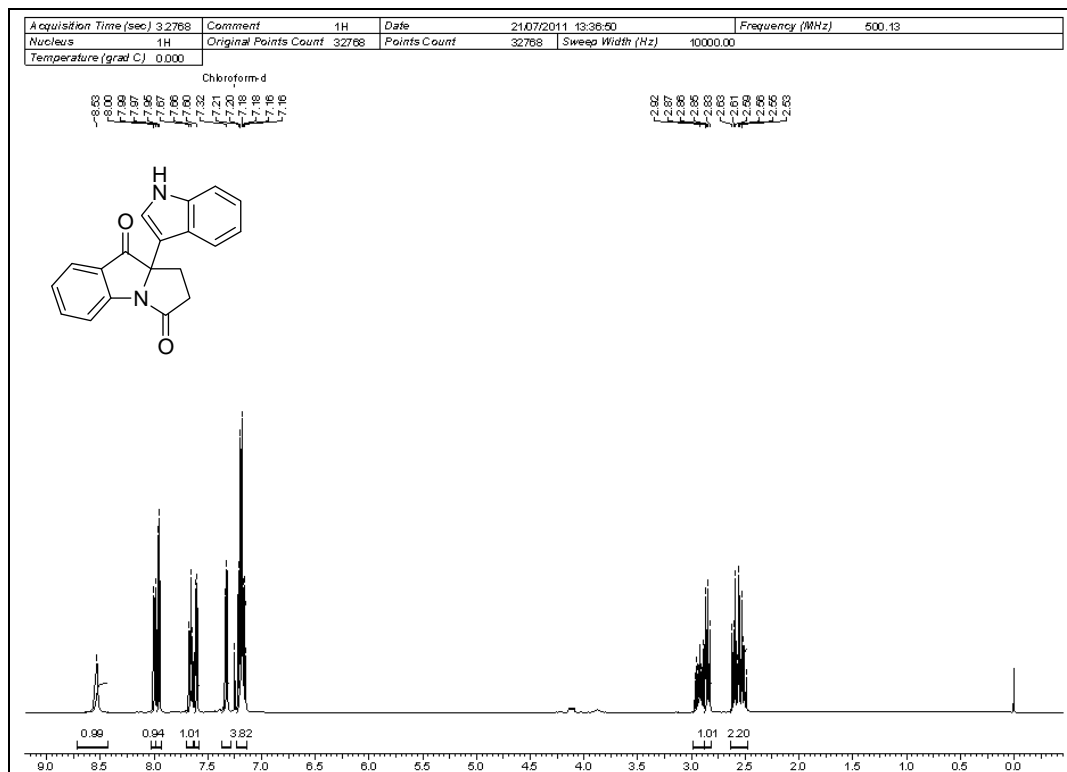
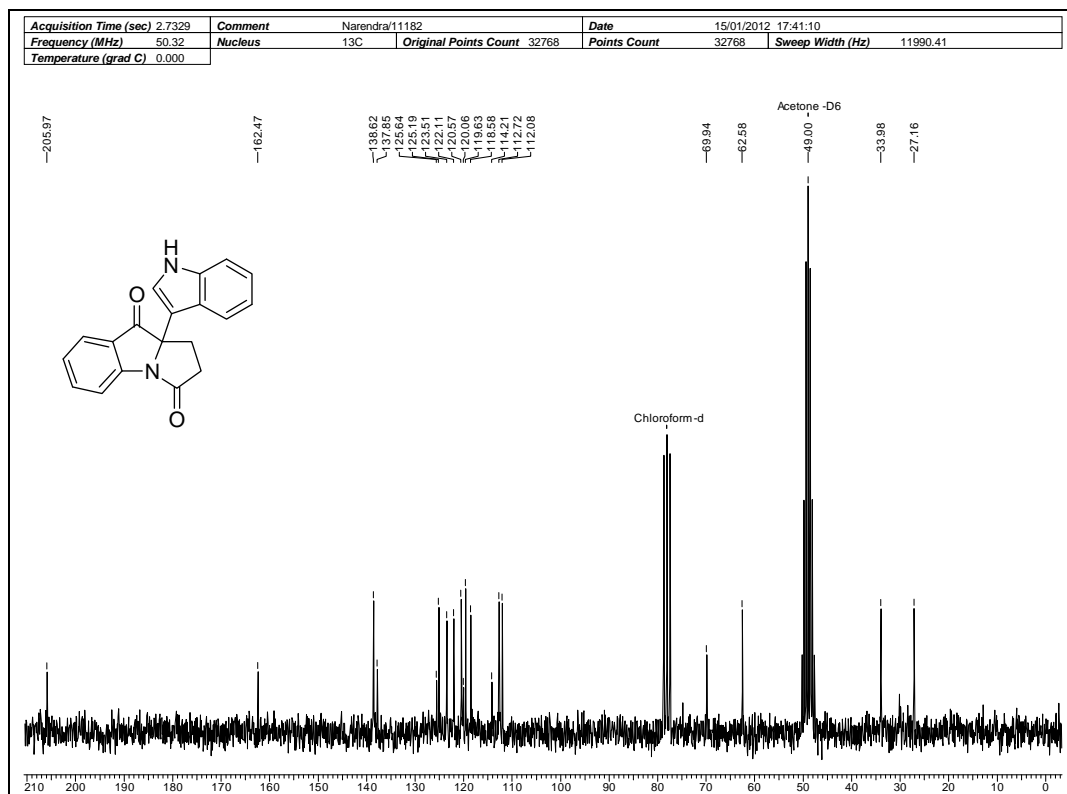
¹H NMR Spectrum of 63 in CDCl₃¹³C NMR Spectrum of 63 in CDCl₃

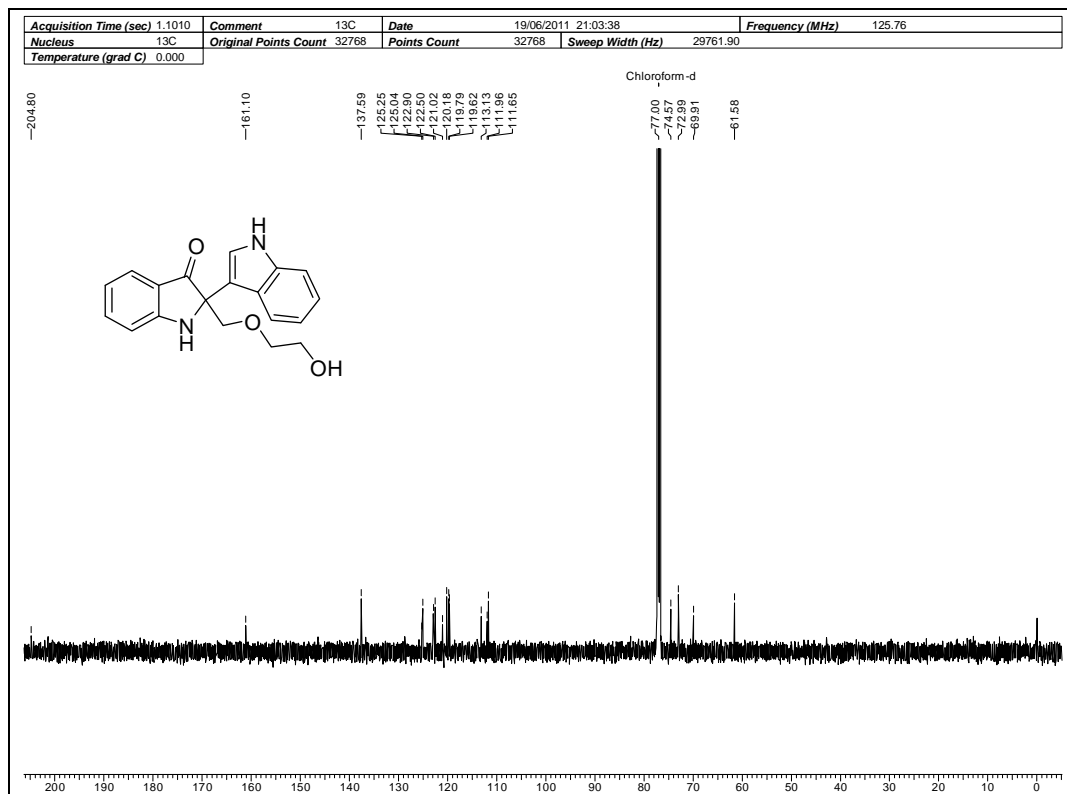
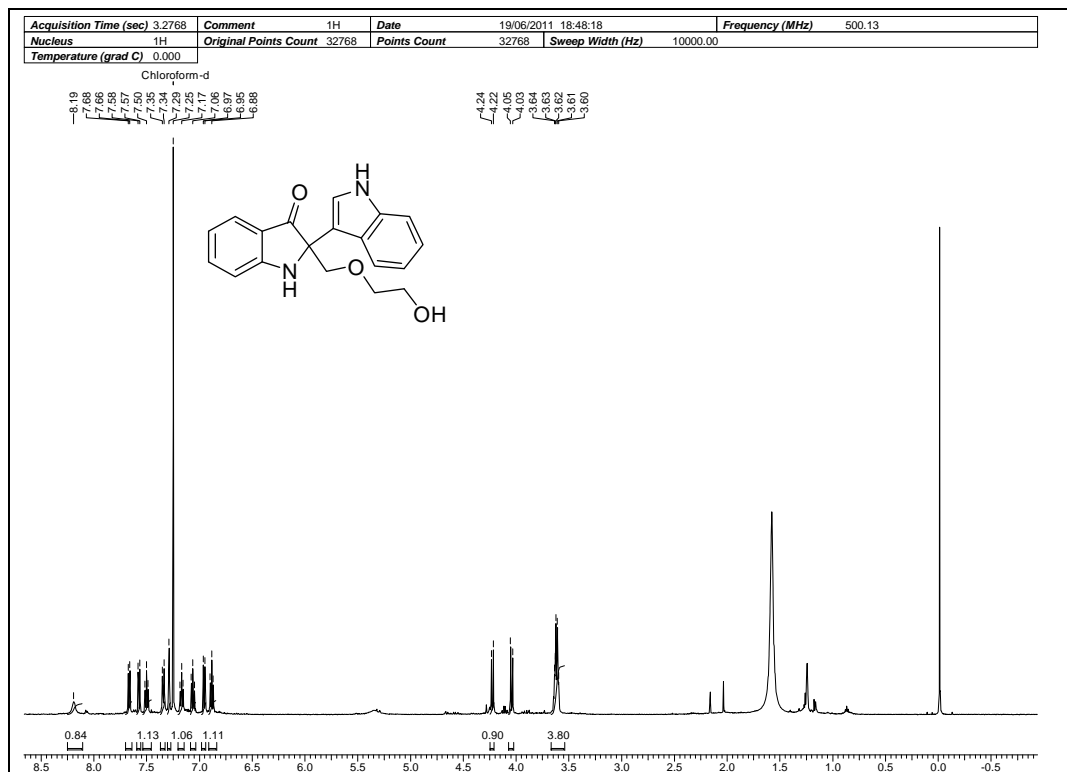
¹H NMR Spectrum of 78 in CDCl₃¹³C NMR Spectrum of 78 in CDCl₃

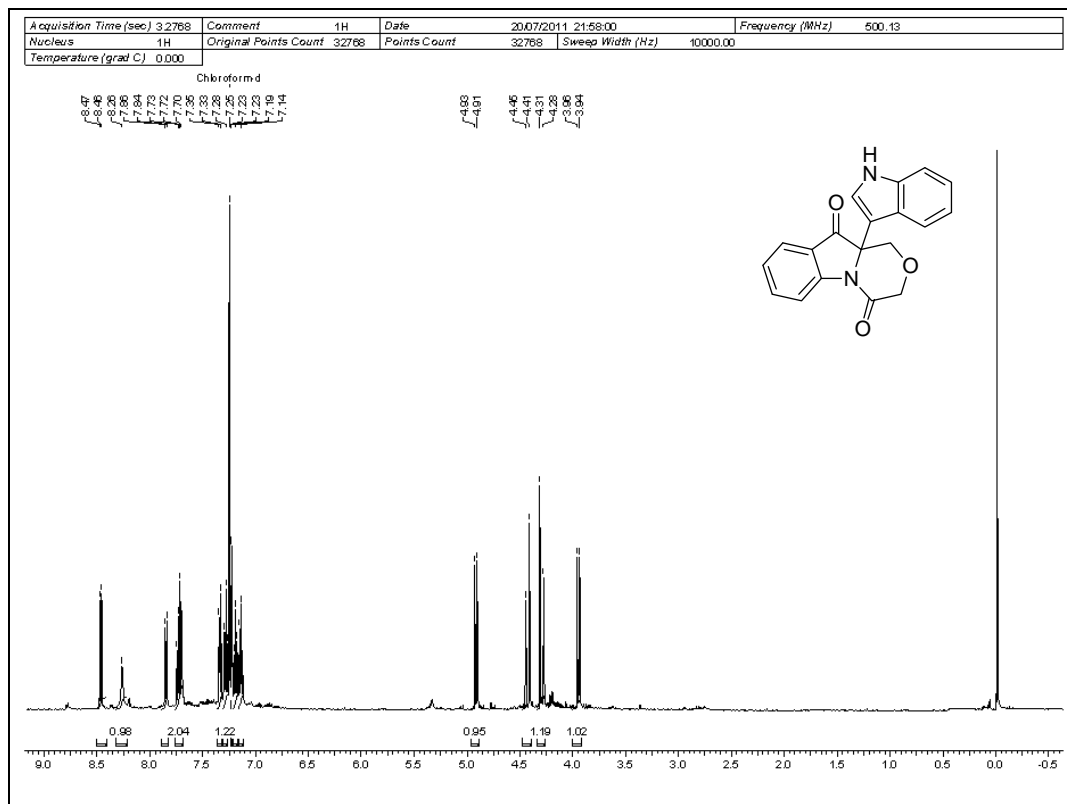
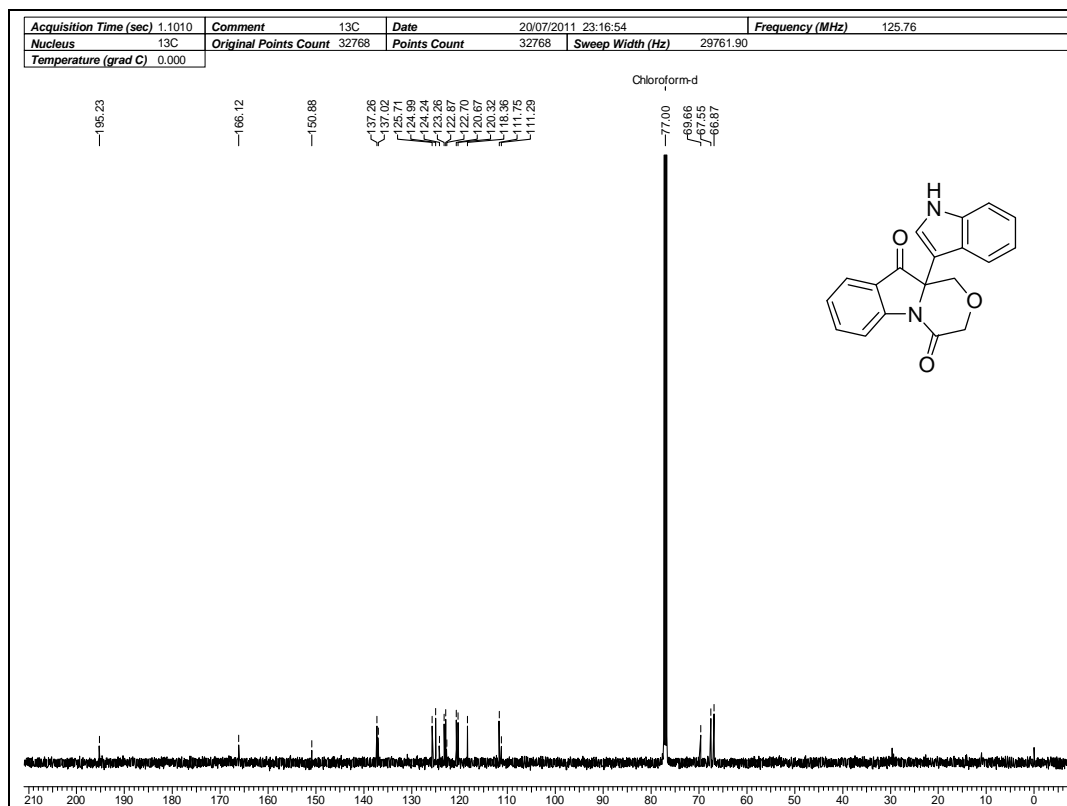
¹H NMR Spectrum of 85 in CDCl₃¹³C NMR Spectrum of 85 in CDCl₃

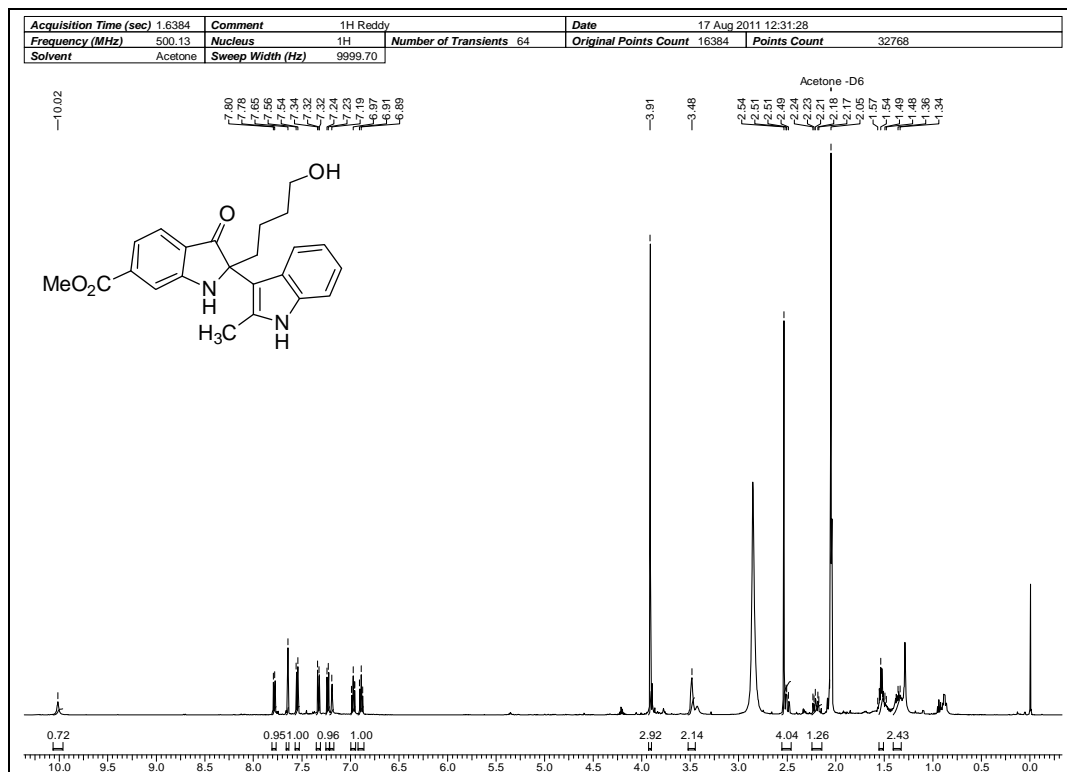
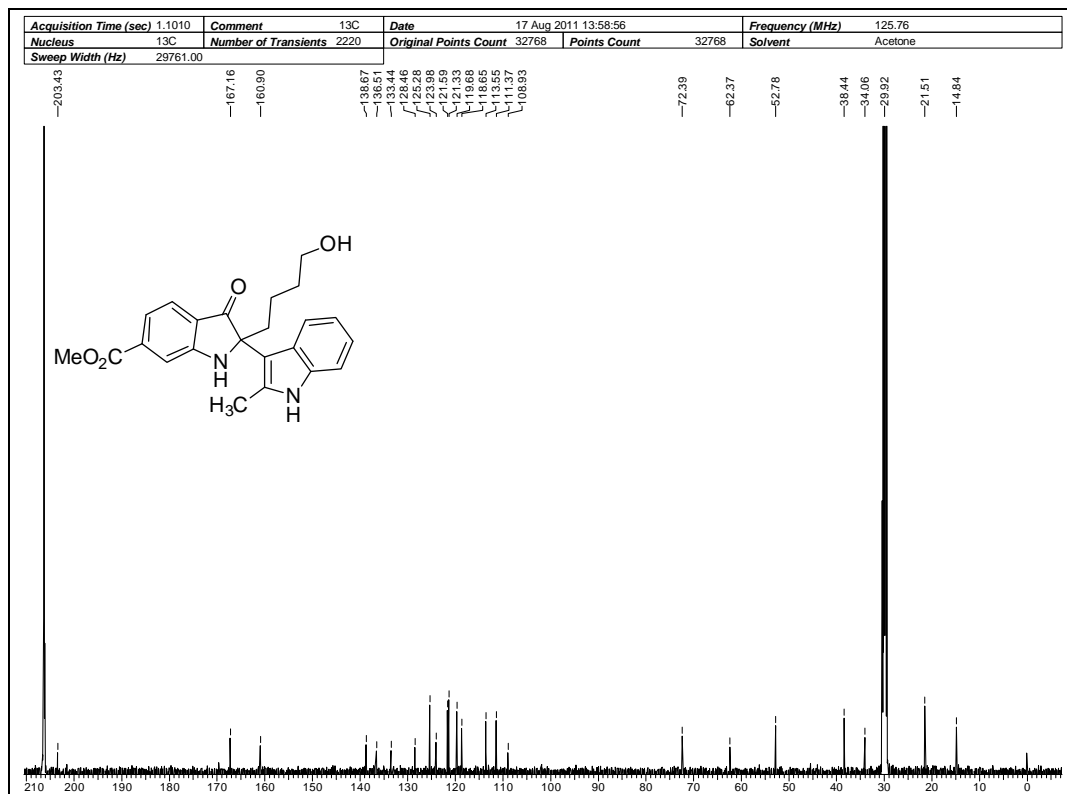


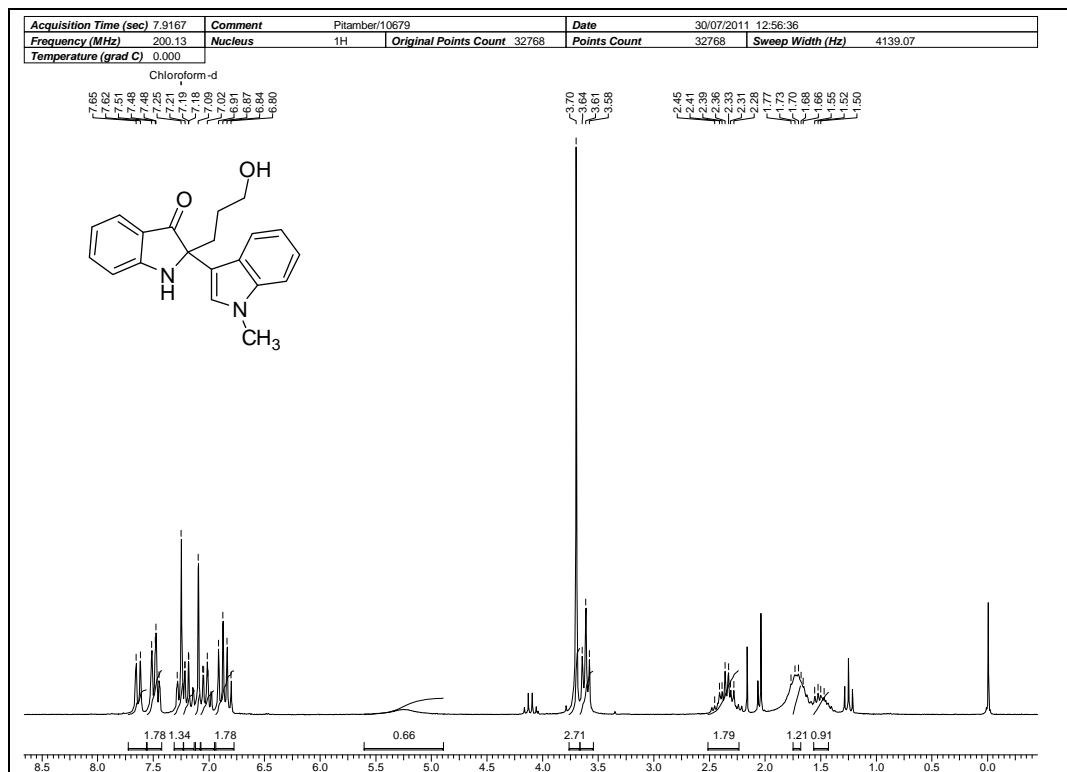
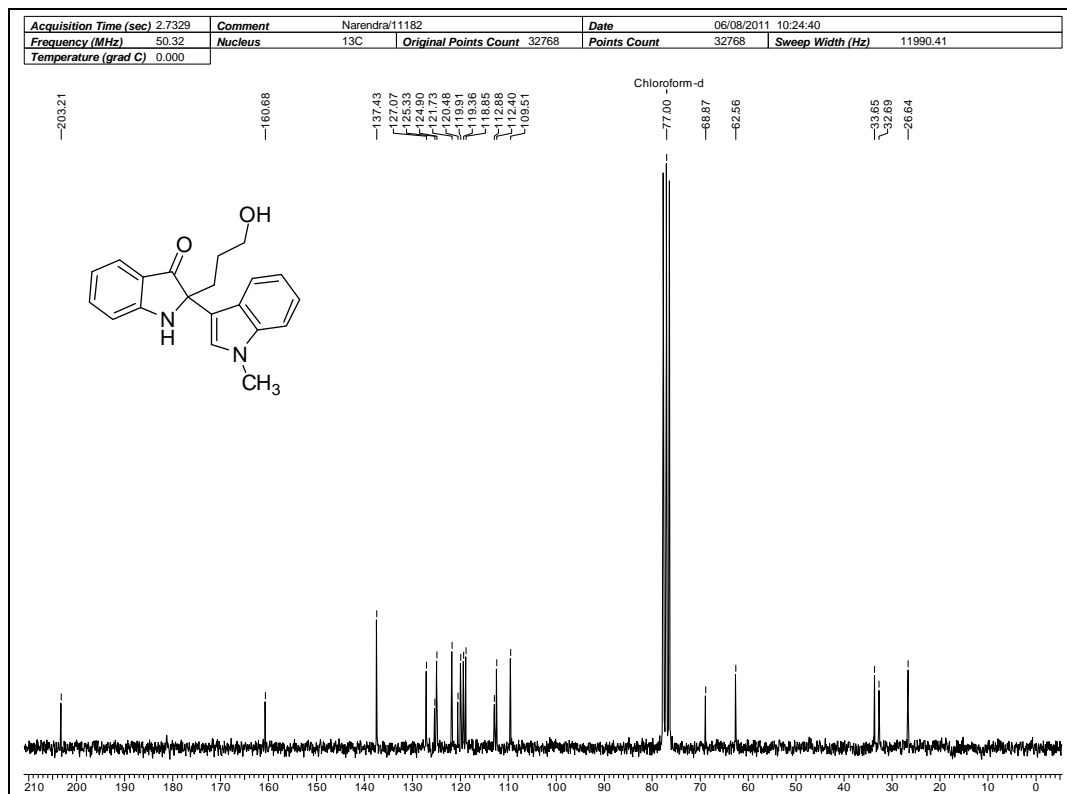
¹H NMR Spectrum of 86 in CDCl₃ and MeOD¹³C NMR Spectrum of 86 in CDCl₃ and MeOD

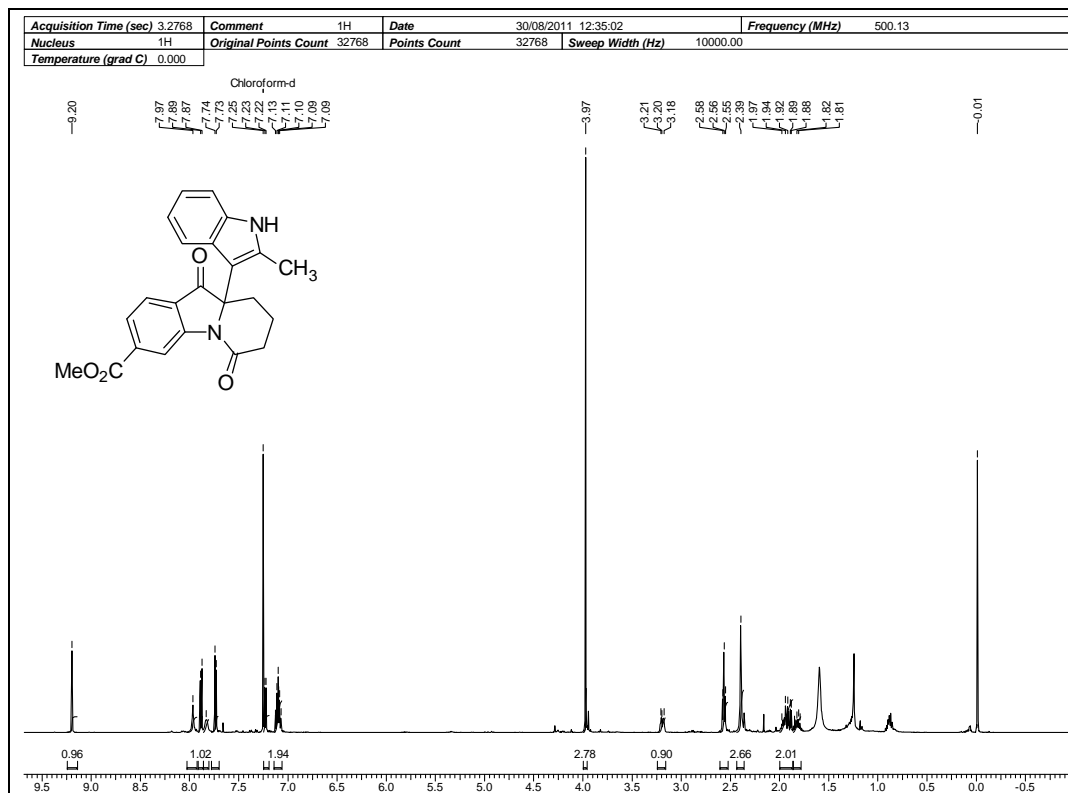
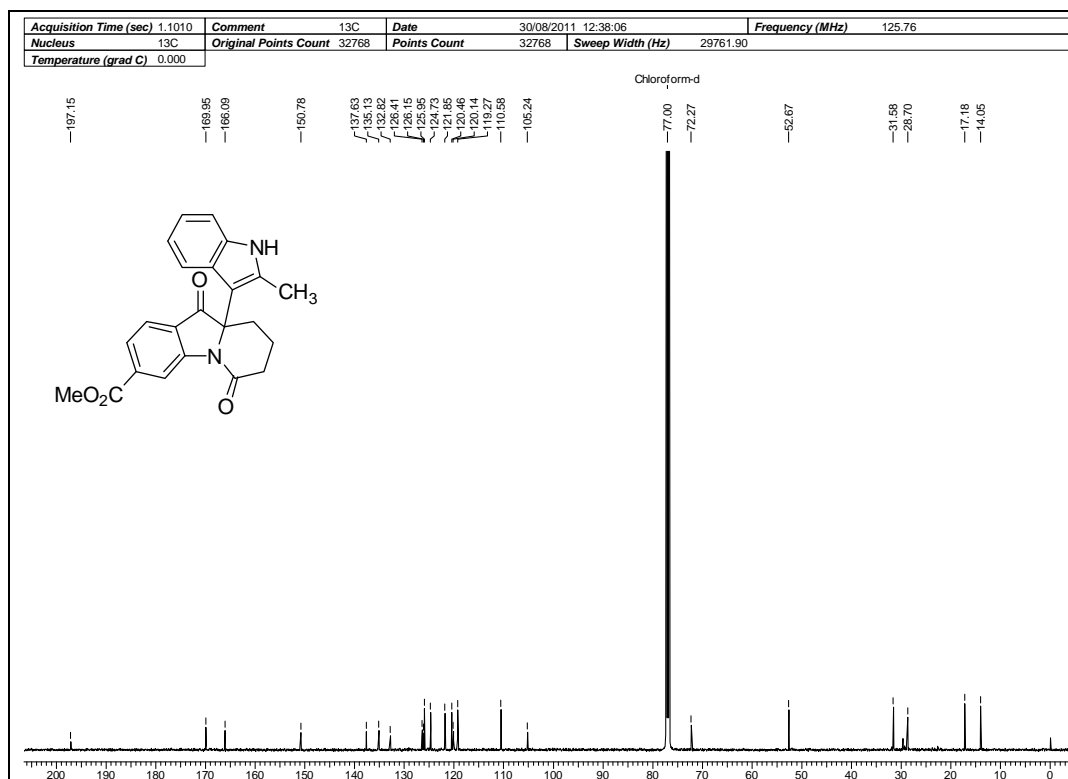
 ^1H NMR Spectrum of 87 in CDCl_3  ^{13}C NMR Spectrum of 87 in CDCl_3 and Acetone- D_6

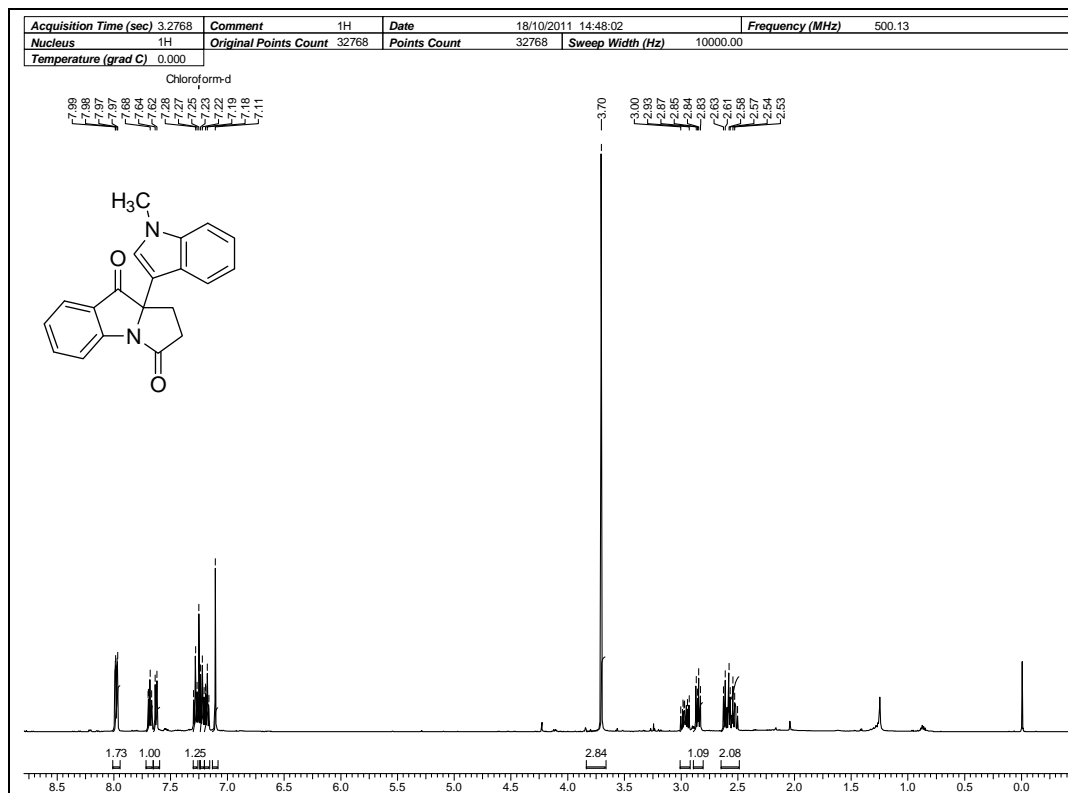
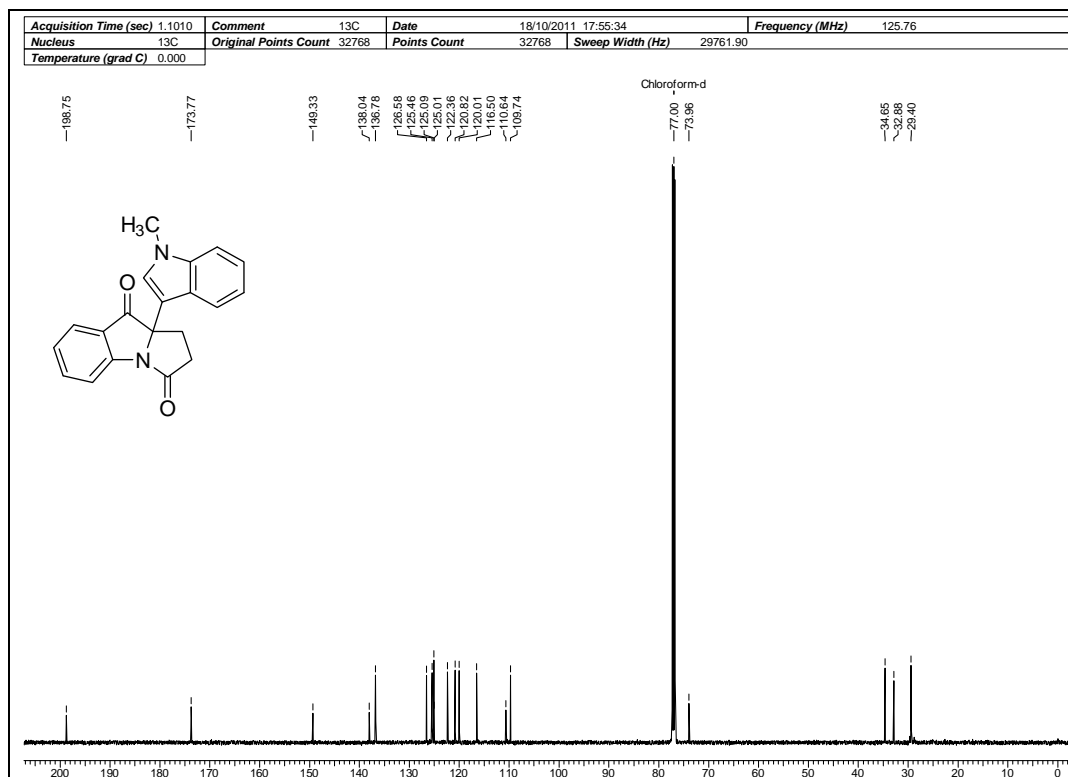


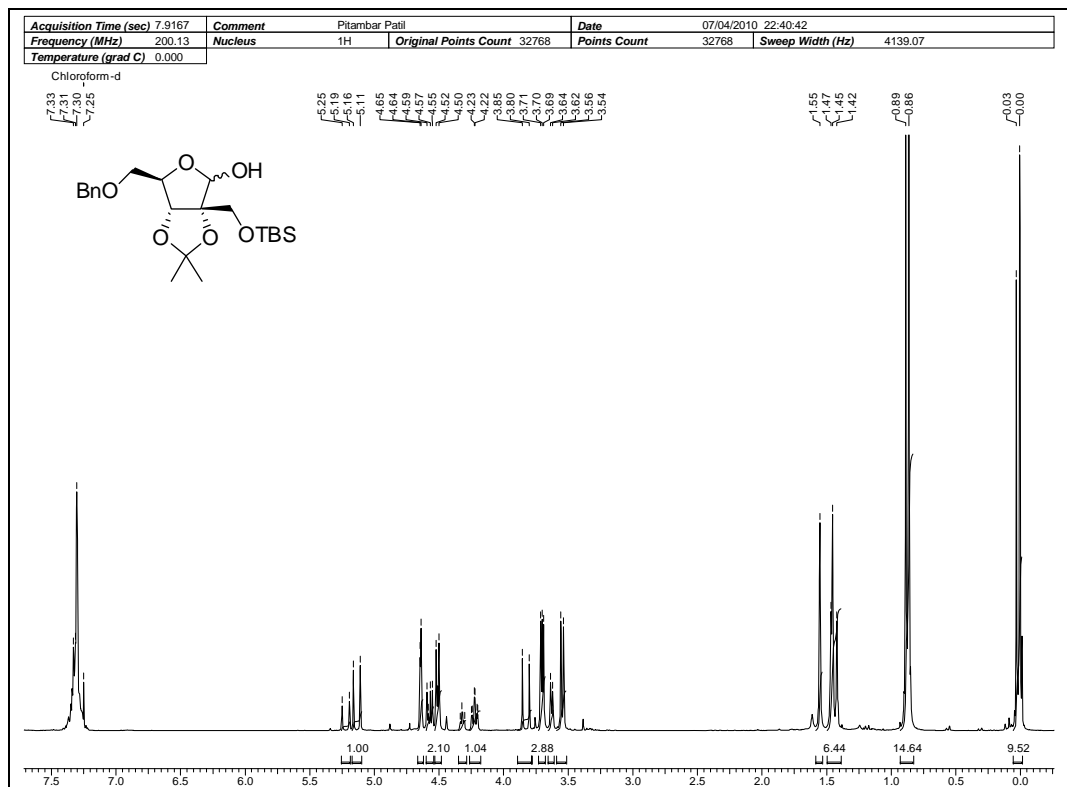
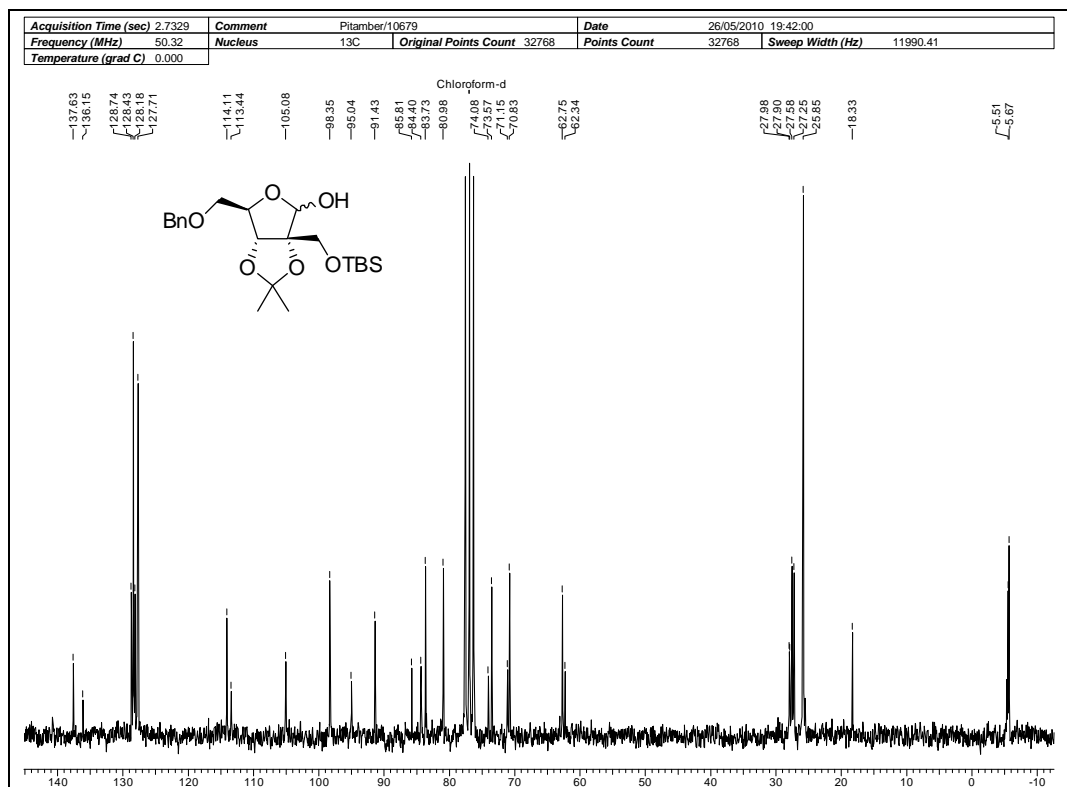
¹H NMR Spectrum of 98 in CDCl₃¹³C NMR Spectrum of 98 in CDCl₃

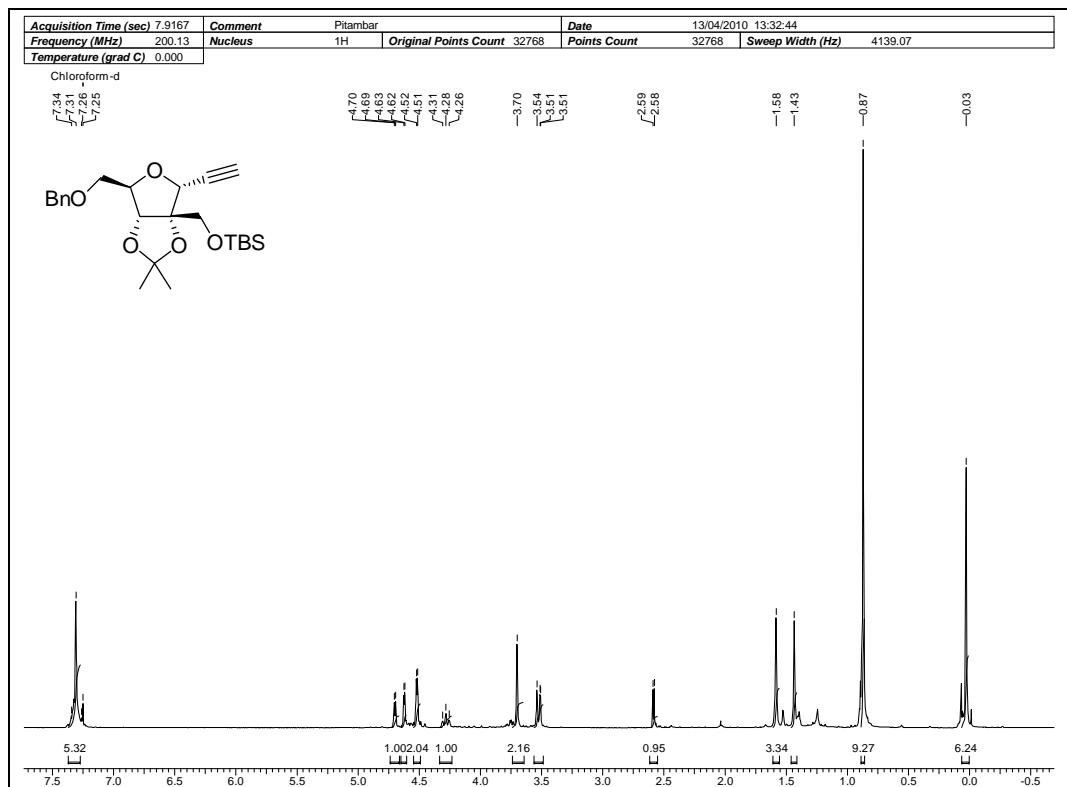
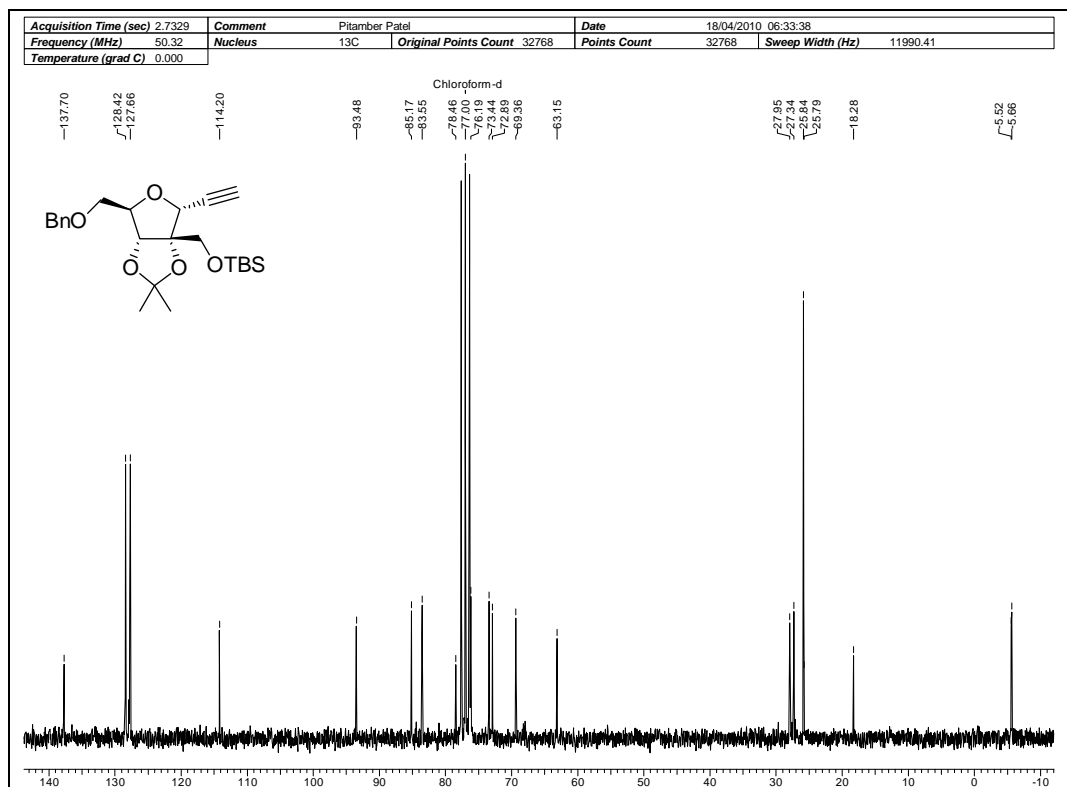
**¹H NMR Spectrum of 101 in Acetone-D₆****¹³C NMR Spectrum of 101 in Acetone-D₆**

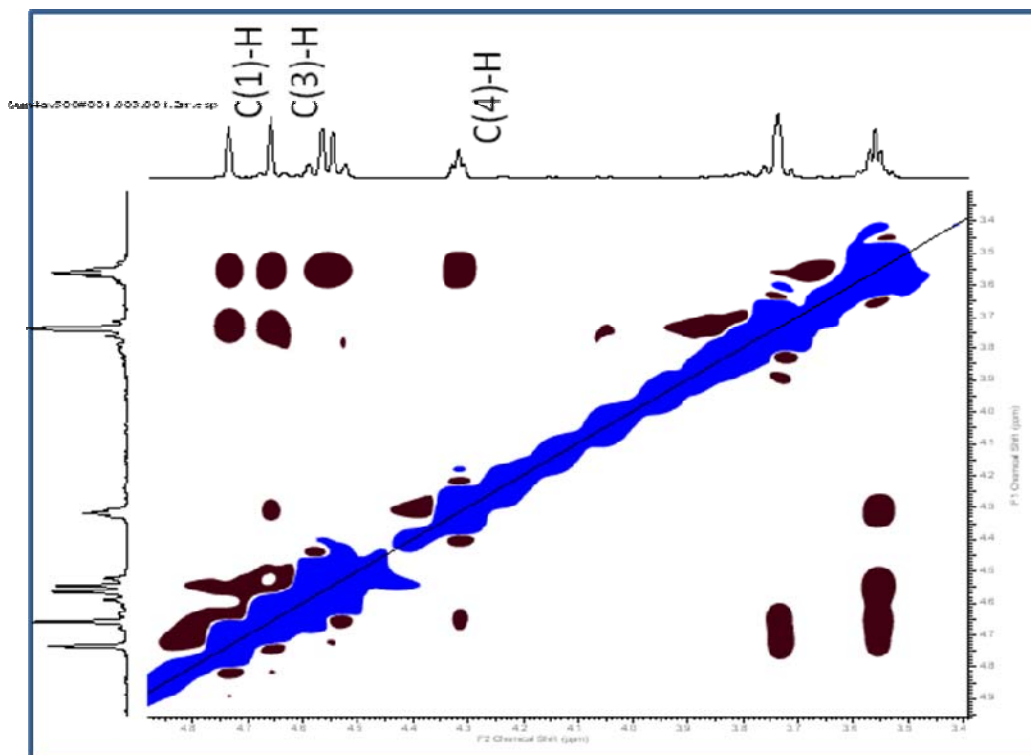
¹H NMR Spectrum of 102 in CDCl₃¹³C NMR Spectrum of 102 in CDCl₃

¹H NMR Spectrum of 104 in CDCl₃¹³C NMR Spectrum of 104 in CDCl₃

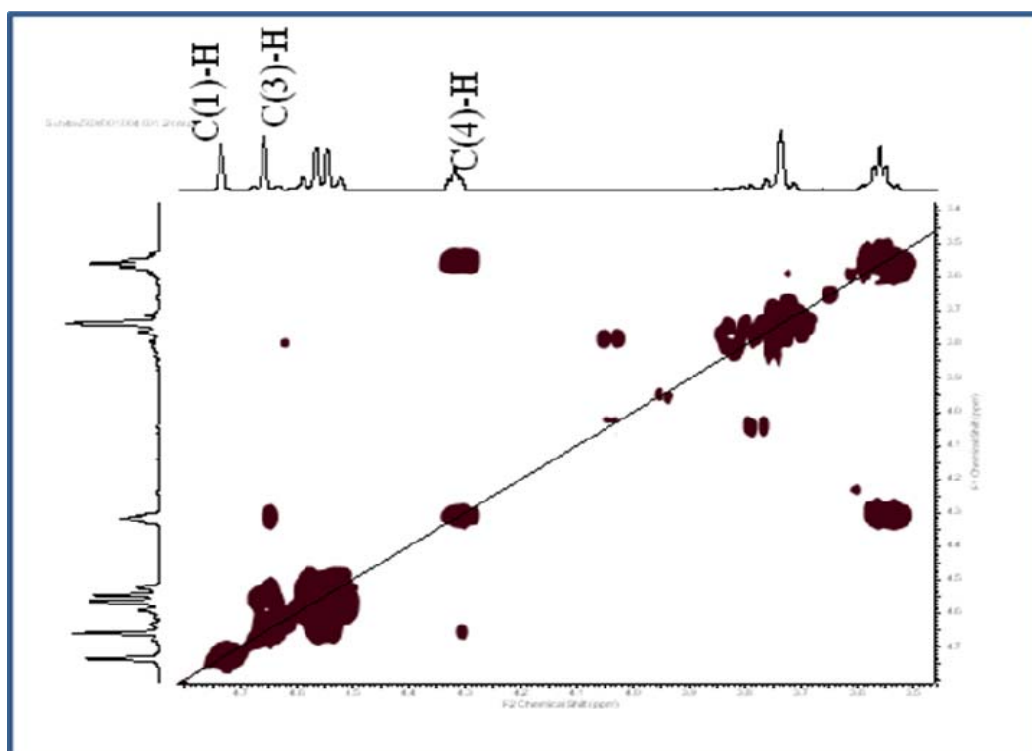
 ^1H NMR Spectrum of 105 in CDCl_3  ^{13}C NMR Spectrum of 105 in CDCl_3

¹H NMR Spectrum of 110 in CDCl₃¹³C NMR Spectrum of 110 in CDCl₃

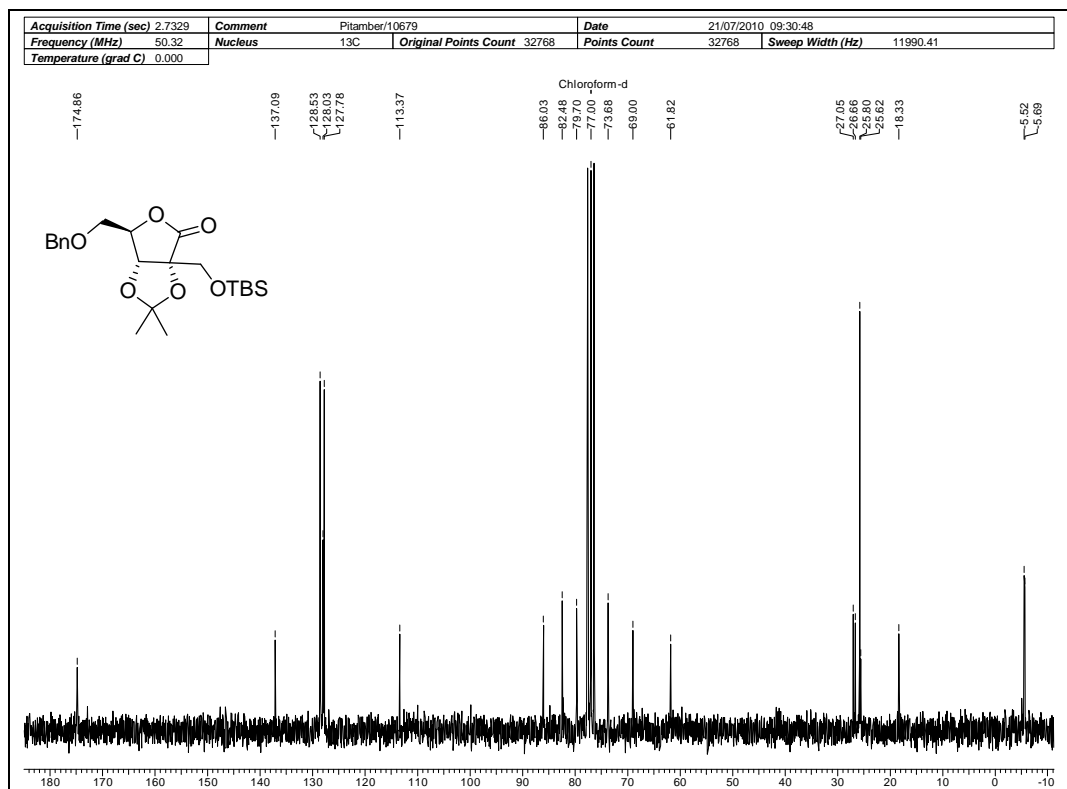
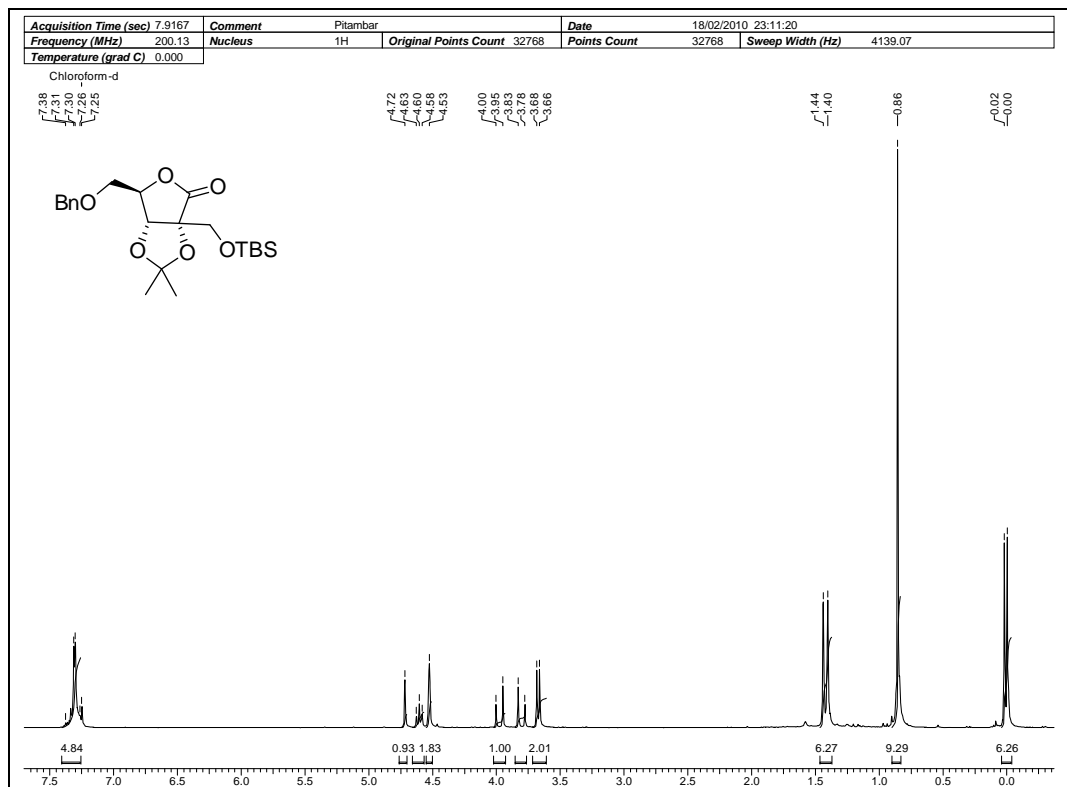
¹H NMR Spectrum of 114 in CDCl₃¹³C NMR Spectrum of 114 in CDCl₃

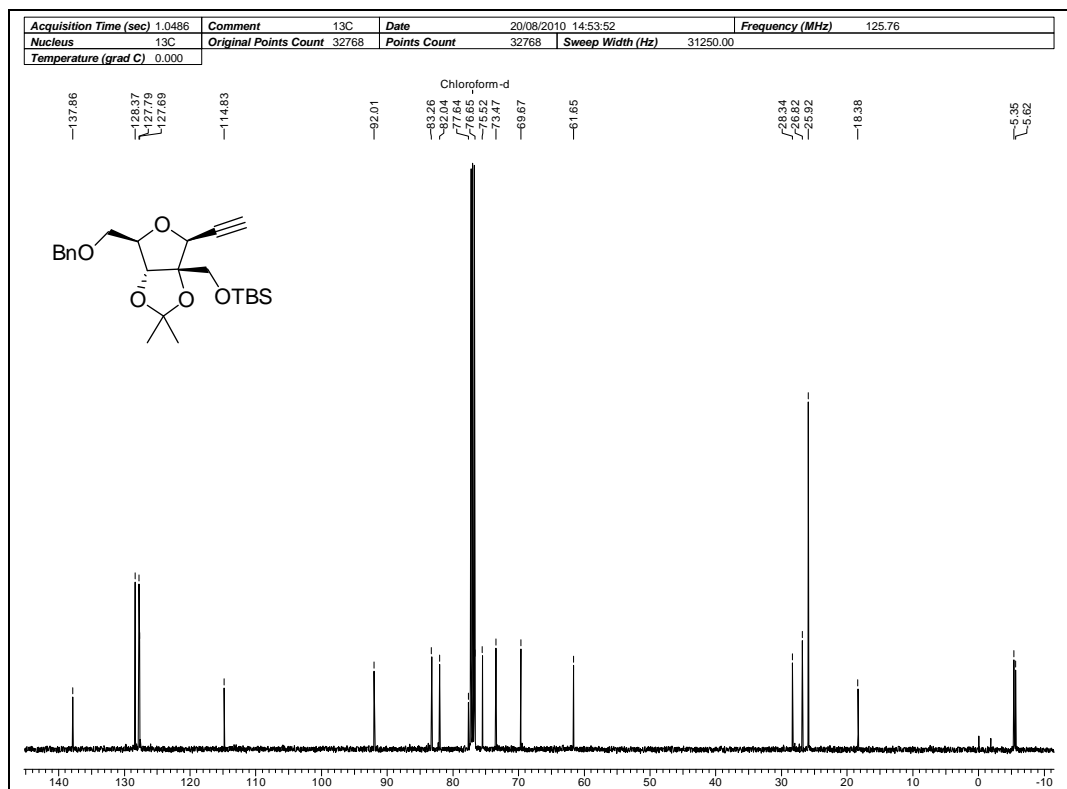
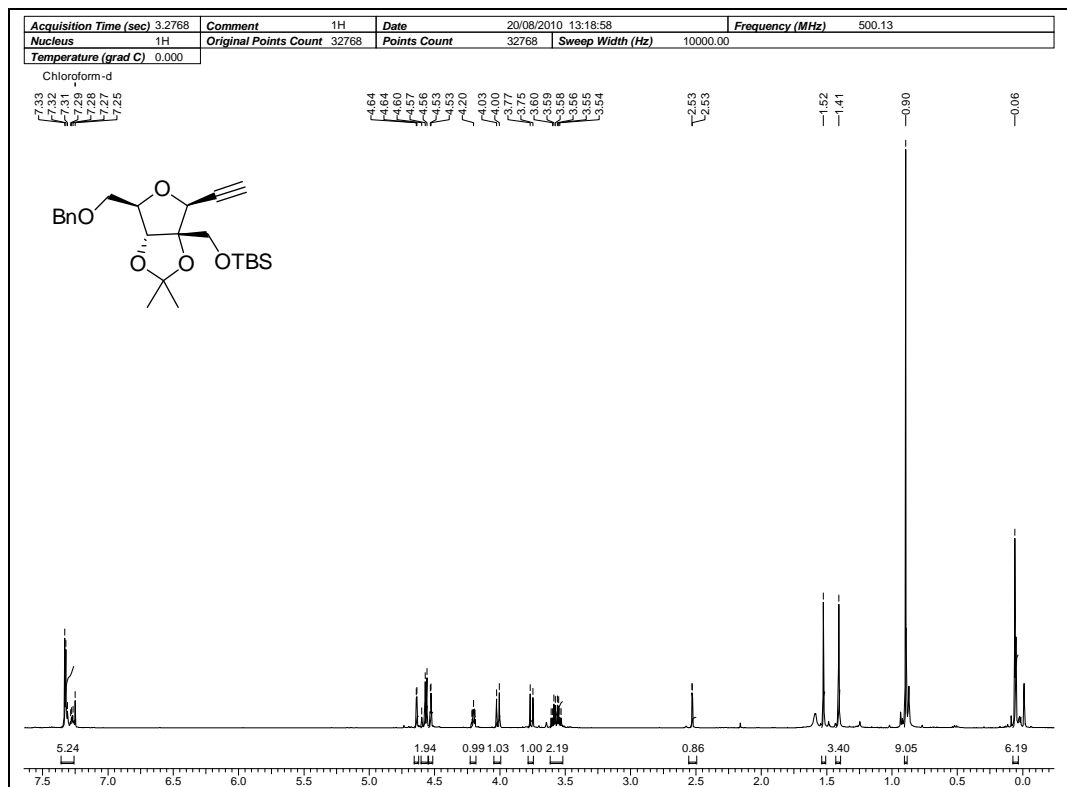


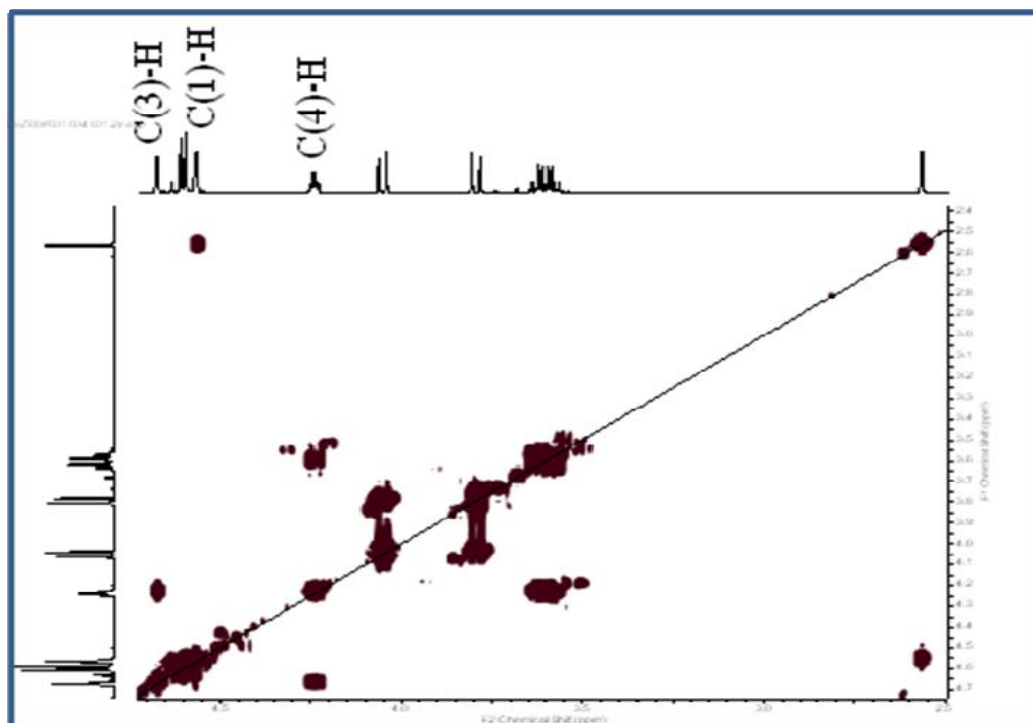
Expanded COSY spectrum of 114



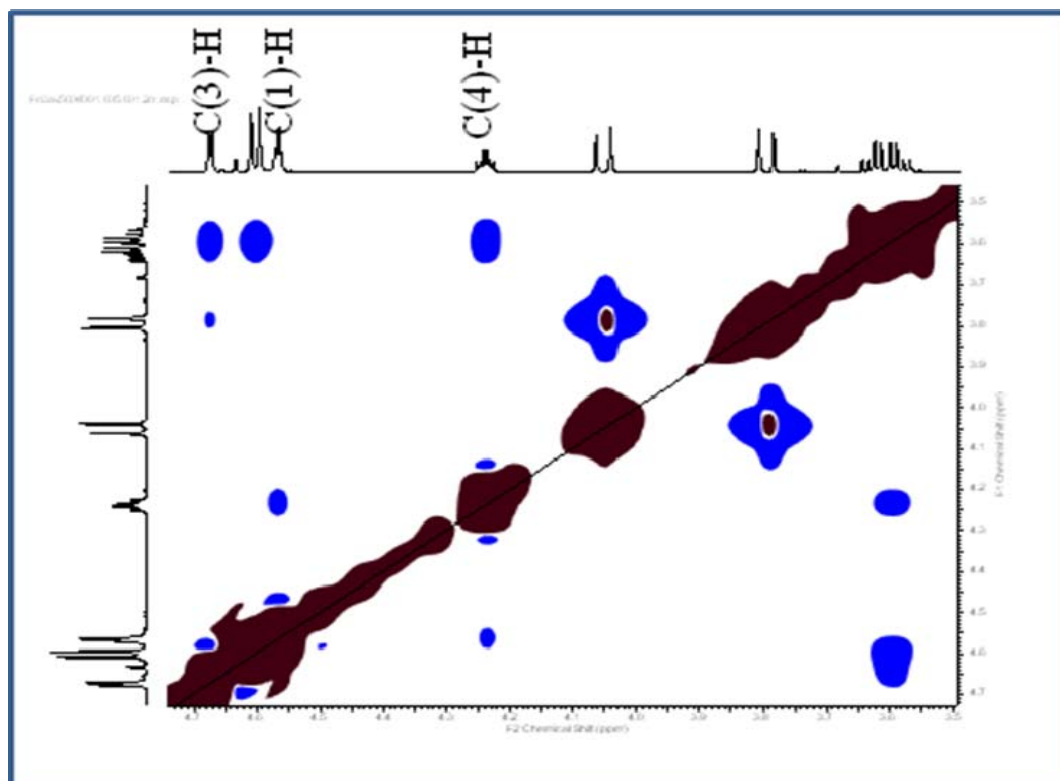
Expanded NOESY spectrum of 114



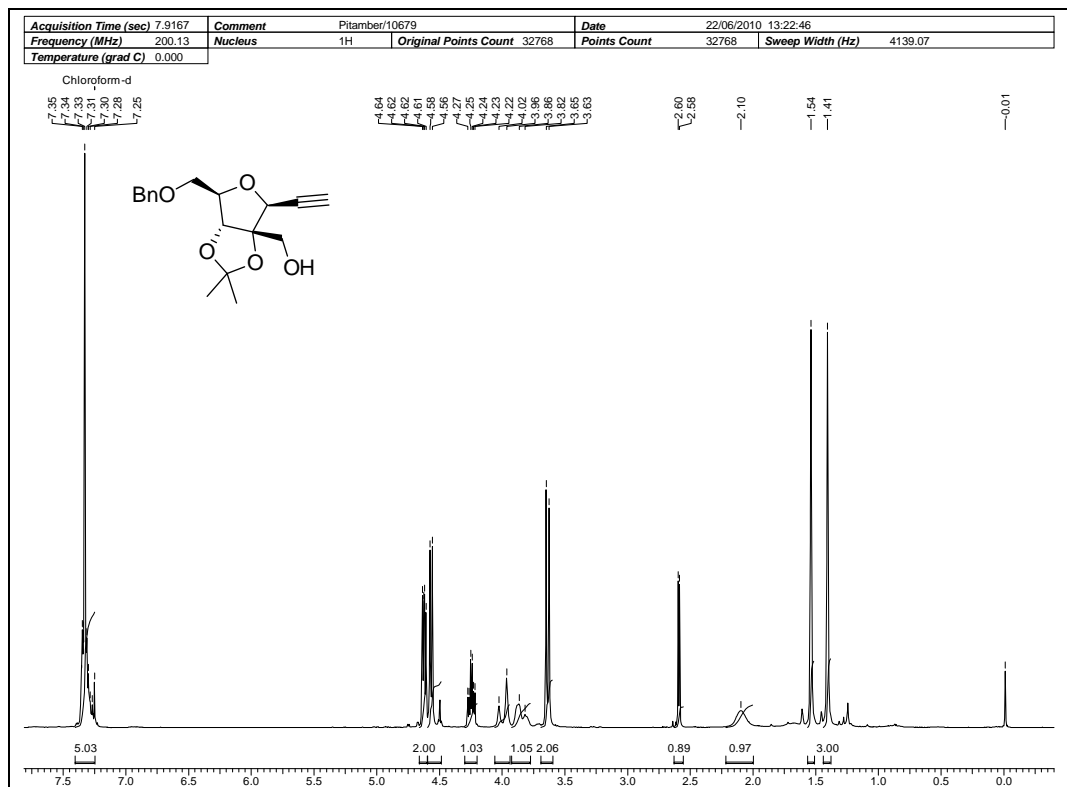
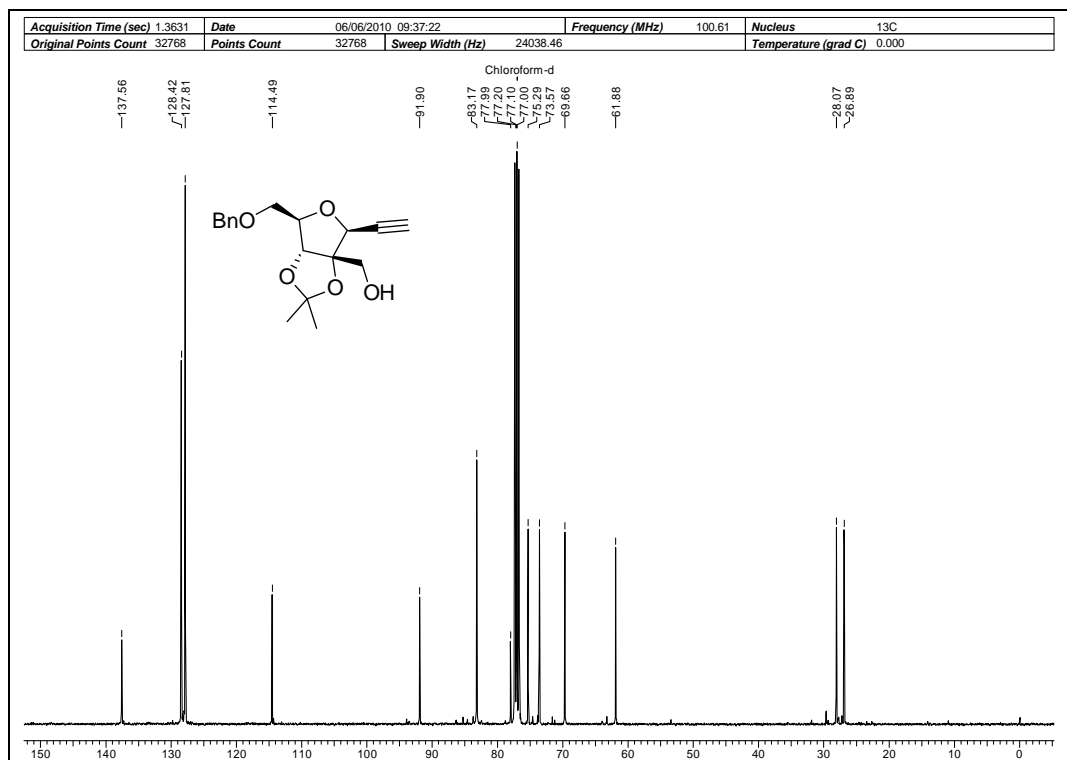


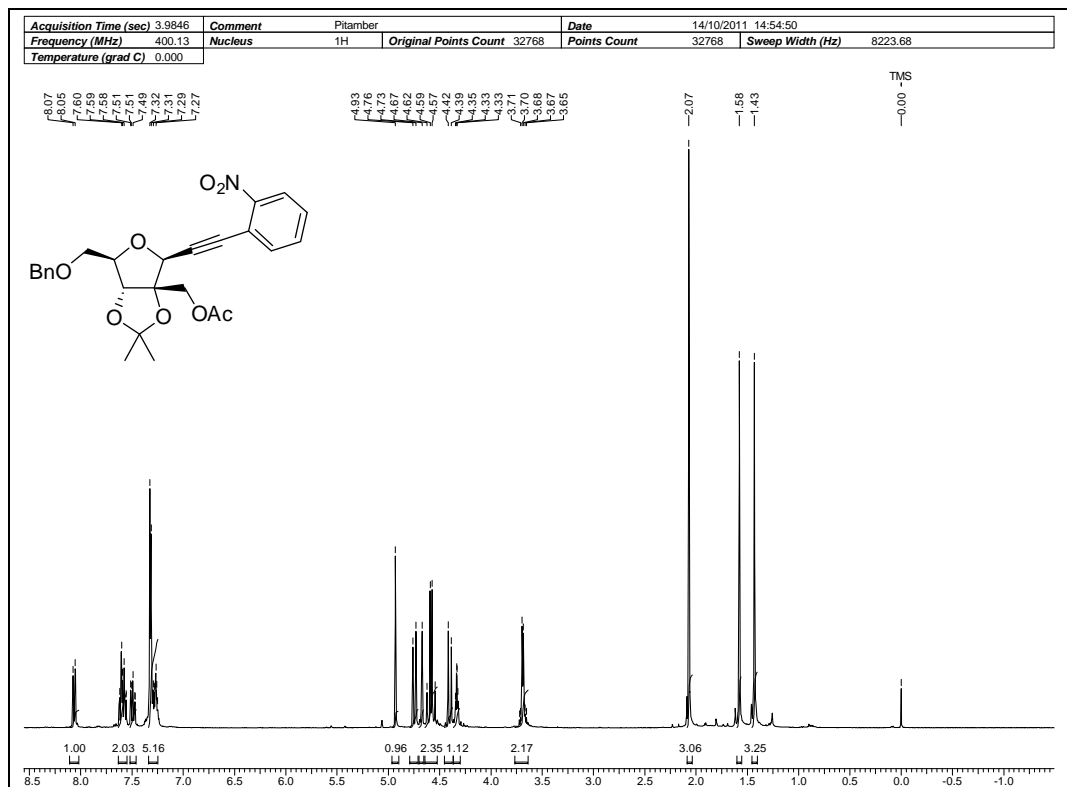
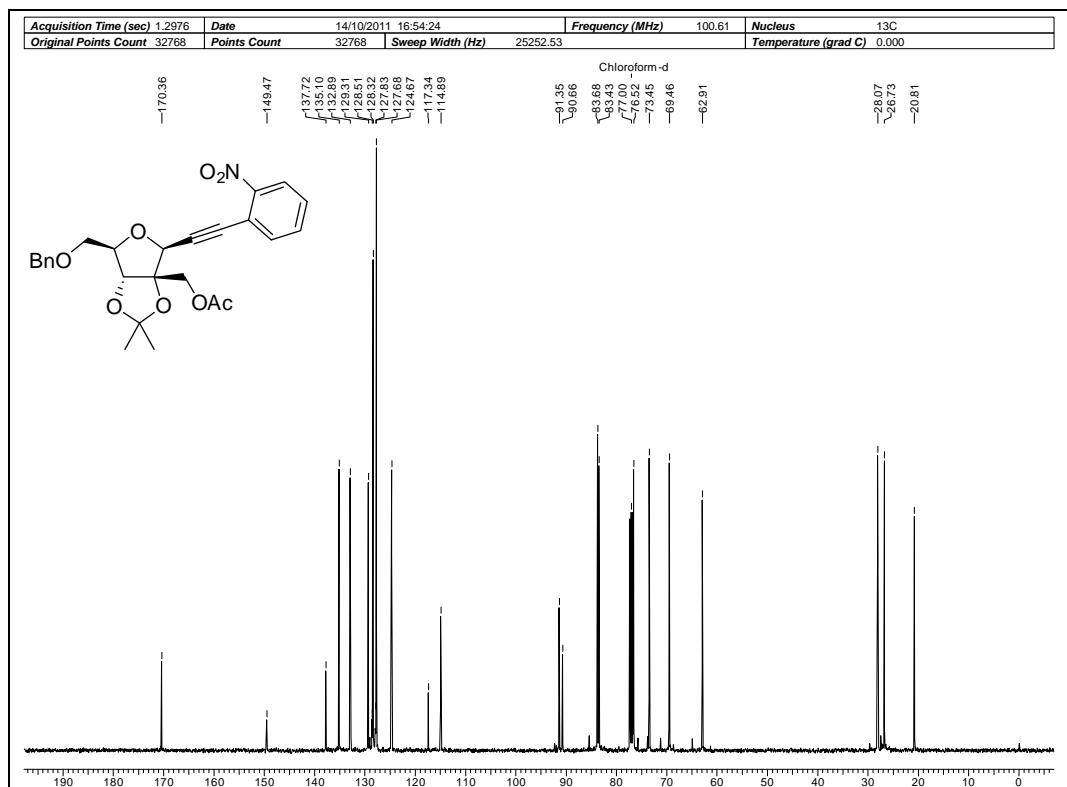


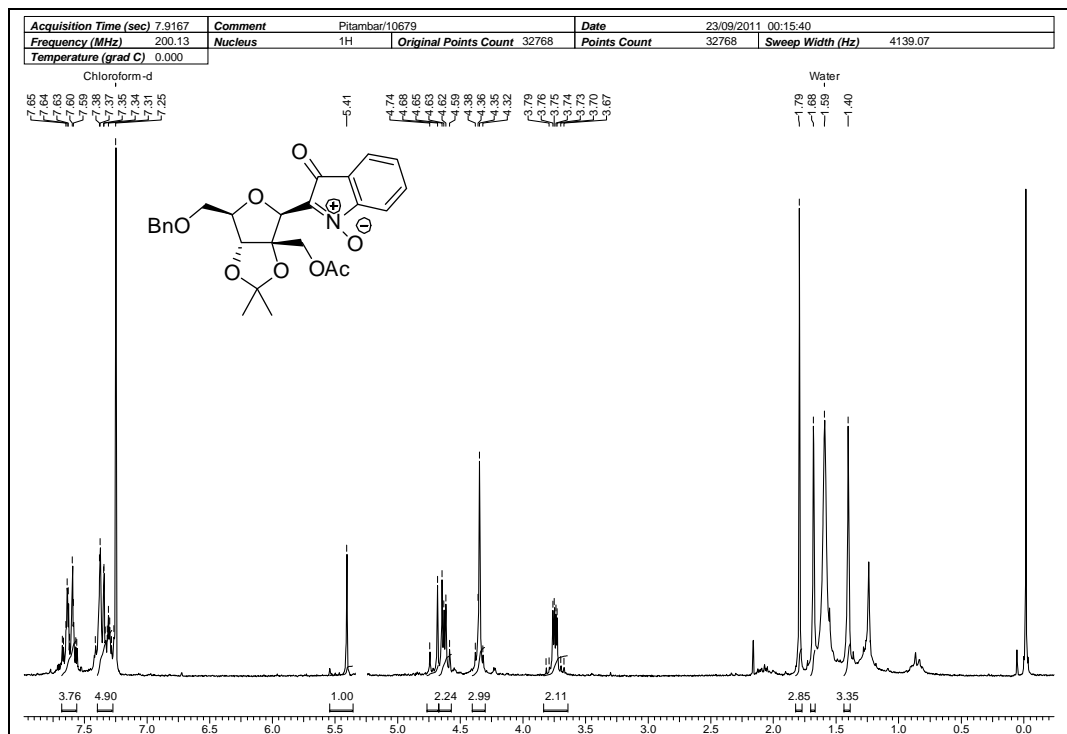
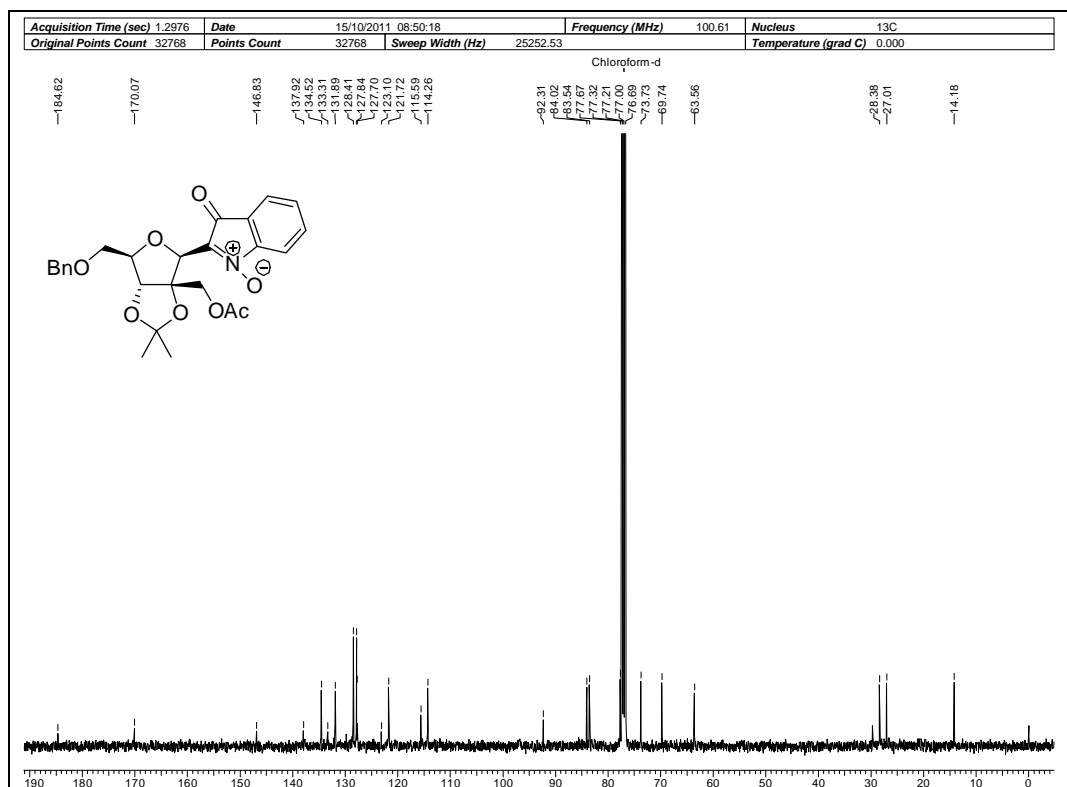
Expanded COSY spectrum of 109

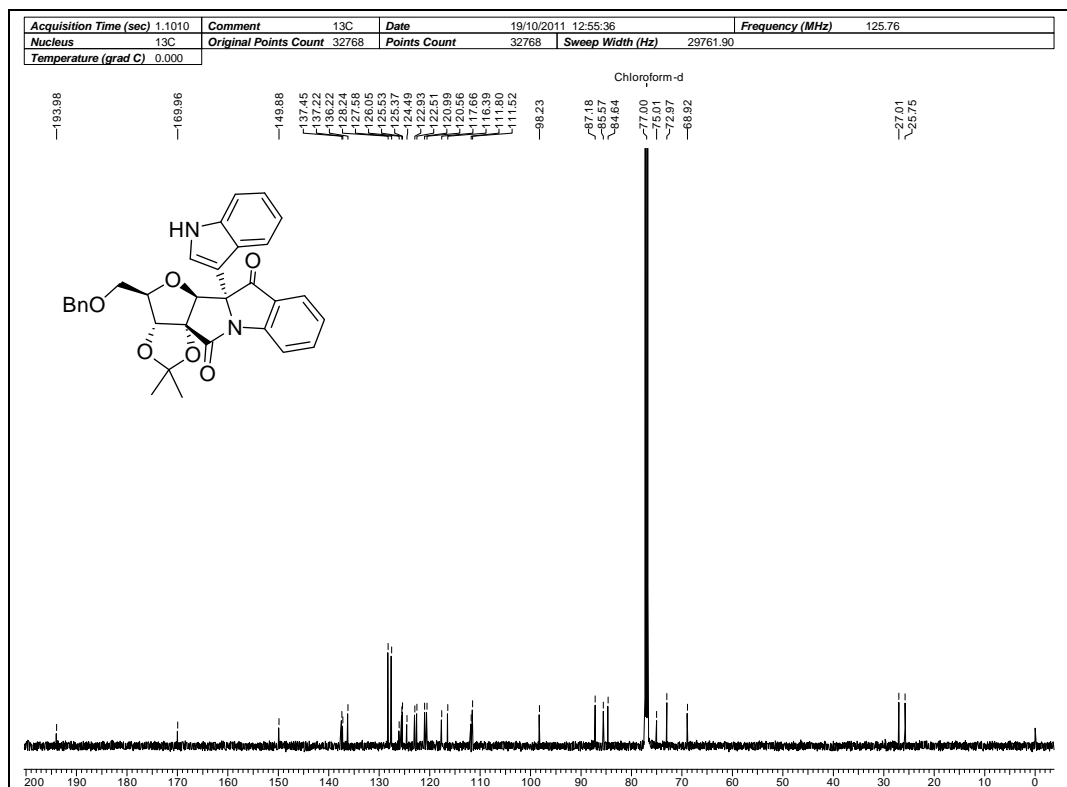
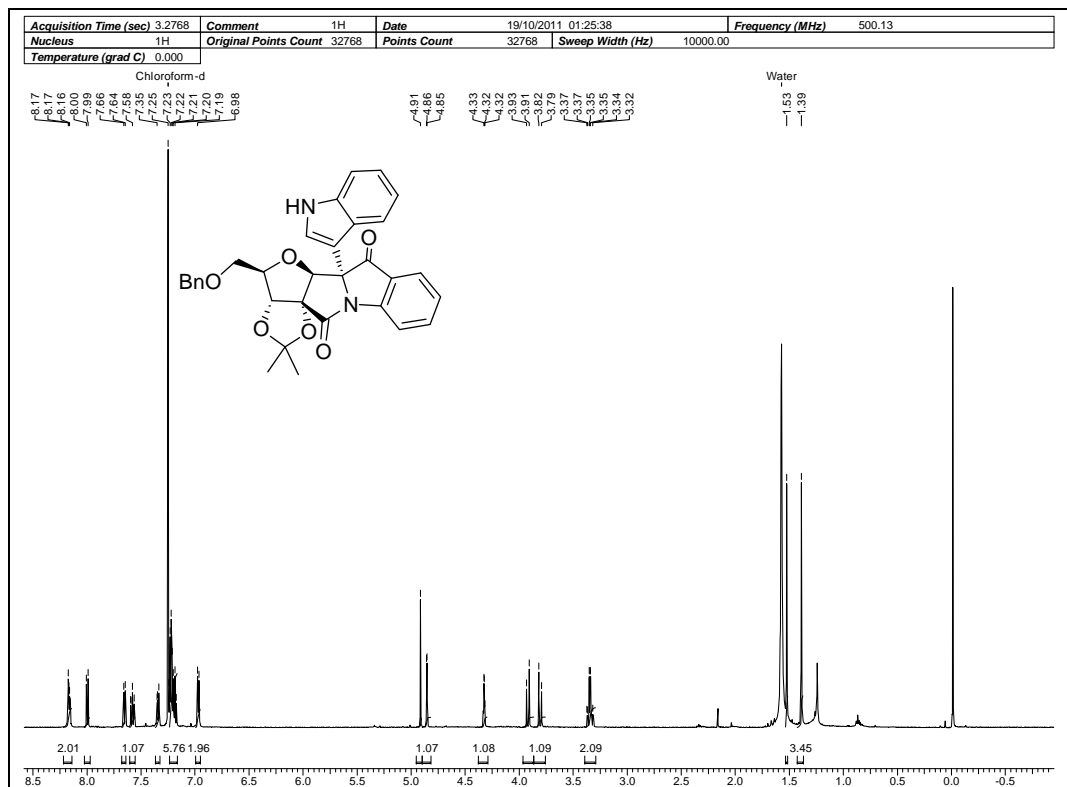


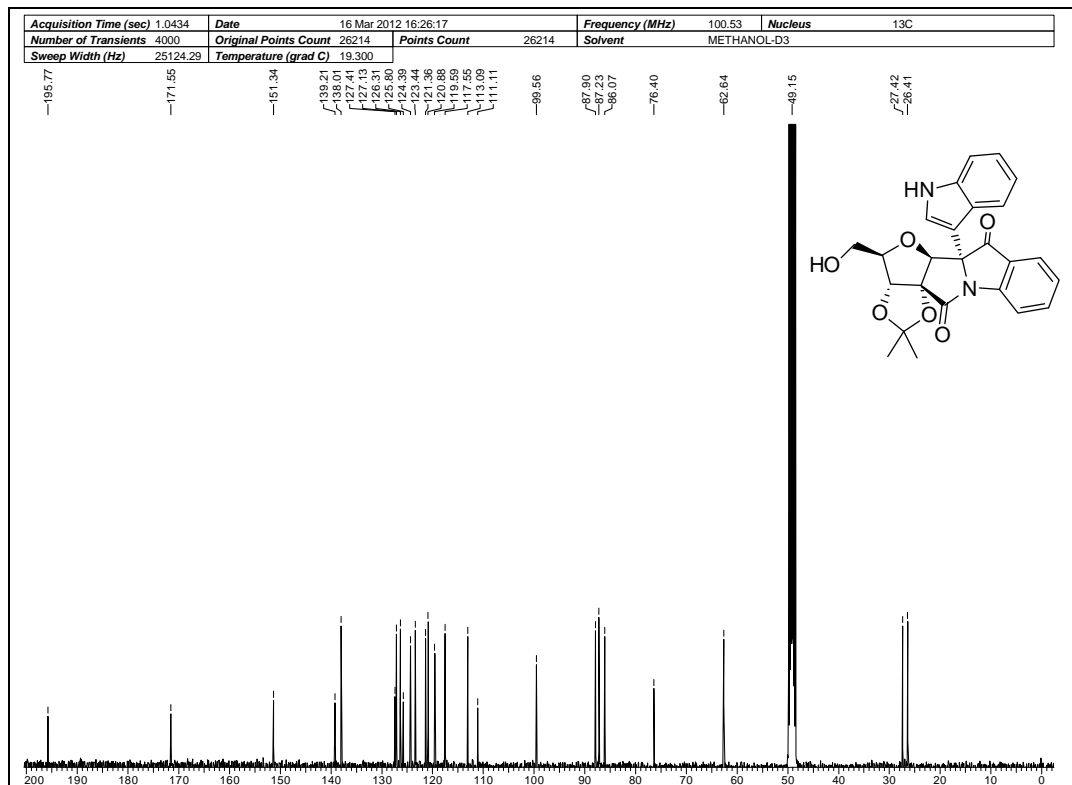
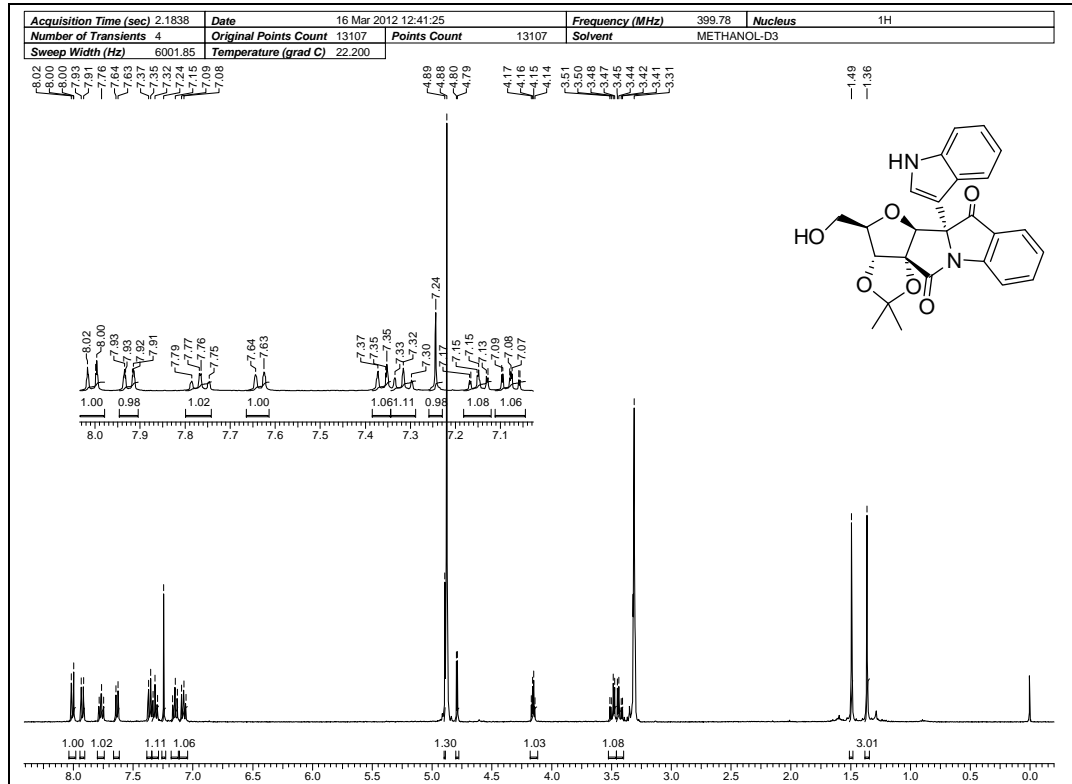
Expanded NOESY spectrum of 109

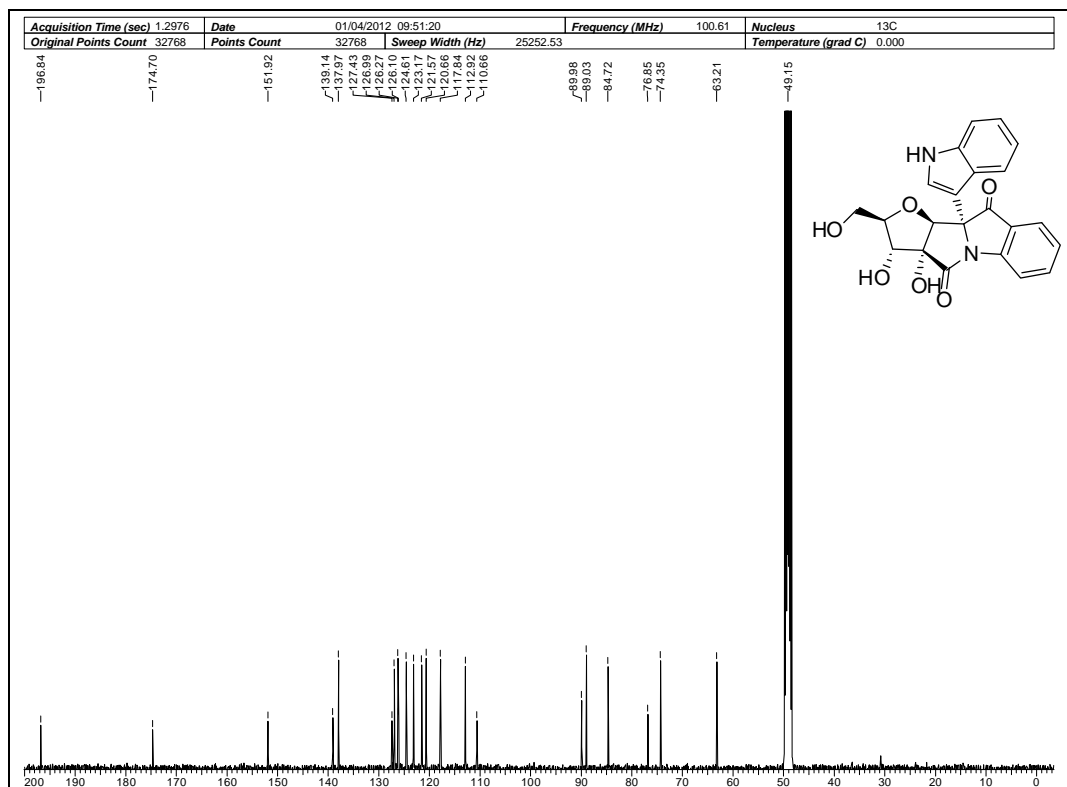
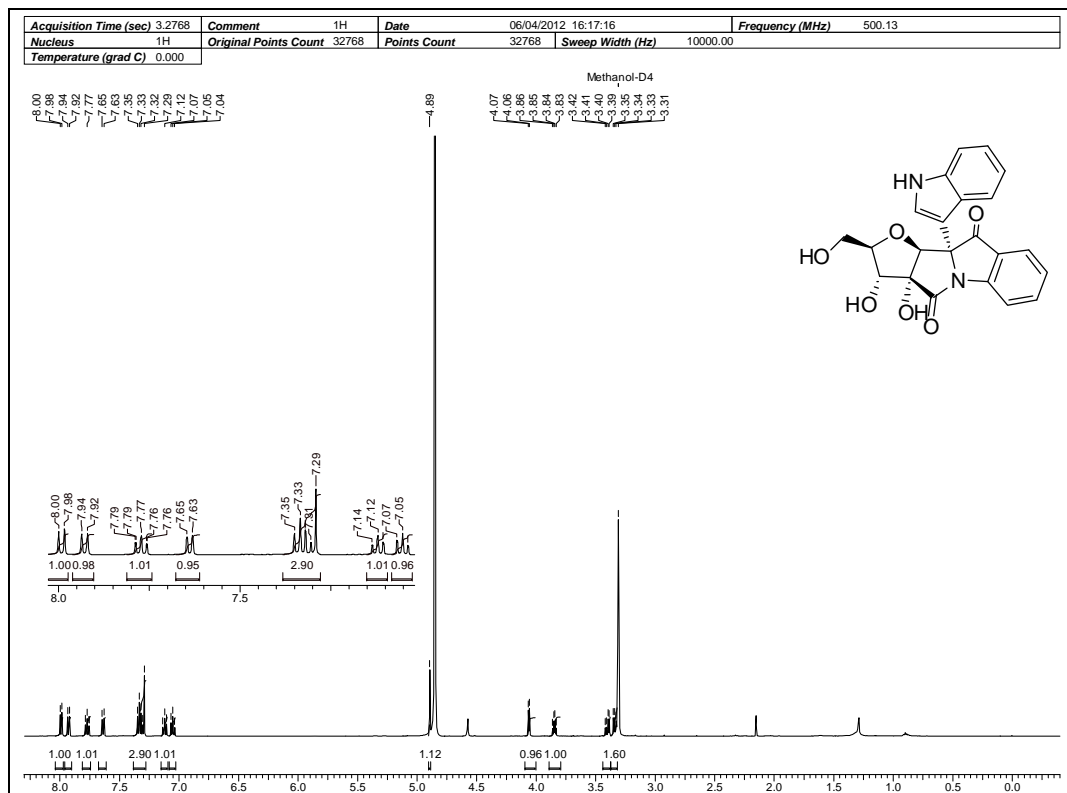
¹H NMR Spectrum of 117 in CDCl₃¹³C NMR Spectrum of 117 in CDCl₃

¹H NMR Spectrum of 119 in CDCl₃¹³C NMR Spectrum of 119 in CDCl₃

¹H NMR Spectrum of 120 in CDCl₃¹³C NMR Spectrum of 120 in CDCl₃







List of Publication

1. "Steric control in Pd-mediated cycloisomerization of sugar alkynols: documentation of a rare allylic epimerization." C. V. Ramana, Pitambar Patel, R. G. Gonnade, *Tetrahedron Lett.* **2007**, *48*, 4771–4774.
2. Multiutility Sophorolipids as Nanoparticle Capping Agents: Synthesis of Stable and Water Dispersible Co Nanoparticles." Manasi Kasture, Sanjay Singh, Pitambar Patel, P. A. Joy, A. A. Prabhune, C. V. Ramana, B. L. V. Prasad, *Langmuir* **2007**, *23*, 11409-11412.
3. "Synthesis of silver nanoparticles by sophorolipids: Effect of temperature and sophorolipid structure on the size of particles" Manasi Kasture, Pitambar Patel, A. A. Kulkarni, A. A. Prabhune, C. V. Ramana, B. L. V. Prasad, *J. Chem. Sci.* **2008**, *120*, 515–520.
4. "A direct method for the preparation of glycolipid–metal nanoparticle conjugates: sophorolipids as reducing and capping agents for the synthesis of water re-dispersible silver nanoparticles and their antibacterial activity." Sanjay Singh, Pitambar Patel, Swarna Jaiswal, A. A. Prabhune, C. V. Ramana, B. L. V. Prasad, *New J. Chem.*, **2009**, *33*, 646–652.
5. "A Combined Experimental and Density Functional Theory Study on the Pd-Mediated Cycloisomerization of *o*-Alkynylnitrobenzenes – Synthesis of Isatogens and Their Evaluation as Modulators of ROS-Mediated Cell Death". Chepuri V. Ramana, Pitambar Patel, K. Vanka, B. Miao, A. Degterev, *Eur. J. Org. Chem.*, **2010**, 5955–5966.
6. "Divergent Pd(II) and Au(III) Mediated Nitro-alkynol Cycloisomerizations." Pitambar Patel, C. V. Ramana, *Org. Boimol. Chem.*, **2011**, *9*, 7327-7334.
7. "Sequential Metal-Mediated Catalytic Transformations: A Modular Assembly of the Central Core of Isatisine A" Pitambar Patel, Narendra Prasad Reddy Bhimreddy, C. V. Ramana, to be communicated.
8. "Total synthesis of Isatisine A" Pitambar Patel, C. V. Ramana, to be communicated.

Erratum
